



ISSN 1580-3155

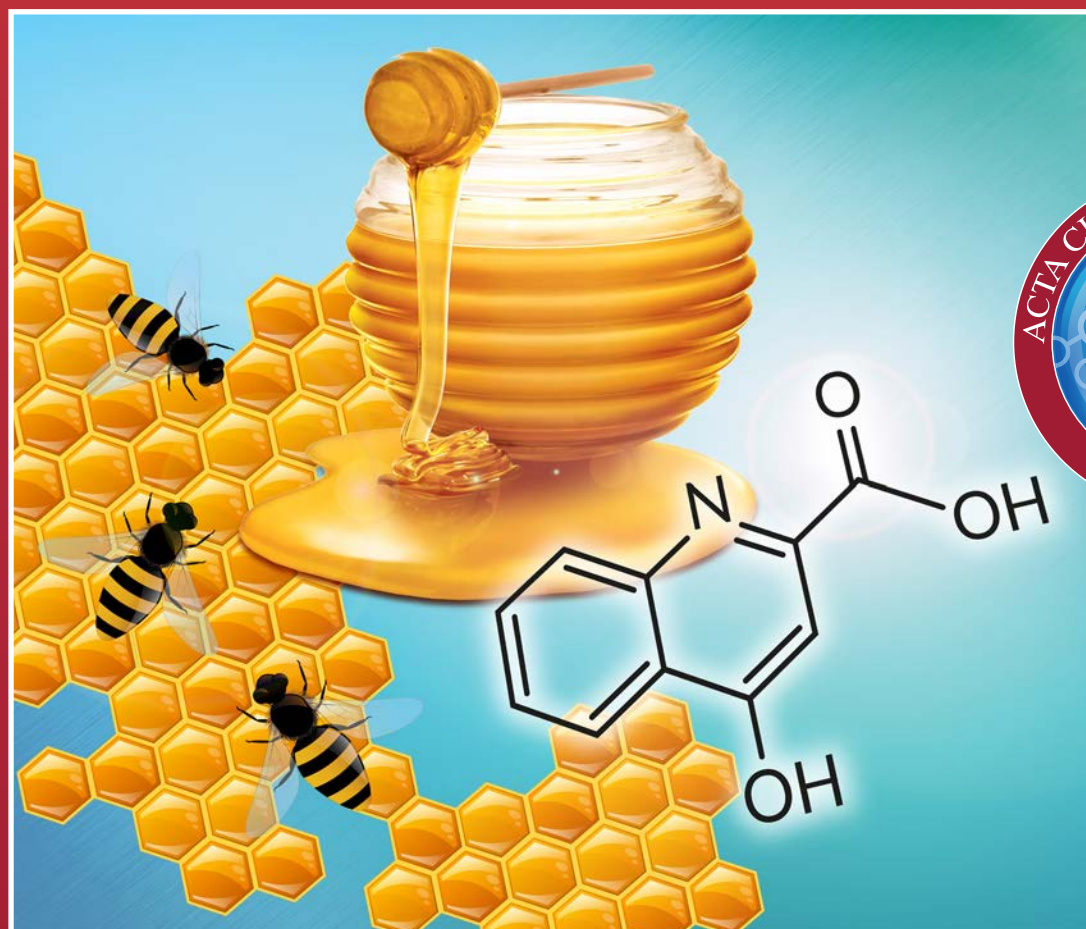
Pages 173–294 ■ Year 2023, Vol. 70, No. 2

Slovensko kemijsko društvo
Slovenian Chemical Society

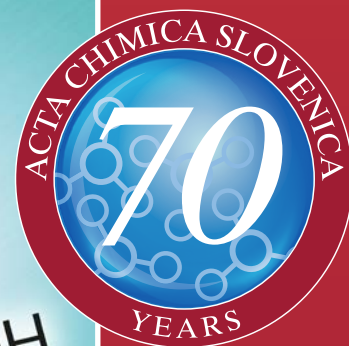


Acta Chimica Slo Acta Chimica Slo Slovenica Acta C

2



70/2023



EDITOR-IN-CHIEF

FRANC PERDIH

University of Ljubljana, Faculty of Chemistry and Chemical Technology, Večna pot 113, SI-1000 Ljubljana, Slovenija
E-mail: ACSi@fkk.uni-lj.si, Telephone: (+386)-1-479-8514

ASSOCIATE EDITORS

Alen Albreht, National Institute of Chemistry, Slovenia
Aleš Berlec, Jožef Stefan Institute, Slovenia
Janez Cerkovnik, University of Ljubljana, Slovenia
Mirela Dragomir, Jožef Stefan Institute, Slovenia
Krištof Kranjc, University of Ljubljana, Slovenia
Matjaž Kristl, University of Maribor, Slovenia
Maja Leitgeb, University of Maribor, Slovenia

Helena Prosen, University of Ljubljana, Slovenia
Aleš Ručigaj, University of Ljubljana, Slovenia
Jernej Stare, National Institute of Chemistry, Slovenia
Irena Vovk, National Institute of Chemistry, Slovenia

ADMINISTRATIVE ASSISTANT

Eva Mihalinec, Slovenian Chemical society, Slovenia

EDITORIAL BOARD

Wolfgang Buchberger, Johannes Kepler University, Austria
Alojz Demšar, University of Ljubljana, Slovenia
Stanislav Gobec, University of Ljubljana, Slovenia
Marko Goličnik, University of Ljubljana, Slovenia
Günter Grampp, Graz University of Technology, Austria
Wojciech Grochala, University of Warsaw, Poland
Danijel Kikelj, University of Ljubljana
Janez Košmrlj, University of Ljubljana, Slovenia
Mahesh K. Lakshman, The City College and
The City University of New York, USA
Blaž Likozar, National Institute of Chemistry, Slovenia

Janez Mavri, National Institute of Chemistry, Slovenia
Jiří Pinkas, Masaryk University Brno, Czech Republic
Friedrich Sreinc, University of Minnesota, USA
Walter Steiner, Graz University of Technology, Austria
Jurij Svete, University of Ljubljana, Slovenia
David Šarlah, University of Illinois at Urbana-Champaign, USA;
Università degli Studi di Pavia, Italy
Ivan Švancara, University of Pardubice, Czech Republic
Gašper Tavčar, Jožef Stefan Institute, Slovenia
Ennio Zangrando, University of Trieste, Italy
Polona Žnidaršič Plazl, University of Ljubljana, Slovenia

ADVISORY EDITORIAL BOARD

Chairman

Branko Stanovnik, Slovenia

Members

Udo A. Th. Brinkman, The Netherlands
Attilio Cesaro, Italy
Vida Hudnik, Slovenia
Venčeslav Kaučič, Slovenia

Željko Knez, Slovenia
Radovan Komel, Slovenia
Stane Pejovnik, Slovenia
Anton Perdih, Slovenia
Slavko Pečar, Slovenia
Andrej Petrič, Slovenia
Boris Pihlar, Slovenia
Milan Randić, Des Moines, USA

Jože Škerjanc, Slovenia
Đurđa Vasić-Rački, Croatia
Marjan Veber, Slovenia
Gorazd Vesnaver, Slovenia
Jure Zupan, Slovenia
Boris Žemva, Slovenia
Majda Žigon, Slovenia

Acta Chimica Slovenica is indexed in: *Academic Search Complete*, *Central & Eastern European Academic Source*, *Chemical Abstracts Plus*, *Chemical Engineering Collection (India)*, *Chemistry Citation Index Expanded*, *Current Contents (Physical, Chemical and Earth Sciences)*, *Digitalna knjižnica Slovenije (dLib.si)*, *DOAJ*, *ISI Alerting Services*, *PubMed*, *Science Citation Index Expanded*, *SciFinder (CAS)*, *Scopus* and *Web of Science*. Impact factor for 2021 is IF = 1.524.



Articles in this journal are published under the
Creative Commons Attribution 4.0 International License

Izdaja – Published by:

SLOVENSKO KEMIJSKO DRUŠTVO – SLOVENIAN CHEMICAL SOCIETY
Naslov redakcije in uprave – Address of the Editorial Board and Administration
Hajdrihova 19, SI-1000 Ljubljana, Slovenija
Tel.: (+386)-1-476-0252; Fax: (+386)-1-476-0300; E-mail: chem.soc@ki.si

Izdajanje sofinancirajo – Financially supported by:

National Institute of Chemistry, Ljubljana, Slovenia
Jožef Stefan Institute, Ljubljana, Slovenia
Faculty of Chemistry and Chemical Technology, University of Ljubljana, Slovenia
Faculty of Chemistry and Chemical Engineering, University of Maribor, Slovenia
University of Nova Gorica, Slovenia

Slovensko kemijsko društvo
Slovenian Chemical Society



Acta Chimica Slovenica izhaja štirikrat letno v elektronski obliki na spletni strani <http://acta.chem-soc.si>. V primeru posvečenih številk izhaja revija tudi v tiskani obliki v omejenem številu izvodov.

Acta Chimica Slovenica appears quarterly in electronic form on the web site <http://acta.chem-soc.si>. In case of dedicated issues, a limited number of printed copies are issued as well.

Transakcijski račun: 02053-0013322846 Bank Account No.: SI56020530013322846-Nova Ljubljanska banka d. d., Trg republike 2, SI-1520 Ljubljana, Slovenia, SWIFT Code: LJBA SI 2X

Oblikovanje ovitka – Design cover: KULT, oblikovalski studio, Simon KAJTNA, s. p. Grafična priprava za tisk: OSITO, Laura Jankovič, s.p.

Graphical Contents



Acta Chimica Slo Acta Chimica Slo Slovenica Acta C

Year 2023, Vol. 70, No. 2

REVIEW ARTICLE

173–183 Chemical, biochemical and environmental engineering

A Critical Review on Corrosion and Fouling of Water in Water Distribution Networks and Their Control

Andi Muhammad Anshar, Bulkis Musa, Muhammad Ayaz, Syahrudin Kasim, Indah Raya, Andrés Alexis Ramírez-Coronel, Shakhawat Chowdhury, Rahman S. Zabibah, Rosario Mireya Romero-Parra, Luis Andres Barboza-Arenas, Yasser Fakri Mustafa and Ali Hussein Demin Al-Khafaji

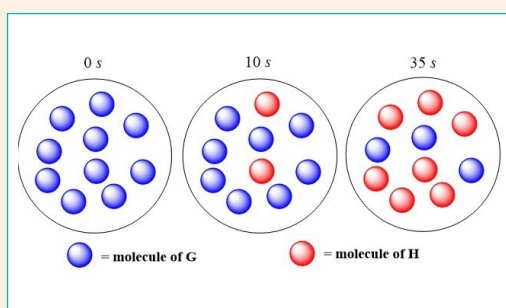


SCIENTIFIC PAPER

184–195 Chemical education

Uncovering Students' Genuine Misconceptions: Evidence to Inform the Teaching of Chemical Kinetics

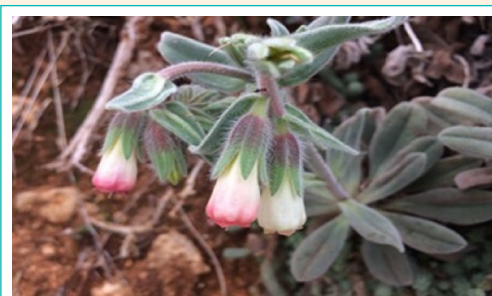
Habiddin Habiddin and Elizabeth Mary Page



196–203 Analytical chemistry

Potential Biochemical Properties of Endemic *Onosma mutabilis*

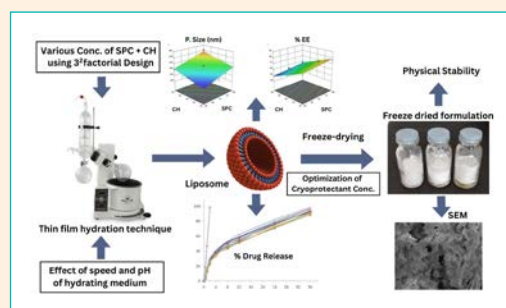
Pelin Eroglu, Mehmet Ulas Civaner, Selda Dogan Calhan, Mahmut Ulger and Riza Binzet



204–217 Biomedical applications

Design, Development and Optimization of Carmustine-Loaded Freeze-Dried Nanoliposomal Formulation Using 3² Factorial Design Approach

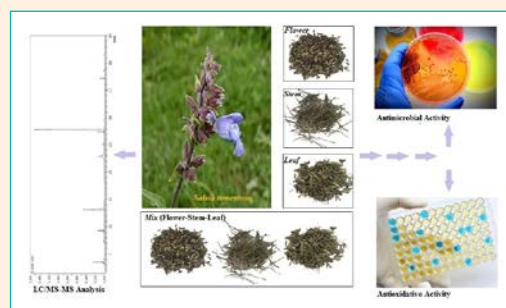
Sandip M. Honmane, Manoj S. Charde and Riyaz Ali M. Osmani



218–225 Biochemistry and molecular biology

Phytochemical Profile, Antioxidant and Antimicrobial Potency of Aerial Parts of *Salvia Tomentosa* Miller

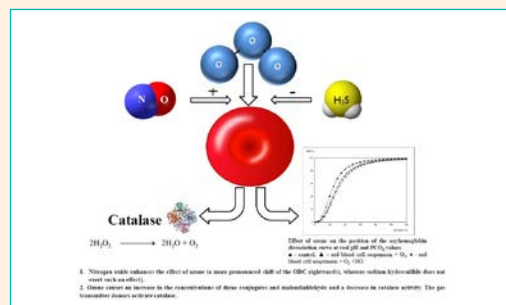
Şehnaz Balkır, Ömer Hazman, Laçine Aksoy, Mustafa Abdullah Yilmaz, Oguz Cakir, Recep Kara and İbrahim Erol



226–230 Biomedical applications

Effect of Ozone on Oxygen Transport and Pro-Oxidant-Antioxidant Balance of Red Blood Cell Suspension

Victor Zinchuk and Elena Biletskaya



231–239 Chemical, biochemical and environmental engineering

Chemical and Antioxidant Profile of Hydroalcoholic Extracts of *Stachys Officinalis* L., *Stachys Palustris* L., *Stachys Sylvatica* L. from Romania

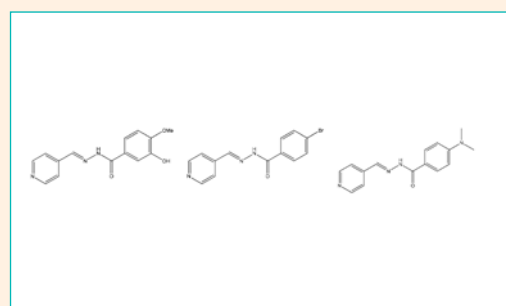
George Florian Apostolescu, Diana Ionela (Stegarus) Popescu, Oana Botoran, Daniela Sandru, Nicoleta Anca Şuţan and Johny Neamtu



240–246 Organic chemistry

Synthesis, Spectroscopic Characterization, Crystal Structures and Antibacterial Activity of Benzohydrazones Derived from 4-Pyridinecarboxaldehyde with Various Benzohydrazides

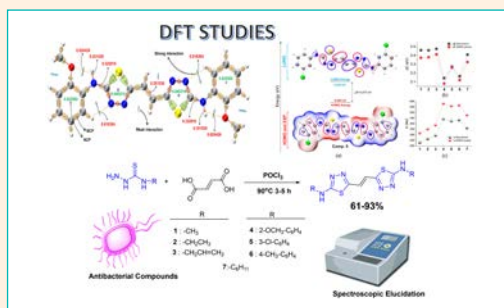
Yi-Xuan Zhou, Wei Li and Zhonglu You



247–260 Applied chemistry

New Bis-1,3,4-Thiadiazoles Based on Fumaric Acid: Preparation, Structure Elucidation, Antibacterial Activities, and Quantum-Chemical Studies

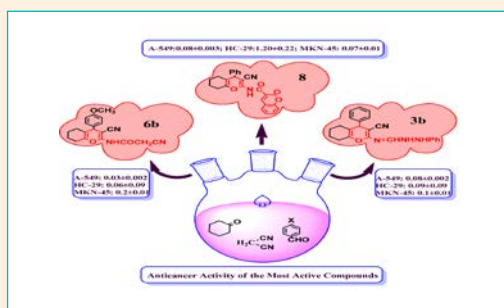
Halit Muğlu, Hasan Yakan, Ghaith Alabed Ibrayke Elefkhakry, Ergin Murat Altuner and M. Serdar Çavuş



261–273 Organic chemistry

Novel 5,6,7,8-tetrahydrobenzo[*b*]pyran Derivatives: Synthesis and Anticancer Activity

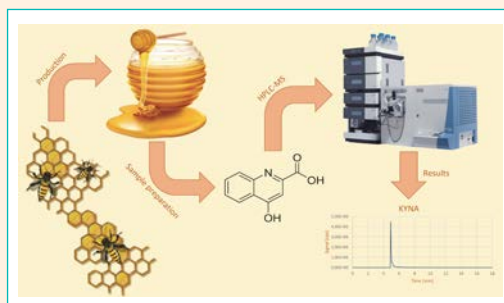
Amira E. M. Abdallah, Rafat M. Mohareb, Maher H. E. Helal and Mariam M. Abd Elkader



274–280 Analytical chemistry

Direct Determination of Kynurenic Acid with HPLC-MS/MS Method in Honey

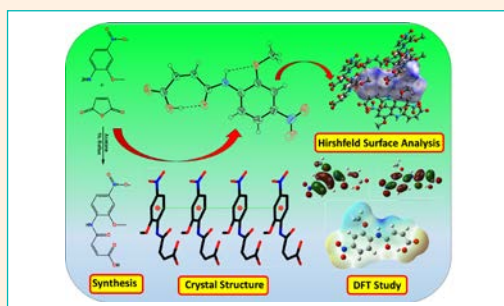
Anže Pavlin, Matevž Pompe and Drago Kočar



281–293 Organic chemistry

Synthesis, SC XRD Based Structure Elucidation, Supramolecular Assembly Exploration Via Hirshfeld Surface Analysis, Computational and QTAIM Study ...

Muhammad Nawaz Tahir, Muhammad Ashfaq, Akbar Ali, Chin Hung Lai, Bojja Rajeshwar Rao, Khurram Shahzad Munawar and Irshad Ali Shahid



Review article

A Critical Review on Corrosion and Fouling of Water in Water Distribution Networks and Their Control

Andi Muhammad Anshar¹, Bulkis Musa^{1*}, Muhammad Ayaz², Syahrudin Kasim¹, Indah Raya^{1*}, Andrés Alexis Ramírez-Coronel³, Shakhawat Chowdhury⁴, Rahman S. Zabibah⁵, Rosario Mireya Romero-Parra⁶, Luis Andres Barboza-Arenas⁷, Yasser Fakri Mustafa⁸ and Ali Hussein Demin Al-Khafaji⁹

¹ Department of Chemistry, Faculty of Mathematics and Natural Science, Hasanuddin University Makassar 90245, Indonesia

² Sensor Networks and Cellular Systems (SNCS) research center, University of Tabuk, Tabuk, Saudi Arabia

³ Research group in educational statistics, National University of Education (UNAE), Azogues, Ecuador

⁴ Department of Civil and Environmental Engineering, King Fahd University of Petroleum & Minerals, Dhahran, Saudi Arabia

⁵ Medical Laboratory Technology Department, College of Medical Technology, The Islamic University, Najaf, Iraq

⁶ Universidad Continental, Lima, Perú

⁷ Universidad Tecnológica del Perú. Lima, Perú

⁸ Department of Pharmaceutical Chemistry, College of Pharmacy, University of Mosul, Mosul-41001, Iraq

⁹ Department of Laboratories Techniques, Al-Mustaqbal University College, Babylon, Hillah, Iraq

* Corresponding author: E-mail: bulkismusa@unhas.ac.id & indahraya@unhas.ac.id

Received: 12-10-2022

Abstract

Corrosion and scaling are among the problems that may arise when storing water in tanks. Several factors affect the corrosion and scaling of water, which include pH, temperature, alkalinity, Ca²⁺ hardness, TDS, concentrations of Cl⁻, SO₄²⁻, CO₃²⁻, and HCO₃⁻. Also, several indices can be measured using these properties such as the Langelier saturation index, Ryznar index, Aggressive index, Larson, Scold index, water quality index, and Puckorius index. These indicators determine the degree of corrosiveness and sedimentation of water. The purpose of this review article was to study the impact of various factors on the corrosiveness and sedimentation of water. To this end, different sources of water in different countries were studied and the impact of physical and chemical parameters on their corrosiveness was investigated. Also, the reaction mechanism of water corrosion inside the pipe was studied. Finally, practical and constructive suggestions were presented to solve the problems of corrosion and sedimentation of desalination water.

Keywords: Corrosion, Fouling, Langelier Saturation Index, Ryznar Index, Inhibitors, Water

1. Introduction

Access to clean and unpolluted water resources is one of the basic human needs for a healthy and sustainable society.^{1,2} Development of industrial and agricultural activities have led to the spread of environmental pollution.³⁻⁶ The natural cycle of life on earth is menaced by the introduction of harmful chemicals. The water transmis-

sion and distribution network is responsible for storing and transporting water.⁷⁻¹⁰ One of the problems that may arise when storing water in tanks is the corrosiveness of the water, resulting in corrosion of facilities (eg, pipes, tanks, etc.). Corrosion of drinking water transmission equipment is a global problem.^{11,12} Corrosion is a physical-chemical reaction between a substance and its surroundings.¹³ Determining water corrosion indices is one

of the effective ways to manage drinking water resources. Corrosion of water can cause economic damage, reduce the useful life of water supply facilities, and illness in consumers.^{14–16} Corrosion in water distribution networks not only destroys equipment, but also reduces the quality of drinking water because of chemical and biological reactions that occur in the water distribution system. Corrosion processes in drinking water pipes depend on the type of pipes, water quality and hydraulic conditions. Qualitative parameters related to water corrosion include pH, alkalinity, degree of buffering, dissolved oxygen, natural organic matter, microorganisms, temperature, inhibitors if used, etc.^{17–20} Duroway et al. (2014) surveyed the impact of water pH on the corrosion of mild steel and realized that the corrosion rate decreases with enhancing pH from 7.2 to 11.2.²¹ Generally, pipe corrosion is prevented by controlling the chemical composition of water and using inhibitors. Due to its chemical properties, desalinated water is known as very corrosive water.^{22,23}

Sedimentation is another fundamental problem in water distribution systems.²⁴ A thin layer of scaling is useful because it can prevent corrosion on the metal surface. However, if the thickness of the deposit on the pipe surface increases, it can cause a lot of damage, including pressure drop, reduced water flow, and reduced heat transfer rate, which leads to an increase in the energy required for pumping. This action reduces thermal conductivity and increases energy consumption.^{25,26}

Generally, various factors affect water corrosion, including pH, CO₂ concentration, hardness, alkalinity, temperature, speed of water, TDS, dissolved oxygen, residual chlorine, fatigue, tension and other factors like cavitation.^{23,27} Prevention of equipment corrosion is usually done by controlling the chemical composition of water and using inhibitors. Inhibitors are chemicals that, when added in low concentrations to a corrosive environment, decline or prevent the reaction between metals and the environment. Vinyl acetate-methacrylic acid and vinyl acetate-acrylic acid have shown high antifouling efficiency at lower pHs and temperatures.²⁸ The corrosion of equipment increases with enhancing water pH. High concentration of sodium and chlorine in water increases the water conductivity, resulting in an increase in water corrosion. According to WHO standards for drinking water, the permissible limit of calcium and TDS is 75 mg/L and 500 mg/L, respectively. Also, the standard value of pH is between 7–8.5. Moreover, the permissible limit of CaCO₃ alkalinity should be between 30–500 mg/L based on WHO standard.²⁵

The Langelier index, along with the Ryznar and Puckorius indices, determines the corrosive or sedimentation status of water in the distribution network. The best case is when the water does not cause corrosion and deposits in the pipes of the water distribution network because both cases reduce the life of the pipes in the water transmission network and are costly. In distribution net-

work management, by measuring the Langelier, Ryznar and Puckorius indices, they try to prevent the corrosion or clogging of the pipes by improving the water quality, which is called water stabilization. Water instability occurs when water quality characteristics such as hardness, alkalinity, temperature, TDS and pH are not balanced.^{29,30} In general, physical, chemical and microbial factors are the three main causes of corrosion. Dissolved oxygen concentration, TDS, alkalinity, pH, CO₂ concentration and residual chlorine are chemical factors in corrosion. Also, temperature, fluid speed, and metal composition of pipes are physical factors³¹ and biological factors include 1) iron bacteria such as Gallionella and Chronotropic³² and 2) sulfate-reducing bacteria such as Desulfovibrio and De Sulfuric Ans.³³

Therefore, considering the problems and damages caused by corrosion and sedimentation in the water transmission and distribution system, it is necessary to reduce its effects by monitoring and controlling the factors affecting this phenomenon. The purpose of this review paper is to investigate various factors on corrosion and fouling in water distribution networks. To this end, the chemical and physical features of water were studied. Then, effective factors on corrosion and fouling were fully investigated. Also, the corrosiveness and sedimentation of water for various water distribution systems were fully studied by several indices such as Langelier, Ryznar, Larson-Scold, Aggressive, and Puckorius. Finally, practical suggestions were presented to improve or fix these problems.

2. Effective Factors on Corrosion and Scaling

Sedimentation in water pipes occurs when divalent metal ions or hardness factors in water are combined with other ions dissolved in water and deposited on the inner wall of the pipe. The main forms of sediments consist of calcium sulfate, magnesium carbonate, calcium carbonate, and magnesium chloride. Based on previous studies, more than 60% of corrosion in pipes and water transmission networks is due to chemical factors, and 40% is caused by biological parameters. The rate of fouling enhances with increasing temperature and salt concentration.³⁴ Sedimentation reduces the amount of water flow inside pipes, reduces heat transfer, increases pressure drop and energy required for pumping, clogs pipes and increases the cost of operation and maintenance of water supply facilities. The effective factors in the occurrence of deposits and clogging of pipes are a function of temperature, pH and concentration of dissolved solids.^{35,36} If the water is corrosive or sedimentary, it will cause many problems in the water transmission and distribution pipes and reduce the life of the facilities. The best pH value of water for preventing corrosion is 7. In fact, water with pH values below 6.5 or above 7.5 will be corrosive. Also, the corrosion rate triplicates

with enhancing temperature from 15.55 to 60 °C.³⁷ Moreover, the presence of some gases such as H₂S can enhance the corrosion of metals. Water containing magnesium or calcium salts (hard water) is less likely to cause corrosion because the minerals coat the inside of the pipe and protect them. Soft water containing sodium salts doesn't cover the pipe and is therefore more corrosive.^{25,27} Figure 1 illustrates various factors affecting the water corrosion and the appropriate amounts for preventing corrosion.

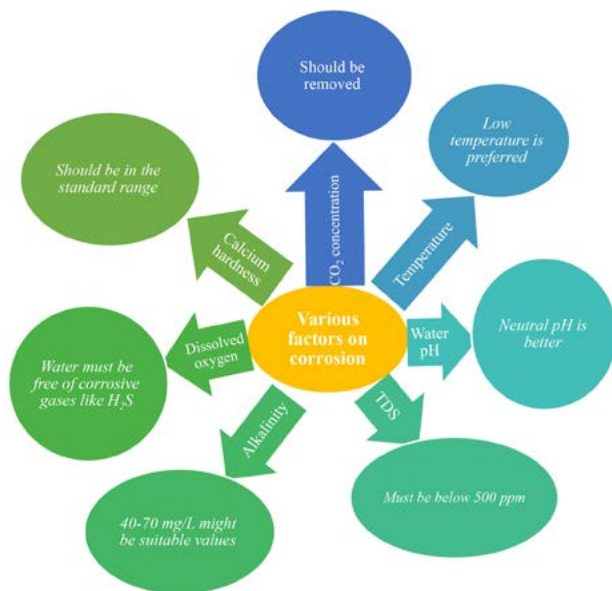


Figure 1. Effective factors and their conditions for preventing water corrosion and fouling

Corrosion is a physical-chemical reaction between a material and water, which changes the substance features. Excessive hardness of water causes corrosion and serious damage to facilities.³⁸ Stable water is water that does not cause corrosion in contact with metals and prevents sedimentation inside water pipes. Two important standards in the water supply network against corrosion are ISO1885 and EN12502.³⁹

Corrosiveness and scaling of water can be determined by Langelier, Ryznar, Aggressive, and Puckorius indices. The Langelier index indicates the state of water in terms of corrosiveness and sedimentation, which depends on various factors such as water acidity, TDS, carbonate concentration, bicarbonate concentration, water temperature and alkalinity. The following relationship is utilized to measure the Langelier saturation index (LSI):

$$LSI = pH - pH_s \quad (1)$$

Where, pH_s is the saturation pH. There are different ways to calculate pH_s . In the first method, the pH_s can be determined through Figure 2. As shown, pHs can be easily determined by having the water temperature, calcium ion

concentration and alkalinity by referring to the graph.³⁸

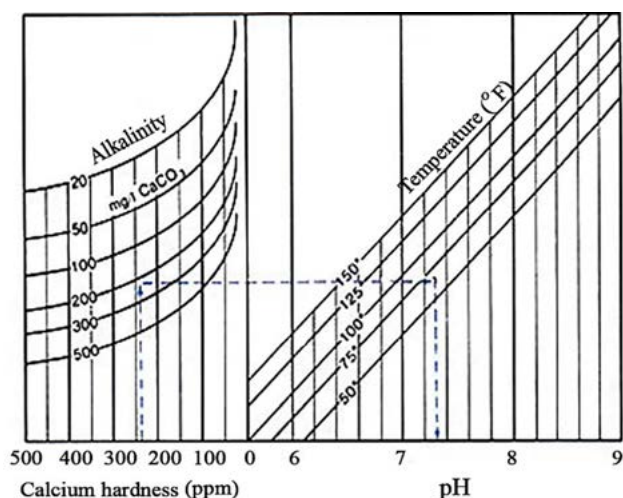


Figure 2. Determination of pHs in terms of Ca hardness, alkalinity, and pH parameters³⁸

In the second method, the following relationship is utilized to calculate pHs:

$$pH_s = (9.3 + A + B) - (C + D) \quad (2)$$

$$A = (\log_{10}^{[TDS]} - 1) / (10 * TDS) \quad (3)$$

$$B = -13.12 * \log_{10}^T - 34.55 \quad (4)$$

$$C = \log_{10}^{[Ca^{2+} \text{ as } CaCO_3]} - 0.5 \quad (5)$$

$$D = \log_{10}^{[Alkalinity \text{ as } CaCO_3]} \quad (6)$$

Where, TDS and T are in terms of mg/l, and kelvin, respectively. For LSI= 0, water is not corrosive or sedimentation. For LSI<0 and LSI>0, water tends to dissolve CaCO₃ and precipitate CaCO₃, respectively. When the index is negative, the water has corrosion potential.^{40,41} Table 1 presents the different modes of the Langelier index and based on that, the desired suggestions are presented to fix them.

Also, the Ryznar index is used as a basis for measuring sediment thickness in urban water supply systems in order to predict the chemical influence of water. The Ryznar stability index (RSI) can be employed to compute the corrosiveness and sedimentation potential of water. The RSI value can be determined using Equation 7. At RSI>7 and RSI<6, water will be corrosive and precipitator, respectively. Also, for RSI between 6–7, the water will be stable.⁴²

$$RSI = 2pH_s - pH \quad (7)$$

The table below presents the degrees of water sedimentation based on RSI values. As reported, an RSI value

Table 1. Different values of the Langelier index and desired suggestions

LSI value	Situation	Suggestion
-5	Intense corrosion	Needs purification
-4	Intense corrosion	Needs purification
-3	Moderate corrosion	Needs purification
-2	Moderate corrosion	Purification might be required
-1	Weak corrosion	Purification might be required
-0.5	Very weak corrosion	Maybe no need for purification
0	Stable	No need for purification
0.5	Weak sedimentation	Maybe no need for treatment
1	Gentle sedimentation	Purification might be required
2	Gentle to moderate sedimentation	Purification might be required
3	Moderate sedimentation	Purification is recommended
4	Intense sedimentation	Purification is recommended

between 6–7 is considered the best amount, so that water leads to little scale or corrosion. Also, Figure 3 indicates the RSI parameter in terms of temperature and pH. As shown, RSI at a certain amount of temperature declines with increasing pH. Also, at constant pH, the value of RSI decreases with enhancing temperature. Considering that the best value of RSI should be between 6 and 7, therefore water under high values of pH and temperature will form severe fouling. Also, water at very low pH and temperature will be corrosive.⁴³

Table 2. RSI values and their interpretations⁴²

RSI value	Case
4–5	Severe fouling
5–6	light fouling
6–7	Little fouling and corrosion
7–7.5	Moderate corrosion
7.5–9	Severe corrosion
>9	Unbearable corrosion

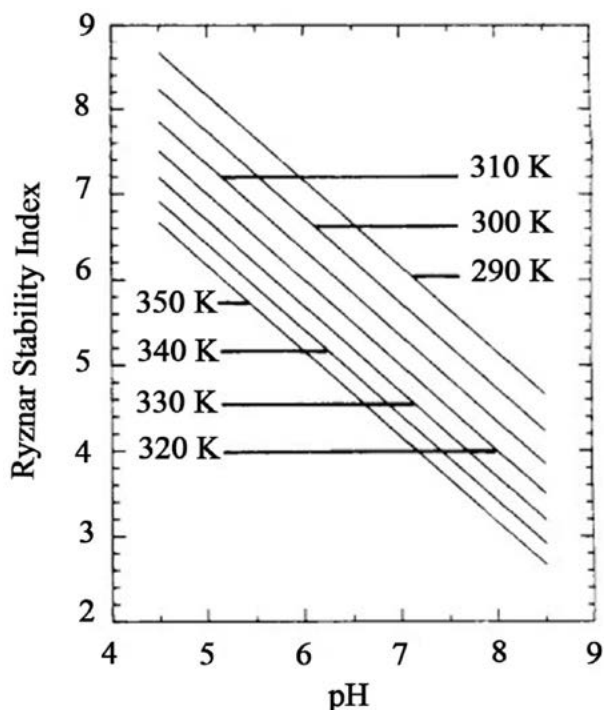
Moreover, the Puckorius index (PI) presents a relationship between scale formation and saturation state. High calcium concentration and low alkalinity of water result in a high level of calcite saturation. PI can be determined as follows:²⁴

$$PI = 2pH_s - pH_{eq} \quad (8)$$

where, pH_s and pH_{eq} are the water pH at saturation state, and the water pH at equilibrium state, respectively. pH_{eq} can be calculated as follows:

$$pH_{eq} = 1.465 * \log(\text{Alkalinity}) + 4.54 \quad (9)$$

where, alkalinity is in terms of mg/L. If $PI > 6$ and $PI < 6$, the water tends to corrode and sediment, respectively.

**Figure 3.** RSI versus pH and temperature⁴³

Furthermore, Larson-Scold index (LRI) is used to show the degree of water corrosiveness for the steel metal surface. LRI is determined through the following equation:

$$LRI = \frac{C(Cl^-) + C(SO_4^{2-})}{C(HCO_3^-) + C(CO_3^{2-})} \quad (10)$$

where, C is the concentration of each ion (m_{eq}/L). If $LRI < 0.8$, the water is not corrosive. Also, for $0.8 < LRI < 1.2$, the water is corrosive and for $LRI > 1.2$, the water will be very corrosive.⁴⁴

Finally, the Aggressive index (AI) is used to monitor corrosion in asbestos pipes and can be used as an indicator of water corrosion. This index is calculated using the actual water pH, calcium hardness, and total alkalinity. In addition, this index is simpler and easier than the Langelier index because it is not affected by temperature or TDS. The following relationship is utilized to calculate AI:

$$AI = [pH + \log(A + H)] \quad (11)$$

where, A and H are alkalinity and total hardness, respectively. If the AI index is equal to or greater than 12, the water will be non-corrosive. It is worth noting that for AI smaller than 10, water is highly corrosive and in values between 10 and 12, it will be moderately corrosive.

Water quality index (WQI) is another significant parameter for determining water quality. WQI indicates the combined impact of various water quality variables. To calculate WQI, each physicochemical factor is assigned a weight (w_i). The value of w_i depends on the impact of each

factor on health or its importance on the quality of water. Then, the relative weight (W_i) for n variables can be calculated as follows:

$$W_i = \frac{w_i}{\sum_{n=1}^n w_i} \quad (12)$$

Also, quality rating can be determined as follows:

$$q_i = \frac{C_i}{S_i} * 100 \quad (13)$$

Where, C_i and S_i are concentration of each chemical factor (mg/L) and the standard value for each factor except for pH (mg/L), respectively. Moreover, the sub-index of the i^{th} factor (SI_i) and WQI are calculated through Eqs. 14 and 15:³⁸

$$SI_i = q_i * W_i \quad WQI = \sum_{i=1}^n SI_i \quad (14)$$

Table 3 presents the water quality in various WQI amounts. As demonstrated, the WQI values below 100 are suitable for water quality.

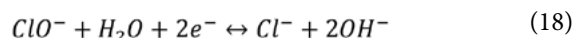
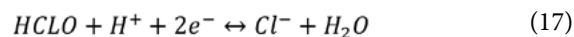
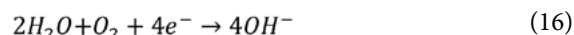
Table 3. WQI values for drinking water and their cases⁴⁵

WQI amount	Description
0–50	Great
50–100	Good
100–200	Poor
200–300	Very poor
>300	Improper

3. Reaction Mechanism

Iron is the most extensively used element in pipes in potable water distribution networks that are utilized to transport drinking water.^{46,47} It is estimated that iron-based pipes make up a large portion of the drinking water distribution system around the world. For example, 67.2% of water distribution pipes in Italy, 56.6% in the US, 75.5% in China, 93% in Innsbruck (Austria), and 91% in Warsaw (Poland) are made of iron.⁴⁷ Corrosion and fouling easily occur in pipes, which involve complex reactions between the pipe surface and the passing water. In the corrosion process in water, iron and oxidants act as anode and cathode (electron acceptor), respectively. Chlorine, dissolved oxygen, hypochlorite ions, and hypochlorous acid are the most common oxidants in water distribution systems.^{46–48} These oxidants can quickly react with zero-valent iron (Fe^0) inside the pipe's wall. Iron hydroxides (i.e., goethite, ferric hydroxide, maghemite) and iron oxides are the main corrosion products that can gently deposit on the pipe wall. The cumulation of corrosion on the pipes increases corrosion resistance and creates an obstacle between the

transferred water and the metal pipe, leading to a decrease in the rate of corrosion. The following reactions can be occurred:⁴⁷



The corrosion process may occur non-uniformly in different locations. Pit corrosion, galvanic, and crevice corrosion are common types of non-uniform corrosion. With the beginning of corrosion in a pipe, corrosion products are produced and accumulate on the pipe surface, which gradually lead to the formation of scales. Figure 4 shows the impact of various factors on the formation of corrosion on the pipe wall.

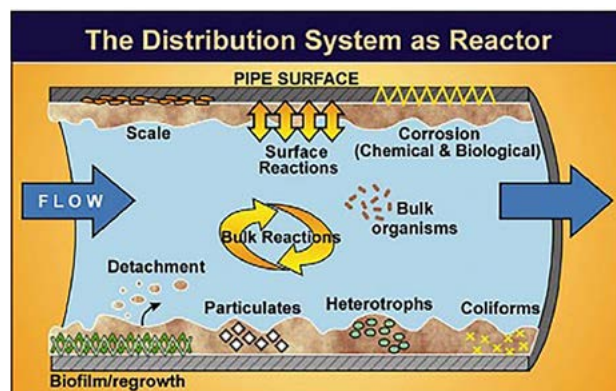


Figure 4. Different factors affecting the formation of corrosion on the pipe wall

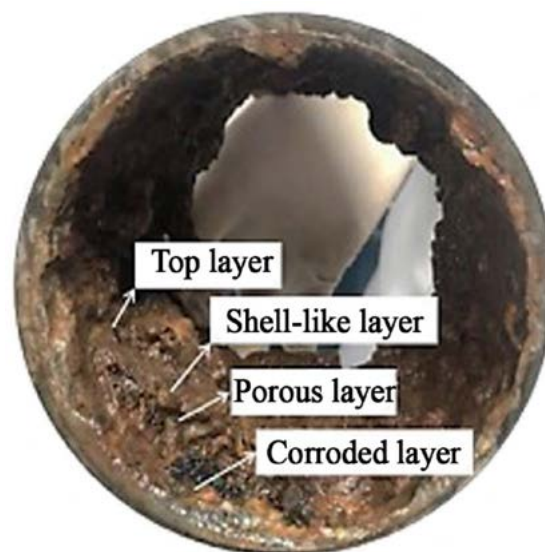


Figure 5. Schematic of corrosion and different layers inside the pipe

Also, the following figure illustrates different layers inside the pipe. As shown, there are 4 layers in iron pipes, which include corroded layer, porous layer, shell-like layer, and top layer. The corroded layer contains zero-valent iron. Also, the porous layer is composed of iron components like ferric hydroxide ($\text{Fe}(\text{OH})_3$), ferrous hydroxide ($\text{Fe}(\text{OH})_2$), goethite ($\alpha\text{-FeOOH}$), siderite, hematite (Fe_2O_3), and lepidocrocite ($\gamma\text{-FeOOH}$). Moreover, the shell-like layer contains the porous core and finally, the top layer is a heterogeneous layer containing silicates, carbonates, phosphates, goethite, iron hydroxide, and lepidocrocite. The corrosion composition depends on various variables like the quality of water, the operation time, and pipe material.⁴⁷

4. Previous Studies

Corrosion is a physical-chemical reaction between a material and its surrounding, which leads to changing the properties of that material. By attacking the inner wall of the pipe, the corrosive water dissolves the materials of the pipes and causes many problems. Economic losses, the formation of by-products, problems with taste, smell, color, staining and increasing turbidity are among the most important problems related to corrosiveness. Langelier, Ryznar, and Puckorius indices are important factors for determining the corrosiveness of water. Many studies have been done on the water's corrosiveness, which are reported in Table 4.

Hasani et al. (2021) suggested that pH, Cl^- concentration, dissolved oxygen, and sulfate should be continuously checked and controlled to prevent water corrosion.⁵⁰ Also, Bouderbala (2021) measured different properties of water such as pH, EC, Cl^- , TDS, COD, BOD, Na^+ , K^+ , Mg^{2+} , SO_4^{2-} , Ca^{2+} , HCO_3^- , NH_4^+ , NO_3^- , NO_2^- , and PO_4^{3-} to determine water quality for irrigation and industrial applications. The outcomes indicated that the WQI is in the range of 50–100, which shows the proper quality of water for irrigation.⁵¹ In other studies, other characteristics such as pH, water temperature, hardness, TDS, electrical conductivity, alkalinity, HCO_3^- , CO_3^{2-} , Ca^{2+} , Mg^{2+} , Na^+ , Cl^- , and SO_4^{2-} were calculated to determine the rate of corrosion and fouling.^{44, 52} In addition to these variables, García-Ávila et al. measured other factors such as sulfate, phosphate, and nitrite to predict and control corrosion.⁵⁵ Eslami et al. (2020) showed that the concentration of Cl^- and SO_4^{2-} has a greater effect on the corrosion and fouling potential of water than other parameters. They proposed that the water pH must be controlled to avoid water corrosion and scaling.⁵²

The morphology and composition of sediments are strongly related to the electrochemical features of water, and with the increase in corrosion and sedimen-

tation, the corrosion current density decreases continuously. By adding sodium hypochlorite disinfection to the groundwater, the water pH increases and results in the formation of calcium carbonate. Calcium carbonate strongly affects the corrosion potential.⁶² Also, controlling water quality before entering the water distribution network is an effective way to prevent corrosion and fouling.³⁶

Shahmohammadi et al. (2018) surveyed the corrosion and sedimentation potential of 46 water supply sources in Sarvabad County (Iran). The Langelier index in some water sources indicated that water tends to dissolve calcium carbonate and in other areas, water tends to form calcium carbonate scale. According to the Ryznar index, the tendency of water to corrode steel pipes increases. The Aggressive index (11.6) showed that the corrosion potential of water is moderate. The corrosion potential of water was also detected by the Puckorius index (7.03).⁵⁶ Therefore, several indicators simultaneously indicate the corrosiveness of water. Furthermore, Maeng et al. surveyed the corrosion potential of river water in Korea. The amount of LSI (−2.97), RSI (12.8), and AI (9.26) showed severe corrosiveness of river water. Also, their results indicated that pH and alkalinity reduce in the rainy season, while calcium hardness has little change throughout the year.⁵⁸ Davoudi et al. (2016) suggested that stabilization of water before entering the distribution network can prevent water corrosiveness.⁶³ According to the study done by Akter et al. in Bangladesh, the water quality index in some cities such as Kurigram Sadar and Rangabali was lower than 50, which indicates the water has excellent quality. However, some cities such as Anwara and Kamalganj had WQI values above 250, indicating very poor water quality. These results indicate that the WQI amount of water below 100 can be suitable for drinking.⁴⁵

Hoseinzadeh et al. (2013) studied the water corrosion and fouling in the water treatment network in Takab city during ten months. According to their results, the amount of LSI was 0.22, which indicates that the water was slightly scale-forming and corrosive. Also, the amount of RSI (7.6) showed that the water is corrosive. Moreover, the AI value (12.63) indicated that the water is non-aggressive. They suggested that corrosion and fouling can be controlled by adjusting the pH and temperature of the water.⁵⁹ Moreover, the LSI value in water sources of Tafila (Jordan) was in the range of −0.39 and −1.5, and the RSI value was in the range of 8.7 and 9.8, which indicates that the water is corrosive. Also, microbiological experiments indicated that three water samples were contaminated with faecal coliform bacteria.⁶¹

In general, it can be concluded that RSI, PI, AI, LSI, and WQI are critical indices for determining water corrosiveness and fouling, which have been widely utilized in previous researches.

Table 4. Characterization of different water sources, problems, and suggestions for solving their problems

City/Country	Effective factors	Description	Their suggestions	Ref.
Thanjavur/India	LSI = 0.13, AI = 12.09, RSI = 7.92, PI = 8.02, LRI = 1.08	Scaling and corrosiveness		30
Bangladesh	WQI for Sadar = 11.79 WQI for Rangabali = 40.05	Excellent quality of water	–	45
Bangladesh	WQI for Alfadanga = 169, WQI for Kendua = 142.5, WQI for Shajahanpur = 135.6, WQI for Debhata = 113, WQI for Bijoyagar = 111.8	Poor quality of water	–	45
Bangladesh	WQI for Rupsha = 92.14 WQI for Patharghata = 75.35	Good quality of water	–	45
Bangladesh	WQI for Anwara = 253.29 WQI for Kamalganj = 258.36	Very poor quality	–	45
Bangladesh	WQI for Shibchar = 371.5	Unsuitable for drinking	–	45
Juja/Kenya	WQI = 131–151	The water quality is very poor	–	49
Ardebil/Iran	LSI = -1.34 RSI = 10.03	Water is corrosive and has a high fouling capability	Water pH, Cl ⁻ , dissolved oxygen and sulfate should be monitored.	50
Oued Fodda dam/ Algeria	WQI = 50–100	Desirable suitable water quality	–	51
Oued Fodda dam/ Algeria	RSI > 7.5 from November to June	Heavy corrosion	–	51
Oued Fodda dam/ Algeria	RSI < 7.5 from July to October	Little corrosion and sedimentation	–	51
Kerman/Iran	LSI < 0, RSI > 7.5, PI > 6, and 10 < AI < 12	Water is corrosive	Controlling pH	52
Iranshahr/Iran	-1.53 < LSI < -0.96, 9.63 < RSI < 10.54, 9.05 < PI < 10.8, 12.04 < AI < 12.91	moderate corrosiveness	–	53
Rudsar/Iran In summer	LSI = -1.05, RSI = 10.04, LRI = 0.19, PI = 10.18, AI = 11.92	Corrosive	–	54
Amlash/Iran In winter	LSI = -1.31, RSI = 9.73, LRI = 0.24, PI = 9.74, AI = 11.5	Corrosive	–	54
Amlash/Iran In summer	LSI = -1.51, RSI = 10.71, LRI = 0.25, PI = 10.72, AI = 11.36	Corrosive	–	54
Rudsar/Iran In winter	LSI = -1.12, RSI = 9.69, LRI = 0.16, PI = 9.19, AI = 11.33	Corrosive	–	54
Azogues/Ecuador	RSI = 6.76, LSI = 0.5, LRI = 6.5	Slightly corrosive	–	55
Sarvabad/Iran	LSI = 0.23, RSI = 7.12, AI = 11.6, PI = 7.03	Moderate corrosion	–	56
Jolfa/Iran For 30 water wells	LSI = 1.15, RSI = 6.92, AI = 12.79, LRI = 0.85, PI = 6.42	Corrosive	–	57
Han, Geum, Nakdong, and Yeongsan in Korea	LSI = -2.97, RSI = 12.8, AI = 9.26	Strong corrosiveness	Controlling pH	58
Takab city/Iran	LSI = 0.22, RSI = 7.6, AI = 12.63	Slightly scale forming and corrosive, non-aggressive	pH and temperature Control	59
Tabriz/Iran In spring and summer	LSI = -0.68, PI = 7.86, AI = 11.23, RSI = 8.43	Corrosive	Adjusting pH	60
Tafila/Jordan	RSI = 8.7 – 9.8 LSI = -0.39 – -1.5	Corrosive	Evaporation of water	61

5. Suggestions for Preventing Corrosion and Fouling

To prevent water corrosion, the saturation index must be bigger than zero to ensure that not only corrosion doesn't take place, but also a thin layer of scale is formed. Therefore, maintaining LSI in the range of 0.6–1 is necessary to control corrosion. In practice, the best way to prevent corrosion is to create a uniform calcium carbonate deposit layer, but some factors that prevent this deposit from forming must be eliminated.^{64,65} Table 5 reports various suggestions to prevent water corrosion and fouling by previous researchers. Corrosion inhibitors are anti-corrosion chemicals. Sodium silicate prevents corrosion by forming a layer on the internal surfaces of metal pipes in the anodic region. Sodium silicate is an effective, economical, and environmentally friendly material that has been used for more than 70 years as a metal protector against the corrosive effects of water.^{66,67} One of the ways to prevent the formation of sediment is to identify the type of sediments in the pipes of the water transmission network. Another effective method to prevent water corrosion is to clean the pipes before installation. This will remove any debris and remarkably increase the life of the pipelines. Adding a cleaning agent to the plumbing will extend its life.^{68,69}

Also, adjusting the water pH or alkalinity can effectively prevent water corrosion in the water distribution network. Acid rain as well as minerals in the walls of the tanks can change the water's pH. Also, the addition of chemicals to water for preventing corrosion can change the pH.⁵⁸

Moreover, microbiological contamination can cause water corrosion. The addition of chlorine to water keeps the water safe and prevents corrosion, resulting in further problems in the municipal supply network. Chlorination in water treatment should be done by professionals be-

cause if it is done incorrectly, it can increase corrosion.^{70,71}

Phosphates can be also utilized to prevent water corrosion. These chemicals act as corrosion inhibitors and prevent the separation of metals from copper and lead pipes. By adding phosphates to the water source, a protective fouling layer is formed inside the pipes, which protects the pipelines from corrosion. The amount of phosphate added to the water source is very small in comparison to the adult diet.⁷² In one study, Karthiga et al. used henna leaf extract as an inhibitor to reduce the corrosiveness potential of soft steel in well water, and after adding 10 mL of henna leaf extract to water, the inhibition efficiency declined by 96%, which indicates the remarkable ability of the aforementioned substance.⁷⁹

Passivators are chemicals utilized to directly interact with minerals in water in the water refinement process. For instance, chlorine dioxide directly prevents manganese and iron to react with copper, lead, and steel pipes.⁷³ Chlorine dioxide, ultraviolet light, chlorine gas, ozone, and hypochlorite are some important passive inhibitors. Each passive inhibitor has advantages and disadvantages. Some of them are more environmentally friendly, but their prices are high. According to the Environmental Protection Agency, the highest concentration of chlorine dioxide and chlorite must be 0.8 and 0.1 mg/L, respectively. Others have corrosive effects on an extensive range of minerals but inhibit corrosion to a lesser extent. Others are very efficient but generate large amounts of waste.⁷⁴

Chemicals react with minerals in the water, while cathodic inhibitors interact with infrastructure piping.^{75,76} Cathodic inhibitors greatly decrease corrosion by creating a protective coating inside metal pipes, such as zinc or calcium. Zinc salts, silicates, calcium carbonate, and polyphosphates are important cathodic inhibitors for controlling water corrosion.^{77,78} In a research done by Lee et al. (2012), the influence of two important inhibitors (e.g., phosphate, silicate, and their mixtures) for controlling

Table 5. Different water sources, their problems, and solutions

Sample	Problem	Solution and result	Ref.
Green water problem and copper pipes	Corrosion	Using silicate inhibitor (10 mg/l) to control corrosion.	48
River water	Strong corrosiveness	Controlling pH in the standard range to prevent corrosion.	58
Water supply source	Corrosiveness and scaling	Adjusting pH is the best way to control corrosion.	60
Water	Corrosion	Microbiological contamination causes water corrosion, and adding chlorine to water prevents corrosion.	70
Copper pipes in household drinking water in Florida	Corrosion	The effect of adding phosphate to water indicated that phosphorus is more concentrated in the areas of corrosion attack and has a good effect on removing copper pipe corrosion.	72
Soft steel in well water	Corrosion	The inhibition efficiency declined by 96% by adding 10 mL of henna leaf extract.	79
Simulated cooling water	Scale	Adding 30 ppb of CaCO ₃ inhibitor for reducing sedimentation.	80
Mild steel in seawater	Corrosion	Adding <i>Azadirachta indica</i> L. extracts led to 98% inhibition efficiency.	81

copper pipe corrosion was investigated. Their results showed that silicate-based inhibitors were the most effective between them to control the pipe corrosion.⁴⁸

6. Conclusions and Practical Suggestions

6.1. Conclusions

Corrosion of water can cause economic damage, reduce the useful life of water supply facilities, and also reduce the quality of drinking water due to chemical and biological reactions and as a result, illness in consumers. Among the economic effects caused by fouling, we can also mention the reduction of water flow inside the pipes, which results in a pressure drop and an increase in the energy required for pumping. Therefore, the water quality must be controlled chemically or physically before entering the water distribution network. In this review article, the physicochemical properties of water such as pH, temperature, hardness, TDS, electrical conductivity, alkalinity, and concentration of HCO_3^- , CO_3^{2-} , Ca^{2+} , Mg^{2+} , Na^+ , Cl^- , and SO_4^{2-} for different water sources around the world were studied to determine the potential of corrosion and fouling. Various indices such as LSI, RSI, PI, AI, LRI, and WQI were also used to evaluate water quality. According to previous studies, LSI value close to zero, RSI between 6 and 7, PI value close to 6, LRI less than 0.8, and AI greater than 12 indicate that the water is not corrosive and does not form sediment. Also, a WQI value less than 100 demonstrates that the quality of water is good for drinking.

6.2. Practical suggestions

In previous studies, various practical suggestions have been presented to eliminate corrosion and water fouling. Accordingly, the adjustment of pH and temperature, the addition of anti-corrosion such as sodium silicate and phosphates, the addition of inhibitors such as chlorine dioxide, ultraviolet light, chlorine gas, ozone, hypochlorite, zinc salts, silicates, calcium carbonate, polyphosphates, and clean the pipes before installation are important ways for preventing corrosion and scaling.

Conflict of Interests Statement

There are no conflicts of interest to declare.

7. References

- R. R. Bhaviya, M. Umadevi, R. Parimaladevi. *Part. Sci. Technol.* **2020**, *38*, 812–820. DOI:10.1080/02726351.2019.1616863
- H. Liang, H. Esmaeili. *Environ. Technol. Innov.* **2021**, *22*, 101498. DOI:10.1016/j.eti.2021.101498
- Z. Wang, X. Liu, S. Q. Ni, X. Zhuang, T. Lee. *Water Res.* **2021**, *202*, 117491. DOI:10.1016/j.watres.2021.117491
- S. Tamjidi, B. K. Moghadas, H. Esmaeili, F. S. Khoo, G. Ghoulami, M. Ghasemi. *Process Saf. Environ. Prot.* **2021**, *148*, 775–795. DOI:10.1016/j.psep.2021.02.003
- Y. Wang, T. Sun, L. Tong, Y. Gao, H. Zhang, Y. Zhang, Z. Wang, S. Zhu. *J. Electroanal. Chem.* **2023**, *928*, 117062. DOI:10.1016/j.jelechem.2022.117062
- Z. Dai, Z. Ma, X. Zhang, J. Chen, R. Ershadnia, X. Luan, M. R. Soltanian. *J. Hydrol.* **2022**, *614*, 128541. DOI:10.1016/j.jhydrol.2022.128541
- A. N. Angelakis, J. B. Rose, eds., *IWA Publishing* **2014**. DOI:10.2166/9781780404851
- K. H. Sambodja, B. P. Samadikun, S. Syafrudin. *IOP Conf. Ser.: Earth Environ. Sci.* **2020**, *448*, 012049. DOI:10.1088/1755-1315/448/1/012049
- X. Peng, J. Zheng, Q. Liu, Q. Hu, X. Sun, J. Li, W. Liu, Z. Lin. *Sci. Total Environ.* **2021**, *791*, 148319. DOI:10.1016/j.scitotenv.2021.148319
- D. Ge, H. Yuan, J. Xiao, N. Zhu. *Sci. Total Environ.* **2019**, *679*, 298–306. DOI:10.1016/j.scitotenv.2019.05.060
- N. Tavanpour, M. Noshadi, N. Tavanpour. *Mod. Appl. Sci.* **2016**, *10*, 166–177. DOI:10.5539/mas.v10n3p166
- S. Sunardi, M. Ariyani, M. Agustian, S. Withaningsih, P. Parikesit, H. Juahir, A. Ismail, O. S. Abdoellah. *Sci. Rep.* **2020**, *10*, 11110. DOI:10.1038/s41598-020-68026-x
- M. Dehghani, F. Tex, Z. Zamanian. *Pak. J. Boil. Sci.* **2010**, *13*, 88–92. DOI:10.3923/pjbs.2010.88.92
- O. S. I. Fayomi, I. G. Akande, S. Odigie. *J. Phys. Conf. Ser.* **2019**, *1378*, 022037. DOI:10.1088/1742-6596/1378/2/022037
- D. Xu, J. Li, J. Liu, X. Qu, H. Ma. *Process Saf. Environ. Prot.* **2022**, *163*, 27–35. DOI:10.1016/j.psep.2022.05.018
- C. Geng, F. Zhao, H. Niu, J. Zhang, H. Dong, Z. Li, H. Chen. *J. Membr. Sci.* **2022**, *664*, 121099. DOI:10.1016/j.memsci.2022.121099
- F. García-Ávila, L. Ramos-Fernández, C. Zhindón-Arévalo. *Rev. Ambient. e Agua.* **2018**, *13*. DOI:10.4136/ambi-agua.2237
- M. M. Islam. A transient model for lead pipe corrosion in water supply systems. *University of Toronto (Canada)*. **2010**.
- Z. Liu, B. Fan, J. Zhao, B. Yang, X. Zheng. *Corros. Sci.* **2023**, *212*, 110957. DOI:10.1016/j.corsci.2022.110957
- J. Tan, L. Liu, F. Li, Z. Chen, G. Y. Chen, F. Fang, J. Guo, M. He, X. Zhou. *Environ. Sci. Technol.* **2022**, *56*, 14350–14360. DOI:10.1021/acs.est.2c01323
- S. I. Durowaye, A. G. F. Alabi, O. I., Sekunowo, B. Bolasodun, I. O. Rufai. *Int. J. Eng. Technol.* **2014**, *4*, 139–144.
- Z. Mi, X. Zhang, C. Chen. *Desalin. Water Treat.* **2016**, *57*, 9728–9735. DOI:10.1080/19443994.2015.1031706
- B. G. Hwang. *Journal of the Korea Academia-Industrial cooperation Society* **2010**, *11*, 2306–2310. DOI:10.5762/KAIS.2010.11.6.2306
- S. Ahmed, M. W. Sultan, M. Alam, A. Hussain, F. Qureshi, S. Khurshid. *J. King Saud Univ. Sci.* **2021**, *33*, 101237.

- DOI:10.1016/j.jksus.2020.101237
25. A. S. Alsaqqar, B. H. Khudair, S. K. Ali. *J. Water Resource Prot.* **2014**, 6, 1344. DOI:10.4236/jwarp.2014.614124
 26. F. B. Asghari, J. Jaafari, M. Yousefi, A. A. Mohammadi, R. Dehghanzadeh. *Hum. Ecol. Risk Assess.* **2018**, 24, 1138–1149. DOI:10.1080/10807039.2017.1407632
 27. R. E. Melchers. *Corros. Sci.* **2006**, 48, 4174–4201. DOI:10.1016/j.corsci.2006.04.012
 28. T. Y. Soror. *The open corrosion Journal* **2009**, 2, 45–50. DOI:10.2174/1876503300902010045
 29. H. C. Vasconcelos, B. M. Fernández-Pérez, S. González, R. M. Souto, J. J. Santana. *Water* **2015**, 7, 3515–3530. DOI:10.3390/w7073515
 30. P. J. Sajil Kumar. *SN Appl. Sci.* **2019**, 1, 1–13. DOI:10.1007/s42452-019-0423-6
 31. M. Mirzabeygi, M. Naji, N. Yousefi, M. Shams, H. Biglari, A. H. Mahvi. *Desalin. Water Treat.* **2016**, 57, 25918–25926. DOI:10.2166/wh.2014.157
 32. H. F. Ridgway, E. G. Means, B. H. Olson. *Appl. Environ. Microbiol.* **1981**, 41, 288–297. DOI:10.1128/aem.41.1.288-297.1981
 33. T. T. T. Tran, K. Kannoorpatti, A. Padovan, S. Thennadil. *R. Soc. Open Sci.* **2021**, 8, 200639. DOI:10.1098/rsos.200639
 34. A. Amouei, H. Asgharnia, H. Fallah, A. R. Yari, M. Mahmoudi. *Arch. Hyg. Sci.* **2017**, 6, 1–9. DOI:10.29252/ArchHygSci.6.1.1
 35. P. Dong, Y. Zhang, S. Zhu, Z. Nie, H. Ma, Q. Liu, J. Li. *Metals* **2022**, 12, 1160. DOI:10.3390/met12071160
 36. S. N. Kazi. Fouling and fouling mitigation on heat exchanger surfaces. In *Heat Exchangers-Basics Design Applications. Intechopen* **2012**. DOI:10.5772/32990
 37. M. L. McFarland, T. L. Provin, D. E. Boellstorff. Drinking water problems: Corrosion. *Texas A&M Agrilife Extension*, **2008**, 51130–19537.
 38. M. R., Uddin, M. M., Hossain, S. Akter, M. E. Ali, M. A. Ahsan. *Water Sci.* **2020**, 34, 164–180. DOI:10.1080/11104929.2020.1803662
 39. K. Pietrucha-Urbanik, D. Skowrońska, D. Papciak. *Coatings* **2020**, 10, 571. DOI:10.3390/coatings10060571
 40. K. M. Zia, R. NAWAZ, I. A. Bhatti, H. N., BHATTI. *J. Chem. Soc. Pak.* **2011**, 30, 182–185.
 41. K. Touati, M. Hila, K. Makhlof, H. Elfil. *Water Sci. Technol. Water Supply* **2017**, 17, 1682–1693. DOI:10.2166/ws.2017.067
 42. B. S. Shankar. *Sch. J. Eng. Tech.* **2014**, 2, 123–27.
 43. H. M. Müller-Steinhagen, C. A. Branch. *Can. J. Chem. Eng.* **1988**, 66, 1005–1007. DOI:10.1002/cjce.5450660617
 44. Z. P. Porsan, A. Zarei, M. Alimohammadi. *Desalin. Water Treat.* **2020**, 195, 19–25. DOI:10.5004/dwt.2020.25895
 45. T. Akter, F. T. Jhohura, F. Akter, T. R. Chowdhury, S. K. Mistry, D. Dey, M. K. Barua, M. A. Islam, M. Rahman. *J. Health Popul. Nutr.* **2016**, 35, 1–12. DOI:10.1186/s41043-016-0041-5
 46. E. Veschetti, L. Achene, E. Ferretti, L. Lucentini, G. Citti, M. Ottaviani. *Toxicol. Environ. Chem.* **2010**, 92, 521–535. DOI:10.1080/02772240903036139
 47. H. Zhang, D. Liu, L. Zhao, J. Wang, S. Xie, S. Liu, P. Lin, X. Zhang, C. Chen. *J. Environ. Sci.* **2022**, 117, 173–189. DOI:10.1016/j.jes.2022.04.024
 48. J. E. Lee, H. D. Lee, G. E. Kim. *Environ. Eng. Res.* **2012**, 17, 17–25. DOI:10.4491/eer.2012.17.1.017
 49. G. M. P. Baloitcha, A. O. Mayabi, P. G. Home. *Heliyon* **2022**, 8, 09141. DOI:10.1016/j.heliyon.2022.e09141
 50. K. Hasani, H. Sadeghi, A. Dargahi, M. Vosoughi, A. Mokhtari, M. Pirasteh. *J. Adv. Environ. Health Res.* **2021**, 9, 201–208. DOI:10.32598/JAEHR.9.3.1210
 51. A. Bouderbala. *Environ. Dev. Sustain.* **2021**, 23, 13340–13363. DOI:10.1007/s10668-020-01215-w
 52. F. Eslami, M. Salari, N. Yousefi, A. H. Mahvi. *Desalin. Water Treat.* **2020**, 179, 19–27. DOI:10.5004/dwt.2020.24999
 53. M. Taghavi, M. H. Mohammadi, M. Radfard, Y. Fakhri, S. Javan. *MethodsX* **2019**, 6, 278–283. DOI:10.1016/j.mex.2019.02.002
 54. J. Alimoradi, D. Naghipour, H. Kamani, G. Asgari, M. Naimi-Joubani, S. D. Ashrafi. *Data Brief* **2018**, 17, 105–118. DOI:10.1016/j.dib.2017.12.057
 55. F. García-Ávila, L. Ramos-Fernández, P. Damián, D. Quezad. *Data Brief* **2018**, 18, 111–123. DOI:10.1016/j.dib.2018.03.007
 56. S. Shahmohammadi, A. Noori, S. Karami, A. Amini, B. Shahmoradi, S. Sobhan Ardakani, S. M. Lee, R. Pawar. *J. Adv. Environ. Health Res.* **2018**, 6, 52–60. DOI:10.22102/jaehr.2018.98342.1037.
 57. M. Yousefi, H. N. Saleh, A. H. Mahvi, M. Alimohammadi, R. Nabizadeh, A. A. Mohammadi. *Data Brief* **2018**, 16, 724–731. DOI:10.1016/j.dib.2017.11.099
 58. M. Maeng, I. Hyun, S. Choi, S. Dockko. *Desalin. Water Treat.* **2015**, 54, 1233–1241. DOI:10.1080/19443994.2014.917991
 59. E. Hoseinzadeh, A. Yusefzadeh, N. Rahimi, H. Khorsandi. *Arch. Hyg. Sci.* **2013**, 2, 41–47.
 60. H. Taghipour, M. Shakerkhatibi, M. Pourakbar, M. Belvasi. *Health Promot. Perspect.* **2012**, 2, 103–111. DOI:10.5681/hpp.2012.013.
 61. A. E. Al-Rawajfeh, E. M. Al-Shamaileh. *Desalination* **2007**, 206, 322–332. DOI:10.1016/j.desal.2006.01.039
 62. H. Zhang, L. Zhao, D. Liu, J. Wang, X. Zhang, C. Chen. *Water Res.* **2020**, 176, 115742. DOI:10.1016/j.watres.2020.115742
 63. M. Davoudi, A. Skandari Torbaghan, M. Sarmadi, J. Salimi, D. Tahan, H. Shirzad. *Journal of Torbat Heydariyeh University of Medical Sciences* **2016**, 4, 4–13.
 64. B. Y. Wu, S. H. Chan. *J. Heat Transfer* **2003**, 125, 147–150. DOI:10.1115/1.1518493
 65. Health Canada. Guidance on controlling corrosion in drinking water distribution systems. **2009**.
 66. Y. Chen, W. Yang. *Water Chemistry* **2019**, 1–22. DOI:10.5772/intechopen.88533
 67. N. Asrar, A. U. Malik, S. Ahmed. *Tech. Rep.* **1998**, 1856–1885.
 68. H. Fossberg, U. Rydningen, C. Merschbrock. *WIT Transactions on Ecology and the Environment* **2017**, 216, 113–122. DOI:10.2495/WS170101
 69. A. C. Hieatt, J. H. Ludwig. Method of cleaning and maintaining water distribution pipe systems. *U.S. Patent* **1994**, 5, 360, 488.

70. P. Bajpai. *Pulp and Paper Industry* **2015**, 103–195.
DOI:10.1016/B978-0-12-803409-5.00008-2
71. R. M. Clark, M. Sivaganesan. Characterizing the effect of chlorine and chloramines on the formation of biofilm in a simulated drinking water distribution system. National Risk Management Research Laboratory, Office of Research and Development, *US Environmental Protection Agency*. **1999**.
72. D. A. Lytle, C. P. White. *J Fail. Anal. and Preven.* **2014**, 14, 203–219. DOI:10.1007/s11668-014-9786-6
73. A. Cantor, P. Jae, K. Park, P. Vaiyavatjamai. The effect of chlorine on corrosion in drinking water systems in chlorine's effect on corrosion in drinking water system. Midwest Technology Assistance Center, Urbana-Champaign, University of Illinois, USA. **2000**.
74. Z. Zhang. Use of chlorine dioxide for Legionella control in hospital water systems, *Doctoral dissertation, University of Pittsburgh*. **2007**. DOI:10.2175/193864707787932423
75. N. Cheng, J. Cheng, B. Valdez, M. Schorr, J. M. Bastidas. *Master Perform.* **2016**, 55, 48–51.
DOI:10.29322/IJSRP.8.5.2018.p7770
76. B. Bai, F. Bai, C. Sun, Q. Nie, S. Sun. *Front. Earth Sci.* **2023**, 10, 1071228. DOI:10.3389/feart.2022.1071228
77. O. Sanni, A. P. Popoola. Gluconates as Corrosion Inhibitor of Aluminum in Various Corrosive Media. *IntechOpen*. **2017**. DOI:10.5772/intechopen.71467
78. M. A. A. Ali. Inhibition of mild steel corrosion in cooling systems by low-and non-toxic corrosion inhibitors. *Doctoral dissertation, The University of Manchester (United Kingdom)*, **2017**.
79. N. Karthiga, P. Prabhakar, S. Rajendren. Inhibition of corrosion of mild steel in well water by an aqueous extract of Lawsonia inermis leaves. *Int. J. Res. Anal. Rev.* **2019**, 6, 437–444.
80. D. Liu. Research on performance evaluation and anti-scaling mechanism of green scale inhibitors by static and dynamic methods. Environmental Engineering. *Ecole Nationale Supérieure d'Arts et Metiers*. **2011**.
81. M. A. Asaad, M. Ismail, N. H. A. Khalid, G. F. Huseien, P. B. Raja. *J. Teknol.* **2018**, 80, 53–59.
DOI:10.17675/2305-6894-2019-8-3-1

Povzetek

Pri shranjevanju vode v rezervoarjih se lahko pojavijo težave, med katerimi sta najpogostejši korozija in nastajanje vodnega kamna. Na procese korozije in nabiranja vodnega kamna vpliva več dejavnikov, kot so pH, temperatura, alkalnost, trdota Ca^{2+} , TDS, ter koncentracije Cl^- , SO_4^{2-} , CO_3^{2-} in HCO_3^- . Z uporabo teh parametrov je mogoče izmeriti različne indekse, med katerimi so Langelierjev indeks nasičenosti, Ryznarjev indeks, Agresivni indeks, Larsonov indeks, Scoldov indeks, indeks kakovosti vode in Puckoriusov indeks. Ti indikatorji nam omogočajo določiti stopnjo korozivnosti in sedimentacije vode, kar je tudi namen tega preglednega članka. Proučevani so bili različni vodni viri v različnih državah, raziskano je bilo, kako fizikalni in kemijski parametri vplivajo na jedkost vode. Prav tako so bili preučeni reakcijski mehanizmi vodne korozije znotraj cevi. Na koncu so predstavljeni praktični in konstruktivni predlogi za reševanje problemov korozije in sedimentacije razsoljene vode.



Except when otherwise noted, articles in this journal are published under the terms and conditions of the Creative Commons Attribution 4.0 International License

Scientific paper

Uncovering Students' Genuine Misconceptions: Evidence to Inform the Teaching of Chemical Kinetics

Habiddin Habiddin^{1,3*} and Elizabeth Mary Page²¹ *Department of Chemistry, Universitas Negeri Malang, Jalan Semarang No. 5 Malang, East Java 65145 Indonesia*² *Department of Chemistry, University of Reading, Whiteknights PO Box 217 Reading Berkshire RG66AH United Kingdom*³ *Department of Science Education, Universitas Negeri Malang, Jalan Semarang No. 5 Malang, East Java 65145 Indonesia** *Corresponding author: E-mail: habiddin_wuni@um.ac.id**Received: 11-13-2022*

Abstract

The aim of this study is to investigate first-year university students' misconceptions in chemical kinetics by analysing data obtained from the four-tier diagnostic instrument of chemical kinetics (FTDICK). 335 first-year chemistry students from two Indonesian and one UK universities participated in this study. The procedure described here is the first of its type to ensure those misconceptions are genuine. Numerous genuine misconceptions within chemical kinetics were revealed among first-year chemistry undergraduates. Although many of the misconceptions found here concur with those results previously published using other instruments, some novel findings were uncovered. These misconceptions can be attributed to a variety of factors including mathematical weakness, carelessness and difficulty in interpreting and extracting information from diagrams, graphs and other non-textual information. On the basis of the results from this study we make some recommendations for improving the effectiveness of chemical kinetics' teaching at this level.

Keywords: Four-Tier Instrument, Teaching Chemistry, Students' Confident Rating, Spurious Misconception

1. Introduction

Chemical kinetics is an essential area of the chemistry curriculum at both secondary and tertiary levels. In some secondary school curricula of some countries, the terminology of reaction rate is preferable. The topic has been of concern to chemical education researchers over the last decade who have long recognised the difficulties students encounter with some concepts. The topic of chemical kinetics has links to many other areas of the chemistry curriculum. It relates to thermodynamics, equilibria, particle theory and aspects of both inorganic and organic chemistry mechanisms.¹ Its applications in industrial processes including the pharmaceutical, agricultural, food and manufacturing industries, the environment and the atmosphere make it a topic whose understanding is of paramount importance to the majority of graduates of science and life sciences degree programmes. Understanding how to measure and control a reaction rate is fundamental to many of these industries and to academic research in a range of disparate disciplines. This

understanding is predicated on an appreciation of the particle nature of matter, kinetic molecular theory, the dynamic aspects of chemical reactions including collision theory and transition-state theory,¹⁻³ all of which are required for success in mastering chemical kinetics. For these reasons a thorough understanding of the concepts is imperative for a whole range of students and educators.

1. 1. A Review of the Literature on Educational Studies in Chemical Kinetics

One recent publication contains an excellent review of research on the teaching and learning of chemical kinetics⁴ and provides a useful summary of student and teacher approaches to the subject. Bain and Towns reviewed a total of 34 publications in English focussing on both secondary and tertiary education. It was a requirement of the studies reviewed that they used instruments such as diagnostic tests and presented data and analyses to answer a proposed research question.

The majority of publications in the chemistry education literature focus on the ideas and concepts students of chemical kinetics develop that do not align with those of the scientific community.² Understanding of the meaning of reaction rate is key to progression in the subject. Confusion over reaction rate and reaction time has been observed.^{5–7} Several studies report the misconception that reaction rate depends upon the stoichiometry of the reaction.^{5,8} Elementary studies in the subject may result in the assumption that reaction rate is always dependent upon reactant concentration.⁹ A widely held misconception revealed in several studies is that an increase in reactant concentration always results in an increase in reaction rate^{5,10–12} including in zero-order reactions.³ Students have been shown to have varying ideas of how rate changes during a chemical reaction. Some report that rate increases to a maximum and then remains constant for a time before decreasing to zero.^{5,6} Others report that rate decreases to a minimum value then remains constant⁹ or that it increases or decreases as reaction proceeds.^{3,5,8,13} Another misconception is that rate is a constant for any order of reaction.^{5,8,9}

The concept of reaction order is one that provokes the most misconceptions. Probably one of the most common misconceptions is that the rate law can be derived from the stoichiometric equation for the chemical reaction.^{5,11,14,15} Other common misconceptions include the belief that increasing the concentration of a reactant always increases the rate^{10,12,15} with a linear relationship between concentration and reaction rate,⁵ and that a change in concentration of a reactant that is zero-order affects the reaction rate.³

Bain & Towns⁴ concluded that more research is needed into the area of teaching and learning in chemical kinetics at the undergraduate level. Although undergraduate students have similar misconceptions to secondary school students in certain concepts,⁵ there are far fewer reports in the literature at the tertiary level. Interestingly, Kolomuc & Tekin⁹ found that some chemistry teachers hold similar misconceptions to grade 11 school students, for example regarding the effect of a catalyst on reaction rate.

There are a number of reasons as listed below and given in the review of Bain and Towns, that demonstrate that a study of student understanding of chemical kinetics at the tertiary level is timely:⁴ the subject is fundamental to many aspects of the chemistry curriculum and has many real-life applications; the subject is perceived as complex and is not well understood and, in some cases, suffers from confused teaching; there are few studies at the undergraduate level that focus solely on the understanding of chemical kinetics; many of the published studies involve pre-degree level students from a single nation (Turkey). Clearly the predominance of findings from a single nation on a subject studied globally could significantly impact upon the overall conclusions.

A variety of tools have been used for exploring student understanding of chemical kinetics and these are cat-

egorised in Bain & Towns's paper.⁴ The format of the tools varies from open-ended and multiple-choice questions through to multi-tier instruments. More recently multiple-tier diagnostic tests have become more widely used in science education research. The first type of such an instrument was developed by Treagust who used a two-tier instrument consisting of an initial tier of multiple-choice questions with one correct answer and a number of distractors followed by a second tier that probes the reason for the selected answer.¹⁶ Although the two-tier instrument is useful in probing student misconceptions and reasoning it is not ideal. If a student is uncertain of the correct answer or how to approach the problem they may select their reason randomly, often selecting the statement of fact with which they are most familiar. This does not mean that they believe their choice of reason is the correct one, just that they believe the reason chosen is a correct scientific statement. A two-tier instrument cannot distinguish between a firmly held reason and a guess or educated guess.¹⁷ To overcome this, three and four-tier instruments have been deployed. Such instruments require respondents to give confidence ratings for their answers and reasons. In a three-tier instrument a mean confidence rating is requested for the answer and reason whereas in a four-tier instrument a separate confidence rating is given for each.

Clearly the four-tier instrument is more useful than the three-tier one. A combined confidence rating leaves uncertainty in the results as to whether the respondent has a certain confidence level in their question, their reason or both. This leads to difficulty in categorising and grading the responses.¹⁸ When a confidence level is attached to both the answer and the reason a greater certainty about understanding and guess work can be achieved.¹⁹ A student with a good understanding of how to solve the problem and why it is correct should display a high confidence level in both tiers. A student with a low confidence in their answer – whether correct or otherwise – and a high confidence in their reason may well have understood and remembered the theory but not how to apply it correctly. The same condition may stand for a student with a low confidence in a correct answer and a low confidence in their incorrect reason. In addition, careful choice of answer and reason distractors on the part of the researcher can provide valuable information on student understanding. The value of a calculated mean confidence rating of both answer and reason should not be understated as it can be useful in providing an overall indication of student understanding of the theory addressed in the question, especially with the additional information relating to confidence in the two tiers.

1. 2. A Comment on the use of Four-Tier Instruments in Classifying Students' Misconceptions

The procedure for assigning students' misconceptions in these previous studies is not fully robust. For ex-

ample, previous literature reporting the use of four-tier instruments^{19–22} applied 6 ratings of confidence, namely: 1 (guess work), 2 (very unconfident), 3 (unconfident), 4 (confident), 5 (very confident) and 6 (absolutely confident). The authors used an average of the confidence rating of the answer tier and the reason tier to determine the overall confidence in the concept investigated with the mid-point value of the scale (3.5) used as the upper limit of a *genuine* misconception. For example, of confidence rating of 6.00 (absolutely confident) in the answer tier and 2.00 (very unconfident) in the reason tier would result in an overall confidence rating of 4.00, suggesting there was no issue in the understanding of this concept despite the fact that responses displayed an element of poor confidence.

In addition, in some studies, students' responses were binary (i.e. sure or unsure) which is also unsatisfactory as it gives students little opportunity to express their degree of confidence in the topic.^{23,24} However, the procedure in justifying students' misconception in those studies might produce a misjudgment in terms of attributing a lack of knowledge or other random errors to be a misconception. For example, the previous literature in the area of four-tier instrument^{19–22} applied 6 ratings of confidence. Literature using this scale (1–6) consider 3.5, i.e. the mid-point of unconfident and confidence, as the limit of a *genuine* misconception.

Employing a confidence rating average between the confidence of answer tier and reason tier to justify a misconception applied in those previous studies in the area may raise a bias and misjudgement. For example, a confidence index of 4.00 could result from absolutely confident (6.00) for A tier and very unconfident (2.00) for R tier and vice versa. Therefore, this limits sound flaw because the point still contains the unconfident element. For this reason, in our study, we avoided employing a confidence average instead of using the confidence for the two tiers as the genuine parameter. In addition, only responses with confidence ratings for both answer and reason tiers of ≥ 3.00 are incorporated in determining students' misconceptions. In other studies,^{23,24} students' confidence ratings are applied in two expressions (sure or not sure). Such this procedure cause inflexibility of students to express the degree of their certainty or confidence rating. The misconceptions identified in this study can be relayed to university authorities, particularly in Indonesia, and deployed in updating the chemistry curriculum for first-year students. Linking information from students' work to curriculum revision is a productive strategy for informing and underpinning science teaching and educational development.²⁵

1. 3. Purposes of the Study and Research Questions

In an extensive review of Chemistry Education Research (CER) Cooper & Stowe²⁶ highlighted three impor-

tant aspects of educational research: the knowledge students should master in a topic and how they apply the knowledge; ensuring students have hold robust scientific concepts; supporting students in their learning based on the evidence of their knowledge. Although they did not outline a single strategy to ensure students' scientific understanding, employing a proper assessment procedure is a powerful tool for understanding the nature of students' knowledge framework, including their misconceptions and prior knowledge. We believe that the FTDICK instrument is a powerful tool that can be used to uncover the students' actual misconceptions and allows these misconceptions to be used as evidence in developing good teaching practices in chemical kinetics. Therefore, this study aims to investigate first-year university students' misconceptions of chemical kinetics by analysing data obtained from a four-tier diagnostic instrument. The goal is to use the findings of the study to enhance the teaching of chemical kinetics, especially at the university level, and to improve student understanding.

2. Method

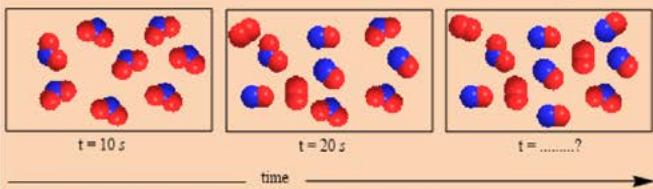
2. 1. Participants

This study involved 83 first-year chemistry students at the University of Reading, UK and 252 students at two Indonesian universities. The study was carried out during the second semester of the first year at each institution. As explained in the previous paper,²⁷ all multiple choice questions were presented and answered in English. The data collection had carried out before students embarked to the chemical kinetics topic in their basic chemistry modules. This is to ensure that all respondents hold an equal prior chemical kinetics class experience.

2. 2. Development of the FTDICK Instrument

The detailed description of the development and validation of the instrument (FTDICK) was described comprehensively in previous paper.²⁷ The validity and reliability of the instrument has been measured and found to be valid and reliable for data collection. All the questions were valid with a confidence level of 95%. The Cronbach Alpha reliability of the instrument was considered acceptable. The final FTDICK consists of 20 four-tier multiple-choice questions with associated reason choices and was used to investigate first-year students' understanding of chemical kinetics (Appendix 1). As highlighted in the previous paper the FTDICK consists of an answer tier (A tier) and a reason tier (R tier), each with a confidence rating attached. The confidence ratings were scaled from 1 (very unconfident) to 5 (very confident). An example of a four-tier question in the FTDICK instrument is depicted in Figure 1.

The decomposition of nitrogen dioxide to nitric oxide and oxygen at a certain temperature is shown pictorially below and is a second order reaction and the equation for the reaction is: $2\text{NO}_2(\text{g}) \rightarrow 2\text{NO}(\text{g}) + \text{O}_2(\text{g})$



The time at the final representation shown above is...

A. 25 s B. 30 s C. 40 s D. 50 s

A Tier

State the confidence rating of your answer

1. Very unconfident 2. Not very confident 3. Average 4. Quite confident 5. Very confident

CR of A Tier

Which one of the following options is the reason for your answer to the question?

A. The value of each successive half-life is half the preceding one

B. The value of $t_{1/2}$ is constant

C. The rate of disappearance of this sample increases with decrease in concentration

D. The value of each successive half-life is twice the preceding one.

R Tier

State the confidence rating of your answer

1. Very unconfident 2. Not very confident 3. Average 4. Quite confident 5. Very confident

CR of R Tier

Figure 1. Example of a four-tier question in the FTDICK instrument

Figure 1 displays each tier of the question in a different colour in order to make the tiers more readily identifiable. The first tier consists of a multiple-choice question with one correct answer and three distractors (incorrect answers). The following tier is the confidence rating (CR) for the A tier named CR(TA). The third tier is the R tier and consists of one correct scientific reason and three incorrect and/or unscientific reasons. The fourth tier is the CR for the R tier and is named CR(TR).

2. 3. Research Design and Data Analysis (Grading Schemes)

This descriptive study describes the first-year chemistry students' understanding of chemical kinetics using the FTDICK instrument. The time allocated for students to work on the questions was 120 minutes. Their answers to the FTDICK instrument were the basis for classifying their understanding of the topic. There are four types of combinations of students' answers and reasons, namely: Correct answer and correct reason (CACR) representing good scientific understanding; Correct answer and wrong reason (CAWR) representing a false positive of students' understanding; Wrong answer and correct reason

(WACR). This represents a false negative of students' understanding. These categories are not discussed widely in this paper. The wrong answer and wrong reason (WAWR) represents an actual student misconception. We focussed only on WAWR combinations in order to ensure all the misconceptions reported are genuine. The confidence ratings of these schemes are assigned as follows: Option A in Question 1 has a CR(TA) = 4.0 meaning the confidence rating average of all students selecting option A as their answer in the A tier in Question 1 is 4.0. The same procedure is also applied for CR(TR) = 4.0. In this study we avoided using an average confidence rating but focussed on the individual confidence ratings for each tier and only incorporated those that had a rating less greater than 3.00 as indicating a *genuine* misconception.

2. 4. Parameters to Classify Students' Misconceptions

Students' misconceptions were determined based on students' wrong answer – wrong reason (WAWR) combinations. The complete criteria for the classification are given in Table 1 below. As explained in the introduction, although CR(TA) and CR(TR) were obtained from the

Table 1. Criteria used to categorise students' misconceptions based on WAWR incidents

No.	CR(TA)	WAWR	CR(TR)	Category
1.	≥ 4.00		≥ 4.00	<i>Genuine</i> : Strong misconception
2.	$3.00 \geq \text{CR(TA)} < 4.00$		$3.00 \geq \text{CR(TR)} < 4.00$	<i>Genuine</i> : Moderate misconception
3.	$2.00 \geq \text{CR(TA)} < 3.00$		$2.00 \geq \text{CR(TR)} < 3.00$	<i>Spurious</i> : Weak misconception
4.	< 2.00		< 2.00	<i>Spurious</i> : Lack of knowledge

average of students' confidence ratings in the answer and reason tiers, only those with CR(TA) and CR(TR) of ≥ 3.00 were taken into account to avoid spurious misconceptions, lack of knowledge and possible guesswork.

It has been stated that this paper is derived from the author's PhD thesis. However, the CR values applied to categorise students' misconception is new and more advanced to ensure the genuineness of the uncovered misconceptions.

2. 5. Pre-university Education in Both Countries Regarding Chemical Kinetics

After carefully checking the chemical kinetics content of the A-level chemistry syllabus in the UK and secondary school in Indonesia, we found that the chemical kinetics content for the two countries is equal.²⁸ Except for Maxwell's distribution, all other concepts in the UK curriculum are accompanied by hands-on experiments. Students in Indonesia are forced to rely on their teachers' explanations and other theoretical exercises to grasp the concepts at hand.

3. Results And Discussion

3. 1. Students' Misconceptions in Chemical Kinetics

The results from our study into students' misconceptions in chemical kinetics have been organised according to the primary concept area in which they lie.

3. 2. Derivation of the Rate Law

Students' misconceptions regarding the rate law were identified using Q4, Q12 and Q17. Several prominent misconceptions were found in this topic.

1. Concentrations of reactants in the rate law have exponents equal to their stoichiometric coefficients in the balanced equation for the chemical reaction.

Question 4 requires students to write the rate law given the order of reaction with respect to the reactants. A small portion of students selecting Q4-AA (CR(TA) = 3.89 and CR(TR) = 3.56) demonstrates that these students are not aware that the rate law must be determined experimentally. A possible reason for this mistake is that examples of rate laws given in chemical kinetics' teaching often align with the coefficients in the balanced chemical equation. This could lead to the conclusion that the exponents in the rate law expression are directly obtained from the coefficients of the reactants in the chemical equation. This misconception has previously been observed.^{5,11,14,15} More selective choice of examples of rate laws and associated chemical equations in chemical kinetics' teaching might help avoid this confusion.

2. The rate law is derived in the same way as the equilibrium coefficient.

The proportion of students (14%) who wrongly selected Q4-CB (CR(TA) = 4.34 and CR(TR) = 3.74) confirmed this as a *genuine* misconception. Answer C assumes that the rate law is derived in the same way as the equilibrium constant from a chemical equation and is based on the law of mass action. This misconception is reinforced by students' responses to Q17-AC (CR(TA) = 4.06 and CR(TR) = 3.85) in which Answer A is obtained by deriving the rate law from the stoichiometric equation. Reason C supports this answer, i.e. *the rate law is obtained directly from the overall reaction equation*.

Also in Question 17, 8% students, with a CR(TA) = 3.58 and CR(TR) = 3.38, believed that for the reaction $\text{NO}_2(\text{g}) + \text{CO}(\text{g}) \rightarrow \text{NO}(\text{g}) + \text{CO}_2(\text{g})$ the rate is given by: $\text{Rate} = k \frac{[\text{NO}][\text{CO}_2]}{[\text{NO}_2][\text{CO}]}$. (answer D) with the reason is that "*the rate law is obtained directly from the overall reaction equation*" (reason C). A smaller proportion chose D as their reason (*the rate law is derived from the law of mass action*) (CR(TR) = 3.00). This is a more logical reason to fit with the incorrect answer D than reason C but is the wrong reason for the correct answer. It is possible that some students are not familiar with the term 'law of mass action' and so avoided this reason. This reinforces the findings of Voska & Heikkinen²⁹ who found students often confuse the law of mass action with the rate law.

3. The rate law in a multi-step reaction is obtained solely from the slow step.

Question 12 requires students to select the correct answer for the rate law in a two-step reaction with an initial fast step, which is an equilibrium reaction, followed by a slow step. 7.16% students selecting Q12-AA (CR(TA) = 3.96 and CR(TR) = 3.96) have ignored the fast step in this multi-step mechanism, in which the intermediate 'I' is produced. A small portion of students with high confidence selected Q12-BC (CR(TA) = 4.30 and CR(TR) = 3.50) and applied the law of mass action to the slow step of the equation. This relatively high confidence rating in the A tier suggests students were quite comfortable with their answers. 11.04% of students selecting Q12-BA (CR(TA) = 3.92, CR(TR) = 3.62) stated that the rate law was obtained from the slow step in the mechanism, having ignored the prior equilibrium fast step. Other students selecting Q12-BB stated that the rate law is obtained from the fast step in the reaction, despite their answer involving reactants and products of the slow step. This could be because the procedure for deriving the rate law from a multi-step mechanism is often covered towards the end of a course on chemical kinetics, so possibly students had little time to internalise the material.

3. 3. The Change in the Concentration of a Reactant or a Product with Time

1. The rate of a reaction can only be expressed in terms of concentrations of reactants.

Question 20 asks students to derive an expression for the rate of a chemical reaction in terms of the rate of disappearance of reactants or products. Students are given data about the rate of disappearance of the only reactant, N_2O_5 , and have to select one correct equation that will represent the rate at which the reaction is proceeding. 10% of students selected Q20-AC (CR(TA) = 4.03 and CR(TR) = 3.48), even though this answer showed that N_2O_5 is being formed and is not disappearing. Only very few students (2.00%) were able to identify both the correct expression for the rate of reaction and the correct reason (Q20-CF) with a strong understanding as demonstrated by the high CR(TA) and CR(TB) with 4.33 for each. This involved working out the relationship between the rate of disappearance of N_2O_5 and the rate of formation of O_2 and using the appropriate sign from the stoichiometric equation.

3. 4. Relationship Between Concentration and Rate

1. Inability to recognise the impact of a change in concentration of a reactant that is zero-order upon the reaction rate

In Q5 students are told that the reaction is zero-order with respect to one of the reactants, CO, and second-order with respect to the other, NO_2 . They have all the information to allow them to determine the rate law. Using this rate law, students were asked to predict the effect of changing the concentration of the second-order reactant, NO_2 , on the rate. Some students (7%) answered that the rate would stay the same because the order with respect to one reactant (CO) is zero (Q5-DD) with CR(TA) of 3.91 and CR(TR) of 3.82). Although only a small proportion of students chose this answer/reason combination, they had a reasonably high confidence in their response and so this is considered a *genuine* misconception. This finding has been reported by Cakmakci³ and Kirik & Boz.⁶

2. When the concentration of two reactants in an experiment is the same a higher reaction rate is obtained because the collision ratio of molecules is more favourable.

This *genuine* misconception was shown by 5% students answering Question 6 who selected Q6-CB with CR(TA) of 4.00 and CR(TR) of 3.59. This assumption may appear to be scientifically logical to students assuming a single-step mechanism. However, this reasoning ignores the influence of the rate-determining step upon the rate of reaction therefore students selecting this combination demonstrate a reasonable understanding of kinetic theory but not of reaction mechanisms.

3. A higher reaction rate is obtained when the concentration of the second-order reactant is the greatest.

This answer and reason combination was selected by a large proportion of students (24%) who answered Q6-AA with a relatively high confidence rating of CR(TA) of 3.88 and CR(TR) of 3.73 confirming a *genuine* misconception.

It is likely that these students failed to apply the appropriate rate law to the concentrations of both reactants in reaction A-D and assumed that the highest concentration of the second-order reactant would maximise the rate. Alternatively, the wrong results could have been obtained by a mathematical error, although the high percentage of students selecting this incorrect answer and related reason would suggest this is a *genuine* misconception.

4. Reaction rate always increases/decreases with time as a reaction proceeds.

For question 19 the hypothetical reaction $\text{G} \rightarrow \text{H}$ is presented in Figure 2 in which each blue sphere represents 0.2 moles of G and each red sphere represents 0.2 moles of H and the container has a volume of 1.00 L. Students were asked to predict the number of moles of G and H remaining after an intermediate length of time, after working out the rate of disappearance of G from the picture given. Calculation of the average rate during the two time periods shows that it is constant and so the reaction is zero order and reason C is the correct reason.

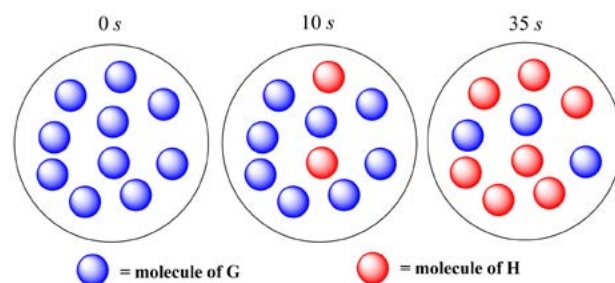


Figure 2. Pictorial representation in Q19

The belief that reaction rate increases with time in this reaction, as shown by students answering Q19-BA (CR(TA) = 3.89 and CR(TR) = 3.44), can be classed as a *genuine* misconception. Previous work has reported that students believe, for example, reaction rate increases to a maximum value, remains constant at that value, and then decreases to zero.^{5,6} Others have reported the alternative conception that an increase in concentration of a reactant always increases the reaction rate.^{10,12,15}

3. 5. Reaction Half-life and Successive Half-lives

1. The decrease in mass of a sample is constant for each successive half-life.

Question 1 is a relatively straightforward question relating to half-life during first-order radioactive decay. 5.1% students had the WAWR combination of Q1-CC with CR(TA) = 4.12 and CR(TR) = 3.65 inferring a *genuine* misconception that the mass change of the sample is constant for each successive half-life. To obtain C students

must misinterpret or misread the question and assume that the half-life of the reaction is 10 minutes. The spread of answers and reasons in this question demonstrates a general lack of clarity in the understanding of half-life.

2. The value for the half-life of a reaction is always constant.

Question 3 uses a pictorial representation and requires students to determine the time at which the concentration of NO_2 has further dropped by a half, given the number of molecules of NO_2 , NO and O_2 . Students are told in the question that the reaction is second order. However, the most popular WAWR combination is Q3-BB (CR(TA) = 4.16 and CR(TR) = 3.91) obtained by assuming this is a first-order reaction. The CR value demonstrates that students are familiar with the concept of a constant half-life for a first-order reaction but are unaware that half-life is not always constant. The confidence ratings imply a *strong* misconception.

Question 11 is deliberately analogous to question 3 except the data are presented textually with information given about the pressure of NO_2 rather than about the number of moles. Again, 16% of students (CR(TA) = 3.83 and CR(TR) = 3.64) selected Q11-BB assuming that the reaction has first-order kinetics and the value of half-life is a constant. This *genuine* misconception demonstrates that students are generally familiar with the half-life of first-order reactions and students often apply the concept of constant half-life to reactions of other orders.

3. 6. Catalysis and Activation Energy

1. Dependence of rate of reaction on activation energy

Question 9 tested students' understanding of the relationship between rate of reaction and temperature given the standard Boltzmann plot showing the distribution of energies of molecules in the same reaction at two different

temperatures. The activation energy of the reaction was marked on the x axis as in Figure 3. Students were asked to select the correct statement that describes the rate of reaction at different temperatures. A small proportion of students (4%) chose Q9-AD (CR(TA) = 3.92 and CR(TR) = 3.67) stating that the reason for the higher rate of Y is that the higher temperature results in a higher activation energy. This misunderstanding was also reported by Yalcinkaya et al.⁷ Other students (5%) stated that reaction X has a higher rate than reaction Y and chose as their reason that reaction X has the higher activation energy (Q9-AA, CR(TA) = 4.00 and CR(TR) = 3.38) although the plot clearly shows that the activation energy for each reaction is the same. This finding contradicts the one revealed by Kolomuc & Tekin⁹ in their survey of chemistry teachers who reported that an increase in temperature decreases the activation energy and so allows for an increase in reaction rate.

The students in our study argued that reaction X (Figure 3) has a higher reaction rate because it has a higher activation energy, although the plot shows that the activation energy in each reaction is the same. The explanation for this genuine misconception could be due to these students failing to correctly interpret the Boltzmann plot given in the question. The diagram is a standard one that commonly appears in textbooks on the topic. However, Justi & Gilbert³⁰ have asserted that teachers often present this diagram without providing an explanation as to the influence of temperature on reaction rate. Similar research published by Orgill & Crippen³¹ explored the manner in which first semester general chemistry students interpreted diagrams when solving questions about electromagnetic radiation. They found that most students avoided using the energy level diagram provided when calculating the wavelength of emitted radiation and preferred to plug figures into the Rydberg equation.

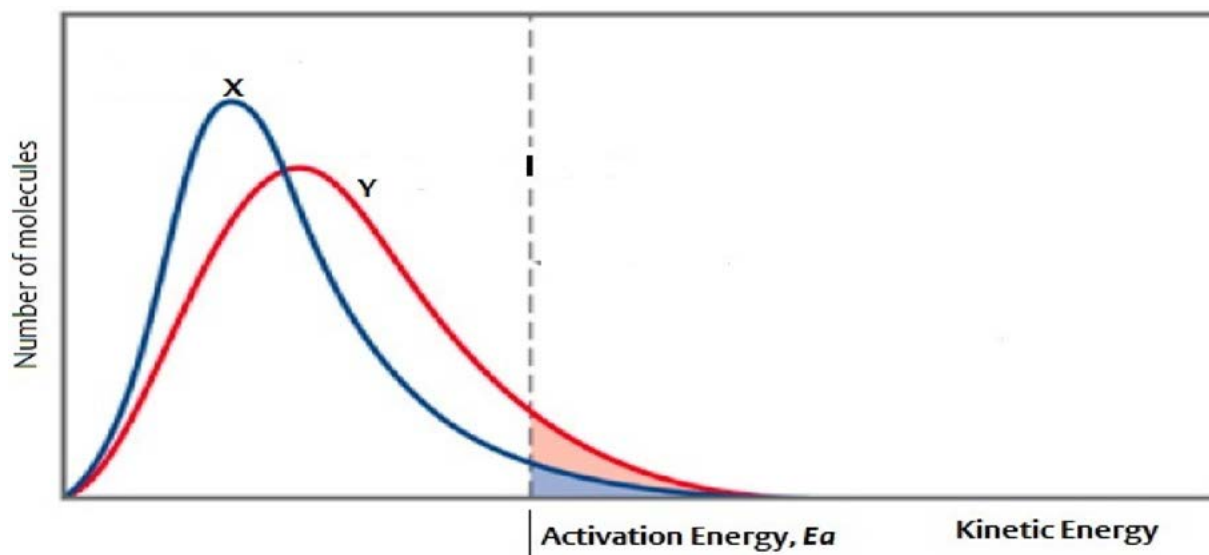


Figure 3. The Boltzmann distribution curves representing reactions of X and Y in Q9

2. An exothermic reaction is the slowest reaction.

Question 10 required students to use plots of energy profiles for four reactions carried out at the same temperature to determine the reaction with the slowest rate. Some of the possible distractors in the reason tier involved statements concerning exothermic and endothermic reaction profiles, an area that has been explored previously in the literature. To correctly answer this question respondents were expected to calculate the activation energy (kJ mol^{-1}) from the y axis values where the scales and maximum values of y were different for each plot.

A small proportion of students chose their answer based on reason A that the reaction with the slowest rate 'has the highest energy in its transition state.' Reaction A actually has the highest energy transition state but not the highest activation energy. The answer that corresponds with this reason is answer A (Q10-AA, $\text{CR}(\text{TA}) = 3.40$ and $\text{CR}(\text{TR}) = 3.60$). Some students chose the correct answer (C) but gave the wrong reason (A) indicating that these students also confused the activation energy and the energy of the transition state, or did not realise they should use values from the plots to determine the energies. This concurs with the finding of ³² who reported students of this topic may confuse an interval on a graph defined by two points with a single point – e.g. activation energy difference with actual potential energy.

Some students with $\text{CR}(\text{TA})$ of 3.44 and $\text{CR}(\text{TR})$ of 4.00 thought that the slowest reaction would be an exothermic reaction. Two exothermic reactions were depicted in the question (A and D). Almost the same number of students selected Q10-AE with a similar confidence rating. A small portion of the total students thought that the slowest reaction would be an exothermic reaction but chose an endothermic profile as their answer. In the literature there are both reports of students and teachers believing that exothermic reactions are slower than endothermic ones^{3,7,9,33}

and conversely that endothermic reactions are slower than exothermic ones.^{3,6,7,14,33} For Question, Some students selected Q14-CD ($\text{CR}(\text{TA}) = 3.57$ and $\text{CR}(\text{TR}) = 4.29$) and arrived at answer C by subtracting the energy of the products from the energy of the transition state for the catalysed reaction rather than subtracting the energy of the reactants from the energy of the transition state. They also believed that the mechanisms for both reactions are the same.

Question 15 gives a pictorial representation of a two-step reaction scheme in which a set of reactants in the presence of a catalyst is converted to a different set of products. Students are asked to identify the catalyst in the reaction mixture. In the cartoons the correct answer is the only molecule that is present at the start and at the end of the reaction and so should be straightforward to spot.

3% students chose the WAWR combination Q15-BA ($\text{CR}(\text{TA}) = 4.56$ and $\text{CR}(\text{TR}) = 4.22$) and 6% of students chose Q15-BC ($\text{CR}(\text{TA}) = 3.80$ and $\text{CR}(\text{TR}) = 3.90$). The molecule depicted in answer B represents a species that is unchanged after the first step of the reaction but not present at the end of the reaction. It is possible that students choosing answer B assumed that the catalyst was the molecule that was unchanged *after the first step*. They chose reason C; *a catalyst increases the rate without being chemically involved in the reaction* despite the fact that all the species depicted are changed at some point during the reaction mechanism and so there is no answer that fits this reason.

3. 7. Factors that Affect Students' Misconceptions

This study suggests that students' misconceptions in the understanding of chemical kinetics can be caused by a number of factors including mathematical weakness, carelessness in reading the information in the question, difficulty in interpreting visual information (tables, diagrams,

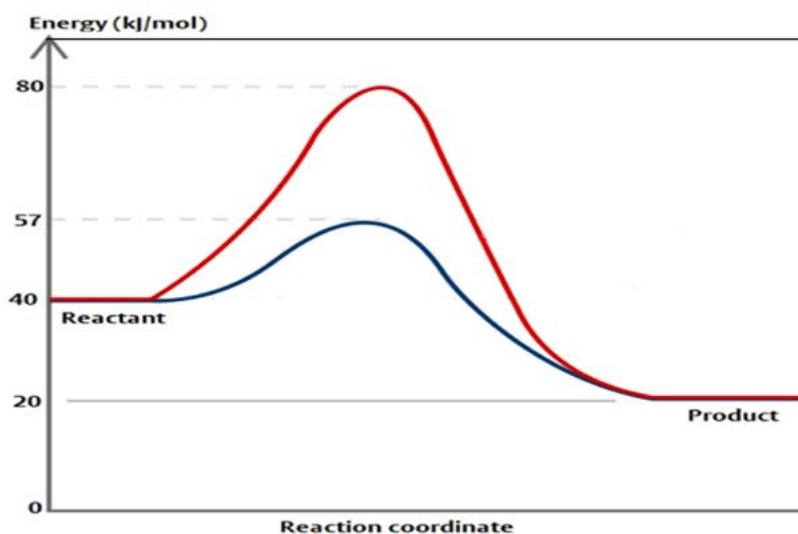


Figure 4. The energy profile describes a catalyzed and an uncatalyzed pathway for a given reaction

graphs etc) and confusion over chemical terminology and vocabulary.

Mathematical difficulties often cause students to introduce errors. In particular, converting a verbal statement to a mathematical/algorithmic operation can create a major challenge for some students. This study also has revealed that many students often answer chemical questions correctly using a formulaic equation by recall and parameter substitution to solve problems without a full understanding of the concepts. This concurs with the previous finding that many first-year students do not understand the significance of equations in chemical kinetics or how to implement the equations to solve a problem³⁴ even though they may recall or be given the actual equation. The study of Rodrigues et al³⁵ revealed that strong ability in symbolic and graphical representations reasoning is a profound way to facilitate students in integrating chemistry and mathematical knowledge.

Another factor affecting students' low performance in this study is carelessness in reading and/or interpreting the question. For example, in question 6, many students only focused on the number of molecules of the second-order reactant and ignored the number of molecules of the first-order reactant without performing the required mathematical calculation. In several circumstances, students only focused on the mathematical operation without a sufficient conceptual understanding. For example, in question 20, many students provided the correct mathematical expression for the rate law with respect to a particular reactant but failed to provide a negative or positive sign showing they did not fully understand the meaning of the relationship between change in concentration with time and rate.

Inability to identify relevant information from a diagram, graph or table can indicate poor conceptual understanding and lead to misconceptions. Extracting data from a visual aid requires additional skills besides simply reading textual information. Students must be able to translate visual clues such as points, lines, intervals, gradients, axis titles, units, colours and other representations into chemical meaning which requires good prior explanations and practice. For example, referring to Figure 3 above (question 9), two reactions are represented as X and Y with the same activation energies. However, many students believed that X has a higher rate than Y as they thought X has the lower activation energy. Because the curve shown is lower for X than Y at the value of the activation energy, some students believed that the activation energy for X is lower and the reaction therefore faster.

Difficulty with chemical terminology is another factor that leads to students' misconceptions observed in this study. This difficulty results in confusion between the precise meaning of chemical terms. For instance, students confuse reaction rate with time of reaction, initial rate, average rate, instantaneous rate and rate with respect to a specific reactant, and the terms rate law, rate expression and rate equation.

In many cases students memorise a scientific definition without having an adequate understanding of its conceptual meaning. For example, students correctly remember that half-life is constant in a first-order reaction but then apply this concept incorrectly to zero and second-order reactions. In another similar example students are taught that reaction rate decreases with time and apply this general concept to all reaction types including zero-order reactions. Students correctly argued that the concentration of a reactant at its half-life is a half of its initial concentration. However, when the question was portrayed in a pictorial format, students found it difficult due to their inability to interpret a visual representation. In addition, as has been reported previously, confusion between chemical kinetics and other topics such as chemical equilibrium and thermodynamics is also a cause of students' misconceptions. For example, many students derived the rate law of a reaction by using the stoichiometric equation in the same way as they would derive the equilibrium constant expression.

4. Conclusions

The results of this study point to several findings as summarised below. The FTDICK instrument is a valid instrument for use in investigating first-year students' misconceptions in chemical kinetics. The procedure employed in this study confirms that results obtained by using this four-tier instrument reveal students' *genuine* misconceptions in chemical kinetics. In addition, incorrect classification of a *spurious* misconception as a *genuine* misconception and vice versa can be avoided. If deployed at an appropriate time in the curriculum the instrument can help educators identify students' misconceptions before embarking on chemical kinetics topics at the tertiary level. More targeted and effective teaching can be designed if staff are aware of students' prior-knowledge misconceptions.

Numerous *genuine* misconceptions within chemical kinetics were revealed among first-year chemistry undergraduates. Although some of these misconceptions align with previous results published in the literature novel findings have been revealed in this study. The study has highlighted common misconceptions in the subject area which, if addressed in a timely manner, will help prevent students' developing further difficulties as they embark on their studies in chemical kinetics at the tertiary level.³⁶

4. 1. Implications for Teaching Chemical Kinetics

The primary aim of this study is to use the results to inform and improve the quality of teaching and learning in chemical kinetics. Based on the analysis of students' answers and confidence ratings there are several implications for the teaching of chemical kinetics.

Students appear to be familiar with the characteristics of first-order reactions but struggle with the kinetics of reactions with different orders. This can be attributed to several factors. One reason is the content of chemistry textbooks. Several general chemistry textbooks devote the largest page allocation to explaining first-order reaction kinetics and zero and second-order reactions receive little attention. In addition, the concept of first-order reactions involves radioactive decay and this improves their confidence in the topic. More emphasis on different reaction orders and their characteristics would enhance students' understanding in this topic.

Several students were found to believe that the exponents in the rate law expression are directly obtained from the stoichiometric coefficients of the reactants in the chemical equation. A possible reason for this is that examples of rate laws given in chemical kinetics' teaching often align with the coefficients in the balanced equation. To avoid this misconception, teachers should provide varied examples of rate laws in which the exponents in the experimentally determined rate laws are not the same as the coefficients in the chemical equations. This can be reinforced through practical work in which students determine the rate law from experimental data.

To address the misconception that an increase in concentration of a reactant always increases the reaction rate, the word "generally" should be used and emphasised when teaching about factors that affect reaction rate. Meanwhile, to avoid the typical misconception that the reaction rate decreases with time for all reactions, chemistry educators should stress that the term 'zero-order' implies that the rate does not depend upon the concentration and therefore the rate is constant through the reaction and does not change as the concentration of reactant decreases and/or increases.

Teaching strategies that can provide better opportunities for students to develop their reasoning skills such as learning cycle and guided inquiry are highly recommended.³⁷ Student-centred teaching such as inquiry-based practical chemistry was found to be effective in improving students' understanding of chemical kinetics.³⁴

The study also showed that students have difficulty when interpreting visual representations. Therefore, more practice should be given in this area, for example by providing information in graphical or pictorial representations when appropriate. As found in Q13, students' inability to differentiate the energy profiles of exothermic and endothermic reactions could be because many textbooks only present the energy profile for an exothermic reaction. Therefore, parallel presentations of the energy profiles for both endothermic and exothermic reactions is highly recommended³⁸. Many recent chemistry textbooks are illustrated by drawings and other pictorial representations in order to help students' reasoning. However, such representations are still limited in the secondary school textbooks in Indonesia. A similar phe-

nomenon was also found in the school textbooks in Greece.²

Evidence from this study implies that students need appropriate guidance in interpreting information. The cognitive theory of multimedia learning suggests that conveying a verbal explanation which is accompanied by an appropriate picture rather than just a textual explanation contributes to students' robust understanding.² Assessment using diagrams and graphs is recommended to improve this skill. Engaging students with technology for enhanced learning, such as a 3D-model^{39,40} could also be a reasonable exercise for teaching and assessing relevant concepts.

As chemical terminology surrounding kinetics is confusing, chemistry educators are advised to provide clear definitions of relevant terms. Some terms have very similar names such as reaction rate and reaction time; rate law, rate expression and rate equation. Educators should ensure that each term is explained carefully to students and sign-post synonyms. Barke et al³⁶ stated that misconceptions inculcated at school are due to incorrect use and understanding of chemical terminology and scientific language. Even chemistry educators can be lax with language in this area. Confusion that exists between some common everyday words and chemical terminologies is one of the barriers to chemistry teaching⁴¹ and can lead to misconceptions.⁴²

Poor mathematical ability may not directly affect students' misconceptions but can lead to weaker understanding and poor performance. However, this issue is clearly a prominent barrier to teaching and learning and should be considered. In Indonesian universities, maths is generally taught to chemistry students as an independent module, distinct from chemical concepts. Students are expected to apply their mathematical knowledge in chemical contexts. In the UK it is more common to provide dedicated 'maths for chemists' modules in an integrated manner in order to support students in performing simple calculations on chemistry topics. This practice should be considered in Indonesian universities, and other education systems where maths is taught separately from chemistry, in order to improve chemistry students' ability in transferring mathematical knowledge to a chemical context. As proposed by another study that the approach to teaching chemistry involving mathematical operation should be reformed.⁴³

Students' difficulty in converting verbal statements to mathematical operations and vice versa is another cause of misconceptions. To address this, more practice should be given in this skill rather than providing examples where numbers can simply be slotted into the appropriate equation. Students' mathematical skills, logical thinking and interpreting information from verbal statements and diagrams are all essential elements for success in physical chemistry.⁴⁴ It may also be useful for exploring a procedure for mapping students' reasoning process, such as Tal-

anquer's Heuristic Approach, as shown by Karakoyun & Asilturk⁴⁵ in acid-base.

4. 2. Limitation of the Study and Future Work

The equal number of Indonesian and UK students hinders a robust comparison of the performance of British and Indonesian students. Also, with only two participant countries, it may not be powerful enough to generalise this study's result internationally. However, it would be prudent to extend the work carried out here to involve students of different nationalities. It would also be instructive to extend the study to further universities in both the UK and Indonesia to obtain a more robust picture of student understanding of chemical kinetics at this level.

A similar four-tier approach is recommended to explore understanding in other physical chemistry topics such as thermodynamics, chemical equilibrium and electrochemistry. Specific areas of organic, inorganic, analytical and biochemistry would also benefit from similar studies. Most importantly, future work should involve using the FTDICK instrument in the teaching of chemical kinetics to empirically evaluate how the instrument can improve the quality of teaching in chemical kinetics at the university level.

Dissemination of the results of this study to chemistry educators and policy makers is essential to enable practitioners, particularly in Indonesia, to design appropriate teaching practices, textbooks and other resources. Agung & Schwartz⁴⁶ stated that the limited number of published studies in Indonesia focusing on students' misconceptions in chemistry, in particular, and the sciences in general, may be the reason why educators and policymakers do not take these students' misconceptions into account. Similarly, Gegious et al² found that school textbooks in Greece have not been influenced by the results of chemical education studies. Unfortunately, chemistry teachers rarely critically evaluate textbooks which are used in their chemistry classes. As a result, many of these textbooks do not help students to gain a better conceptual understanding.²

Acknowledgements

We would like to thank the Directorate General of Higher Education, Ministry of Research, Technology and Higher Education, the Republic of Indonesia for a PhD scholarship to one of us. This paper is derived from my PhD thesis at The University of Reading, but we applied a different approach in categorising students' misconceptions for some reasons.

Ethical Statement

Approval for the study described was granted by the university ethics board. All students gave informed consent to partake in the study.

Statements and Declarations

We declare that this study has no potential conflicts of interest, including financial funding.

5. References

1. R. Justi, in J. K. Gilbert, O. de Jong, R. Justi, D. F. Treagust, J. H. Van Driel (Eds.): *Chemical Education: Towards Research-based Practice*, Springer Netherlands, Netherlands, **2002**, pp. 293–315.
2. T. Gegios, K. Salta, S. Koinis, *Chem. Educ. Res. Pract.* **2017**, *18*, 151–168. DOI:10.1039/C6RP00192K
3. G. Cakmakci, *J. Chem. Educ.* **2010**, *87*, 449–455. DOI:10.1021/ed8001336
4. K. Bain, M. H. Towns, *Chem. Educ. Res. Pract.* **2016**, *17*, 246–262. DOI:10.1039/C5RP00176E
5. G. Cakmakci, J. Leach, J. Donnelly, *Int. J. Sci. Educ.* **2006**, *28*, 1795–1815. DOI:10.1080/09500690600823490
6. O. T. Kirik, Y. Boz, *Chem. Educ. Res. Pract.* **2012**, *13*, 221–236. DOI:10.1039/C1RP90072B
7. E. Yalçinkaya, Ö. Taştan-Kirik, Y. Boz, D. Yıldıran, *Res. Sci. Technol. Educ.* **2012**, *30*, 151–172. DOI:10.1080/02635143.2012.698605
8. B. Bektasli, G. Cakmakci, *Educ. Sci.* **2011**, *36*, 273–287. DOI:10.1007/s10755-011-9196-6
9. A. Kolomuç, S. Tekin, *Eurasia J. Phys. Chem. Educ.* **2011**, *3*, 84–101. DOI:10.51724/ijpce.v3i2.194
10. J. H. Van Driel, *Chem. Educ. Res. Pract.* **2002**, *3*, 201–213. DOI:10.1039/B2RP90016E
11. T. Turányi, Z. Tóth, *Chem. Educ. Res. Pract.* **2013**, *14*, 105–116. DOI:10.1039/C2RP20015E
12. Ö. Tastan, E. Yalçinkaya, Y. Boz, *J. Turkish Sci. Educ.* **2010**, *7*, 47–60.
13. M. W. Hackling, P. J. Garnett, *Eur. J. Sci. Educ.* **1985**, *7*, 205–214. DOI:10.1080/0140528850070211
14. G. Cakmakci, C. Aydogdu, *Chem. Educ. Res. Pract.* **2011**, *12*, 15–28. DOI:10.1039/C1RP90004H
15. S. Kingir, O. Geban, *Hacettepe Univ. J. Educ.* **2012**, *43*, 306–317. DOI:10.1007/s11165-012-9326-x
16. D. F. Treagust, *Int. J. Sci. Educ.* **1988**, *10*, 159–169. DOI:10.1080/0950069880100204
17. S. Hasan, D. Bagayoko, E. L. Kelley, *Phys. Educ.* **1999**, *34*, 294–299. DOI:10.1088/0031-9120/34/5/304
18. H. O. Arslan, C. Cigdemoglu, C. Moseley, *Int. J. Sci. Educ.* **2012**, *34*, 1667–1686. DOI:10.1080/09500693.2012.680618
19. B. Sreenivasulu, R. Subramaniam, *Res. Sci. Educ.* **2014**, *44*, 801–828. DOI:10.1007/s11165-014-9400-7
20. I. Caleon, R. Subramaniam, *Res. Sci. Educ.* **2010**, *40*, 313–337. DOI:10.1007/s11165-009-9122-4
21. B. Sreenivasulu, R. Subramaniam, *Int. J. Sci. Educ.* **2013**, *35*, 601–635. DOI:10.1080/09500693.2012.683460
22. Y. K. Yan, R. Subramaniam, *Chem. Educ. Res. Pract.* **2018**, *19*, 213–226. DOI:10.1039/C7RP00143F
23. I. Kaniawati, N. J. Fratiwi, A. Danawan, I. Suyana, A. Samsudin, E. Suhendi, *J. Turkish Sci. Educ.* **2019**, *16*, 110–122.

24. L. A. R. Laliyo, S. Hamdi, M. Pikoli, R. Abdullah, C. Panigoro, *Eur. J. Educ. Res.* **2021**, *10*, 825–840. DOI:10.12973/eu-jer.10.2.825
25. L. F. Gerard, M. Spitulnik, M. C. Linn, *J. Res. Sci. Teach.* **2010**, *47*, 1037–1063. DOI:10.1002/tea.20367
26. M. M. Cooper, R. L. Stowe, *Chem. Rev.* **2018**, *118*, 6053–6087. DOI:10.1021/acs.chemrev.8b00020
27. H. Habiddin, E. M. Page, *Indones. J. Chem.* **2019**, *19*, 720–736. DOI:10.22146/ijc.39218
28. A Level GCE Chemistry H432, OCR, <https://www.ocr.org.uk/qualifications/as-and-a-level/chemistry-a-h032-h432-from-2015/> (assessed: February 12, 2023).
29. K. W. Voska, H. W. Heikkinen, *J. Res. Sci. Teach.* **2000**, *37*, 160–176. DOI:10.1002/(SICI)1098-2736(200002)37:2<160::AID-TEA5>3.0.CO;2-M
30. R. Justi, J. K. Gilbert, *Sci. Educ.* **1999**, *8*, 287–307. DOI:10.1023/A:1008645714002
31. M. Orgill, K. Crippen, *J. Coll. Sci. Teach.* **2010**, *40*, 78–84.
32. N. Glazer, *Stud. Sci. Educ.* **2011**, *47*, 183–210. DOI:10.1080/03057267.2011.605307
33. M. Sozibilir, T. Pinarbasi, N. Canpolat, *Eurasia J. Math. Sci. Technol. Educ.* **2010**, *6*, 111–121.
34. S. Chairam, E. Somsook, R. K. Coll, *Res. Sci. Technol. Educ.* **2009**, *27*, 95–115. DOI:10.1080/02635140802658933
35. J. G. Rodriguez, S. Santos-Diaz, K. Bain, M. H. Towns, *J. Chem. Educ.* **2018**, *95*, 2114. DOI:10.1021/acs.jchemed.8b00584
36. H. D. Barke, A. Hazari, S. Yitbarek, *Misconceptions in Chemistry: Addressing Perceptions in Chemical Education*, Springer Berlin Heidelberg, **2008**.
37. M. S. Cracolice, J. C. Deming, B. Ehlert, *J. Chem. Educ.* **2008**, *85*, 873–878. DOI:10.1021/ed085p873
38. G. M. Bowen, W. M. Roth, *Res. Sci. Educ.* **2002**, *32*, 303–327. DOI:10.1023/A:1020833231966
39. D. Dolničar, B. Boh Podgornik, V. Ferik Savec, *Acta Chim. Slov.* **2022**, *69*, 167–186.
40. T. Thayban, H. Habiddin, Y. Utomo, M. Muarifin, *Acta Chim. Slov.* **2021**, *68*, 736–743. DOI:10.17344/acsi.2021.6836
41. D. Gabel, *J. Chem. Educ.* **1999**, *76*, 548–554. DOI:10.1021/ed076p548
42. P. J. Garnett, P. J. Garnett, M. W. Hackling, *Stud. Sci. Educ.* **1995**, *25*, 69–96. DOI:10.1080/03057269508560050
43. M. Rusek, K. Vojří, I. Bártová, M. Klečková, V. Sirotek, J. Štrofová, *Acta Chim. Slov.* **2022**, *69*, 371–377. DOI:10.17344/acsi.2021.7250
44. R. A. Hoban, O. E. Finlayson, B. C. Nolan, *Int. J. Math. Educ. Sci. Technol.* **2013**, *44*, 14–35. DOI:10.1080/0020739X.2012.690895
45. G. Önal Karakoyun, E. Asiltürk, *Acta Chim. Slov.* **2021**, *68*, 645–657. DOI:10.17344/acsi.2021.6666
46. S. Agung, M. S. Schwartz, *Int. J. Sci. Educ.* **2007**, *29*, 1679–1702. DOI:10.1080/09500690601089927

Povzetek

Namen študije je raziskati napačno razumevanje študentov prvega letnika univerzitetnega študija o kemijski kinetiki z analizo podatkov, pridobljenih s štiristopenjskim diagnostičnim pristopom za kemijsko kinetiko (FTDICK). V tej študiji je sodelovalo 335 študentov prvega letnika kemije z dveh indonezijskih in ene britanske univerze. Opisani postopek je prvi te vrste, ki zagotavlja, da so ta napačna razumevanja resnična. Med študenti prvega letnika študija kemije so se razkrila številna napačna razumevanja na področju kemijske kinetike. Čeprav se mnoga od ugotovljenih napačnih razumevanj ujemajo z rezultati, ki so bili predhodno objavljeni z uporabo drugih pristopov, je bilo odkritih tudi nekaj novih ugotovitev. Ta napačna razumevanja je mogoče pripisati različnim dejavnikom, vključno z matematično šibkostjo, neprevidnostjo in težavami pri razlagi in pridobivanju informacij iz diagramov, grafov in drugih nebesedilnih informacij. Na podlagi rezultatov te študije podajamo nekaj priporočil za izboljšanje učinkovitosti poučevanja kemijske kinetike na tej stopnji.



Except when otherwise noted, articles in this journal are published under the terms and conditions of the Creative Commons Attribution 4.0 International License

Scientific paper

Potential Biochemical Properties of Endemic *Onosma mutabilis*

Pelin Eroglu,^{1,*} Mehmet Ulas Civaner,¹ Selda Dogan Calhan,² Mahmut Ulger³ and Riza Binzet⁴

¹ Department of Chemistry, Faculty of Science, Mersin University, 33343, Mersin, Turkey

² Department of Pharmaceutical Biotechnology, Faculty of Pharmacy, Mersin University, 33169, Mersin, Turkey

³ Department of Pharmaceutical Microbiology, Faculty of Pharmacy, Mersin University, 33169, Mersin, Turkey

⁴ Department of Biology, Faculty of Science, Mersin University, 33343, Mersin, Turkey

* Corresponding author: E-mail: pelineroglu@mersin.edu.tr

Phone: +90 324 3610001/14560

Received: 01-04-2023

Abstract

The *Onosma L.* (Lithospermae, Boraginaceae) genus contains many plant species with therapeutic properties due to its rich phytochemicals. *Onosma mutabilis* Boiss. & Hausskn. ex Boiss. (*O. mutabilis*) is the species for which there is not enough information on its characteristics.

Objective: The total phenolic content, antioxidant activity, possible bioactive compounds, and antibacterial activities of ethanolic extracts of leaf, stem, root, and flower parts of endemic *O. mutabilis* were investigated.

Conclusions: The total phenolic content of all *O. mutabilis* extracts was in the range of 9.2–31 mg gallic acid equivalent (GAE)/g of extract. According to the results of antioxidant activity, the IC₅₀ antioxidant capacity values determined by the 1,1-diphenyl-2-picrylhydrazyl (DPPH) method were between 4.39–29 µg/mL, while the equivalent trolox antioxidant activity determined by the cupric reducing antioxidant values (CUPRAC) was 0.45–0.78 mmol of trolox equivalents (TE)/g of extract. Bioactive compounds have been analysed using gas chromatography coupled with mass spectrometry (GC/MS) and were found to contain 29 different chemical components. All plant extracts tested showed effective antibacterial activity against *A. baumannii* (ATCC 02026) (62.5 µg/mL MIC value) when compared to the reference drug Ampicillin (125 µg/mL).

Keywords: *Onosma mutabilis*, phenolic compounds, antioxidant activity, antibacterial activity.

1. Introduction

Onosma L. (1762: 196) (Lithospermae, Boraginaceae) is a large genus in the world. It is distributed from the northwest of Africa to Europe and Asia and mainly in Turkey and Iran^{1,2}. The total number of *Onosma* species known from Turkey is 103^{3,4}. When the high rate of endemism in Turkey (57.84%) was taken into account, it was seen that Turkey was the centre of diversity of the *Onosma* genus. *Onosma* species is widely used worldwide in traditional medicine. The various parts of *Onosma* species are known to be used for the treatment of various disorders such as bronchitis, hemorrhoids, tonsillitis, pain relief, and relief of blood disorders in Turkey.^{5,6}

On the other hand, antioxidant enzymes produced by our body's defence system are critical to maintain the

oxidant-antioxidant balance. In addition, plant-derived antioxidant substances have been reported to be effective against degenerative diseases caused by oxidative stress.⁷ For this reason, the determination of the effects of therapeutically effective plants on free radical-induced oxidative damage attracts the attention of many researchers. Despite the unique bioactive composition of plants, the phytochemical content of approximately 15% was investigated and the biological activity of 6% was screened.⁸ Antimicrobial compounds isolated from medicinal plants are effective against different bacteria.^{9,10} In addition, the emergence of multidrug-resistant pathogens in recent times has had adverse effects on public health. This encourages new research and the development of more effective drugs to replenish therapeutic drug reservoirs.¹¹ How-

ever, the chemical components and antioxidant and antimicrobial properties of endemic plants grown in various countries and used for medicinal purposes still need to be discovered. Therefore, active research on plants is necessary to identify potential candidates as safer and more effective agents in the future.

To our knowledge, only one study has been conducted to determine the phytochemical content of *O. mutabilis*. In the study performed by Jabbar et al.¹² different extraction solvents were used, and it was reported that 18 different bioactive species were detected. Cytotoxicity studies have been carried out on different cell lines, but no studies have been carried out on the antibacterial activities of the plant.

In this study, we have identified the phenolic compound, chemical composition, antioxidant and antibacterial activity of the ethanolic extract obtained from roots, stems, flowers, and leaves of endemic *O. mutabilis*.

2. Experimental

2.1. Chemicals and Instruments

The Folin-Ciocalteu reagent and ethanol (99%) were supplied from Merck (Darmstadt, Germany), gallic acid (3,4,5-trihydroxybenzoic acid, abbreviated as GA), anhydrous sodium carbonate (Na_2CO_3) was obtained from Fluka (USA). DPPH (1,1-diphenyl-2-picrylhydrazyl radical), BHT (2,6-Di-tert-butyl-4-methylphenol), and Mueller-Hinton broth (Sigma 70192) and Resazurin dye (Sigma R7017) were obtained from Sigma-Aldrich (St. Louis, MO). The soxhlet apparatus was supplied by Isolab (Wertheim, Germany). A Rotary evaporator (Buchi B-491, Germany), UV-1601 spectrophotometer (UV-1601, Shimadzu, Japan), GC/MS (GC: 7890 A, MS: 5975 C, Agilent, USA) were used throughout this work.

2.2. Plant Materials

The samples of *O. mutabilis* were identified and collected by Dr. Riza Binzet from Mersin (Location: C5 Mersin, Mersin-Gözne, around Darisekisi, rocky slopes and scrub, 36°58'10.91"N 34°34'11.79"E, 780 m) (Fig. 1).



2.3. Preparation of Plant Extracts

Fresh leaves, roots, stem, and flower samples of *O. mutabilis* were air dried in the shade at room temperature (25 °C) for three weeks. Then the leaves, roots, stems and flowers samples were reduced to powder separately with a blender (Blender 8011ES Model HGB2WTS3, 400 W) and kept in glass bottles at room temperature. Ten grams of powdered samples were extracted in 300 mL of ethanol solvent using the Soxhlet extraction method for 6 hours. Ethanol was evaporated at 50–60 °C using a Rotary Evaporator with bath water. Stock solutions were prepared at concentrations of 1 mg/mL of each part of the plant. Extracts were kept before analysis in a sealed vial at +4 °C.

2.4. Determination of the Total Phenolic Content

The content of phenolic compounds in extracts obtained from different parts of the plant analysis according to the Folin-Ciocalteu method.¹³ 1 mL of Folin-Ciocalteu reagent was added to 1 mL of ethanolic plant solution (1 mg/mL). The sample was kept in the dark for five minutes. Then 2 mL of Na_2CO_3 solution (20%, (w/v)) and 2 mL of water were added to the reaction medium. After incubation at room temperature for 30 minutes in the dark, the absorbance was measured at 714 nm. The total polyphenol content was calculated using the gallic acid calibration curve and reported as mg of gallic acid equivalent per gram of extract (mg GAE/g E).

2.5. DPPH Radical Scavenging Assay

The free radical scavenging of the ethanolic extracts obtained from different parts of *O. mutabilis* by the DPPH-test according to the method established by Ilokiassanga et al.¹⁴ First, a stock solution of dried plant extracts was prepared with ethanol at a concentration of 1 mg/mL. The solutions of ethanolic extracts of *O. mutabilis* prepared in each concentration range (100–1000 $\mu\text{g/mL}$) were analysed. 100 μL of the extract solutions were mixed with 100 μL of freshly prepared DPPH (0.2 mM). The mixture ob-



Fig. 1 (a) Habitus and (b) map of the distribution of *O. mutabilis*.

tained was slightly shaken and incubated at room temperature for 30 min in the dark. BHT was used as a reference. The absorbance values of the sample solutions and BHT were measured at 517 nm using ELISA (Thermo Scientific™ Multiskan™ FC). The tests were repeated 3 times. The percent inhibition of the DPPH free radical scavenging activity was calculated with Eq. (1):

$$\% \text{ Inhibition} = \left[\frac{\text{Abs control} - \text{Abs sample}}{\text{Abs control}} \right] \times 100 \quad (1)$$

Radical scavenging activity was indicated as IC_{50} , which shows the concentration of plant extracts required to inhibit 50% of the free radicals DPPH.

2. 6. Cupric Reducing Antioxidant Capacity (CUPRAC) Assay

CUPRAC assay,¹⁵ and the results were expressed as Trolox equivalents. In detail, 1 mL of 1.0×10^{-2} M copper chloride solution, 7.5×10^{-3} M neocuproin solution and 1 M (pH = 7) ammonium acetate buffer are added to the test tube, respectively. Then Trolox and distilled water are added. Solutions prepared with a total volume of 4.1 mL are kept closed for 30 minutes under room conditions. At the end of this period, the absorbance values are measured at 450 nm against the reference solution without a sample.

2. 7. Antibacterial activity

The antibacterial activity and minimum inhibitory concentration (MIC) values of extracts obtained from different parts of the plant were tested using REMA.¹⁶ The following five bacteria were tested in this study: *Staphylococcus aureus* ATCC 25925, *Bacillus subtilis* ATCC 6633, *Aeromonas hydrophila* ATCC 95080, *Escherichia coli* ATCC 25923, *Acinetobacter baumannii* ATCC 020226.

2. 8. Determination of MIC Values for *O. mutabilis*

Antibacterial activity was evaluated using the microdilution assay in 96-well sterile polystyrene microplates. Extract at concentrations of 1000 µg/mL was prepared by dissolving in DMSO and filtered through a 0.22 µm microporous filter. Each well in the microplate was filled with 100 µL of Mueller-Hinton broth (Sigma 70192). The working solutions of the extracts with serial twofold dilutions were adjusted to 500–0.24 µg/mL. Ampicillin was used as the standard drug in the study and the dilution of the standard drug was carried out in the same way. The bacterial suspension was prepared from standard bacterial strains at 0.5 McFarland density. This suspension was then diluted with sterile distilled water (1/20). 10 µL of this suspension was added to the corresponding wells. Thus, the final bacterial density in the wells was adjusted to 5×10^5

CFU/mL (CLSI 2012). The working solution of Resazurin (resazurin sodium salt, Sigma R7017) was prepared in 0.01% (w/v) distilled water and sterilised by passing through a 0.22 µm membrane filter. 10 µL of sterilised resazurin was added to the wells. Plates were covered with a plastic film (ThermoFisher Scientific MicroAmp® optical adhesive film, 4360954) to prevent evaporation. The plates were then incubated at 37 °C for 24 hours. At the end of the period, the colour change in the plates was visually evaluated. The change in resazurin from blue to pink or colourless was considered bacterial growth. The MIC value was determined as the lowest concentration of plant samples that prevents the growth of bacteria that prevented resazurin from turning blue to pink or colourless. All antibacterial activity assays were repeated three times.

2. 9. Determination of Bioactive Compounds

The essential compounds of *O. mutabilis* were analysed with a7890A GC system with an inert MSD of 5975C and a capillary column [Agilent Technologies 19091S-433-HP5-MS]. The injection temperature was 285 °C. The volume of injection was 2 µL. The GC temperature programme was used as follows: At 40 °C, holding there for 5 min, 40 to 220 °C at a rate of 4°C/min and holding at 220 °C for 5 min, and then increased from 220 to 280 °C at a rate of 5°C/min and holding there for 15 min, from 280 to 300 °C at a rate of 15 °C/min and holding there for 5 min. Spectra were obtained in the range of 50–550 m/z. Helium gas was used as the carrier gas with a flow rate of 1 mL/min. The maximum temperature was 325 °C. Total analysis time: 82.5 min. The chemical components of the extract were identified by matching the retention times and mass spectral fragmentation patterns with those of the compounds resulting from data from the NIST/EPA/NIH mass spectral library (NIST05a.L).

3. Results and Discussion

3. 1. Total Phenolic Content Analysis

Composed of an aromatic hydroxyl core, plant phenolics are one of the most important groups of compounds that work as primary antioxidants and free radical scavengers. Spectrophotometric measurements were performed based on the blue colour of the phosphomolybdic-phosphotungstic-phenol complex formed in the Folin-Ciocalteu method,¹⁷ which is widely used in the determination of the total phenolic content. The total phenolic content of the *O. mutabilis* extracts, expressed as gallic acid equivalents, are shown below in Fig. 2

In this study, the findings we obtained for the phenolic content of *O. mutabilis* are compatible with the literature. In a study with *O. mutabilis* grown in Iran, the total phenolic content of the methanolic extract of this plant species was determined to be 37.24 mg equivalent rutin equivalents/g extract.¹² Sarikurkcu et al.^{18,19} determined the total

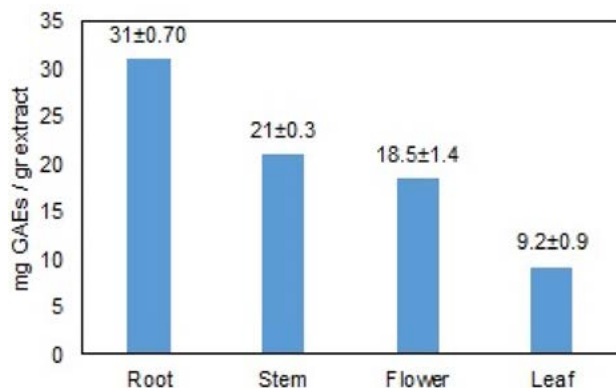


Fig. 2 Total phenolic contents of the ethanolic extracts of different parts of *O. mutabilis*. The values presented represent the mean of three experiments \pm SD.

phenolic content of the methanolic extracts of *O. gigantea* and *O. rascheyana* to be 9.12 μ mol GAEs/g and 31.55 mg GAE / g, respectively. Furthermore, Kirkan et al.²⁰ *Onosma tauricum* var. *tauricum* species and showed that the total phenolic content of this plant is 16.20 μ mol GAEs/g. In a study with another *Onosma* species (*Onosma chlorotricum*) the total phenolic content was determined as 56.10 mg GAE / g of dry extract.²¹ Emsen et al.,²² analysed the ethyl acetate extracts of *O. bozakmanii* and determined the total phenolic content as 36.29 μ g GAE/mg extract.

3. 2. Antioxidant Activity

The antioxidant activity of the ethanolic extracts of *O. mutabilis* was evaluated using DPPH and CUPRAC methods. The DPPH method is widely used because its assay is reliable, simple, fast, and sensitive and determines the antioxidant activity in vitro of several natural bioactive compounds.^{23,24} Basically, in this method, there is a decrease in the strong absorbance of DPPH at 517 nm due to the reaction of proton transfer to the DPPH free radical by the antioxidant.²⁵

Table 1 shows the IC₅₀ values of the ethanolic extract of different parts of *O. mutabilis*. Free radical scavenging ability is expressed as the IC₅₀ value. The IC₅₀ value is the amount of antioxidant required to reduce 50% of the initial concentration of DPPH.²⁶ A low IC₅₀ value means high free radical scavenging activity.²⁷ The IC₅₀ values of the roots, stems and flowers were the highest with 5.37, 4.39 and 8.02 μ g/mL, respectively. The phenolic content of the plant is proportional to the concentration of the extract and indicates that it has very high antioxidant activity.²⁸

While the CUPRAC method shows the ability of the extract to reduce Cu metal, the results are proportional to the total amount of copper reduced by antioxidant compounds through electron transfer. The CUPRAC assays were expressed as mmol of Trolox equivalent/g of extract.

The extracts of *O. mutabilis* gave CUPRAC values with a total antioxidant capacity ranging between 0.45 and

Table 1. Antioxidant activities (DPPH, and CUPRAC) of ethanolic extracts from different parts of *O. mutabilis**.

Sample	DPPH assay (IC ₅₀ μ g/mL)	CUPRAC (mmol TE/g extract)
Root	5.37 \pm 0.23	0.78 \pm 0.22
Stem	4.39 \pm 0.29	0.45 \pm 0.26
Flower	8.02 \pm 0.57	0.52 \pm 0.34
Leaf	29 \pm 0.63	0.67 \pm 0.36
BHT	1.75 \pm 0.18	0.64 \pm 0.28

* The values presented are the mean of three experiments \pm SD.

0.78 as mmol Trolox equivalent/g. The highest antioxidant capacity determined by the CUPRAC analysis was recorded for the root extract. This is followed by flower, leaf, and stem extracts, respectively (Table 1). The highest reduction potential determined by the CUPRAC assay was also observed in the root extract.

Our results support previous studies on the antioxidant capacities of other medicinal plants in the Boraginaceae family. Researchers used methanol extracts, unlike us, in the research carried out on different types of this plant. Jabbar¹² investigated the antioxidant activity of *O. mutabilis* methanol extracts using the DPPH method and reported an IC₅₀ value of 3.54 mg/mL, respectively.

Saravanakumar et al.²⁹ investigated the free radical scavenging activity of the methanolic extract of *O. bracteosa* plant with the DPPH test and showed that the IC₅₀ value was 4.58 mg/mL. Furthermore, Sarikurkcu et al.,³⁰ determined the antioxidant activities of methanolic extracts of *O. frutescens* with DPPH and CUPRAC tests as 1.14 and 0.53 mg/mL, respectively, and showed that they have high antioxidant potential. Kumar et al.,³¹ recorded the DPPH IC₅₀ value of methanolic *O. hispidum* root extract as 2.73 μ g/mL. Kirkan et al.³², determined that methanol extracts of *O. cappadocica* showed high activity based on the DPPH scavenging test and the CUPRAC test. In addition, another study by Kirkan et al.²⁰ showed that methanolic extracts of *O. tauricum* var. *tauricum* exhibited a high antioxidant potential when tested with the DPPH and CUPRAC methods.

It can be said from the results that the ethanolic extracts of *O. mutabilis*, especially the roots and stem, have quite high antiradical activities, with radical scavenging values close to that of the standard. The difference in free radical scavenging activity in various parts of *O. mutabilis*, such as the root, stem, flower, and leaves, may be related to its chemical composition. It is difficult to compare the results of different methods used to determine antioxidant activity, such as CUPRAC and DPPH.³³ Therefore, the results are not given comparatively.

3. 3. Antibacterial Activity

The MIC values of the extracts, compared to the standard bacterial strains used in the study, were determined to be in the range of 250–31.25 μ g/mL. The test-

ed extracts had higher antibacterial activity against *A. baumannii* with a 62.5 µg/mL MIC value, compared to the reference drug ampicillin with a 125 µg/mL MIC value.

Based on the results, it was determined that the MIC values of the extracts against *A. hydrophila* were 62.5 µg/mL. It was determined that the results showed a lower antibacterial effect compared to the reference drug, but a result close to the MIC value (31.25 µg/mL) of ampicillin. Although the MIC results of the plant extracts (31.25 µg/mL) for *B. subtilis*, a Gr (+) bacterium, were higher than the MIC results of the other four bacteria, the activity was found to be lower when compared to the MIC value of ampicillin (0.9 µg/mL). The plant extracts were defined to show low activity against standard bacterial strains of *S. aureus* and *E. coli* (Table 2).

acid and derivatives of fatty acids such as ethyl linoleate and hexanamide have been found.

Butanoic acid was found only in the leaf part of the plant; hexadecanoic acid was found in all parts of the plant, but in different concentrations. Relative rates of hexadecanoic acid, which has a strong antimicrobial and anti-inflammatory^{36,37} effect, are mainly flower, leaves, roots, and stem, respectively. Hexanamide and 14-pentadecanoic acid were found only in the root of the plant and linoleic acid was detected only in the flower of the plant. Furthermore, ethyl linoleate was found in the flower and root part of the plant; 9,12,15-octadecatrienoic acid was detected in the flower and leaves of the plant. Octadecanoic acid was found in all parts of the plant. Fatty acids are compounds with important structural functions. Studies have shown that fatty acids such as stearic acid, oleic acid, and linoleic acid

Table 2. MIC (µg/mL) values of extracts and reference drugs tested against standard bacterial strains.

	<i>S. aureus</i> (ATCC25925)	<i>E. coli</i> (ATCC25923)	<i>A. baumannii</i> (ATCC02026)	<i>B. subtilis</i> (ATCC6633)	<i>A. hydrophila</i> (ATCC95080)
Root	125	125	62.5	31.25	62.5
Stem	125	125	62.5	31.25	62.5
Flower	250	125	62.5	31.25	62.5
Leaf	125	125	62.5	31.25	62.5
Ampicillin	31.25	15.62	125	0.9	31.25

A lot of research is focused on studying the antimicrobial activity of various parts of plants of the family Boraginaceae. In various studies, root extracts from different species of *Onosma* have been shown to be effective against Gr (+) bacteria.³⁴ In our study, the MIC value of root extracts of *O. mutabilis* against *S. aureus* was 125 µg/mL and against *B. subtilis* was 31.25 µg/mL. In other studies, the MIC values of *O. dichroanthum* root extracts against Gr (+) bacteria were in the range of 0.156–0.312 mg/mL.³⁴ Dousti and Nabipor²¹ showed that by the MIC assay *O. chlorotricum* Boiss methanol extracts showed higher antibacterial activity against Gr (+) bacteria than Gr (-) bacteria. Halim et al.,³⁵ reported that *O. Bracteatum* extracts inhibited Gr (+) bacteria more than G (-) bacteria.

3. 4. Chemical Composition Analysis

Using GC-MS analysis of *O. mutabilis* flower, leaf, stem, and root extracts, a total of 29 compounds with high-quality peaks were detected (Table 3). The results showed that there are different compounds in the flower, leaf, stem, and root parts of the plant, and that the rates of these compounds varied by their peak areas. In our study, based on the results of the GC-MS analysis of *O. mutabilis* flower, leaf, stem and root extracts, fatty acids such as butanoic acid, hexadecanoic acid, 14-pentadecanoic acid, linoleic acid, 9,12,15-octadecatrienoic acid, octadecanoic

reduce inflammation due to their antioxidant properties, albeit indirectly, in vascular endothelial cells. Therefore, it has been suggested that treatment using these parts of the plant could reduce the risk of atherosclerosis and cardiovascular disease.³⁸ Phytol is an important diterpene with antimicrobial, antioxidant and anticancer activities.^{36,39,40} Neophytadiene, another important bioactive compound found in the flower and stem parts of *O. mutabilis*, has analgesic, antipyretic, anti-inflammatory, antimicrobial and antioxidant effects.⁴¹ The compound 14β-Pregnane, found in the root part of *O. mutabilis* at a concentration of 1%, has a steroid structure and is a defence chemical with preventive and therapeutic effects against diabetic retinopathy.⁴² Another bioactive compound detected based on GC-MS results is β-Sitosterol, commonly known as phytosterol. Phytosterols, found in plant cell membranes, are chemically similar to mammalian cell-derived cholesterol. It has been shown in many in vitro and in vivo studies that β-sitosterol has various biological effects, including anxiolytic and sedative effects, analgesic, immunomodulatory, antimicrobial, anticancer, anti-inflammatory, and lipid-lowering effects; it is also hepatoprotective and showed a protective effect against nonalcoholic fatty liver disease.⁴³ Hydrocarbons, another important group of organic compounds, are found in the flower, leaf, stem and root extracts of *O. mutabilis*. Hexadecane, tri-tetracontane, heptadecane, octadecane, nonadecane, tricosane, hexacosane, tetra-

Table 3. Phytochemical contents of flower, leaf, stem, and root samples of *O. mutabilis* analyzed by GC-MS.

Compound	Chemical Formula	Flower	Leaf	Stem %	Root	t _R (min)	CAS NO
Butanoic acid	C ₄ H ₈ O ₂	–	2.65	–	–	9.67	016844-99-8
1H-Indole	C ₈ H ₇ N	3.40	1.24	1.24	2.99	18.21	000120-72-9
Decaborane	B ₁₀ H ₁₄	–	5.37	–	–	29.1	017702-41-9
Hexadecane	C ₁₆ H ₃₄	–	–	–	0.43	35.74	000638-36-8
Tri-tetracontane	C ₄₃ H ₈₈	–	–	–	0.20	35.85	007098-21-7
Heptadecane	C ₁₇ H ₃₆	–	–	–	1.35	37.23	000629-78-7
Octadecane	C ₁₈ H ₃₈	–	–	–	4.06	39.60	000593-45-3
Neophytadiene	C ₂₀ H ₃₈	2.45	6.84	–	–	41.03	000504-96-1
Hexanamide	C ₆ H ₁₃ NO	–	–	–	1.57	43.51	998195-79-6
Hexadecanoic acid	C ₁₆ H ₃₂ O ₂	10.5	4.07	0.85	8.69	44.18	000057-10-3
14β-Pregnane	C ₂₁ H ₃₆	–	–	–	1.00	44.55	998433-89-7
1,7-Dimethyl Phenanthrene	C ₁₆ H ₁₄	–	–	–	8.63	45.85	000483-87-4
Phytol	C ₂₀ H ₄₀ O	–	4.63	–	–	47.51	000150-86-7
Azaperone	C ₁₉ H ₂₂ FN ₃ O	–	–	–	3.51	48.08	001649-18-9
Linoleic acid	C ₁₈ H ₃₂ O ₂	2.06	–	–	–	48.23	998405-19-4
Ethyl linoleate	C ₂₀ H ₃₆ O ₂	4.81	–	–	5.23	48.55	000544-35-4
14-Pentadecenoic acid	C ₁₅ H ₂₈ O ₂	–	–	–	7.52	48.66	017351-34-7
9,12,15-Octadecatrienoic acid	C ₁₈ H ₃₆ O ₂	14.0	3.97	–	–	48.73	001191-41-9
Octadecanoic acid	C ₁₈ H ₃₆ O ₂	4.71	17.1	17.1	10.04	49.22	000111-61-5
Hexacosane	C ₂₆ H ₅₄	–	–	3.12	–	51.42	000630-01-3
Tetracosane	C ₂₄ H ₅₀	–	–	4.40	–	54.14	000646-31-1
Nonadecane	C ₁₉ H ₄₀	4.04	1.73	5.75	0.74	56.83	000629-92-5
Tricosane	C ₂₃ H ₄₈	2.63	1.32	0.57	–	57.65	000638-67-5
Heneicosane	C ₂₁ H ₄₄	–	–	5.82	–	58.08	000629-94-7
Docosane	C ₂₂ H ₄₆	–	–	9.82	–	58.48	000629-97-0
Heptacosane	C ₂₇ H ₅₆	5.45	–	–	–	59.72	000593-49-7
Octacosane	C ₂₈ H ₅₈	–	–	8.51	–	60.73	000630-02-4
Eicosane	C ₂₀ H ₄₂	0.68	7.31	4.63	–	61.78	000112-95-8
β-Sitosterol	C ₂₉ H ₅₀ O	1.49	–	–	–	68.91	000083-46-5

cosane, eicosane, heneicosane, heptacosane, docosane, and octacosane are among the hydrocarbons detected based on GC-MS results. Among these compounds, eicosane is interesting for its antibacterial activity,⁴⁴ heneicosane for its antimicrobial effect,⁴⁵ and tetracosane, heptadecane, hexadecane for its antioxidant and antimicrobial properties.^{44,46,47} Decaborane, which is found in the leaf part of *O. mutabilis*, attracts attention due to its toxic and volatile properties.⁴⁸ 1H-Indole, an aromatic organic compound, was detected in all parts of the plant, including flowers, leaves, stems, and roots. In the study by Jabbar in 2021 that evaluated the phytochemical content, antioxidant properties and toxicity of *O. mutabilis*, the plant was examined as a whole and the contents of flowers, leaves, stems, and roots of the plant were not compared in terms of phytochemicals. However, according to our results, the parts of the flower, leaves, stem and root of the plant contain different bioactive species at different rates. On the contrary, among the 29 compounds found in our study, unlike Jabbar's previous report, many different compounds have been detected, mainly phytol, neophytadiene, 14β-Pregnane, 1H-Indole, linoleic acid, ethyl linoleate, 14-pentadecenoic acid, 9,12,15-octadecatrienoic acid, octadecanoic acid, tricosane,

hexacosane, tetracosane, heneicosane, heptacosane, docosane, and octacosane. Therefore, endemic *O. mutabilis* can be considered as a bioactive agent with superior potential for pharmacological and chemical applications.

4. Conclusion

Ethanol extracts obtained from different parts of *O. mutabilis* collected from the Mersin region of Turkey have antioxidant and antibacterial effects due to the large number of bioactive compounds (hexadecanoic acid and β-sitosterol, etc.). Our results show that there is a positive correlation between the amount of phenolic substances and free radical scavenging activities. In our study, the root and stem showed the highest antioxidant activity, respectively. Furthermore, it was found that the root, stem, leaf, and flower extracts of the plant were effective against *A. baumannii* bacteria known as a nosocomial infection agent. Due to the limited information on the anticancer, anti-inflammatory, antifungal, and many other molecular-level properties of the plant, more studies are needed for its pharmaceutical and industrial use.

Funding:

The authors would like to thank to Mersin University Scientific Research Project Unit for financial support (Project no: 2017-2-TP2-2516).

5. Reference

- L. Cecchi, A. Coppi, F. Selvi. *Phytotaxa*. **2016**, 288, 201–213. DOI:10.11646/phytotaxa.288.3.1
- M. Firat, R. Binzet. *Adansonia* **2021**, 43, 185-195. DOI:10.5252/adansonia2021v43a16
- R. Binzet, Ö. Eren. *Phytotaxa* **2018**, 356, 117-130. DOI:10.11646/phytotaxa.356.2.2
- R. Binzet. *Turk J Bot* **2016**, 40, 194-200. DOI:10.3906/bot-1410-23
- A. Tosun, K. E. Akkol, O. Bahadir, E. Yeşilada. *J. Ethnopharmacol.* **2008**, 120, 378-381. DOI:10.1016/j.jep.2008.09.007
- U. Ozgen, M. Ikbal, A. Hacimuftuoglu, P. J. Houghton, F. Gocer et al. *J. Ethnopharmacol.* **2006**, 104, 100-103. DOI:10.1016/j.jep.2005.08.052
- V. López, S. Akerrreta, E. Casanova, J. M. García-Mina, R. Y. Cavero et al. *Plant Food Hum. Nutr.* **2007**, 62, 151-155. DOI:10.1007/s11130-007-0056-6
- R. Verpoorte. *J. Pharm. Pharmacol.* **2000**, 52, 253-262. DOI:10.1211/0022357001773931
- L. Yarmolinsky, M. Bronstein, J. Gorelick. *Isr. J. Plant Sci.* **2015**, 62, 294-297. DOI:10.1080/07929978.2015.1067076
- Z. Wang, Y. Zhou, X. Shi, X. Xia, Y. He et al. *Food Biosci.* **2021**, 42, 101206. DOI:10.1016/j.fbio.2021.101206
- N. Aelhidar, A. Nafis, A. Kasrati, A. Goehler, J. A. Bohnert et al. *Ind. Crop. Prod.* **2019**, 130, 310-315. DOI:10.1016/j.indcrop.2018.12.097
- A. A. Jabbar. *Food Sci. Nutr.* **2021**, 9: 5755-5764. DOI:10.1002/fsn3.2544
- P. Ersan, Ö. Sönmez, B. Gözmen. *J. Iran. Chem. Soc.* **2020**, 17, 871-879. DOI:10.1007/s13738-019-01824-x
- S. B. Iloki-Assanga, L. M. Lewisluján, C. L. Laraespinoza, A. A. Gilsalido, D. Fernandezangulo et al. *BMC Res. Notes* **2015**, 8: 1-14. DOI:10.1186/s13104-015-1388-1
- R. Apak, K. Güçlü, M. Özyürek, S. Çelik. *E. Microchim. Acta* **2008**, 160, 413-419. DOI:10.1007/s00604-007-0777-0
- A. W. Bauer, W. M. Kirby, J. C. Sherris, M. Turck. *Am. J. Clin. Pathol.* **1966**, 45, 493-496. DOI:10.1093/ajcp/45.4_ts.493
- V. L. Singleton, R. Orthofer, R. M. Lamuela-Raventos. *Methods Enzymol.* **1999**, 299, 152-178. DOI:10.1016/S0076-6879(99)99017-1
- C. Sarikurkcu, B. Kirkan, M. S. Ozer, O. Ceylan, N. Atilgan, M. Cengiz, B. Tepe. *Ind. Crop. Prod.* **2018**, 115, 323-329. DOI:10.1016/j.indcrop.2018.02.040
- C. Sarikurkcu, E. Demir, M. S. Ozer, R. Binzet. *Int. J. Plant Pharm.* **2022**, 2, 128-135.
- B. Kirkan, C. Sarikurkcu, M. S. Ozer, M. Cengiz, N. Atilgan, O. Ceylan, B. Tepe. *Ind. Crop. Prod.* **2018**, 125, 549-555. DOI:10.1016/j.indcrop.2018.09.043
- B. Dousti, F. Nabipor. *J. Biotechnol. Comp. Biol. Bionanotechnol.* **2021**, 102, 377-386. DOI:10.5114/bta.2021.111095
- B. Emsen, B. Surmen, H. S. Karapinar. *Plant Biosyst.* **2022**, 1-10. DOI:10.1080/11263504.2023.2165561
- H. Koraqi, FC Ajazi, K. Kimete Lluga-Rizani, S. Kazlauskaitė. *Croat. J. Food Sci. Technol.* **2022**, 14: 1-8. DOI:10.17508/CJFST.2022.14.1.12
- M. M. Ebulue. *ASEAN J. Sci. Eng.* **2022**, 3, 69-78. DOI:10.17509/ajse.v3i1.45017
- J. R. Soares, T. C. P. Dins, A. P. Cunha, L. M. Ameida. *Free Rad. Res.* **1997**, 26, 469-478. DOI:10.3109/10715769709084484
- T. H. Lee, C. H. Lee, P. Y. Ong, S. L. Wong, N. Hamdan et al. *S. Afr. J. Bot.* **2022**, 148: 170-179. DOI:10.1016/j.sajb.2022.04.026
- F. B. Mukeba, J. B. Mukoko, M. M. Mayangi et al. *Eur. J. Med. Plants* **2020**, 31: 33-47. DOI:10.9734/ejmp/2020/v31i12030355
- H. Kikuzaki, M. Hisamoto, K. Hirose, K. Akiyama, H. Tani-guchi. *J. Agric. Food Chem.* **2002**, 50: 2161-8. DOI:10.1021/jf011348w
- K. Saravanakumar, C. Sarikurkcu, R. T. Sarikurkcu, M. H. Wanga. *Ind. Crop. Prod.* **2019**, 142, 111878. DOI:10.1016/j.indcrop.2019.111878
- C. Sarikurkcu, S. S. Sahinler, B. Tepe. *Ind. Crop. Prod.* **2020**, 154, 11263. DOI:10.1016/j.indcrop.2020.112633
- N. Kumar, A. Singh, D. K. Sharma, K. Kishore. *Int. J. Pharm. Biol. Sci.* **2017**, 7 (3), 30-35.
- B. Kirkan, C. Sarikurkcu, A. S. Tepe. *Biointerface Res. Appl. Chem.* **2023**, 13 (1): 1-10. DOI:10.33263/BRIAC131.088
- M. Rafi, L. Wulansari, D. A. Septaningsih, T. F. Purnomo, R. Auliatifani, K. Khaydanur et al. *J. Trop. Life Sci.* **2021**, 11, 375-382. DOI:10.11594/jtls.11.03.14
- P. Z. Moghaddam, M. Mazandarani, M. R. Zolfaghari, M. T. Badelehand, E. A. Ghaemi E. *Afr. J. Microbiol. Res.* **2012**, 6, 1776-1781. DOI:10.5897/AJMR11.1225
- A. Halim, M. A. Zeb, M. Sajid, T. U. Rahman, K. F. Khattak, S. Ullah, et al. *J. Microbiol. Exp.* **2015**, 3: 00074. DOI:10.15406/jmen.2015.02.00074
- M. Saha, P. K. Bandyopadhyay. *Microb. Pathog.* **2020**, 141: 103977. DOI:10.1016/j.micpath.2020.103977
- V. Aparna, K. V. Dileep, P. K. Mandal, P. Karthe, C. Sadasivan et al. *Chem. Biol. Drug Des.* **2012**, 80, 434-439. DOI:10.1111/j.1747-0285.2012.01418.x
- D. Richard, K. Kefi, U. Barbe, P. Bausero, F. Visioli. *Pharmacol. Res.* **2008**, 57, 451-455. DOI:10.1016/j.phrs.2008.05.002
- C. C. M. P. Santos, M. S. Salvadori, V. G. Mota, L. M. Costa, A. A. C. Almedia et al. *J. Neurosci.* **2013**, 949452. DOI:10.1155/2013/949452
- Y. Song, S. K. Cho. *Biochem. Anal. Biochem.* **2015**, 4: 1-7. DOI:10.4172/2161-1009.1000211
- S. Vats, T. Gupta. *Physiol. Mol. Biol. Plants* **2017**, 23, 239-248. DOI:10.1007/s12298-016-0407-6
- D. Durak, Y. Kalender. *Folia Biol.* **2007**, 55, 133-141. DOI:10.3409/173491607781492551
- S. Babu, S. Jayaraman. *Biomed. Pharmacother.* **2020**, 131, 110702. DOI:10.1016/j.biopha.2020.110702

44. O. Boussaada, S. Ammar, D. Saidana, J. Chriaa, I. Chraif et al. *Microbiol. Res.* **2008**, *163*, 87–95. DOI:10.1016/j.micres.2007.02.010
45. V. Vanitha, S. Vijayakumar, M. Nilavukkarasi, V. N. Punitha, E. Vidhya, P. K. Praseetha. *Ind. Crop. Prod.* **2020**, *154*, 112748. DOI:10.1016/j.indcrop.2020.112748
46. T. Rhetso, R. Shubharani, M. S. Roopa, V. Sivaram. *Future J. Pharm. Sci.* **2020**, *6*, 1–9. DOI:10.1186/s43094-020-00100-7
47. S. Yogeswari, S. Ramalakshmi, R. Neelavathy, J. Muthumary. *Glob. J. Pharmacol.* **2012**, *6*, 65–71. DOI:10.1080/00431672.2012.666178
48. G. B. Dunks, K. Palmer-Ordonez, E. Hedaya, P. Keller, P. Wunz. *Inorg. Synth.* **1984**, *22*, 202–207. DOI:10.1002/9780470132531.ch46

Povzetek

Rod *Onosma L.* (Lithospermae, Boraginaceae) vsebuje številne rastlinske vrste, ki imajo zaradi številnih fitokemikalij terapevtske lastnosti. *Onosma mutabilis* Boiss. & Hausskn. ex Boiss. (*Onosma mutabilis*) je vrsta, za katero ni dovolj podatkov o njenih značilnostih.

Cilj: Raziskali smo skupno vsebnost fenolov, antioksidativno aktivnost, možne bioaktivne spojine in antibakterijske aktivnosti etanolnih izvlečkov listov, stebela, korenin in cvetnih delov endemične *O. mutabilis*.

Zaključki: Skupna vsebnost fenolov v vseh ekstraktih *O. mutabilis* se je gibala med 9,2 in 31 mg ekvivalentov galne kisline (GAE)/g ekstrakta. Glede na rezultate antioksidativne aktivnosti so bile vrednosti antioksidativne kapacitete IC₅₀, določene z metodo 1,1-difenil-2-pikrilhidrazil (DPPH), med 4,39 in 29 µg/ml, medtem ko je bila ekvivalentna antioksidativna aktivnost trolox, določena z merjenjem reducirajoče antioksidativne vrednosti bakrovih ionov (CUPRAC), 0,45–0,78 mmol trolox ekvivalentov (TE)/g ekstrakta. Bioaktivne spojine so bile analizirane z uporabo plinske kromatografije v povezavi z masno spektrometrijo (GC/MS) in ugotovljeno je bilo, da vsebujejo 29 različnih kemičnih sestavin. Vsi testirani rastlinski izvlečki so pokazali učinkovito antibakterijsko delovanje proti *A. baumannii* (ATCC 02026) (vrednost minimalne inhibitorne koncentracije (MIC) 62,5 µg/ml) v primerjavi z referenčnim zdravilom ampicilin (125 µg/ml).



Except when otherwise noted, articles in this journal are published under the terms and conditions of the Creative Commons Attribution 4.0 International License

Scientific paper

Design, Development and Optimization of Carmustine-Loaded Freeze-Dried Nanoliposomal Formulation Using 3² Factorial Design Approach

Sandip M. Honmane^{1,2*}, Manoj S. Charde² and Riyaz Ali M. Osmani³

¹ Department of Pharmaceutics, Annasaheb Dange College of B. Pharmacy, Ashta, Shivaji University, Kolhapur 416301, Maharashtra, India.

² Department of Pharmaceutical Chemistry, Government College of Pharmacy, Karad, Shivaji University, Kolhapur 415124, Maharashtra, India.

³ Department of Pharmaceutics, JSS College of Pharmacy, JSS Academy of Higher Education and Research, Mysuru 570015, Karnataka, India

* Corresponding author: E-mail: sandiphonmane@gmail.com
Mob: +918600392878

Received: 01-05-2023

Abstract

The objective of the current study was to develop and optimize a novel lyophilized liposomal formulation of anticancer agent carmustine, or bis-chloroethyl nitrosourea (BCNU) for prolonged release that could overcome the dose-dependent side effects and improve its bioavailability at the site of action. The optimization was done using a 3² factorial design approach wherein soya phosphatidylcholine (SPC) and cholesterol (CH) as independent variables. The optimized formulation (F4) exhibited high entrapment efficiency (81.57%) with an average vesicle size of 141.7 nm and a –22.6 mV Zeta potential. *In-vitro* drug release studies from all formulations revealed that the BCNU was released for up to 36 hours following the Higuchi matrix release model. The TEM, FTIR, DSC, PXRD, and SEM analyses confirm the formation of liposomes. BCNU-loaded nanoliposomal formulation demonstrated prolonged release, suggesting that it could be used to supplement cancer therapy efficiently with a reduction in dose-dependent side effects.

Keywords: Carmustine; Nanoliposomes; 3² Factorial design; Release kinetics; Freeze-drying.

1. Introduction

Despite the fact that cancer has been the second leading cause of mortality in the 21st century (besides cardiac ailments), it is plausibly the most complex disease and a serious health threat to people.^{1,2} Currently, to treat cancer, physicians use chemotherapy, hormone treatment, gene therapy, surgery, and radiation therapy. Usually, cancer is treated with chemotherapy. On the other hand, high doses of chemotherapy drugs have undesired side effects and can be harmful to the body.³ In comparison to conventional chemotherapy, the nanocarrier-targeted drug delivery system offers the advantage that it reduces drug exposure to healthy tissues and the risk of organ and tissue damage, which reduces the development of multi-drug resistance and improves bioavailability.^{4–7} Moreover, a nano-

carrier drug delivery system can also reduce toxicity and chemotherapy costs while achieving a long biological half-life and controlled drug release of chemotherapeutic drugs. Over time, a variety of nanocarriers have been developed for the delivery of tumor-specific drugs, including micelles, liposomes, inorganic nanoparticles, polymeric nanoparticles, nanorods, and others.^{8,9}

Liposomes might be one of the most promising drug delivery systems. It consists of one or more concentric phospholipid bilayers formed from synthetic or natural phospholipids that surround an aqueous core. They can include both hydrophilic and lipophilic molecules while yet being dispersed in water as a result of a phospholipid bilayer. These features make liposomes a special nano-carrier for the delivery of biological therapeutics.^{10,11} Furthermore, because liposomes are comprised of naturally oc-

curing substances found in biological membranes, they offer the advantages of being biodegradable and non-toxic. Currently, liposomes are a desirable delivery system because of their flexibility, structure, and colloidal size.¹² Liposomes have been produced using a variety of manufacturing techniques and lipid compositions in sizes ranging from nanometres to micrometres. More flexible liposomes can be created by altering the bilayer elements, which produce hard, impermeable, or porous and stable vesicles.¹³ For their improved solubility, precise drug targeting, and controlled release of different formulations, liposomes are widely preferred nowadays.¹⁴ According to the results of numerous experimental studies, cancer cells prefer nanoparticles up to 500 nm due to their enhanced penetration and retention effects (EPR). Nanoparticles as small as 500 nm can extravasate because the blood arteries in tumor cells are more permeable than those in healthy tissue.^{15,16}

The sole FDA-approved chemotherapeutic drug to treat high-grade gliomas (HGG) is carmustine or BCNU.¹⁷ It is a non-specific, alkylating antineoplastic drug that is used to treat many malignant neoplasms, including brain tumors.¹⁸ Multiple pathways are used by BCNU to cause tumor cytotoxicity, and it frequently disrupts DNA transcription and replication.¹⁹ In addition, BCNU binds to and alters (carbamoyletes) glutathione reductase enzyme leading to cell death.²⁰

BCNU's short half-life of about 15 to 30 minutes and high toxic side effects (lung fibrosis and bone marrow suppression) limit its efficacy in treating glioma; these are among its most significant disadvantages. Furthermore, it has poor bioavailability due to hepatic metabolism.^{21–23} Therefore, an advanced novel prolonged-release formulation is needed for the efficient delivery of BCNU to the brain and other related malignancies, which may help reduce the dose as well as any dose-related side effects.

Therefore, the current work sought to evaluate the effects of polymer concentration and other process variables to create and optimize a nanoliposomal formulation with the desired size range, high entrapment efficiency, and prolonged release of BCNU, an anticancer drug.

2. Materials and Methods

2.1. Materials

BCNU was received as a gift sample from Emcure Pharmaceuticals Ltd., Pune, Maharashtra, India. SPC was provided by the German company lipoid GmbH as a gift sample. CH, chloroform, and methanol were purchased from Loba Chemie Pvt. Ltd. Mumbai, Maharashtra, India. The other solvents and materials employed were of an analytical standard.

2.2. Optimization of the Solvent System

The solvent system for the lipid phase was optimized using several combinations of organic solvents, specifical-

ly, methanol and chloroform and the homogeneity of the film was assessed as depicted in Table 1.

Table 1. Optimization of the solvent system

Trial	Chloroform (mL)	Methanol (mL)	Observation
1	3	0	Uniform, transparent film
2	3	1	Non-uniform sticky flocks
3	3	2	Non-uniform sticky flocks
4	3	3	Non-uniform sticky flocks
5	0	3	Non-uniform sticky flocks

2.3. Optimization of Process Parameters for Preparation of Liposomes

Using chloroform as an organic solvent, preliminary optimization of the speed of rotation and hydration medium for uniform film formation and maximal drug entrapment efficiency of liposomes was investigated. To create a thin and uniform film, which controls the liposomal preparation process's result, the speed of rotation was changed from 30 revolutions per minute (rpm) to 90 rpm during film deposition under vacuum as depicted in Table 2. The drug's ability to become entrapped in liposomes depends on the pH of the phosphate buffer. Entrapment efficiency was calculated after the pH of the hydration buffer was changed to levels closer to the drug's pKa using phosphate buffer saline (PBS) solution pH 5.0, 6.8, and 7.4 as depicted in Table 2.

Table 2. Optimization of process parameters

Parameters	Variable	Observation
Speed of (rpm) rotary evaporator	30	A thin and uniform film
	60	A non-uniform film with flocks at the centre of round bottom flask (RBF)
	90	A non-uniform film with flocks at the centre of RBF
The pH of Hydrating medium	5.0	F4 (38.48 %)
	6.8	F4 (57.59 %)
	7.4	F4 (81.57 %)

2.4. Preparation of Liposomes

A small modification to the thin film hydration process was used to produce blank and BCNU-loaded liposomes. SPC and CH were dissolved in chloroform as an organic phase at various molar ratios, along with BCNU (5 mg), to obtain a 60 mg/mL lipid phase concentration in a 250 mL rotary flask. The flask was attached to a rotary evaporator (Aditya Scientific, Hyderabad) that revolved at 30 rpm while immersed in a water bath that was maintained at 40 °C temperature and vacuumed for an hour to form the film.^{10,11} Table 3 depicts the components of the liposomal formulation.

After the organic phase had evaporated, the flask was placed in a desiccator overnight to remove any remaining organic solvent residues from the film. The following day, a liposome with a 10 mg/mL lipid concentration was produced by thoroughly hydrating the thin film with PBS solution, pH 7.4, for one hour at a constant rotation of 160 rpm. To transform the produced liposomes from multilamellar to unilamellar vesicles, they were subjected to Ultra Turrax (IKA T25) at 7000 rpm for 15 min. Then they were passed through a high-pressure homogenizer (HPH) (GEA Lab, Panda PLUS 1000) at 200 bar pressure for 50 cycles to reduce particle size and obtain uniform sized-liposomes at the required nanometre size. The produced nanoliposomes were stored at 4 °C for further use.

Table 3. Optimization of BCNU-loaded liposomal formulation using a 3²-factorial design

Formulation code	Factors [A:B] (mg)	SPC:CH Molar Ratio	Lipid: Drug ratio (mg)
F1	60(-1):20(-1)	1:0.67	16:1
F2	60(-1):40(0)	1:1.33	20:1
F3	60(-1):60(+1)	1:2	24:1
F4	70(0):20(-1)	1:0.57	18:1
F5	70(0):40(0)	1:1.14	22:1
F6	70(0):60(+1)	1:1.71	26:1
F7	80(+1):20(-1)	2:1	20:1
F8	80(+1):40(0)	1:1	24:1
F9	80(+1):60(+1)	1:1.5	28:1

2. 5. Full Factorial Design

The BCNU-loaded liposomes were developed using a 3² factorial design. In this approach, the quantities of SPC (A) and CH (B) were evaluated as independent variables. The fixed responses used were vesicle size (Y_1) and percent drug entrapment (PDE) (Y_2). By taking each control variable at three distinct levels nine alternative combinations were made, as depicted in Table 3. Later, the best-fit model derived from fit summary and analysis of variance (ANOVA) was used to examine the impact of various control variables on dependent variables. Design-Expert® software point prediction method was used to achieve the predicted formulation and verify optimization.

2. 6. Characterization of BCNU Loaded Liposome

2. 6. 1. Particle Size

The mean vesicle size and size distribution of blank and BCNU-loaded liposomes were measured using a device based on the dynamic light scattering method (HORIBA scientific SZ-100). The liposomal dispersion was di-

luted with distilled water (1:100 v/v ratio, dispersant viscosity 0.896 mPa.s) using an ultrasonicator for 15 minutes to obtain a stable suspension. A portion of the suspension was transferred to a quartz cuvette (four openings). Size analysis was performed using a 90° angle of detection for 120 seconds at room temperature. Analysis was performed in triplicates.³

2. 6. 2. Zeta Potential

Using Zetasizer (HORIBA scientific SZ-100), the surface charge of liposomes was measured. Before being positioned in measuring cells (cuvette with the carbon electrode, 6 mm), all compositions were diluted with distilled water (1:100 v/v). The measurement of average zeta potential and charge on the liposomes was done by subjecting the formulation for 60 seconds run time. Analysis was performed in triplicates.³

2. 6. 3. Entrapment Efficiency

To calculate the total quantity of drug (A) present in the formulation, 2 mL of the liposomal formulation was suspended in 2 mL of methanol to break up the liposomal matrix. This mixture was then centrifuged at 10,000 rpm at 1 °C temperature using a cooling centrifuge (REMI CM-12 Plus) for 30 minutes. The produced pellet was rinsed by overtaxing with a 1 mL PBS solution (pH 7.4) to remove the free drug deposited on the liposome's surface. The resultant dispersion was mixed with 10 ml of PBS solution (pH 7.4) and filtered using a 0.2-micron microsyringe filter. Using a UV/visible spectrophotometer (Shimadzu 1800, Japan), the absorbance was measured at 229 nm to determine the quantity of BCNU in the filtrate.³ For the determination of free drug concentration (B), 2 mL of a drug-loaded liposomal mixture was centrifuged at 10,000 rpm at 1 °C for 30 minutes using a cooling centrifuge. The supernatant was discarded and diluted it with 10 mL of PBS solution (pH 7.4). The resultant solution was filtered through a microsyringe filter (0.2 µm), and absorbance was measured at 229 nm using a UV/visible spectrophotometer.³ The entrapment efficiency was calculated by using a formula-

$$PDE = \frac{A-B}{A} \times 100$$

Where 'A' is the total amount of drug and 'B' is the free drug concentration.

2. 6. 4. Transmission Electron Microscopy

TEM images were used to examine the structural integrity of BCNU-loaded liposomes (using Hitachi S-7500). A few drops of diluted liposomal dispersion were applied to a 200-mesh carbon-coated copper grid and photographed at 30,000x magnification and 100 kV.¹⁰

2. 6. 5. *In-vitro* Drug Release Study

An *in-vitro* drug release study of optimized liposomal formulation (F4) and pure drug (BCNU) was carried out by the diffusion method using a dialysis bag. The treated cellophane membrane (molecular weight cutoff [MW-CO] 12 kDa, Thermo Fisher Scientific) was tied at both ends after filling the liposomal sample (equivalent to 5mg of BCNU) in it and placed into the 100 mL beaker containing 50 mL of PBS solution pH 7.4 as a dissolution medium. A magnetic stirrer was used to agitate the dissolving media at 100 rpm while maintaining the temperature at 37 ± 1 °C. 2 mL samples were taken from the receiver at periodic intervals up to 36 h and replaced with equal quantities of fresh dissolving liquid. Using a UV/Visible spectrophotometer, a spectrometric analysis was performed at 229 nm to obtain drug content. Three separate recordings of each reading were taken.²⁴

2. 6. 6. Kinetic Modeling of Release Profiles

Several kinetic models, including zero order, first order, Higuchi matrix, Korsmeyer-Peppas, and Hixson-Crowell, were used to fit the data from *in-vitro* drug release studies of liposomal formulations. The best-suited model was chosen, based on the correlation coefficient with the highest value.³

2. 6. 7. Physical Stability of Liposomal Formulation

As per the ICH guidelines, stability experiments were carried out for the optimized formulation (F4) to evaluate the physical stability. The liposomal formulation (F4) was stored at room temperature (25 ± 2 °C / 60 ± 5 %RH) and in the refrigerator (4 ± 2 °C) for three months. The samples were collected at predetermined intervals of initial, 30, 60, and 90 days to assess their physical appearance, mean vesicle sizes, size distributions, and amounts of drug entrapment as previously mentioned.^{10,25}

2. 6. 8. Optimization of Cryoprotectant and Freeze-Drying Process

The cryoprotectant concentration and formulation parameters that are most likely to affect the freeze-drying cycle and the quality of the finished product were studied. A drug-loaded liposomal sample (F4) was centrifuged for 30 minutes at 10,000 rpm (REMI CM-12 Plus). The supernatant was discarded after centrifugation, and the sediment was collected in glass vials for freeze-drying. Along with the liposomal formulations, the cryoprotectant mannitol was used in various concentrations (lipid: mannitol 1:0w/w, 1:5w/w, 1:10w/w, and 1:15w/w). To produce homogenous ice nucleation, the above mixture was frozen overnight at -50 °C (1 °C/min) in a deep freezer. After

that, it was freeze-dried using Christ, Alpha 1-2 LDplus. The aqueous solvent was then sublimated by maintaining the sample at -50 °C and 0.011 mBar for 12 h. The temperature and pressure were then raised to -20 °C (1 °C/min) and 1.0 mBar for 6 h. Secondary drying was done to remove bound water. For this, the shelf temperature was raised by 1 °C every minute and maintained at 20 °C and 1.6 mBar for almost 3 h. After the process was completed, the vials were sealed with rubber caps and kept at 4 °C for further analysis.²⁶

2. 6. 9. Moisture Content

The Karl Fisher method was used to calculate the remaining moisture (RM) in the freeze-dried cake. 0.1 g of the sample was transferred to the titration cell. The water content was determined using a Metrohm 870 KF Titrino plus KF titrator.

2. 6. 10. Compatibility Studies

Using an FTIR spectrometer (Bruker Alpha II), the FTIR spectra of pure BCNU, physical mixtures, and freeze-dried formulation were recorded and analyzed between the wavelengths of 4000 and 650 cm^{-1} .

2. 6. 11. Differential Scanning Calorimetry

Using the Mettler Toledo DSC 822e instrument, DSC analysis of pure BCNU and a freeze-dried formulation were carried out to check the compatibility. Zinc and indium were used as standards to calibrate the temperature and enthalpy scales. Samples were heated in hermetically sealed aluminium containers at a constant rate of 10 °C/min from -60 to 200 °C. Liquid nitrogen was used at a flow rate of 40 mL/min to create an inert atmosphere.

2. 6. 12. Powder X-ray Diffraction

PXRD is a crucial method for determining whether a substance is crystalline or amorphous. Using a powder X-ray diffractometer (AXS D8 Advances, Bruker Ltd., Germany) diffractograms of a pure drug and formulation were obtained with tube anode Cr spanning the range of 10 – 70 °/ 2θ employing copper as the X-ray target and a 1.54 Å wavelength.

2. 6. 13. Scanning Electron Microscopy

A scanning electron microscope (JSM-6360, Jeol Instruments, Japan) was used to examine the surface morphology of the BCNU-loaded freeze-dried liposomal formulation. With a 15 kV accelerating voltage, photomicrographs were taken of the sample while it was mounted on a double-faced gold-coated adhesive tape.²⁷

3. Results and Discussion

3. 1. Development of the Solvent System

This system used organic solvents to dissolve the lipid phase and form a thin, uniform, and non-sticky film. Since the nature of the film affects the liposomal size and entrapment efficiency. Different compositions of chloroform and methanol were assessed for film formation. From the blend of organic solvents, a thick and sticky film was observed at the centre of the RBF, while chloroform alone produced a thin, uniform, and non-sticky film at the sides of the RBF. The results are depicted in Table 1.

3. 2. Optimization of Process Parameters for Preparation of Liposomes

For the preparation of liposomes, process parameters like the speed of rotation and pH of the hydrating medium were studied for thin, uniform non-sticky film formation and entrapment efficiency, respectively. From the observations, it was found that at slow speed, RBF (30 rpm) produced a uniform non-sticky film at the sides, while at high speed (60 rpm and 90 rpm), lipid phase aggregated at the centre, possibly due to a high central force. The effect of hydrating buffer pH on entrapment efficiency was studied as the pH of hydrating buffer effect on entrapment of the drug into the lipid phase. Entrapment efficiency was varied at different pH values (5.0, 6.8, and 7.4). High entrapment efficiency was observed at a pH of 7.4 as the drug (BCNU) is unionized in aqueous fluid at that pH and more soluble in the lipidic phase while more ionized form at less pH and decreases entrapment into the lipid phase.¹⁸ The results are depicted in Table 2.

3. 3. Full Factorial Design

When compared to unsaturated phospholipids, hydrogenated SPC is more stable and biocompatible. Based on earlier research, SPC and CH concentrations were chosen to produce stable liposomes devoid of any aggregation or fusion, with small vesicles and higher drug entrapment efficiencies. This reveals that the amount of SPC and CH is the more important element in liposome production. Optimized concentrations of SPC (60–80 mg) and CH (20–60 mg) were adequate to synthesize liposomes with small vesicle sizes, excellent drug entrapment, and no aggregation or sedimentation. A full factorial design was employed to investigate the factors systematically. Using DESIGN EXPERT® (version 8.0) software, the impact of different independent variables such as SPC (A) and CH (B) was examined by response surface plots. Figure 1 displays the response to the impacts of independent factors for liposomal vesicle size (Y_1) and PDE (Y_2). The following equations were produced, via regression and graphical analysis of data obtained from the experimental runs, where F ratios were statistically significant ($p < 0.05$), and Adj- R^2 val-

ues ranged from 0.8 to 1. The data was well-fit by these model equations.

The effect on vesicle size (Y_1) and PDE (Y_2) was observed to be significant by ANOVA and the linear equation was found as follows:

$$Y_1 = +153.13 + 8.47A + 6.83B \quad (1)$$

$$Y_2 = +63.68 + 3.88A - 10.84B \quad (2)$$

The response surface plots and regression equations mentioned above make it clear that the SPC and CH, at varying concentrations, produce a positive association concerning the vesicle size of BCNU-encapsulated liposomes. An increase in lipid concentration within the bilayer led to an increase in size. The level of CH was found to be closely correlated with a slight but substantial ($p < 0.05$) decline in entrapment efficiency. Similar outcomes for several lipophilic medications, such as alpha-tocopherol,²⁸ ciprofloxacin,²⁹ and triamcinolone acetonide,³⁰ have previously been observed. In the liposomal bilayer, CH molecules are positioned between the nearby phospholipid molecules. As a result, they take up some area and compete with BCNU for inclusion in the bilayer. Moreover, CH makes the bilayer stiffer, making it more challenging to incorporate drug molecules.

The adjusted determination coefficient ($R^2 = 0.8948$ and 0.8873 for Y_1 and Y_2 , respectively) and predicted determination coefficient ($R^2 = 0.8217$ and 0.8227 for Y_1 and Y_2 , respectively) values were comparable and showed the high significance of the model. By rejecting the null hypothesis, these “p” values of 0.05 (Prob > F) show that the model terms are significant. The “p” values for vesicle size and PDE were 0.0005 and 0.0006, respectively. For 3^2 factorial design model, the sum of the “p” values and the “adjusted R^2 ” values reveals a substantial synergistic association between both independent variables at $P < 0.05$.

3. 4. Characterization of BCNU Loaded Liposome

3. 4. 1. Particle Size

The mean vesicle size of the various drug-loaded liposomal formulations, which had 20–60 mg CH and 60–80 mg SPC, was found to be between 141.0 and 170.9 nm. For drug-loaded liposomes, the polydispersity index ranged from 0.31 to 0.53, indicating narrow vesicle size dispersion shown in Table 4. A slightly small range of size distribution was present in every liposomal formulation. The amount of SPC and CH present was significantly related to the size of the drug-loaded liposomes. Rather than the lipid content in the liposomal dispersion, the CH enhances the stiffness of the membrane. Figure 2 shows a typical particle size distribution profile obtained for the optimized formulation (F4).

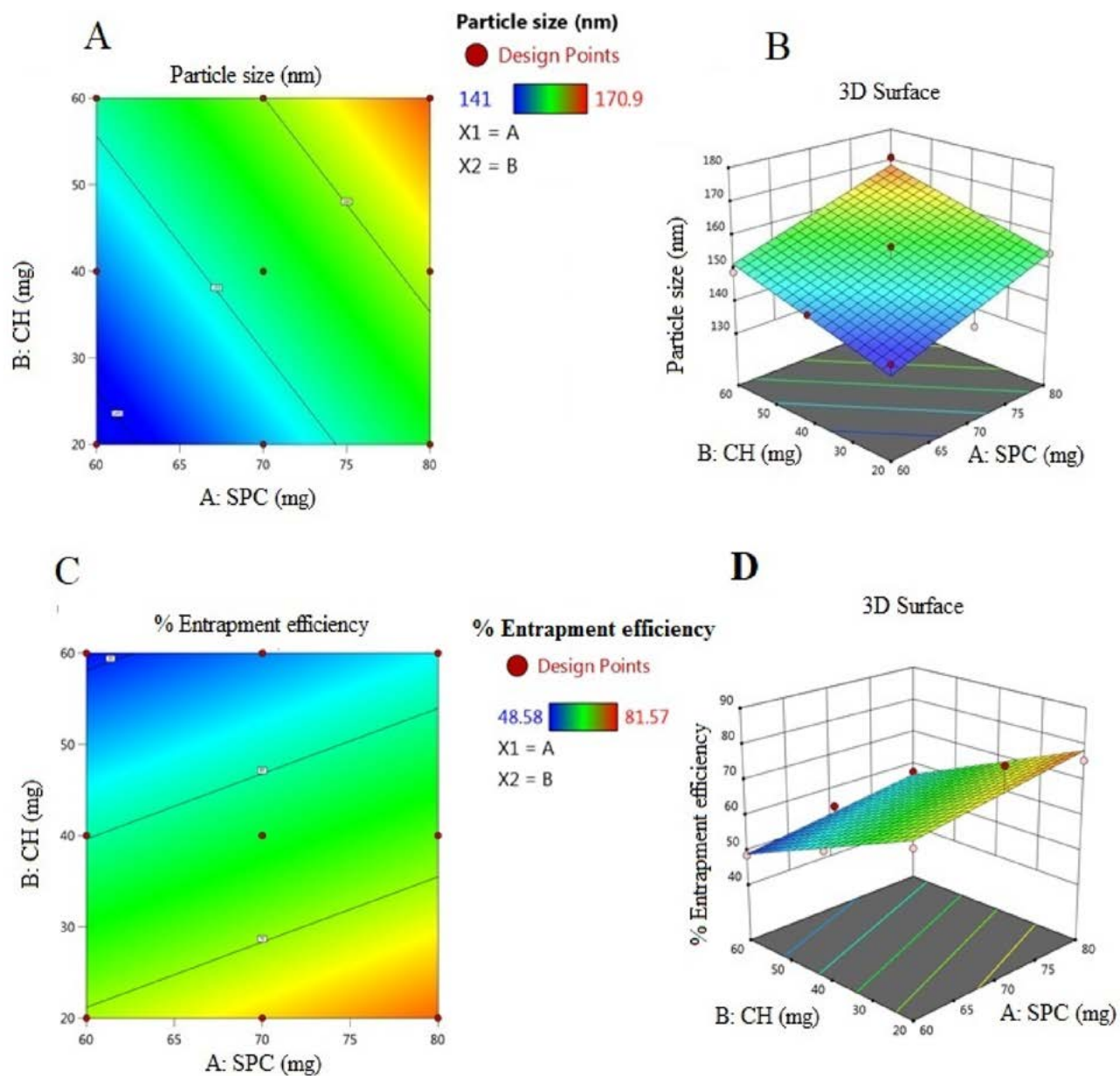


Figure 1. Linear plots (A, C) and Surface response plots (B, D) for particle size and % entrapment efficiency respectively

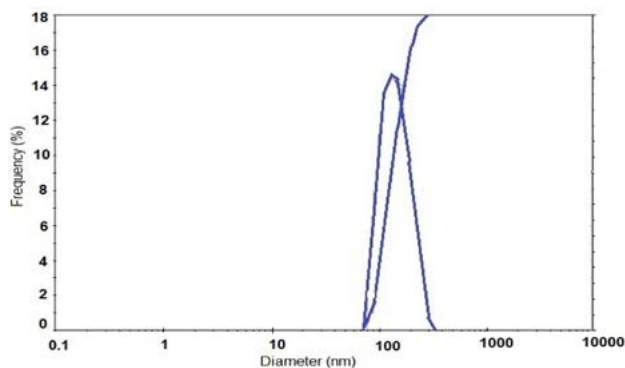


Figure 2. A typical particle size distribution curve of optimized formulation (F4)

3. 4. 2. Zeta Potential

Zeta potential measurements provide information on particle charge and the stability of the dispersion. Zeta potential shows the degree of repulsion between the charged particles in the dispersion. High zeta potential indicates highly charged particles, which avoids particle aggregation owing to electrostatic repulsion. If the zeta potential is low, attraction overcomes repulsion and the dispersion forms aggregates. A zeta potential value of +30 mV to −30 mV is thought to be optimal for good stabilization.³¹ High zeta potential values, between ±20 and ±40 mV, offer system stability and are less prone to agglomeration formation or particle size growth. However, it should be noted that zeta potential

values are not an absolute measure of nanoparticle stability.³¹

The zeta potential of freshly prepared liposomes ranged from -18.9 mV to -32.7 mV revealing that they had enough charge and mobility to prevent vesicle aggregation (Table 4). The Zeta potential of the optimized formulation (F4) was depicted in Figure 3.

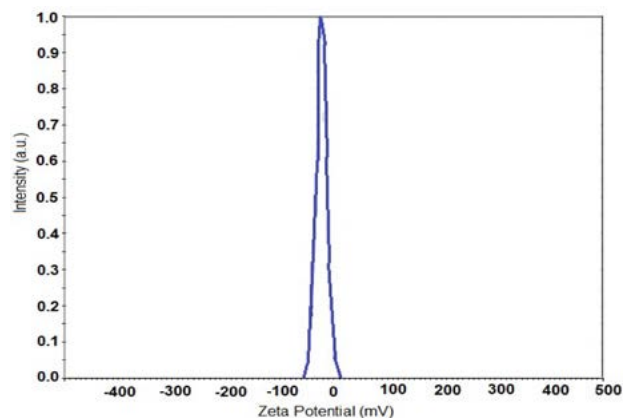


Figure 3. Zeta potential of optimized formulation (F4)

3. 4. 3. Percentage Drug Entrapment

PDE is measured as the drug retention in liposomes as a percentage of the total drug. Percent entrapment efficiency for all formulations was found to be between 48.58% – 81.57% depicted in Table 4. The amount of SPC and CH optimized for liposomal formulation by considering the small vesicle size and maximum entrapment efficiency because these characteristics predominantly affect the encapsulation of the drug. Furthermore, smaller vesicle size offers better uptake by the cells and augmented drug deposition. Entrapment of the drug may be directly related to the overall surface area, as there are a higher number of vesicles more quantity of the drug will be entrapped. As the particle size decreases, the surface area increases that subsequently results in an increase in drug

encapsulation. PDE in liposomes demonstrates that drug entrapment efficiency in the liposomes decreases with decreasing SPC concentrations. This is because the lipid bilayer is saturated with respect to the drug and has a restricted capacity for entrapment due to its low SPC content.

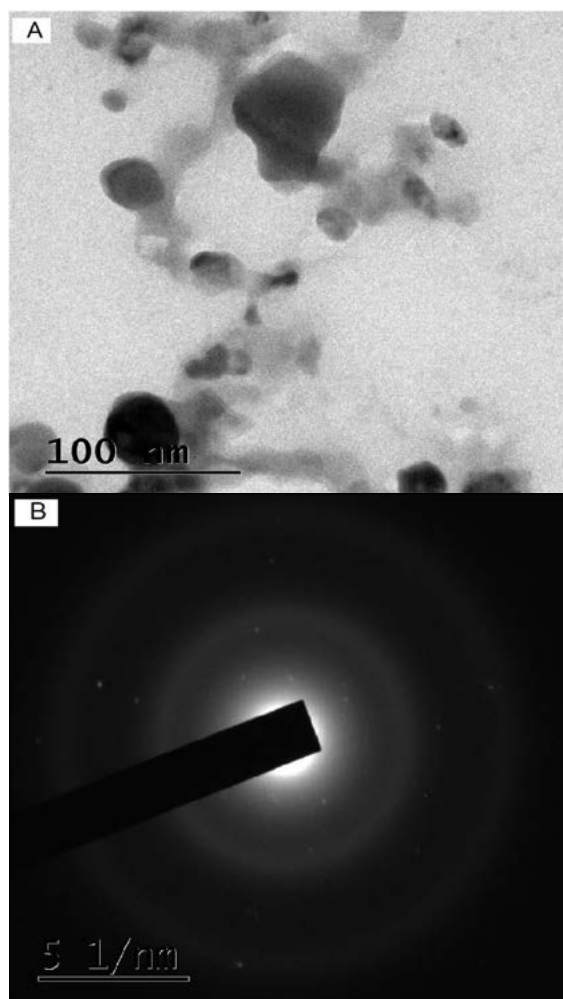


Figure 4. HR-TEM (A) and SAED (B) images of optimized formulation (F4)

Table 4. Vesicle size, PDI, Zeta potential, and PDE of different batches of liposomal formulations

Formulation codes	Before HPH		After HPH		Zeta Potential (mV)	PDE
	Vesicle size (nm)	PDI	Vesicle size (nm)	PDI		
Blank	131.2±0.34	0.453±0.04	95.1±0.42	0.207±0.06	-21.4±0.32	-
F1	215.9±0.42	0.703±0.06	141.0±0.38	0.331±0.08	-11.5±0.42	64.64±0.43
F2	213.2±0.16	0.474±0.02	145.2±0.23	0.472±0.04	-23.2±0.12	58.94±0.74
F3	256.2±0.26	0.416±0.07	149.0±0.52	0.422±0.02	-36.1±0.26	48.58±0.63
F4	219.8±0.46	0.487±0.04	141.7±0.24	0.251±0.03	-22.6±0.36	81.57±0.92
F5	223.2±0.24	0.400±0.06	156.8±0.68	0.382±0.09	-32.6±0.35	61.36±0.34
F6	248.2±0.57	0.290±0.07	158.5±0.44	0.385±0.06	-25.8±0.48	54.60±0.64
F7	254.4±0.46	0.494±0.09	154.7±0.26	0.531±0.04	-18.4±0.16	75.61±0.83
F8	262.5±0.63	0.396±0.09	160.4±0.44	0.315±0.06	-28.9±0.23	62.22±0.93
F9	275.0±0.28	0.951±0.11	170.9±0.34	0.381±0.07	-30.2±0.28	57.60±0.46

Each value represents Mean ± SD, $n = 3$.

Based on the PDE data, it was revealed that when CH concentration increased, it provided rigidity to the bilayer and decreased PDE. Due to the high drug entrapment efficiency and small vesicle size of the F4 formulation, it was determined to be pertinent.

3. 4. 4. TEM Analysis

The TEM image of the optimized formulation (F4) showed spherical liposomes with a small vesicle size with an average particle size of 141.7nm (Figure 4A). Figure 4B showed the selected area electron diffraction (SAED) pattern of liposomes that confirms the formation of liposomes. This supports the results of particle size.

3. 4. 5. In-Vitro Drug Release Studies

The *in-vitro* drug release from the liposomal formulations and the pure BCNU was assessed using a PBS solution with a pH of 7.4. All formulations showed drug release up to 36 h, except the pure BCNU solution, which was released in less than 2 h. All formulations showed more than 90 % drug release within the 36 h (Figure 5). Formulation F4 showed a 96.64 % drug release over 36 h. which indicate controlled release of drug over a prolonged period of time.

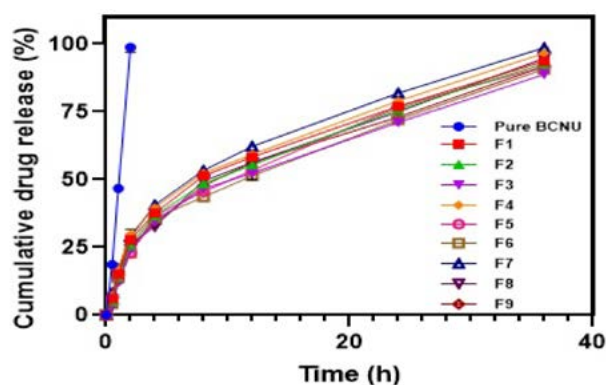


Figure 5. Cumulative % drug release from BCNU liposomes, and pure BCNU

3. 4. 6. Release Kinetic

The data obtained from the *in-vitro* drug release investigation of developed liposomes was fitted into kinetic models to identify the drug release mechanism. For the optimal fitting, the correlation coefficient value (R^2) was used. The values of R^2 for formulations ranged from 0.887 to 0.989. The correlation data for various models for all formulations are displayed in Table 5. According to the measured R^2 values, the Higuchi matrix kinetic model best describes the *in vitro* drug releases from BCNU liposomes. It demonstrates that a diffusion process was adopted to release the drug from the liposomes.

Table 5. Mathematical models in drug release kinetics of liposomal formulations

Formulation codes	Zero order (R^2)	First order (R^2)	Higuchi Matrix (R^2)	Hixon Crowell (R^2)	Korsmeyer-Peppas (R^2)
F1	0.887	0.974	0.980	0.977	0.939
F2	0.900	0.977	0.984	0.981	0.933
F3	0.893	0.978	0.981	0.972	0.899
F4	0.893	0.949	0.981	0.977	0.941
F5	0.913	0.987	0.989	0.986	0.963
F6	0.917	0.973	0.986	0.980	0.920
F7	0.893	0.924	0.984	0.978	0.959
F8	0.905	0.959	0.987	0.978	0.954
F9	0.901	0.972	0.983	0.976	0.901

3. 4. 7. Physical Stability of Liposomal Formulation

The stability of the liposomal formulation is a further essential factor in the development of an effective drug delivery system. As a result, we tested the durability of the improved liposomal formulation in various settings, including room temperature (25 °C / 60 %RH) and the refrigerator (4 °C). At initial, 30, 60, and 90-day intervals, all liposomal formulations were assessed and determined to be stable. At various storage conditions, caking and discoloration were not seen.

As a function of temperature, the mean particle size and formulation entrapment percentage were assessed. The results were depicted in Table 6 and a graphical representation of the change in particle size and entrapment efficiency is shown in Figure 6. Liposomes stored at 4 °C and 25 °C do not differ significantly in mean particle size. The entrapment efficiency showed a little decline, indicating a considerable loss of BCNU from the formulation over time when held at 25 °C. Therefore, based on the findings of the stability study, it is advised that the liposomal formulation be kept in a refrigerator for better stability.

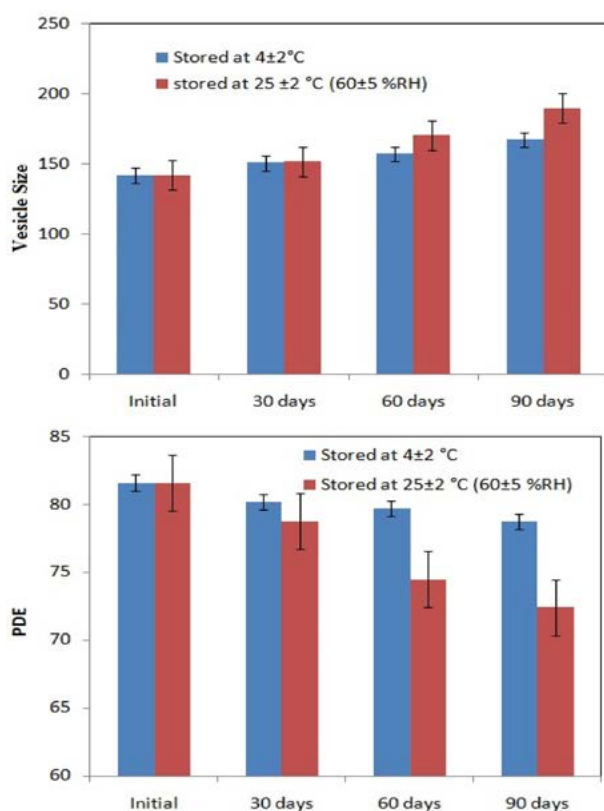
3. 5. Optimization of Cryoprotectant and Freeze-Drying Process

Optimization of the cryoprotectant concentration used in the formulation is essential, along with careful consideration of the process parameter, to enable efficient stability of the liposomes with retaining formulation properties. We need to maintain the product's primary drying temperature below either the glass transition temperature (T_g') or the somewhat higher collapse temperature (T_c) per guidelines for pharmaceutical freeze-drying. Typically, T_c and T_g' can be used interchangeably because they are 1 to 2 °C apart. According to earlier research, the liposomal formulation with mannitol has a T_g' of between -30 and -32 °C. Considering these values, the shelf temperature during primary drying was kept at -50 °C.²⁶

Table 6. The average particle size and PDE of the formulation (F4) stored at various temperatures

Storage temperature	4±2 °C			25 ±2 °C (60±5 %RH)		
Parameter	Vesicle size (nm)	PDE	Zeta Potential (mV)	Vesicle size (nm)	PDE	Zeta Potential (mV)
Initial	141.7±0.24	81.57±0.92	-22.6±0.36	141.7±0.24	81.57±0.92	-22.6±0.36
30 days	150.4±0.32	80.16±0.42	-22.0±0.18	151.4±0.38	78.74±0.23	-24.6±0.12
60 days	156.9±0.25	79.68±0.12	-25.1±0.27	170.3±0.54	74.46±0.32	-25.3±0.24
90 days	167.1±0.37	78.72±0.14	-26.6±0.14	189.4±0.24	72.39±0.42	-25.5±0.18

Each value represents Mean ± SD, *n* = 3.

**Figure 6.** Physical stability of liposomes (F4) stored at different storage conditions; particle size (A) and % drug entrapment (B)

In the first section of the investigation, we explored how freeze-dried liposome stability was affected by mannitol content. This was accomplished by lyophilizing liposomal suspension in the presence of mannitol while varying the weight ratio of lipids to carbohydrates from 1:0 to 1:15. The stability of liposomes during freeze-drying was evaluated by measuring the proportion of the drug that was retained in the liposomes and comparing the size and PDI before and after freeze-drying. Since the drug retained after freeze-drying is closely correlated to the lipid phase transition and the aggregation of particles, it is considered the most sensitive measure that reflects all the harm caused by freeze-drying.

The physicochemical properties of the liposomes were examined before freeze-drying. The liposomes were 141.7 nm in size with a 0.251 PDI, indicating a nar-

row size distribution displayed in Table 4. In the case of non-cryoprotected liposomes, vesicle aggregation/fusion occurred during freeze-drying was evidenced by the size and PDI of the liposomes obtained after rehydration being significantly higher when freeze-dried without a cryoprotectant (control). It reveals that the freeze-drying process without cryoprotectant affects the integrity of the liposomes. Most of the drug that was encapsulated leaked during the process. In contrast, lyophilized formulations with cryoprotectant content demonstrated increased stability as evidenced by narrow size distribution with controlled vesicle size, and less amount of drug leakage shown in Table 7. However, the stability of the liposomes was significantly impacted by the cryoprotectant concentration. A Lipid: mannitol weight ratio of 1:15 during freeze-drying of liposomes produced vesicles that were two times larger than those of the fresh liposomes.

The distribution of population sizes within a given sample is essentially represented by PDI. The PDI's numerical value range is 0.0 (uniform or monodisperse) to 1.0. (Polydisperse). A PDI of 0.3 and below is thought to be acceptable in drug delivery applications using lipid-based carriers, such as liposome and nanoliposome formulations, and it denotes a homogenous (narrow) distribution of phospholipid vesicles.³² Table 7 findings show that the freeze-drying procedure did not affect the PDI of rehydrated liposomes that included cryoprotectant in a different weight ratio, with the liposomes having a similar PDI to liposomes before the freeze-drying process (below 0.3). The size distribution of the liposomes was relatively wide, having a value of 0.661 at high lipid-to-mannitol ratios, 1:15, indicating that aggregation/fusion occurs during the processing. Over a limited range, the weight ratio of carbohydrate to lipid increased while the percentage of drug entrapment was reduced when more carbohydrate was added. The liposome membrane integrity was found to be best preserved at an intermediate ratio of 1:10 (lipid-to-mannitol). Previous literature has reported similar outcomes.³³

Uniform cakes have been seen for all samples with an RM ≤ 5%. For all samples, the secondary drying process eliminated unfrozen water rather slowly, especially when it was done at a temperature of 20 °C. Table 7 displays the RM of cakes and the rehydrated liposomes' characteristics.

Table 7. The effects of mannitol concentration on vesicle size, PDI, PDE, Zeta potential, and RM of a freeze-dried liposomal formulation (F4).

Parameters	Lipid: mannitol weight ratio			
	1:0 (Control)	1:5	1:10	1:15
Vesicle size (nm)	416.6±0.46	237.3±0.62	191.4±0.46	218.5±0.54
PDI	0.933±0.07	0.299±0.08	0.226±0.06	0.661±0.04
PDE	56.40±0.57	72.60±0.53	80.48±0.68	74.67±0.56
Zeta potential (mV)	-26.7±0.38	-27.1±0.64	-28.5±0.49	-23.8±0.32
RM (%)	2.72±0.34	2.20±0.23	2.42±0.32	2.90±0.15

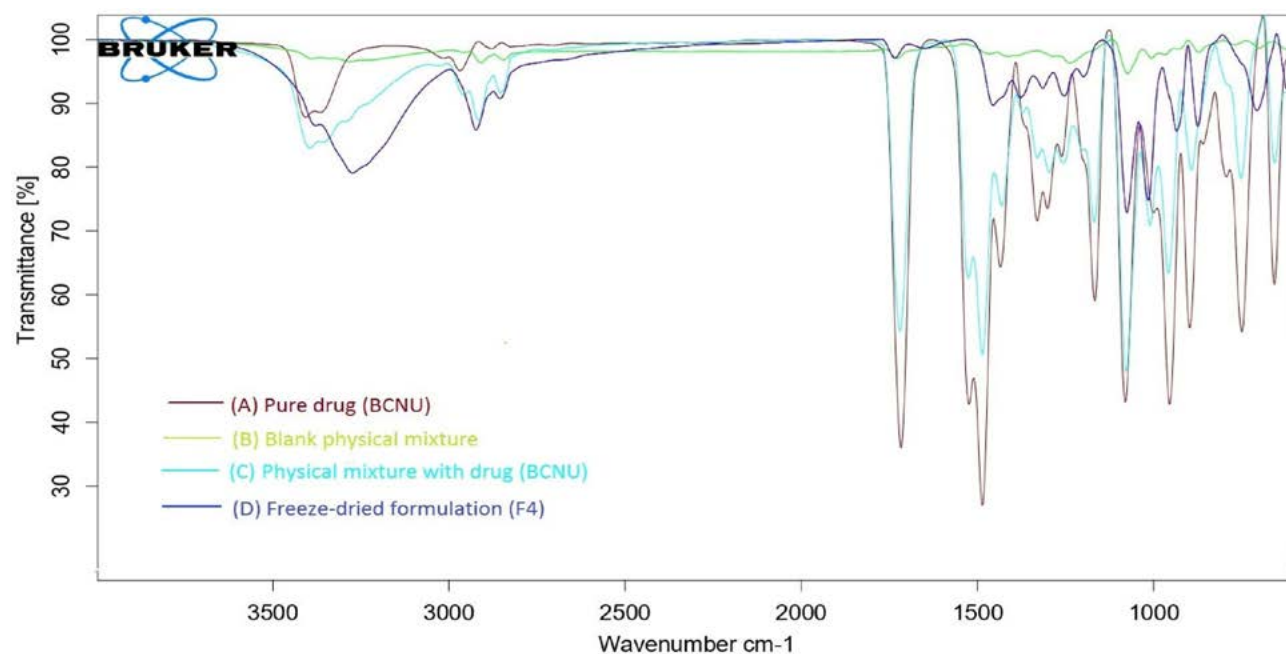
Each value represents Mean ± SD, $n = 3$.

3. 6. Compatibility Studies

Utilizing FTIR tests, it was assessed whether the drug was compatible with other excipients and formulations. Using an ATR-FTIR spectrometer, the infrared spectrum of a pure drug (BCNU) and a physical mixture of a BCNU with excipients and formulation were recorded (Figure 7). The distinctive peaks of the BCNU FTIR spectrum may be seen to correspond to COO^- groups at 1278 and 1456 cm^{-1} and to the double bond $\text{C}=\text{H}$ at 1134 cm^{-1} . Additionally, peaks at 626, 1318, 1354, and 1432 cm^{-1} were observed, which, respectively, corresponded to aromatic CH bending, C-N stretch, aliphatic CH bending, and CH_2 bending. Typical characteristic peaks of the BCNU were also seen in the FTIR spectrum of the physical mixture and formulation with no obvious change from the spectra of the individual drug and excipients. This demonstrated that mannitol, the drug, lipids, and cholesterol did not interact chemically. These findings are consistent with previous research.²¹

3. 7. DSC study

DSC studies were used to analyse the thermal behaviour of pure BCNU, physical mixture and its formulation. The results are displayed in Figure 8. The DSC of pure BCNU shows a prominent endothermic peak at 31 °C and -141.4 J/g, indicating the melting of pure BCNU. The SPC endothermic peak was observed at 48.0 °C (the temperature of the phase transition) and had an enthalpy of -0.551 J/g, whereas the mannitol endothermic peak was observed at 161.0 °C and had an enthalpy of -157.4 J/g. At 148 °C, the typical cholesterol peak was discovered. It might be accounted for by the lipids' nanocrystalline structure in liposomes. The absence of an endothermic peak for BCNU in the formulation indicated that the lipid matrix had completely dissolved BCNU. The retention of the characteristic endothermic peak of mannitol in the formulation suggested its crystallinity and did not interact chemically. The conclusions of the DSC analysis were further supported by the PXRD data.

**Figure 7.** FTIR spectra of the pure drug (BCNU), physical mixture, and optimized formulation (F4)

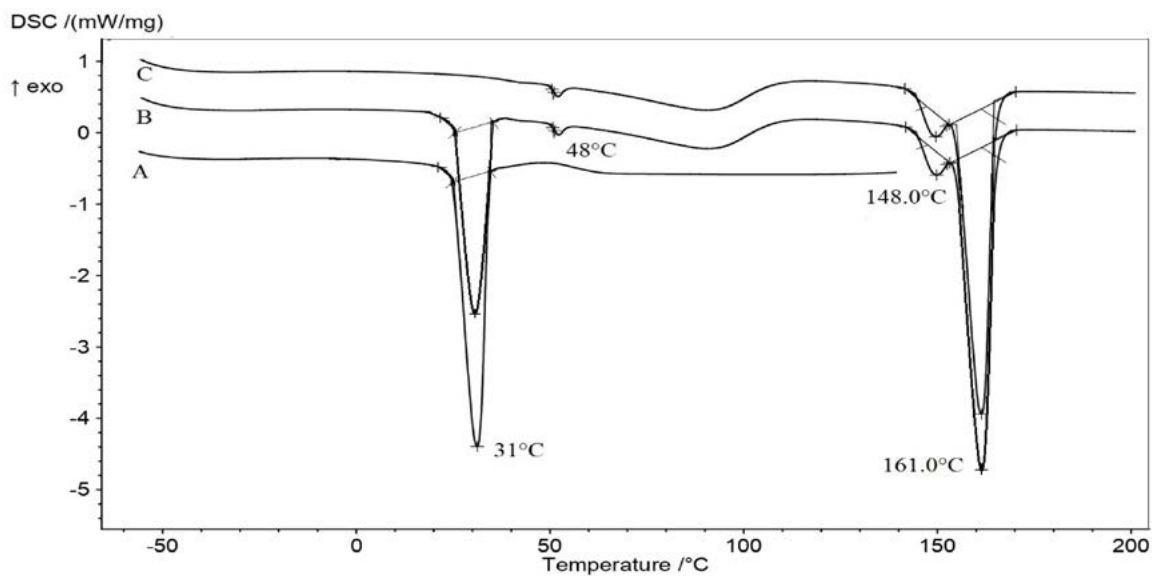


Figure 8. DSC thermogram of the pure drug (BCNU) (A), physical mixture (B), and freeze-dried formulation (F4) (C)

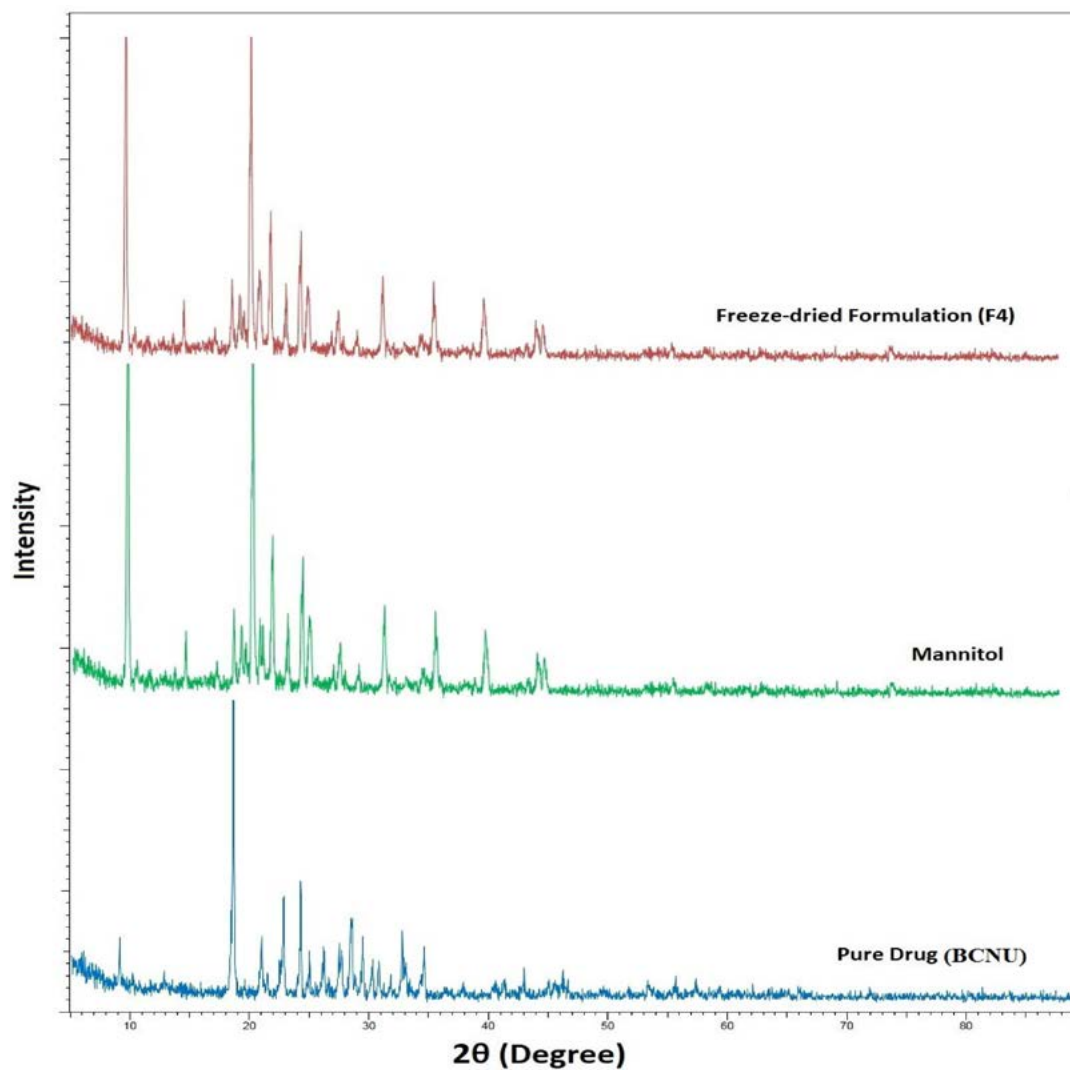


Figure 9. PXRD of the pure drug (BCNU), mannitol, and freeze-dried formulation (F4)

3. 8. PXRD

Figure 9 displays the PXRD of a lyophilized formulation (F4) and pure BCNU. Typical diffraction peaks remarkably at 2θ diffraction angles of 8.58° , 18.66° , 21.18° , 23.88° , 28.60° , 29.52° , 33.11° , and 34.90° were used to identify the crystalline nature of BCNU. The pure BCNU exhibits an intense crystalline peak between 5° and 50° . However, the peak of the pure drug (BCNU) in the lyophilized liposomal formulation (F4) was reduced; indicating a decrease in crystallinity. It was anticipated that BCNU was dispersed as a molecule in the thin lipid film layer. While the intense peak in the formulation might be due to the crystalline nature of mannitol.

3. 9. SEM

The microstructure of the product can be directly observed and the impact of the freeze-drying procedure on cake morphology can be determined by performing a microscopic examination of the freeze-dried cake. Figure 10 depicts a crystalline, porous matrix at a 200-fold magnification. Previous literature has reported similar outcomes.³³ The conclusions of the SEM analysis were further supported by the PXRD data.

icle size, entrapment efficiency, zeta potential, and drug leakage after freeze-drying, to list a few. SPC and CH were investigated in various compositions using a 3^2 -factorial design to fabricate nanoliposomes for targeted drug delivery. Surface response plots and regression equations showed a positive association between the vesicle size of BCNU-loaded liposomes and the SPC and CH at various ratios. A higher lipid content led to an increase in the size and stiffness of the liposomal bilayer. *In vitro* drug release and release kinetics investigations of BCNU-loaded liposomes revealed that the drug is released through a diffusion mechanism and the Higuchi matrix model is followed over a prolonged period. Stability studies showed that lipid compositions are stable under refrigerated storage (4°C) conditions. FTIR and DSC analysis data demonstrated that mannitol as a cryoprotectant protects the liposomal structure at an optimum concentration during freeze-drying. In contrast, SEM microscopy revealed that the mannitol leads to the porous microstructure of the final product at an optimum concentration with some extent of crystallinity.

The crystalline nature of mannitol in the final lyophile provided mechanical strength to the final cake. In order to maintain mannitol in a crystalline state in the

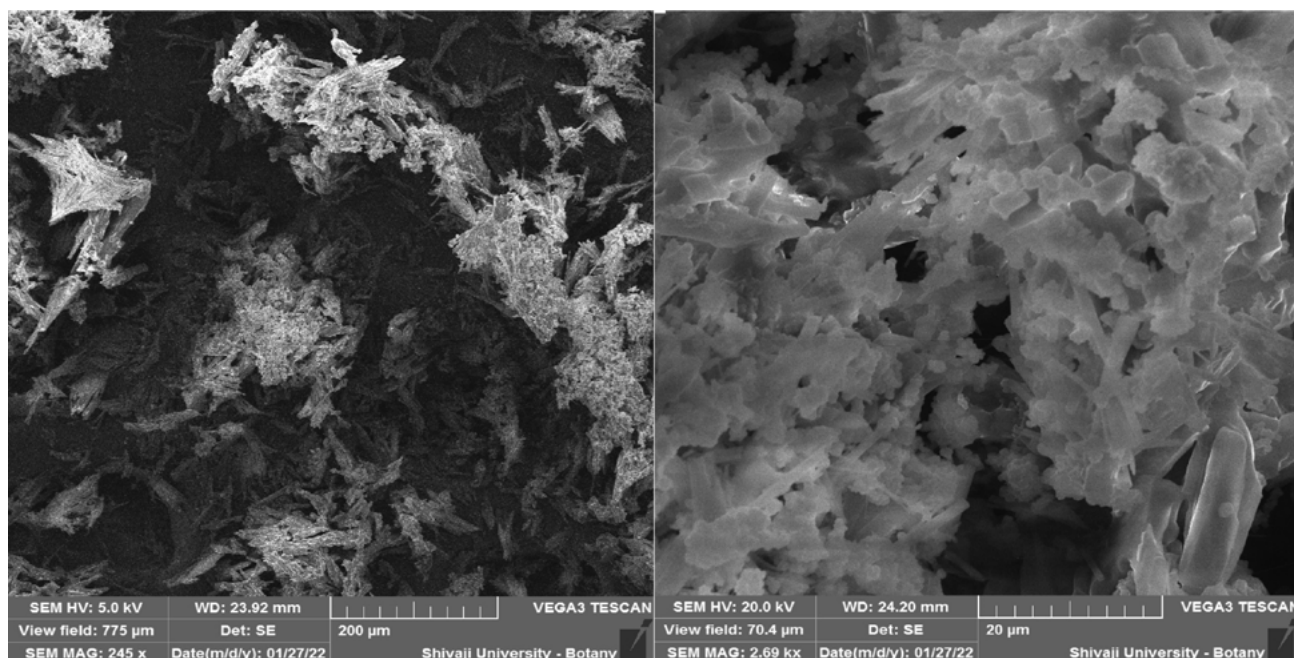


Figure 10. SEM images of freeze-dried formulation (F4)

4. Conclusions

For improving the characteristics and performance of nanoliposomal formulation of the anticancer drug (BCNU), we have assessed and examined the impact of various process parameters on formulation properties such as ves-

final product, it is necessary to ensure that mannitol does not crystallize when the system is in the glassy state ($T < T_g'$). As a result, it is evident from the outcomes of testing the parameters for the BCNU nanoliposomal formulation that it may minimize the dosing frequency and effectively be targeted at the site of action. Moreover, it will reduce the adverse effects brought on by the anticancer agent BCNU's high dose and non-targeted distribution. The pharmacokinetics and

pharmacodynamics properties of these formulations can be explored through *in vivo* bioavailability studies to develop an efficient drug delivery system for augmented anticancer therapy.

5. Future Prospects

The utilization of organic solvents in liposome-based pharmaceuticals has certain limitations. These solvents must be eliminated during the drug production process, which requires adhering to strict safety and regulatory standards. As a result, there is a rise in production expenses due to the need for further purification and waste management procedures. There are various techniques available to decrease the size and distribution of the initial hetero-dispersed liposome suspensions. Among these techniques, homogenization is widely employed as it is applicable for large-scale production and yields a desirable size reduction and distribution. This involves pumping the hetero-dispersed liposome preparation through a small reaction tank under high pressure in a cyclic manner until the desired average liposome size is attained. To decrease the size of liposomes, another technique is to subject them to sonication or ultrasonic irradiation, which generates shear forces during the process. Another effective size reduction method involves extruding the liposomes through membranes with uniform pore sizes to achieve uniform liposome preparation.

While the thin film hydration technique is a useful method for synthesizing liposomes, there are certain drawbacks that must be addressed. These include the need to use and completely remove organic solvents, the formation of multilamellar vesicles, and a broad distribution of particle sizes. Further investigation into the process design and preparation of liposomes through thin film hydration with homogenization techniques on an industrial scale is crucial. This is due to the current lack of continuous production at high levels and the drawbacks linked with the utilization of organic solvents. Nonetheless, before proceeding with large-scale liposome production, it is necessary to thoroughly examine the impact of each parameter of the thin film hydration-assisted process.

Author contribution statement

All authors listed have significantly contributed to the development and the writing of this article.

Funding statement

A grant from Shivaji University, Kolhapur, 416 0004 Maharashtra, India under the Research Initiation Scheme (SU/C. & U. D. Section/97/170 Dated: 31/08/2021), supported this work.

Acknowledgement

We gratefully acknowledge lipoid GmbH, Germany for providing a gift sample of phospholipid. The authors also would like to thank the Principal and management of Annasaheb Dange College of B. Pharmacy, Ashta, Maharashtra, India for providing the facility to complete this research.

Declarations

Conflict of Interest

The authors declare that they have no conflict of interest.

6. References

1. M. Fang, C. W. Peng, D. W. Pang, *Cancer Biol Med.* **2012**, *9* (3), 151–163. DOI:10.7497/j.issn.2095-3941.2012.03.001.
2. D. Bikiaris, *Biochem. Pharmacol.* **2012**, *1*, 1–5. DOI:10.4172/2167-0501.1000e122
3. S. M. Honmane, S. M. Chimane, S. A. Bandgar, S. S. Patil, *Indian J. Pharm. Educ. Res.* **2020**, *54* (2), 376–384. DOI:10.5530/ijper.54.2.43
4. Y. H. Bae, and K. Park, *J. Control. Release.* **2011**, *153*, 198–205. DOI:10.1016/j.jconrel.2011.06.001
5. J. L. Markman, A. Rekechenetskiy, E. Holler, *Adv. Drug Deliv. Rev.* **2013**, *65*, 1866–1879. DOI:10.1016/j.addr.2013.09.019
6. L. S. Jabr-Milane, L. E. Vlerken, S. Yadav, *Cancer Treat. Rev.* **2008**, *34*, 592–602. DOI:10.1016/j.ctrv.2008.04.003
7. D. S. Spencer, A. S. Puranik, N. A. Peppas, *Curr. Opin. Chem. Eng.* **2015**, *7*, 84–92. DOI:10.1016/j.coche.2014.12.003
8. M. Kanapathipillai, A. Brock, D. E. Ingber, *Adv. Drug Deliv. Rev.* **2014**, *79–80*, 107–118. DOI:10.1016/j.addr.2014.05.005
9. A. Jhaveri, P. Deshpande, V. Torchilin, *J. Control. Release.* **2014**, *190*, 352–370. DOI:10.1016/j.jconrel.2014.05.002
10. S. Honmane, S. Salunkhe, A. Hajare, N. Bhatia, S. Mali, *Int. Res. J. Pharm.* **2014**, *5* (2), 70–74. DOI:10.7897/2230-8407.050214
11. S. Honmane, A. Hajare, H. More, S. Salunkhe, *J. Liposome Res.* **2019**, *23*, 1–11. DOI:10.1080/08982104.2018.1531022
12. T. A. Elbayoumi, V. P. Torchilin, *Methods Mol. Biol.* **2010**, *605*, 1–27. DOI:10.1007/978-1-60327-360-2_1
13. A. Akbarzadeh, R. Rezaei-Sadabady, S. Davaran, *Nanoscale Res. Lett.* **2013**, *8*, 102. DOI:10.1186/1556-276X-8-102
14. A. Khan, K. S. Allemailem, S. A. Almatroodi, A. Almatroodi, A. H. Rahmani, *3 Biotech.* **2020**, *10* (4), 163. DOI:10.1007/s13205-020-2144-3
15. L. Brannon-Peppas, and J. O. Blanchette, *Adv Drug Deliv. Rev.* **2004**, *56*, 1649–1659. DOI:10.1016/j.addr.2004.02.014
16. S. Feng, and S. Chien, *Chem. Eng. Sci.* **2003**, *58* (18), 4087–4114. DOI:10.1016/S0009-2509(03)00234-3
17. C. G. Hadjipanayis, and W. Stummer, *J Neurooncol.* **2019**, *141*, 479–486. DOI:10.1007/s11060-019-03098-y
18. Carmustine. [(Accessed on 25 August 2020)]; Available online: <https://go.drugbank.com/drugs/DB00262>.

19. S. H. Lin, and L. R. Kleinberg, *Expert Rev. Anticancer Ther.* **2008**, 8 (3), 343–359. DOI:10.1586/14737140.8.3.343
20. N. Doroshenko, and P. Doroshenko, *Eur. J. Pharmacol.* **2004**, 497 (1), 17–24. DOI:10.1016/j.ejphar.2004.06.043
21. S. Yi, F. Yang, C. Jie, G. Zhang, *Artif. Cells Nanomed. Biotechnol.* **2019**, 47, 3438–3447. DOI:10.1080/21691401.2019.1652628
22. V. T. De Vita, P. P. Carbone, A. H. Jr. Owens, G. L. Gold, M. J. Krant, J. Edmonson, *Cancer Res.* **1965**, 25, 1876–1881.
23. B. R. O'Driscoll, S. Kalra, H. R. Gattamaneni, A. A. Woodcock, *Chest.* **1995**, 107, 1355–1357. DOI:10.1378/chest.107.5.1355
24. D. Bi, L. Zhao, H. Li, Y. Guo, X. Wang, M. Han, *Int. J. Pharm.* **2019**, 559, 76–85. DOI:10.1016/j.ijpharm.2019.01.033
25. H. Ola, S. A. Yahiya, O. N. El-Gazayerly, *Saudi Pharm J.* **2010**, 18 (4), 217–224. DOI:10.1016/j.jsps.2010.07.003
26. Z. Hua, B. Li, Z. Liu, D. Sun, *Drying Technology.* **2003**, 21 (8), 1491–1505. DOI:10.1081/DRT-120024489
27. S. Honmane, A. Kadam, S. Choudhari, R. Patil, S. A. Ansari, V. Gaikwad, *J. Drug Deliv. Sci. Technol.* **2021**, 64, 102578. DOI:10.1016/j.jddst.2021.102578
28. H. Tabandeh, and S. A. Mortazavi, *Iran J Pharm Res.* **2013**, 12 (Suppl), 21–30.
29. K. M. Hosny, *AAPS PharmSciTech.* **2010**, 11 (1), 241–246. DOI:10.1208/s12249-009-9373-4
30. B. Clares, V. Gallardo, M. M. Medina, M. A. Ruiz, *J. Liposome Res.* **2009**, 19(3), 197–206. DOI:10.1080/08982100902736571
31. C. Freitas, R. H. Müller, *Int J Pharm.* **1998**, 168 (2)221–229. DOI:10.1016/S0378-5173(98)00092-1
32. I. Khan, R. Needham, S. Yousaf, C. Houacine, Y. Islam, R. Bryan, S. K. Sadozai, M. A. Elrayess, A. Elhissi, *J. Drug Deliv. Sci. Technol.* **2021**, 66, 102822. DOI:10.1016/j.jddst.2021.102822
33. B. Sylvester, A. Porfire, P. J. Van Bockstal, S. Porav, M. Achim, T. Beer, I. Tomuță, *J Pharm Sci.* **2018**, 107 (1), 139–148. DOI:10.1016/j.xphs.2017.05.024

Povzetek

Cilj raziskave je bil razviti in optimizirati novo liofilizirano liposomsko formulacijo protirakave učinkovine karmustin, ali bis-klometil nitrosourea (BCNU), za podaljšano sproščanje, s čimer bi lahko odpravili od odmerka odvisne stranske učinke in izboljšali biološko uporabnost na mestu delovanja. Optimizacija je bila izvedena z uporabo 3²-faktorskega pristopa, pri čemer sta bila sojin fosfatidilholin (SPC) in holesterol (CH) neodvisni spremenljivki. Optimizirana formulacija (F4) je pokazala visoko učinkovitost vključevanja (81,57 %) s povprečno velikostjo veziklov 141,7 nm in zeta potencialom -22,6 mV. In vitro študije sproščanja učinkovine iz vseh formulacij so pokazale, da se BCNU sprošča do 36 ur po Higuchijevem modelu matičnega sproščanja. Analize TEM, FTIR, DSC, PXRD in SEM potrjujejo nastanek liposomov. Nanoliposomska formulacija z BCNU je izkazovala podaljšano sproščanje, kar kaže, da bi jo lahko učinkovito uporabili za dopolnilno zdravljenje raka z zmanjšanjem od odmerka odvisnih stranskih učinkov.



Except when otherwise noted, articles in this journal are published under the terms and conditions of the Creative Commons Attribution 4.0 International License

Scientific paper

Phytochemical Profile, Antioxidant and Antimicrobial Potency of Aerial Parts of *Salvia Tomentosa* Miller

Şehnaz Balkır¹, Ömer Hazman¹, Laçine Aksoy^{1*}, Mustafa Abdullah Yılmaz²,
Oguz Cakir², Recep Kara³ and İbrahim Erol¹

¹ Department of Chemistry, Faculty of Science and Arts, Afyon Kocatepe University, 03200, Afyonkarahisar, Turkey

² Dicle University Science and Technology Research and Application Center, 21280, Diyarbakir, Turkey

³ Afyon Kocatepe University, Faculty of Veterinary Medicine, Department of Food Hygiene and Technology, Afyonkarahisar

* Corresponding author: E-mail: sehnazblkr@hotmail.com

Received: 01-11-2023

Abstract

Antioxidant activity, antimicrobial potency and components of the aerial parts (leaf, stem, flower and mixture) of *Salvia tomentosa* Miller were determined qualitatively and quantitatively in this study. Aqueous extracts of *Salvia tomentosa* (ST) were prepared by using the flower, leaf and stem parts and all the above-ground parts of the plant (flower-leaf-stem mixture) for this purpose. The radical scavenging activity, total antioxidant/oxidant status, antimicrobial potential, phenolic substances and qualitative/quantitative analyzes of the components in the extracts were determined. ST-stem phenolic acid amount (599 ± 34 mg gallic acid equivalent (GAE)/g extract) was found to be close to the standard substance caffeic acid (651 ± 3 mg GAE/g extract). Total antioxidant status of ST-mix (3.4 ± 0.1 mmol Trolox Equiv./L) and ST-stem (3.4 ± 0.1 mmol Trolox Equiv./L) and natural antioxidant Vitamin C (3.6 ± 0.1 mmol Trolox Equiv./L) were not statistically different. The extract produced by using *S. tomentosa* aerial parts (flower-stem-leaf) showed stronger antioxidant and antimicrobial activity than the aqueous extracts obtained separately from the flower, stem and leaf of the plant. However, it was determined that the components of the separately prepared flower, stem and leaf extracts and the extract components obtained from the aerial parts were largely similar. At the same time, it was observed that there were significant differences in the presence of these components.

Keywords: *Salvia tomentosa* Miller, antimicrobial, antioxidant, LC-MS/MS

1. Introduction

Salvia tomentosa is a perennial semi-shrub with white or lilac-purple flowers up to 55 cm tall. It blooms between April and September. It grows in forests of *Pinus brutia*, *Pinus nigra*, *Quercus pubescens* and on limestone and volcanic slopes. The leaves are used as herbal tea.^{1–3} *Salvia* species contain many bioactive compounds that can be classified as monoterpenes, diterpenes, triterpenes and phenolic compounds. The most common monoterpenes are; α -thujone and β -thujone, 1,8-cineole and camphor, diterpenes; carnosol, carnosic acid, rosmadial and manool, triterpenes; oleanolic and ursolic acids. Phenolic components are phenolic acids such as caffeic, vanillic, ferulic and rosmarinic acids, and flavonoids such as luteolin, apigenin and quercetin.^{4–6} Sage taxa grown in Turkey were classified by Başer⁷ (2002) according to the main compo-

nents of essential oil. According to this classification, *Salvia tomentosa* belongs to the pinene group; the plant which contains 0.6–1.3% essential oil, contains 6–29% α -pinene and 5–33% β -pinene.^{7–9}

The use of herbal medicines for therapeutic purposes, the fact that fragrant plants constitute the main raw material of perfumery, food and cosmetics industry, and the emergence of new areas of use increases the demand for medicinal and aromatic plants day by day and causes the industrial sector to consume these plants as raw materials intensively.^{10, 11} Like many other medicinal plants, *S. tomentosa* was extensively collected from its natural habitat, and this careless collection has caused some plants to become extinct. Therefore, these plants are grown in order to promote sustainable and standard agricultural production.¹² It is stated that the essential oil of *Salvia tomentosa* aerial parts significantly inhibits the growth of Gram-posi-

tive and Gram-negative bacteria tested except *Pseudomonas aeruginosa* in the literature.¹³ In another study, it is stated that the plant has antioxidative effects.¹⁴ In this study, the biological activity and phytochemical content of the parts of *Salvia tomentosa* consumed as tea are presented in detail.

2. Materials and Methods

2.1. Plant Material and Extraction Protocol

Salvia tomentosa is a perennial plant. The stem of the plant consists of upright, four-sided, usually branched, hairy and sessile glands extending up to 1 m. Leaves simple, narrowly oblong to ovate, 2–11 x 0.8–5 cm, rounded to cordate at base, entire to oblong-cubic. The petiole is 1.7–5.5 cm. Verticillasters 4–10 flowered, distant or dense at the top. The crowns are lilac, purple or white. They usually grow in the forests of *P. brutia* and *P. nigra*, on limestone or magmatic slopes, at an altitude of 90–2000 m. *Salvia tomentosa* was collected in 2020 from Ardıçlı village, Keçiborlu, Isparta, Turkey (37° 48' 8.9928" and 30° 12' 13.4676"). Separate aqueous extracts were prepared by using the flower (ST-flower), leaf (ST-leaf) and stem (ST-stem) parts of the plant and the total aerial parts of the plant (flower-leaf-stem mixture, ST-mix). The plant, which was allowed to dry well in the shade. Each separated part was crushed into powder with the help of a special blender (Waring 32BL80, Connecticut, USA). The water extract from the samples was obtained using the maceration method. Water was placed in glass bottles and heated in a water bath until boiling. The powder sample was added to glass bottles. The plant-water suspension in glass bottles was incubated in the dark at room temperature for 24 hours. At the end of the incubation, the mixture in the glass bottle was passed through filter paper (Whatman, Grade 589/1) and the plant particles were separated from the filtrate. In order to remove the solvent in the filtrate, the filtrate was placed in the balloon of the rotary evaporator (Heidolph, 562-00000-00-0, Germany) under vacuum. Solutions containing dense extract and poured into glass petri dishes were kept in dark at room temperature until the solvent evaporated completely (2–3 days). Extracts obtained in dry form were stored at +4 °C to be used in qualitative, quantitative and biological activity analyses.¹⁵

2.2. Qualitative and Quantitative Analysis of Phytochemicals in Extracts

Determination of Total Phenolic Acid amount

Total phenolic acid content was measured by the modified Folin-Ciocalteu method. The reference material caffeic acid was used in order to compare the amounts of phenolic substances in the extracts in the analysis. A

standard curve of gallic acid was created for this purpose. The standard solutions of gallic acid at different concentrations (100, 200, 400, 600, 800 µg/mL) were prepared. Folin-Ciocalteu reagent was added to the prepared solutions of plant extract, caffeic acid and standards in the analyses. Sodium carbonate was added and incubated for 2 hours at room temperature. The absorbance of the mixture was measured spectrophotometrically at 760 nm against water. The total amount of phenolic acid in 1 mg of the extracts was calculated as gallic acid equivalent (µg GAE/mg extract) using the absorbance obtained as a result of the analysis of the plant extracts and the straight equation obtained from the gallic acid standard curve.¹⁶

Determination of Components in Extracts and Concentrations

Qualitative and quantitative determination of the components in the extracts were made by LC-MS/MS system in the laboratories of Dicle University Science and Technology Application and Research Center. The reverse phase UHPLC system used in the LC-MS/MS system preferred in the analysis; It consisted of an autosampler (SIL-30AC), a column furnace (CTO-10ASvp), a gradient pump system (LC-30AD) and a degaser (DGU-20A3R). Chromatographic separation was performed using a column (Agilent Poroshell 120 EC-C18) (150 mm×2.1mm, 2.7 µm). The column temperature was set to 40 °C. The elution gradient was composed of mobile phase A (ultra pure water+5 mM ammonium formate+0.1% formic acid) and mobile phase B (ultrapure water +5 mM ammonium formate+0.1% formic acid).¹⁵

The gradient elution profile used was as follows: 20–100% B (0–25 min), 100% B (25–35 min), 20% B (35–45 min). In addition, the mobile phase flow rate and injection volume were determined as 0.5mL/min and 5 µL, respectively. For mass spectrometry detection of the LC-MS/MS system used, a Shimadzu LCMS-8040 model sequential mass spectrometer equipped with an electrospray ionization source operating in both positive and negative modes was used. LC-ESI-MS/MS data was acquired and processed with LabSolutions software (Shimadzu). MRM (multiple reaction monitoring) mode was used for the quantification of phytochemicals. The MRM method has been optimized for the selective detection and quantification of phytochemicals based on the screening of specific major ion-fragmentation ion transitions. Collision energies (CE) are optimized to achieve optimum phytochemical fragmentation and maximal migration of desired fragmentation ions. Applied MS operating conditions: drying gas (N₂) flow, 15 L/min; nebulizer gas (N₂) flow, 3 L/min; DL temperature, 250 °C; The heat block temperature was determined as 400 °C and the interface temperature as 350 °C. The amounts of phenolic acid species whose amounts were determined in the extracts were expressed as mg-analyte/g-extract.¹⁷

2. 3. Determination of Biological Activity of Extracts

Free Radical Scavenging Activity

Free radical scavenging activity of *S. tomentosa* and standard antioxidant substances (Butylated Hydroxy Toluene-BHT and Vitamin C) used in the study were determined by DPPH (1,1-diphenyl-2-picrylhydrazyl) radical. A calibration curve was created using different concentrations of DPPH solution. Using the curve equation obtained from the calibration chart and sample absorbances, it was determined how much DPPH radical each sample inhibited. Extracts and standards were added to the solution containing DPPH radical and their absorbance was measured at 517 nm. Concentrations from the measured absorbances were determined by the calibration curve. % inhibitions were determined using the formula below.¹⁵

$$\text{Inhibition rate (\%)} = \left[\frac{(\text{Absorbance}_{\text{control}} - \text{Absorbance}_{\text{sample}})}{\text{Absorbance}_{\text{control}}} \right] \times 100$$

Total Antioxidant Status (TAS), Total Oxidant Status (TOS) Levels

Total Antioxidant Status (TAS) levels were measured using spectrophotometric commercial kits (Rel Assay, Gaziantep, Turkey). In order to determine TAS levels, 0.5–2 mmol/L Trolox was used as a standard. TAS levels were determined as mmol Trolox Equivalent/L according to the calibration graph taken from the ELISA reader using three standards (0.5 mmol/L Trolox, 1mmol/L Trolox and 2 mmol/L Trolox) according to the kit protocol.

TOS levels were determined at 540 nm by spectrophotometric method using commercial kits (Rel Assay, Gaziantep, Turkey). To determine TOS levels, a calibration curve was created using three H₂O₂ standards (5 μmol/L, 10 μmol/L and 20 μmol/L) according to the kit protocol. The results were determined as μmol H₂O₂ Equiv./L. Oxidative stress index (OSI) levels were determined by dividing the TOS level of each sample by the TAS level.¹⁸

Evaluation of Antimicrobial Efficacy of Extracts

Microdilution method was used to determine the antimicrobial activity of extracts of *Salvia tomentosa*. Stock solutions were prepared from all extracts at a concentration of 60 mg/mL. 1/2, 1/4, 1/8, 1/16, 1/32 and 1/64 dilutions were prepared from these stock solutions, respectively. 10⁷ CFU/mL of 1% (v/v) bacterial solutions were added to the same volume of extract solutions from the dilutions and incubated at 37°C for 24 hours. Minimum inhibitory concentration (MIC) is inhibited value after incubation; The lowest extract concentrations at which bacterial growth was inhibited were evaluated by both measuring at 450 nm and inoculation into the medium.¹⁹

2. 4. Statistical analysis

The extracts used in the study were prepared in triplicate, and the measured results were expressed as mean ± standard deviation (mean ± SD). SPSS 20 package program was used in the statistical analysis of the data in this study. Differences between groups were determined by one-way analysis of variance (one-way ANOVA). The difference between which groups was determined at p < 0.05 significance value according to Duncan's multiple range test.

3. Results

Plants have many activities such as antioxidant, antimicrobial and anticarcinogenic effects due to the secondary metabolites they synthesize and possess.²⁰ The amount of phenolic acid, which is one of the secondary metabolites in *S. tomentosa*, was determined by modifying the method.¹⁶ The amounts of phenolic substances expressed as mg gallic acid equivalent (GAE)/g-extract in the samples were interpreted by comparing the amount of phenolic substance in the extracts with the amount of phenolic substance in the caffeic acid. The data obtained are presented in Figure 1. It was determined that the total amount of phenolic substance was the least in the aqueous extract obtained from the flower part of the plant. The extracts of the stem (ST-stem), leaf (ST-leaf), flower (ST-flower) and aerial parts of the plant (stem-leaf-flower; ST-mix) have high total phenolic content close to caffeic acid were determined. These data show that especially the stem and leaf of the plant are rich in phenolic content. The amount of phenolic acid in ST-flower was found to be statistically significantly lower (p < 0.05) than the others.

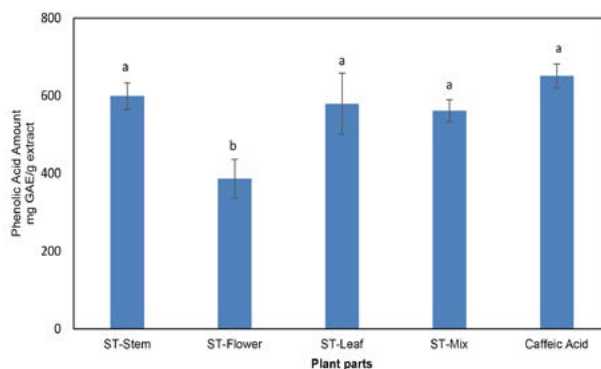


Figure 1. The total amount of phenolic substances detected in the extracts and the standard. ST-Stem; Aqueous extract of stem of *Salvia tomentosa*, ST-Flower; Aqueous extract of flower of *Salvia tomentosa*, ST-Leaf; Aqueous extract of leaf of *Salvia tomentosa*, ST-Mix; Aqueous extract of a mixture of stem, leaf and flower of *Salvia tomentosa*. (a, b) The difference between the means labelled with different letters is statistically significant (p < 0.05).

LC-MS/MS system was used to determine the phytochemicals contained in *Salvia tomentosa*. The components

of the aerial parts of the plant are shown separately in Table 1. When the amount of components in the extracts is examined in general, it can be said that especially three components are more intense than *S. tomentosa* extracts compared to other components. These components are rosmarinic acid, quinic acid and fumaric acid, respectively. When the extracts were analyzed separately, the presence and concentrations of 16 components in ST-stem extract, 15 components in ST-flower extract, and 17 components in ST-leaf and ST-mix extracts were determined. Hesperidin, quinic acid, fumaric acid, aconitic acid, protocatechuic acid, gentisic acid, protocatechuic aldehyde, chlorogenic acid, caffeic acid, salicylic acid, apigenin, o-coumaric acid, rosmarinic acid, cosmoisin, luteolin are chemicals found in all parts of the plant.

Table 1. Types and amounts of some phytochemicals in *Salvia tomentosa* extract

Plant parts	Concentration (mg analyte/g extract)			
	ST-Stem	ST-Flower	ST-Leaf	ST-Mix
Hesperidin	5.507	0.081	0.718	2.060
Quinic acid	25.628	29.217	32.247	37.750
Fumaric acid	10.888	0.923	7.592	11.155
Aconitic acid	0.525	0.677	0.373	0.391
Protocatechuic acid	0.851	1.829	0.694	0.568
Gentisic acid	0.231	0.546	0.209	0.168
Protocatechuic aldehyde	0.883	0.712	1.046	0.844
Chlorogenic acid	1.632	1.242	1.429	1.757
Caffeic acid	2.247	0.560	2.245	2.339
Salicylic acid	1.596	2.102	1.473	0.799
Apigenin	0.003	0.006	0.057	0.035
o-Coumaric acid	0.042	0.037	0.056	0.032
Rosmarinic acid	50.235	61.590	89.892	83.625
Cosmoisin	0.077	0.931	0.793	0.560
Luteolin	0.017	0.035	0.348	0.210
Hesperetin	0.071	ND	0.025	0.077
Naringenin	ND	ND	0.011	0.011

ND: Not detected. ST-Stem; Aqueous extract of stem of *Salvia tomentosa*, ST-Flower; Aqueous extract of flower of *Salvia tomentosa*, ST-Leaf; Aqueous extract of leaf of *Salvia tomentosa*, ST-Mix; Aqueous extract of a mixture of stem, leaf and flower of *Salvia tomentosa*

It was determined that the major component determined in all of the extracts obtained from *S. tomentosa* was rosmarinic acid. The amount of rosmarinic acid is quite high when compared to other ingredients.

One of the commonly used methods to determine the antiradical activity of a sample is the method using the DPPH radical. In this method, sample (extract) at certain concentrations is added to the DPPH radical dissolved at a certain concentration in a suitable solvent. The percentages of inhibition of DPPH radical by using the solutions of extracts and standards (BHT and Vitamin C) of *S. tomen-*

tosa obtained at the same concentrations are presented in Figure 2. When the data are examined, it is seen that the ST-leaf extract is statistically significantly ($p < 0.05$) lower than all other extracts. It can be mentioned that the other extracts (ST-stem, ST-flower and ST-mix) have close radical scavenging effects, such as BHT and Vitamin C, which are antioxidants used for comparison.

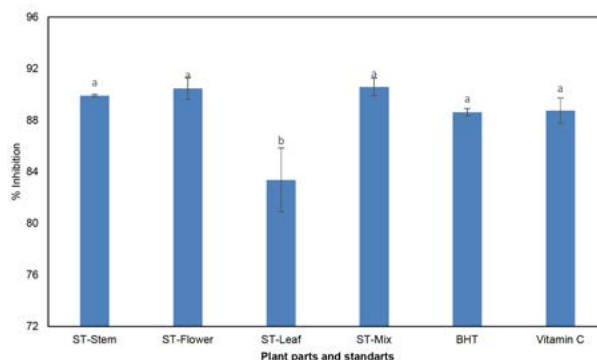


Figure 2. DPPH radical inhibition ratios of the extracts. ST-Stem; Aqueous extract of stem of *Salvia tomentosa*, ST-Flower; Aqueous extract of flower of *Salvia tomentosa*, ST-Leaf; Aqueous extract of leaf of *Salvia tomentosa*, ST-Mix; Aqueous extract of a mixture of stem, leaf and flower of *Salvia tomentosa*. BHT; Butylated Hydroxy Toluene. (a,b) The difference between the means labelled with different letters is statistically significant ($p < 0.05$).

Spectrophotometric method were used to determine the antioxidant and oxidant capacity of extracts of *S. tomentosa*. Oxidative stress indexes of the samples were determined using these antioxidant and oxidative capacity datas. It was evaluated that the antioxidant activity of the extracts with low oxidative stress index data was higher. Antioxidant and oxidant capacity, oxidative stress indexes values were shown in Figure 3.

As a result of the analysis, it was determined that the extract with the highest antioxidant capacity among the extracts of *S. tomentosa* belonged to ST-stem and ST-mix. TAS levels of ST-flower and ST-leaf extract were found to be statistically significantly ($p < 0.05$) lower than other extracts and Vitamin C. When TOS levels were examined, it was determined that the TOS level of ST-stem extract was the lowest, while the TOS level of ST-flower extract was the highest. OSI values obtained by dividing the TOS levels of the extracts of *S. tomentosa* by the TAS levels, express the capacity of a plant to create oxidative stress in the organism from which it is taken. The OSI values of the ST-stem extract, which were determined to have the highest TAS levels and the lowest TOS levels, were found to be the lowest. It was observed that the extract with the highest OSI value was ST-leaf.

When the analyzes made on behalf of the antioxidant activity of the extracts were examined in general, the phenolic substance amounts, DPPH scavenging effects and TAS levels of the ST-stem and ST-mix extracts of the

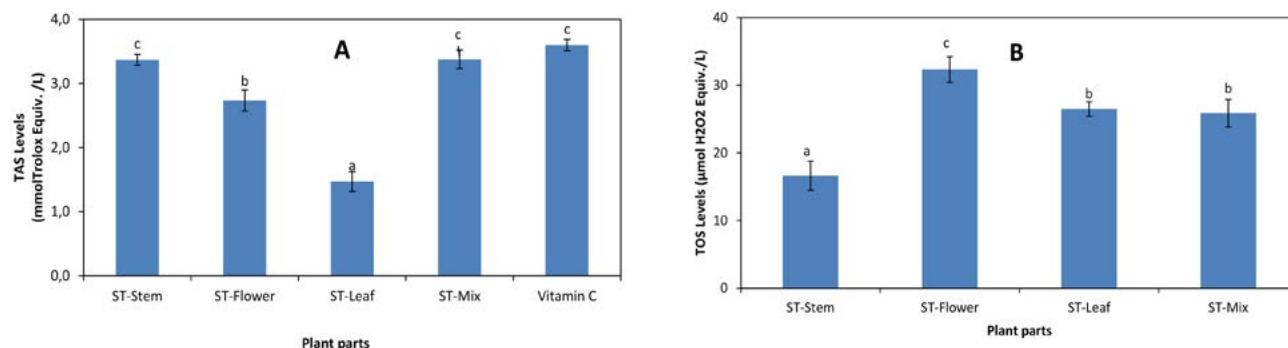


Figure 3. A: Total antioxidant capacities of extracts of *Salvia tomentosa*. B: Total oxidant capacities of extracts of *Salvia tomentosa* (a, b, c) The difference between the means labelled with different letters is statistically significant ($p < 0.05$)

plant were found to be higher than the other leaf and flower extracts.

The antimicrobial activity of extracts of *S. tomentosa* was determined by microdilution method and given in Table 2. When the data were examined, it was found that the lowest 1/16 dilution of ST-flower extract was effective on *Escherichia coli* O157:H7, *Staphylococcus aureus* and *Candida albicans*; The lowest 1/8 dilution of ST-leaf extracts was effective on *Listeria monocytogenes*, *Salmonella typhimurium* and *Candida albicans*; The lowest 1/16 dilu-

tion of ST-Stem extracts was effective on all agents (*L. monocytogenes*, *S. typhimurium*, *S. aureus*, *C. albicans*) except *E. coli* O157:H7; All dilutions of ST-mix extract were found to be effective on *L. monocytogene* and *C. albicans*.

Based on the data obtained from Table 2, considering the doses corresponding to each dilution ratio, the MIC values of the extracts are presented in Table 3. It was determined that ST-mix was the most effective inhibitory extract for all microorganisms used. This data shows that

Table 2. Antimicrobial activity of *Salvia tomentosa* extracts

Extract	Dilution Rate	<i>E. coli</i>	<i>L. monocytogenes</i>	<i>S typhimurium</i>	<i>S. aureus</i>	<i>C. albicans</i>
ST-Flower	1/2	+	+	+	+	+
	1/4	+	+	+	+	+
	1/8	+	+	+	+	+
	1/16	+	–	–	+	+
	1/32	–	–	–	–	–
	1/64	–	–	–	–	–
ST-Leaf	1/2	+	+	+	–	+
	1/4	+	+	+	–	+
	1/8	–	+	+	–	+
	1/16	–	–	–	–	+
	1/32	–	–	–	–	–
	1/64	–	–	–	–	–
ST-Stem	1/2	+	+	+	+	+
	1/4	+	+	+	+	+
	1/8	+	+	+	+	+
	1/16	–	+	+	+	+
	1/32	–	–	–	–	–
	1/64	–	–	–	–	–
ST-Mix	1/2	+	+	+	+	+
	1/4	+	+	+	+	+
	1/8	+	+	+	+	+
	1/16	+	+	+	–	+
	1/32	–	+	–	–	+
	1/64	–	+	–	–	+

ST-Stem; Aqueous extract of stem of *Salvia tomentosa*, ST-Flower; Aqueous extract of flower of *Salvia tomentosa*, ST-Leaf; Aqueous extract of leaf of *Salvia tomentosa*, ST-Mix; Aqueous extract of a mixture of stem, leaf and flower of *Salvia tomentosa*

the use of the aerial part of the plant together is more beneficial in terms of providing antimicrobial activity.

Table 3. MIC values of extracts

Microorganisms	ST-Flower	ST-Leaf	ST-Stem	ST-Mix
<i>E. coli</i>	3.75	15	7.5	1.875
<i>L. monocytogenes</i>	7.5	7.5	3.75	0.9375
<i>S. typhimurium</i>	7.5	7.5	3.75	1.875
<i>S. aureus</i>	3.75	–	3.75	7.5
<i>C. albicans</i>	3.75	3.75	3.75	0.9375

ST-Stem; Aqueous extract of stem of *Salvia tomentosa*, ST-Flower; Aqueous extract of flower of *Salvia tomentosa*, ST-Leaf; Aqueous extract of leaf of *Salvia tomentosa*, ST-Mix; Aqueous extract of a mixture of stem, leaf and flower of *Salvia tomentosa*. MIC; Minimum concentration at which microorganism growth is inhibited

4. Discussion

Metabolites consist of intermediate products formed by the effect of metabolic activities. Metabolites have functions such as energy generation, building blocks, stimulating enzymes and additionally inhibiting them, being under the influence of catalyst, defense and other organisms, giving odor. Primary metabolites are directly involved in processes involved in normal growth, development and reproduction. Although secondary metabolite species are not directly related to these processes, they contribute to the maintenance of these processes by the plant. Secondary metabolites may contribute to the adaptation of the species to its specific conditions. These compounds, which enable plants to have their unique color, taste, aroma and texture, also play an important role in many metabolic events that occur in the plant.^{21, 22} In addition to contributing to the resistance mechanism in the body at the time of disease in plants, they are produced as a defense mechanism for plants and increases as stress increases. Phenolic compounds are synthesized during the normal development of plants and when the plant is sick and injured. In addition, phenolic production is dependent on environmental conditions and are synthesized when exposed to UV rays, at low temperatures and during periods when nitrogen, phosphate and iron content are low.^{21, 22}

In a study, the phenolic composition and antioxidant properties of wild and cultured *S. tomentosa* were investigated. Total phenolics of *S. tomentosa* were found between 49.27 and 66.15 mg GAE/dw. The total phenolic content of the grown samples was determined to be higher than that of the wild samples. 17 different phenolic compounds containing 7 phenolic acids and 10 flavonoids were identified and quantified in *S. tomentosa*. Rosmarinic acid was measured as the main component of *S. tomentosa*. It is followed by caffeic acid, morin, p-coumaric acid and myricetin.²³ In the present study, the phenolic acid amounts of plant parts

ranged from 386.48 to 599.24 mg GAE/g extract. Identified and quantified phenolic substances are respectively, rosmarinic acid (50.235 mg/g extract), quinic acid (25.628 mg/g extract), fumaric acid (10.888 mg/g extract), hesperidin (5.507 mg/g extract), caffeic acid (2.247 mg/g extract), chlorogenic acid (1.632 mg/g extract) and salicylic acid (1.596 mg/g extract).

Rosmarinic acid is one of the most abundant phenolic substances in all *S. tomentosa* extracts. In many studies, it is stated that rosmarinic acid has antiviral, antibacterial, anti-inflammatory and antioxidant effects.²⁴ In a study, biotechnological production of rosmarinic acid, which is found in high amounts in *Salvia officinalis*, has been suggested.²⁵ A high amount of rosmarinic acid is also expected in *S. tomentosa*, another species from the *Salvia* family. It can be said that rosmarinic acid, the major component of *S. tomentosa*, has an important role in the formation of antioxidant and antimicrobial activity of the extracts.

Fumaric acid and its derivatives are among the well-known antioxidants that provide various health benefits due to their potent free radical scavenging properties, anti-inflammatory and immunomodulatory effects.^{26, 27} These data in the literature may be related to the wound healing activity of *Salvia tomentosa* due to its high fumaric acid content.

When the analysis made on behalf of the antioxidant activity of the extracts are examined in general, the phenolic substance amounts, DPPH scavenging effects and TAS levels of the ST-stem and ST-mix extracts of the plant were found to be higher than the other ST-leaf and ST-flower extracts. It is seen that the antioxidant active substance levels of hesperidin and fumaric acid in ST-stem extract, and hesperidin, fumaric acid and rosmarinic acid in ST-mix extract are higher than other extracts. Among these components, besides the antioxidant activities of fumaric acid and hesperidin, antimicrobial activities are prominent in the literature.^{28–30}

In addition, the antioxidative properties of ST-flower extract (except for DPPH radical scavenging activity) were found to be lower than other extracts, while TOS levels were found to be high. This may be due to the fact that the levels of hesperidin, fumaric acid and caffeic acid in the flower extract are lower than in other extracts. While the antioxidative property of ST-flower extract was low, DPPH radical scavenging activity was found to be high. Some antioxidants act by preventing the formation of free radicals, while other antioxidants act by scavenging existing radicals. Therefore, there may be more components in the flower extract that increase the radical scavenging activity of the extracts. It is seen that the amounts of some components (aconitic acid, protocatechuic acid, gentisic acid, salicylic acid and cosmoisin) are higher in the flower extract.

The second component, which was determined to be higher in ST-stem and ST-mix extracts compared to other extracts, is hesperidin. Hesperidin, which has a

flavonoid structure, protects the organism against oxidants with its strong antioxidant property in biological systems³¹, and also protects the body against infections with its antiviral and antibacterial activity.³² Recent studies on wound healing show that hesperidin is very effective in healing wounds that develop due to various diseases or that may occur in daily life²⁵. For thousands of years, extract of St. John's Wort (*Hypericum perforatum*) flour obtained with olive oil have been used traditionally in the treatment of burns and open wounds and in the removal of their scars. Considering that one of the major components of St. John's wort is hesperidin³³, the effectiveness of hesperidin can be better understood in terms of wound healing activity. From this point, it is expected that the extract of *Salvia tomentosa*, which contain plenty of hesperidin, prepared with water, have antimicrobial effects.

It was determined that the ST-mix extract showed stronger antioxidant and antimicrobial activity than those obtained from parts of the plant. However, it was determined that the components of the ST-flower, ST-stem and ST-leaf extracts and the components of the ST-mix extract were largely similar. On the other hand, it was observed that there were significant differences in the proportion of the same type of components. This probably caused the different antimicrobial and antioxidant activities of each extract in the components they contained in different proportions.

5. Conclusions

The phenolic and flavonoid contents of the aqueous extracts of the ST-flower, ST-stem, ST-leaf and ST-mix parts of *S. tomentosa* were determined qualitatively and quantitatively. The phenolic content of the fractions was found to be quite high except for ST-flower. Rosmarinic acid, quinic acid and fumaric acid are phenolic substances found in high amounts in all parts of the plant. Total antioxidant levels of ST-stem and ST-mix are quite high. It has been determined that plant parts are very effective radical scavengers expect for ST-leaf. In addition, it was determined that the most effective extracts from *S. tomentosa* in terms of antibacterial activities were ST-stem and ST-mix. It has been interpreted that the antimicrobial and antioxidant activities between the extracts may be due to the component differences in their contents. It is thought that the obtained data will contribute to the literature in order to explain the phytotherapeutic activity of *Salvia tomentosa* Miller.

Acknowledgements

This work is supported by the Scientific Research Project Fund of Afyon Kocatepe University (AKU-BAP) under the Project number 19.FEN.BİL.36.

6. References

- V. Papageorgiou, C. Gardeli, A. Mallouchos, M. Papaioannou, M. Komaitis, *J. Agr. Food Chem.* **2008**, *56*, 7254–7264. DOI:10.1021/jf800802t
- M.Z. Haznedaroglu, N.U. Karabay, U. *Fitoterapia* **2001**, *72*, 829–831. DOI:10.1016/S0367-326X(01)00335-5
- Y. Lu, L. Foo, *Phytochemistry* **2002**, *59*, 117–140. DOI:10.1016/S0031-9422(01)00415-0
- N. Tan, S.T. Yazıcı, Y.C. Yeşil, B. Demirci, Tan E. *Rec. Nat. Prod.* **2017**, *11*, 456–461. DOI:10.25135/rnp.57.16.12.086
- M. Jakovljević, S. Jokić, M. Molnar, M. Jašić, J. Babić, H. Jukić, I. Banjari, *Plants* **2019**, *8*, 1–30. DOI:10.3390/plants8030055
- E. Hanlidou, R. Karousou, D. Lazari, *Chem. Biodivers.* **2014**, *11*, 1205–1215. DOI:10.1002/cbdv.201300408
- K.H.C. Başer, *Pure Appl. Chem.* **2002**, *74*, 527–545. DOI:10.1351/pac200274040527
- T. Aşkun, K.H.C. Başer, G. Tümen, M. Kürkcüoğlu, *Turk. J. Biol.* **2010**, *34*, 89–95. DOI:10.3906/biy-0809-2
- G. Ozek, T. Ozek, K.H.C. Baser, E. Hamzaoglu, A. Duran, *Chem. Nat. Compd.* **2007**, *43*, 667–671. DOI:10.1007/s10600-007-0224-9
- Z. Dumanoglu, S. Mokhtarzadeh. *TURKJANS* **2020**, *7*, 596–602. DOI:10.30910/turkjans.663891
- S. Mokhtarzadeh, B. Demirci, H.G. Ağalar, K.M. Khawar, N. Kırimer, *Rec. Nat. Prod.* **2019**, *13*, 121–128. DOI:10.25135/rnp.86.18.04.105
- I. Erdogan-Orhan, E. Baki, S. Senol, G. Yilmaz, *J. Serb. Chem. Soc.* **2010**, *75*, 1491–1501. DOI:10.2298/JSC100322115E
- M.Z. Haznedaroglu, N.U. Karabay, U. Zeybek. *Fitoterapia* **2001**, *72*, 829–831. DOI:10.1016/S0367-326X(01)00335-5
- B. Tepe, D. Daferera, A. Sokmen, M. Sokmen, M. Polissiou, *Food Chem.* **2005**, *90*, 333–340. DOI:10.1016/j.foodchem.2003.09.013
- Ö. Hazman, L. Aksoy, A. Büyükben, R. Kara, M. Kargioğlu, İ.H. Cigerci, M.A. Yılmaz, *Indian J. Exp. Biol.* **2022**, *60*, 743–752. DOI:10.56042/ijeb.v60i10.55070
- K. Slinkard, V.L. Singleton, *Am. J. Enol. Vitic.* **1977**, *28*, 49–55. DOI:10.5344/ajev.1974.28.1.49
- M.A. Yılmaz, *Ind. Crops Prod.* **2020**, *149*, 112347. DOI:10.1016/j.indcrop.2020.112347
- L. Aksoy, İ. Güzey, M. Düz, *Turk. J. Pharm. Sci.* **2022**, *19*, 76–83. DOI:10.4274/tjps.galenos.2021.86422
- S.S. Shaikh, A.S. Bawazir, B.A. Yahya, *Turk. J. Pharm. Sci.* **2022**, *19*, 145–152. DOI:10.4274/tjps.galenos.2021.02058
- B. Tepe, D. Daferera, A. Sokmen, M. Sokmen, M. Polissiou, *Food Chem.* **2005**, *90*, 333–340. DOI:10.1016/j.foodchem.2003.09.013
- S. Neugart, S. Baldermann, F.S. Hanschen, R. Klopsch, M. Wiesner-Reinhold, M. Schreiner, *Scient. Hort.* **2018**, *233*, 460–478. DOI:10.1016/j.scienta.2017.12.038
- M. Wink, *Nat. Prod. Commun.* **2008**, *3*, 1205–1216. DOI:10.1177/1934578X0800300801
- C. Dinçer, I. Tontul, I. B. Çam, K.S. Özdemir, A. Topuz, H.Ş. Nadeem, S.T. Ay, R. S. Göktürk. *Turk. J. Agric. For.* **2013**, *37*, 561–567. DOI:10.3906/tar-1211-72

24. H. Guan, W. Luo, B. Bao, Y. Cao, F. Cheng, S. Yu, Q. Fan, L. Zhang, Q. Wu, M. Shan. *Molecules* **2022**, *27*, 3292. DOI:10.3390/molecules27103292
25. M. Petersen, M.S. Simmonds, *Phytochemistry* **2003**, *62*, 121–125. DOI:10.1016/S0031-9422(02)00513-7
26. S.A. Scuderi, A. Ardizzone, I. Paterniti, E. Esposito, M. Campolo. *Antioxidants* **2020**, *9*, 630. DOI:10.3390/antiox9070630
27. A. Shakya, G.K. Singh, S.S. Chatterjee, V. Kumar, *J. Intercult. Ethnopharmacol.* **2014**, *3*, 173–178. DOI:10.5455/jice.20140912021115
28. U. Wollina, *Indian Dermatol. Online J.* **2011**, *2*, 111. DOI:10.4103/2229-5178.86007
29. M. Vabeiryureilai, K. Lalrinzuali, G.C. Jagetia, *Burns*. **2022**, *48*, 132–145. DOI:10.1016/j.burns.2021.04.016
30. W. Li, A.D. Kandhare, A.A. Mukherjee, S.L. Bodhankar, *Excli. J.* **2018**, *17*, 399–419. DOI: 10.17179/excli2018-1036
31. P.K. Wilmsen, D.S. Spada, M. Salvador, *J. Agric. Food Chem.* **2005**, *53*, 4757–4761. DOI:10.1021/jf0502000
32. H.W. Kim, H.J. Woo, J.Y. Yang, J.B. Kim, S.H. Kim, *Int. J. Mol. Sci.* **2021**, *17*, 10035. DOI:10.3390/ijms221810035
33. C. Sarikurkcu, M. Locatelli, A. Tartaglia, V. Ferrone, A.M. Juszcak, M.S. Ozer, B. Tepe, M. Tomczyk, *Molecules* **2020**, *6*, 1202. DOI:10.3390/molecules25051202

Povzetek

V tej študiji smo kvalitativno in kvantitativno določili antioksidativno aktivnost, protimikrobno učinkovitost in sestavine nadzemnih delov (listov, stebela, cvetov in mešanice) rastline *Salvia tomentosa* Miller. Vodne izvlečke *S. tomentosa* (ST) smo pripravili z uporabo cvetov, listov in stebel ter vseh nadzemnih delov rastline (mešanica cvetov, listov in steblo). Določili smo aktivnost odstranjevanja radikalov, skupni antioksidativni/oksidativni status, protimikrobni potencial, fenolne snovi in kvalitativne/kvantitativne analize sestavin v ekstraktih. Ugotovljeno je bilo, da je količina fenolnih kislin v ST-stebelu (599 ± 34 mg ekvivalenta galne kisline (GAE)/g ekstrakta) blizu količini standardne snovi kofeinske kisline (651 ± 31 mg GAE/g ekstrakta). Skupni antioksidativni statusi mešanice ST ($3,4 \pm 0,1$ mmol ekvivalenta troloxa /L), stebela ST ($3,4 \pm 0,1$ mmol ekvivalenta troloxa /L) in naravnega antioksidanta vitamina C ($3,6 \pm 0,1$ mmol ekvivalenta troloxa /L) se statistično niso razlikovali. Izvleček, pridobljen z uporabo nadzemnih delov *S. tomentosa* (cvet-steblo-listi), je pokazal močnejše antioksidativno in protimikrobno delovanje kot vodni izvlečki, pridobljeni ločeno iz cvetov, stebela in listov rastline. Ugotovljeno je bilo, da so si sestavine ločeno pripravljenih izvlečkov cvetov, stebela in listov ter sestavine izvlečka, pridobljenega iz nadzemnih delov, v veliki meri podobne. Hkrati pa je bilo ugotovljeno, da obstajajo pomembne razlike v prisotnosti teh sestavin.



Except when otherwise noted, articles in this journal are published under the terms and conditions of the Creative Commons Attribution 4.0 International License

Scientific paper

Effect of Ozone on Oxygen Transport and Pro-Oxidant-Antioxidant Balance of Red Blood Cell Suspension

Victor Zinchuk* and Elena Biletskaya*

Grodno State Medical University, Department of Normal Physiology, 230009, Gorkogo str, 80, Grodno, Belarus

* Corresponding author: E-mail: zinchuk@grsmu.by; Tel.: +37529-7859027
biletskaya.e@inbox.ru; Tel.: +37529-2689339

Received: 01-31-2023

Abstract

Introduction: Ozone affects blood oxygen transport and the pro-oxidant-antioxidant balance. However, the role of blood formed elements and gas transmitters in these processes still remains unclear. The aim of the present study was to investigate the effect of ozone on oxygen transport and the pro-oxidant-antioxidant balance in a red cell suspension.

Methods: The red cell suspension was incubated with ozone at a concentration of 6 mg/l and substances affecting the synthesis of gas transmitters (nitroglycerin, sodium hydrosulfide). Parameters of blood oxygen transport and pro-oxidant-antioxidant balance were determined.

Results: The effect of ozone on blood oxygen transport was found which was manifested in an increase in oxygen partial pressure and the degree of oxygenation. The index of hemoglobin –oxygen affinity $p50_{\text{actual}}$ was raised and a shift of the oxyhemoglobin dissociation curve rightwards was noticed. The addition of the gas transmitter donor, nitric oxide, enhanced the effect of this gas on the parameters of oxygen transport in the erythrocyte suspension

Conclusion: We found that ozone induced a change in oxygen-binding properties of the erythrocyte suspension which is a mechanism of action of the above gas on the adaptive processes in the body realized directly at the level of erythrocytes.

Keywords: Ozone, red blood cells, gas transmitter, hemoglobin oxygen affinity, nitric oxide, hydrogen sulfide

1. Introduction

Ozone (O_3) exerts various physiologic effects on the organism: increases the rate of erythrocyte glycolysis, improving oxygen delivery to tissues, and activates the enzymatic link of the antioxidant system (glutathione, peroxidase, catalase and superoxide dismutase).¹ Our earlier studies demonstrated the effect of O_3 on blood oxygen transport, which was manifested by a distinct shift of the oxyhemoglobin dissociation curve (ODC) rightwards and elevated concentrations of the gas transmitters hydrogen sulfide (H_2S) and nitric oxide (NO).² An effect of ozone on hemoglobin – oxygen affinity (HOA) due to activation of the gas transmitter system is suggested.³ Red blood cells possess their own mechanisms of NO synthesis and can serve as an essential source of NO under hypoxia.⁴ Moreover, erythrocytes were shown to contain 3-mercaptopyruvate sulfotransferase, contributing to H_2S production.⁵

However, NO-synthase activity is not only inherent to red blood cells; it is also a characteristic of leukocytes and thrombocytes. Thrombocytes were demonstrated to contain two isoforms of NO-synthase (inducible and en-

dothelial), and the application of flow cytometry allowed Mahaj et al. to detect inducible NO-synthase in leukocytes.^{6,7} Therefore, it was necessary to investigate the ability of red blood cells to respond to the action of ozone.

The purpose of this work was to study the effect of ozone on oxygen transport in a red blood cell suspension.

2. Materials and Methods

2. 1. Materials and Study Design

Venous blood was drawn with a heparin-pretreated syringe (50 U/ml).

This study was conducted, using a suspension of red cells from the blood of albino Sprague Dawley male rats fed a standard laboratory diet. The experimental protocol was approved by the Ethical Committee of Grodno State University (approval No1 of January 14, 2019).

To separate blood plasma and erythrocytes, blood samples were centrifuged at 3000 r.p.m. over 10 min and washed twice with a cold isotonic solution. Thereafter the

obtained red blood cell suspension was divided into 4 groups of samples of ten 1.2 ml samples in each group (the hematocrit level was 40%) (Figure 1). An isotonic solution of sodium chloride was enriched with an ozone-oxygen mixture for 4–5 minutes using an ozone generator UOTA-60-01 (Medozon, Russia), which makes it possible to measure ozone concentrations by an optical method in the ultraviolet range, which is provided by the technical capabilities of the device.

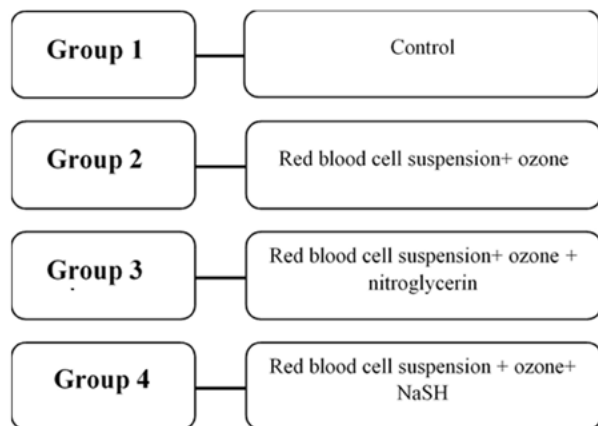


Figure 1: Study design

Group 1 samples (control) contained the erythrocyte suspension (1.2 ml) + isotonic solution of sodium chloride (1.1 ml). The contents of Group 2 samples were as follows: the red blood cell suspension (1.2 ml) + 1 ml of the ozonized isotonic solution of sodium chloride (O_3 concentration was 6 mg/l) + 0.1 ml of the isotonic solution of sodium chloride. The samples of Group 3 were composed of the red blood cell suspension (1.2 ml) + 1 ml of the ozonized isotonic solution of sodium chloride (O_3 concentration was 6 mg/l) + 1 ml of the solution containing the gas transmitter nitroglycerin (SchwarzPharma AG) at the final concentration of 0.05 mmol/l. Group 4 samples contained the red blood cell suspension (1.2 ml) + 1 ml of the ozonized isotonic solution of sodium chloride (O_3 concentration was 6 mg/l) + 0.1 ml of the solution containing the gas transmitter sodium hydrosulfide (Sigma-Aldrich) at the final concentration of 0.38 mmol/l. The contents of each sample were mixed. The incubation time was 60 min. Thus, we had control without ozonation (Group 1), the ozonized red blood cell suspension (Group 2) and the red blood cell- and gas-transmitter-containing suspensions (Groups 3 and 4).

2. 2. Methods

2. 2. 1. Blood Oxygen Transport (Hemoglobin-Oxygen Affinity)

Parameters of blood oxygen transport and acid-base status were measured using a Stat-Profile pHox plus L gas

analyzer at 37°C. Partial pressures of oxygen (pO_2) and carbon dioxide (pCO_2), the degree of oxygenation (SO_2), standard bicarbonate (SBC), actual base excess/standard base excess (ABE/SBE), hydrogen carbonate (HCO_3^-), pH and total plasma carbonic acid (TCO_2) were determined. Hemoglobin-oxygen affinity was assessed spectrophotometrically by $p50_{actual}$ (pO_2 corresponding to 50% Hb saturation with oxygen). The Severinghaus formulas were used to calculate $p50_{standard}$ and ODC position.⁸

2. 2. 2 Pro-Oxidant/Antioxidant System

The activity of free radical processes was evaluated by the contents of primary (diene conjugates, DC) and intermediate (malondialdehyde, MDA) products of lipid peroxidation (LPO) in the red blood cell suspension. The level of DC was measured spectrofluorimetrically (an SM 2203 spectrofluorimeter, SOLAR) by a method based on the intensity of absorption of diene structures of lipid hydroperoxides at 233 nm, in comparison with the blank samples in which the biological material was substituted by distilled water.⁹ The DC content was expressed as U/ml. The concentration of MDA (TBARS) was assessed by the interaction with 2'-thiobarbituric acid (TBA) which, when heated in acidic medium, causes the formation of a pink trime-thine complex.¹⁰ The intensity of color was determined spectrophotometrically at a wavelength of 55 nm with a PV12 51 SOLAR spectrophotometer and compared to control. The MDA concentration was expressed as $\mu\text{mol/l}$.

To determine catalase activity in hemolysates, we used the method of Koroliuk based on spectrophotometrical recording of the amount of the colored product of the reaction of H_2O_2 with ammonium molybdate having a maximum absorption at a wavelength of 410 nm.¹¹ The activity of catalase was expressed as $\text{mmol } H_2O_2/\text{min/g Hb}$. The amount of the enzyme catalyzing the formation of 1 mmol of the product per 1 min under the experimental conditions was taken as the unit of activity.

2. 2. 3. Statistical Analysis

The correspondence of the study data to the normal distribution law was tested by the Shapiro-Wilk test. With consideration for this criterion, non-parametric statistics with application of Statistica 10.0 software (StatSoft Inc., Tulsa, Oklahoma, USA) was used. Three and more independent groups were compared by the Kruskal-Wallis one-way analysis-of-variance-by ranks test. Allowing for the small sample and multiple comparisons, the significance of the data obtained was evaluated using the Mann-Whitney U-test. The Wilcoxon signed ranks test was applied for paired in-group comparisons of the indices levels using repeated measures ANOVA. The results were presented as a median (Me), the interquartile range between the 25th and the 75th percentile. The data were considered significant at the level of $P < 0.05$.

3. Results and Discussion

The O₃ treatment of the red blood cell suspension resulted in an increase in the fundamental indices of blood oxygen transport: SO₂ by 121.8 % (P < 0.05), pO₂ by 74.1% (P < 0.05) (Table 1). Under these conditions, the value of HOA parameter p50_{actual} was increased by 21.4% (P < 0.05) and the ODC was shifted rightwards (Figure 2) compared to the control group. The value of p 50_{standard} was also observed to rise. No significant changes were found when analyzing the acid-base balance parameters. Nitroglycerin enhanced the effect of ozone on the oxygen transport in the red blood cell suspension. The values of SO₂ and pO₂ increased by 12.5% and 21.0 (P < 0.05), respectively, in comparison with the samples pretreated with the ozonized isotonic solution of sodium chloride. Under these conditions, the HOA parameter p50_{actual} increased by 7.5% (P < 0.05) and the ODC was shifted rightwards more distinctly (Figure 2). The H₂S donor (sodium hydrosulfide) did not exert a similar effect.

The treatment of the red blood cell suspension with the ozonized saline solution caused an 85.3% elevation of the MDA content in the red blood cell suspension and the concentration of DC was increased by 77.4% (P < 0.05) in comparison with the control group (Table 2), whereas catalase activity was decreased by 44.5% (P < 0.05). The addition of the gas transmitter donors, nitroglycerine and sodium hydrosulfide, did not cause any changes in the LPO indices. However, it raised catalase activity by 46.1%

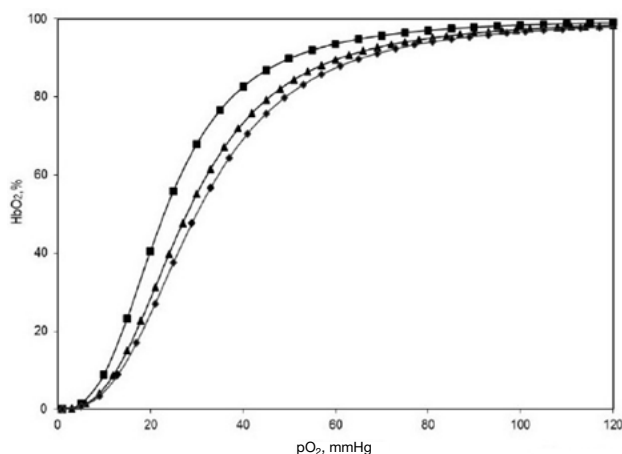


Figure 2: Effect of ozone on the position of the oxyhemoglobin dissociation curve at real pH and pCO₂ values. ■ – control; ▲ – red blood cell suspension + ozone; ◆ – red blood cell suspension + ozone + NO.

(P < 0.05) and 43.8% (P < 0.05), respectively compared to the group of samples containing the ozone – treated red blood cell suspension.

In comparison with other blood formed elements, red blood cells are an important target for the action of ozone. Due to the hexose monophosphate shunt, ozone promotes activation of 2,3-diphosphoglycerate mutase (DPGM), which finally results in conversion of erythrocyte 1,3-DPGM to 2,3-DPGM that, binding to the hemoglobin β-chain, may bring about an ODC shift right-

Table 1: Effect of ozone on oxygen transport in red blood cell suspension (median [25th; 75th percentile])

Parameter	Control (n = 10)	Red blood cell suspension + ozone (n = 10)	Red blood cell suspension + ozone + NO (n = 10)	Red blood cell suspension + ozone + H ₂ S (n = 10)
SO ₂ , %	26.96 [26.00; 32.10]	59.80 [56.30; 62.20]*	67.30 [62.70; 67.70]*#	58.10 [57.90; 58.70]*Ψ
pO ₂ , mmHg.	18.15 [17.40; 19.60]	31.60 [30.10; 34.50]*	38.25 [37.40; 39.20]*#	31.05 [28.70; 31.30]*Ψ
pH, units	7.305 [7.287; 7.356]	7.331 [7.321; 7.352]	7.313 [7.293; 7.315]#	7.318 [7.312; 7.353]
pCO ₂ , mmHg.	5.25 [4.70; 5.90]	4.70 [4.50; 5.10]	6.45 [4.30; 8.70]	6.45 [5.20; 8.20]#
HCO ₃ ⁻ , mmol/L	2.70 [2.30; 3.30]	2.45 [2.30; 2.70]	3.25 [2.30; 4.20]	3.30 [2.80; 4.18]#
TCO ₂ , mmol/L	2.85 [2.40; 5.90]	2.60 [2.40; 2.90]	3.5 [2.40; 4.50]	3.45 [2.83; 4.50]#
ABE, mmol/L	-23.60 [-24.60; -20.40]	-23.65 [-23.80; -23.60]	-23.30 [-24.10; -22.40]	-23.20 [-23.48; -22.30]#
SBE, mmol/L	-19.90 [-21.00; -17.10]	-20.60 [-20.70; -20.30]	-20.05 [-20.30; -19.50]#	-20.80 [-21.15; -20.53]Ψ
SBC, mmol/L	9.00 [8.50; 10.80]	8.60 [8.60; 8.90]	8.85 [8.40; 9.40]	8.75 [8.40; 9.38]
p50 _{actual} , mmHg	22.96 [22.40; 23.97]	27.88 [27.49; 27.92]*	29.99 [29.79; 31.13]*#	27.55 [27.49; 27.85]*Ψ
p50 _{standard} , mmHg	20.63 [20.20; 21.60]	25.40 [23.00; 26.90]*	28.35 [27.40; 29.00]*#	23.40 [23.40; 23.60]*Ψ

Note: changes compared to control (*), red blood cell suspension + ozone (#), Red blood cell suspension + ozone + NO (Ψ).

Table 2. Effect of ozone on indices of pro-oxidant-antioxidant balance of red blood cell suspension (median [25th; 75th percentile])

Parameter	Control (n = 10)	Red blood cell suspension + ozone (n = 10)	Red blood cell suspension + ozone + NO (n = 10)	Red blood cell suspension + ozone + H ₂ S (n = 10)
MDA, μmol /L	8.73 [7.63; 9.21]	16.18 [11.84; 17.57]*	14.60 [11.57; 17.84]*	15.55 [14.73; 16.31]*
DK, U/mL	16.62 [15.50; 18.23]	29.48 [17.54; 34.87]*	28.48 [25.29; 29.26]*	28.50 [27.12; 29.89]*
Catalase, mmol H ₂ O ₂ /min/g Hb	13.53 [12.19; 14.02]	7.51 [6.18; 9.88]*	10.97 [10.23; 11.47]*#	10.80 [10.04; 11.60]*#

Note: changes compared to control (*), red blood cell suspension + ozone (#).

wards.¹² We believe that in addition to the above mechanism, other mechanisms can be involved in this process, in particular those mediated through gas transmitters. Red blood cells contain the constitutive isoform of NO synthase, which produces NO.¹³ Blood plasma shows nitrites/nitrates, but during inhibition of erythrocyte NO synthase, their concentration considerably decreases, which proves that red blood cell NO is exported via anion exchanger 1 in the form of secondary nitrogen species to which hemoglobin is unlikely to bind, thus providing for a free NO pool.¹⁴ Our findings show that the addition of the exogenous donor nitric oxide (nitroglycerin) increases the effect of O₃ on blood oxygen transport in the red blood cell suspension. However, the hydrogen sulfide donor (sodium hydrosulfide) does not have this effect. It is known that NO is capable of changing HOA.¹⁵ Its release from red blood cells is controlled by the blood pO₂ level, whereas the O₃ treatment promotes an increase in this parameter.¹⁶ According to our findings, red blood cells directly respond to the effect of ozone, and this response is manifested with involvement of the gas transmitters, independently of leukocytes and thrombocytes.

Exposure of blood to O₃ leads to production of reactive oxygen species, inducing activation of lipid peroxidation in cell membranes and the development of oxidative stress.¹⁷ Continuous exposure of red blood cells to the multitude of different oxidants contributes to the formation of their potent intracellular antioxidant defense system, with gas transmitter mechanisms occupying a special place in the hierarchy of these processes.¹⁸ Due to its oxidative activity, ozone stimulates the antioxidant system of erythrocyte defense and improves cell deformability.¹⁹ Reactive oxygen species are neutralized to give hydrogen peroxide, which finally results in an increase in catalase activity.²⁰ However, in our studies, the activity of the enzyme decreased, thus providing evidence for an imbalance between antioxidants and free radicals. In the membrane fraction of red blood cells, ozone, as a source of oxygen, reacts with NO to form the powerful oxidant peroxynitrite.²¹ Subsequent oxidation of methemoglobin by peroxynitrite may induce synthesis of globin radicals, which enhance pro-oxidant activity in red blood cells.²² In turn, NO and hydrogen sulfide are also capable of affecting the me-

tabolism of antioxidants due to the gas transmitter enzymes and their reaction products and this feature was noticed in the groups of samples with nitroglycerin and hydrogen sulfide which showed elevated catalase activity compared to the group containing the ozone-treated red blood cell suspension.²³

Thus, we found ozone-induced changes in parameters of blood oxygen transport of the erythrocyte suspension, which is one of the mechanisms of the action of ozone on adaptive processes in the body which are directly realized by red blood cells.

4. Conclusion

1. The exposure of the red blood cell suspension to ozone improved its oxygen transport indices: the increase in pO₂ and SO₂ as well as the ODC shift rightwards were found.
2. Although the addition of nitroglycerin enhanced the effect of ozone on the oxygen transport in the red blood cell suspension under the above experimental conditions (the distinct ODC shift rightwards), sodium hydrosulfide did not exert a similar effect.
3. Ozone induced an elevation of the DC and MDA concentrations as well as a decrease of catalase activity. The gas transmitter donors did not enhance oxidative stress, but activated catalase.

Acknowledgments

Funding

This study was financially supported by the National Anti-Doping Laboratory, Republic of Belarus, Draft State Programs for Scientific Research No. 30-24/549-21.

Author contributions

VZ designed, organized, and wrote the article; designed the outline; solved queries related to scientific publications from the journals. EB performed Pubmed searches, aided in writing, and critiqued the literature. All authors have read and approved the manuscript provided.

Institutional Review Board Statement

The study was conducted according to the guidelines of the Declaration of Helsinki, and Ethical Committee of the Grodno State Medical University (approval No. 1) approved the study on January 14, 2019.

5. References

1. K. Re, J. Gandhi, R. Liang, S. Patel, G. Joshi, N. L. Smith, I. Reid, S. A. Khan, *Med. Gas Res.* **2023**, *13*, 1-6. DOI:10.4103/2045-9912.351890
2. V. V. Zinchuk, E. S. Biletskaya, *Biophysics.* **2020**, *65*, 779-783. DOI:10.1134/S0006350920050231
3. V. V. Zinchuk, D. D. Zhadko, *Nitric Oxide* **2019**, *84*, 45-49. DOI:10.1016/j.niox.2019.01.007
4. V. Kuhn, L. Diederich, T. C. S. Keller, C. M. Kramer, W. Lückstädt, C. Panknin, T. Suvorova, B. E. Isakson, M. Kelm, M. M. Cortese-Krott, *Antioxid. Redox Signal.* **2017**, *26*, 718-742. DOI:10.1089/ars.2016.6954
5. M. M. Cortese-Krott Red blood cells as a “central hub” for sulfide bioactivity: Scavenging, metabolism, transport, and cross-talk with nitric oxide. *Antioxid. Redox Signal.* **2020**, *33*, 1332-1349. DOI:10.1089/ars.2020.8171
6. E. Gkaliagkousi, J. Ritter, A. Ferro Platelet-derived nitric oxide signaling and regulation. *Circ Res.* **2007**, *101*, 654-662. DOI:10.1161/CIRCRESAHA.107.158410
7. S. Maharaj, K. D. Lu, S. Radom-Aizik, F. Zaldivar, F. Haddad, H.W. Shin, S.Y. Leu, E. Nussbaum, I. Randhawa, D. M. Cooper. *Nitric Oxide* **2018**, *72*, 41-45. DOI:10.1016/j.niox.2017.11.002
8. J. W. Severinghaus, *J Appl Physiol.* **1966**, *21*, 1108-1116. DOI:10.1152/jappl.1966.21.3.1108
9. R. Mendes, C. Cardoso, C. Pestana, *Food Chem.* **2009**, *112*, 1038-1045. DOI:10.1016/j.foodchem.2008.06.052
10. A. T. Diplock, M. C. R. Symons, C. A. Rice-Evans Techniques in free radical research: (Laboratory techniques in biochemistry and molecular biology, volume 22), Elsevier, Amsterdam, **1991**.
11. M. A. Koroliuk, L. I. Ivanova, I. G. Maïorova, V. E. Tokarev, *Lab. Delo* **1988**, *1*, 16-19.
12. V. Bocci, *Free Radic. Res.* **2012**, *46*, 1068-1075. DOI:10.3109/10715762.2012.693609
13. S. Kishimoto, T. Maruhashi, M. Kajikawa, S. Matsui, H. Hashimoto, Y. Takaeko, T. Harada, T. Yamaji, Y. Han, Y. Kihara, K. Chayama, C. Goto, F. M. Yusoff, A. Nakashima, Y. Higashi, *Sci. Rep.* **2020**, *10*, 11467-1-9. DOI:10.1038/s41598-020-68319-1
14. K. J. Richardson, L. Kuck, M. J. Simmonds, *Am. J. Physiol. Heart Circ. Physiol.* **2020**, *319*, 866-872. DOI:10.1152/ajpheart.00441.2020
15. A. G. Tsai, M. Intaglietta, H. Sakai, E. Delpy, C. D. La Rochelle, M. Rousselot, F. Zal, *Curr. Drug Discov. Technol.* **2012**, *9*, 166-172. DOI:10.2174/157016312802650814
16. S. Zheng, N. A. Krump, M. M. McKenna, Y. H. Li, A. Hanemann, L. J. Garrett, J. S. Gibson, D. M. Bodine., P. S. Low. *J. Biol. Chem.* **2019**, *294*, 2519-2528. DOI:10.1074/jbc.RA118.006393
17. C. H. Wiegman, F. Li, B. Ryffel, D. Togbe, K. F. Chung, *Front. Immunol.* **2020**, *11*, 1957-1-9. DOI:10.3389/fimmu.2020.01957
18. R. Franco, G. Navarro, E. Martínez-Pinilla, *Antioxidants*, **2019**, *8*, 46-1-10. DOI:10.3390/antiox8020046
19. I. H. Akbudak, V. Kucukatay, O. Kilic-Erkek, Y. Ozdemir, M. Bor-Kucukatay, *Clin. Hemorheol. Microcirc.* **2019**, *71*, 365-372. DOI:10.3233/CH-180417
20. F. Dei Zotti, R. Verdoy, D. Brusa, I. I. Lobysheva, J. L. Balligand, *Redox Biol.* **2020**, *34*, 101399-1-10. DOI:10.1016/j.redox.2019.101399
21. F. Dei Zotti, I. I. Lobysheva, J. L. Balligand, *PLoS One* **2018**, *13*, e0200352-1-20. DOI:10.1371/journal.pone.0200352
22. J. M. Rifkind, E. Nagababu. *Antioxid. Redox Signal.* **2013**, *18*, 2274-2283. DOI:10.1089/ars.2012.4867
23. D. D. Guerra, K. J. Hurt, *Biol. Reprod.* **2019**, *101*, 4-25. DOI:10.1093/biolre/ioz038

Povzetek

Uvod: Ozon vpliva na prenos kisika v krvi in na prooksidativno-antioksidativno ravnovesje, vendar vloga sestavin kri in plinskih prenašalcev pri teh procesih še vedno ostaja nejasna. Namen te raziskave je bil proučiti vpliv ozona na prenos kisika in prooksidativno-antioksidativno ravnovesje v suspenziji rdečih krvničk.

Metode: Suspenzijo eritrocitov smo inkubirali z ozonom v koncentraciji 6 mg/l in snovmi, ki vplivajo na sintezo plinskih prenašalcev (nitroglicerina, natrijev hidrosulfid). Določeni so bili parametri prenosa kisika v krvi in prooksidativno-antioksidativno ravnovesje.

Rezultati: Ugotovili smo vpliv ozona na prenos kisika v krvi, ki se je kazal v povečanju delnega tlaka kisika in stopnje oksigenacije. Indeks dejanske afinitete hemoglobina do kisika p50 se je povečal, opazen pa je bil tudi premik disociacijske krivulje oksihemoglobina v desno. Dodatek donorskega plinskega prenašalca, dušikovega oksida, je povečal učinek tega plina na parametre prenosa kisika v suspenziji eritrocitov.

Zaključek: Ugotovili smo, da je ozon povzročil spremembo lastnosti vezave kisika v suspenziji eritrocitov, kar predstavlja mehanizem delovanja omenjenega plina na prilagoditvene procese v telesu, ki se dogajajo neposredno na ravni eritrocitov.



Except when otherwise noted, articles in this journal are published under the terms and conditions of the Creative Commons Attribution 4.0 International License

Scientific paper

Chemical and Antioxidant Profile of Hydroalcoholic Extracts of *Stachys Officinalis* L., *Stachys Palustris* L., *Stachys Sylvatica* L. from Romania

George Florian Apostolescu¹, Diana Ionela (Stegarus) Popescu², Oana Botoran², Daniela Sandru³, Nicoleta Anca Şuţan^{4,*} and Johny Neamtu⁵

¹ Doctoral school, Faculty of Pharmacy, University of Medicine and Pharmacy of Craiova, 2 Petru Rareş Street, 200349 Craiova, Romania

² National Research and Development Institute for Cryogenics and Isotopic Technologies–ICSI Ramnicu Valcea, 4th Uzinei Street, 240050 Ramnicu Valcea, Romania

³ Department of Agricultural Sciences and Food Engineering, Lucian Blaga University of Sibiu, Doctor Ion Raţiu 7, 550012 Sibiu, Romania

⁴ Department of Natural Sciences, University of Pitesti, Targul din Vale 1, 110040 Pitesti, Romania

⁵ Faculty of Pharmacy, University of Medicine and Pharmacy of Craiova, 2-4 Petru Rares Str., 200349 Craiova, Romania

* Corresponding author: E-mail: anca.sutan@upit.ro
Tel.: +40 348 453 260

Received: 02-04-2023

Abstract

Stachys officinalis L., *Stachys palustris* L., *Stachys sylvatica* L. (Lamiaceae) are widely used as herbal remedies. In this study, comparative assessment of the phenolic acids, flavonoids, anthocyanin, and tannins content, together with antioxidant activity of the extracts obtained from flowers, leaves and stems was performed. Phenolic acids determined by the HPLC method reached highest values in flower extract of *S. palustris*, stem extract of *S. officinalis*, and leaf extracts of *S. sylvatica*. Flavonoids were found at values exceeding 100 mg quercetin equivalents (QE)/g dry weights in all three species, based on the spectrophotometric method. Anthocyanins were detectable only in extracts from flowers. *S. officinalis* stood out for the highest content of anthocyanins and tannins. Antioxidant activity was present in all three species studied, with *S. palustris* standing out for the most intense ferric reducing antioxidant power. The results obtained lead to the validation of applicability of these plants for curative and food purposes, given their variety and richness in bioactive compounds and antioxidants.

Keywords: *Stachys*; Phenolic Compounds; Flavonoids; Anthocyanin; Tannins; Antioxidant

1. Introduction

Many plants are known for their therapeutical effects in the treatment of certain diseases, but more and more are being discovered, and nowadays there is an ever-increasing return to nature and what it has to offer. Advanced or classical extraction technologies of valuable components lead to the completion of information in this field, the results being visible both in the scientific and commercial areas.

One of the often refferened families in folk medicine is *Lamiaceae*, with genera and species identified world-

wide, most of them presenting exceptional curative properties. The genus *Stachys* is represented by 300–400 species, native or acclimatized, natural or ornamental, their importance and complex chemical composition being validated by the increasingly varied research that is being carried out and the possibility of superior exploitation of their bioactive potential.^{1,2}

Recent studies revealed antioxidant, enzyme inhibition, antidiabetic, anti-cholinesterase and anti-tyrosinase properties of *Stachys cretica* subsp. *mersinaea* (Boiss.) Rech.f., cytotoxic and antifungal activities of *Stachys parv-*

iflora L., *Stachys cretica* subsp. *bulgarica* Rech.f. (SC), *Stachys byzantina* K. Koch (SB), *Stachys thirkei* K. Koch, antibacterial activity against Gram-positive microorganisms of *Stachys byzantina* K.Koch, *S. officinalis* and *S. sylvatica*, nephroprotective, anti-inflammatory, hepatoprotective and anticancer properties of *Stachys pilifera* Benth, antiphlogistic effects of *S. alpina*, *S. germanica*, *S. officinalis* and *S. recta* antidepressant activity and apoptotic effect of *Stachys pilifera* Benth.^{3–11} Antioxidant activities were mentioned for all the above species. Nutritional value was also showed by a number of studies for species such as *Stachys affinis* Bunge, *Stachys lavandulifolia* Vahl. var. *lavandulifolia*, *Stachys sieboldii* Miq.^{12–14}

The chemical composition of the extracts differs depending on the species,^{6,9} on the solvent, on the different parts of plants used for extraction¹⁵ and the geographical area that the plants grow,^{16,17} and so are the antioxidant and antimicrobial properties.^{16,18}

In the central area of Romania (Sibiu County), seven species of *Stachys* genus have been identified so far: *Stachys alpina* L., present on the valleys and slopes of the Cibin and Făgăraș mountains; *Stachys annua* L. found on the montan hills at altitudes between 300 m and 700 m; *Stachys germanica* L. found on hills and montan hills at altitudes of 320–550 m; *Stachys officinalis* L. identified in hilly-mountain areas at altitudes between 330–1250 m; *Stachys palustris* L. growing sporadically at high altitudes between 300 m and 900 m; *Stachys recta* L. present in the hilly-mountainous area at altitudes between 260–800 m; *Stachys sylvatica* L. present frequent on mountain hills at high altitudes comprised 340–1470 m.¹⁹

Considering the therapeutic and nutritional potential of the species of the genus *Stachys*, this study provides a comprehensive and comparative evaluation of polyphenols and antioxidant profile of extracts obtained from flowers, leaves and stems of the three species grown in the central area of Romania (Sibiu County): *S. officinalis*, *S. palustris* and *S. sylvatica*. Although other reports include chemical profile of *Stachys* sp., this is the first study that shows the chemical and antioxidant profile differentiated according to the aerial part of the plant and provide important clues regarding the optimal exploitation of plants, through the use of plant organs with abundant bioactive compounds.

2. Experimental

2.1. Plant Samples and Description of the Area of Interest

Plant samples: *Stachys officinalis* L. (hemicryptophyte, Eurasia), *Stachys palustris* L. (hemicryptophyte, circumpolar), and *Stachys sylvatica* L. (hemicryptophyte, Eurasia) were collected in July 2022, in the maximum flowering period from depression Mărginimii groups. The

area that was studied is located between coordinates: 45°45'23"N 23°55'28"E and 45°45'58"N 23°54'29"E, at an altitude between 560 m and 610 m that covers the media between villages Fântânele (Cacova) and Sibiel from Mărginimea Sibiului.

Depression Mărginimii groups is located at the foothills of Mountains Cindrel and is formed by two depressions, one of Sibiu and the other of Săliște, separated by Măgura Beleuța with an altitude of 630 m. Depression is characterized by gradually hill Miocene aged at the foothills of mountains, meadows, and terraces, attributes that frame it in the contact area. The climate is distinguished according to the landscape, with the depression area showing warm sides, rich in precipitation, and more significant in winter. The solar radiation exceeds 115 kcal/cm²/year overall. Air temperature oscillates depending on the landscape, depression area presenting an annual average temperature of 9 °C and northwest winds. Rainfall totals over 600 mm, with summer showers. Woody and herbaceous species are specific to the foothill area. The xerophiles meadows from the Depression Mărginimii (of Săliște) stand out through boreal plant diversity, dominated by plants original from Eurasia, followed by those Europeans and Central-European. Floristic species from this area were botanically researched with results that led to a very thorough and complete inventor.¹⁹

Plant samples of *S. officinalis*, *S. palustris*, and *S. sylvatica* were recorded within the CCBIA from L. Blaga University, Sibiu, Romania under no. 314/1, 314/2, and 314/3 respectively.

2.2. Chemicals and Reagents

The chemicals and reagents used in the process were sodium nitrite (NaNO₂) 5%, aluminum chloride hexahydrate (AlCl₃ · 6H₂O) 10%, sodium hydroxide (NaOH) 1M, quercetin, potassium chloride (KCl) 0.025M, sodium acetate (CH₃COONa) 0.4M, hydrochloric acid (HCl), cyanidin-3-glucoside, reagent Folin-Ciocalteu, sodium carbonate (Na₂CO₃) 20%, tannic acid, casein, 0.5% formic acid in H₂O, methanol (CH₃OH), ferric-tripyridyltriazine (Fe³⁺-TPTZ), Trolox (6-hydroxy-2,5,7,8-tetramethylchroman-2-carboxylic acid) from Fluka (Germany) and Sigma-Aldrich (Germany). The HPLC standards were caffeic acid, chlorogenic acid, p-coumaric acid, ferulic acid, m-coumaric acid, sinapic acid, trans-cinnamic acid, benzoic acid, ellagic acid, gallic acid, p-hydroxybenzoic acid, rosmarinic acid, syringic acid, and vanillic acid from Sigma-Aldrich (Germany).

2.3. Preparation of *Stachys* sp. Extracts

Flowers, stems, and leaves of *S. officinalis*, *S. palustris*, and *S. sylvatica* were dried separately at a temperature of 40 °C until the constant mass. Each 50 g of shredded dried material was soaked in a 500 mL solution of aqueous

80% methanol for 3 days at a temperature of 18 °C in a covered container. The samples were decanted, filtered with a Buchner vacuum pump (Whatman filter paper No. 1001 090), and concentrated in a rotary evaporator. The dry extracts were resuspended in distilled water to a concentration of 1:1 mg/ml.

2. 4. Determination of Phenolic Acids (PAs)

PAs were quantified through the HPLC method proposed by Baczek et al.²⁰ slightly modified, and by consulting other methods that were already applied on plant extracts.^{21,22} Phenolic acids were identified following the HPLC system Smartline, KNAUER GmbH (Berlin, Germany), equipped with a quaternary pump, automatic injection and DAD detector, set to the following λ wavelengths: 280 nm, 320 nm, 360 nm. Briefly, C18 columns (Zorbax SB – Aq: 250 mm \times 4.6 mm i.d., 5.0 μ m p.s) were used. For the mobile phase, a solution of deionized H₂O and phosphoric acid (pH 3.5) was used as eluent A, and acetonitrile (pH 3.5) as eluent B, with the follows ratio: 0.00 min – 20% B; 0.45 min – 20% B; 5.50 min – 30% B; 5.55 min – 90% B; 6.50 min – 95% B; 6.51 min – 20% B; 15.00 min – STOP. A volume of 2 μ L extract was injected into the column for chromatographic analysis, and the flow rate was 1 mL/min, at the temperature of 35 °C and 15 min total time of analysis. The identification and quantification of phenolic acids was achieved by comparison with selected standards, using calibration curves for each individual compound. The experiments were performed in triplicate and the results were expressed in μ g/g extract.²⁴

2. 5. Determination of Total Flavonoid Content (TFC)

Flavonoids were determined based on the spectrophotometric method described by Popescu et al.²³ The aqueous extracts (5 mL) were homogenized with 5% NaNO₂ solution (0.3 mL) and incubated for 5 minutes. Later a solution of AlCl₃ · 6H₂O 10% (0.5 mL) was added and the mixture was left to react in darkness. After 15 minutes of reaction 2 mL of 1M NaOH solution was added and made up to 10 mL with distilled water. The samples were read with UV-1900 SHIMADZU spectrophotometer (Shimadzu Corporation, Kyoto, Japan) at a wavelength of 510 nm. The TFC was expressed in mg quercetin equivalents /gram of dry weight (mg QE/g DW).

2. 6. Determination of Total Monomeric Anthocyanin Pigment Content

The colorimetric method based on the difference of absorbance of anthocyanins at a change in pH (pH 1 and pH 4.5) was applied for determination of total monomeric anthocyanin pigment (MAPC) content.²⁴ Depending on their concentration, the difference in the absorbance of

MAPC was read at a wavelength of 520 nm, respectively 700 nm, using UV-1900 SHIMADZU spectrophotometer (Shimadzu Corporation, Kyoto, Japan). Results obtained in mg/L cyanidin-3-glucoside were converted into mg/g.²⁴

2. 7. Determination of Total Tannin Content (TTC)

For the assessment of TTC, comparative quantification of total polyphenols determined through Folin-Ciocalteu method and express the results in μ g tannic acid equivalents/ml (μ g TAE/ml) and polyphenols residuals in casein was applied. The difference between the total level of polyphenols and polyphenols residuals represents the TTC expressed in mg tannic acid equivalents /g dry weight (mg TAE/g DW).^{25,26}

2. 8. Determination of Ferric Reducing Antioxidant Power (FRAP)

Antioxidant properties of the extracts were evaluated based on the reduction of Fe³⁺-TPTZ in Fe²⁺-TPTZ by antioxidants ingredients from the samples. FRAP was monitored using the spectrophotometric method described by Lachowicz-Wisniewska et al.²⁷ Briefly, 1 mL of each aqueous extracts was homogenized with 3 mL Fe³⁺-TPTZ, absorbance being read at a wavelength of 593 nm with UV-1900 SHIMADZU spectrophotometer (Shimadzu Corporation, Kyoto, Japan), after 10 minutes of incubation. The results are expressed in mg Trolox equivalents/g of dry weight (mg TE/g DW).

2. 9. Multivariate Analysis

In order to explain the significant correlations between quality parameters (phenolic acids data), principal component analysis (PCA) was the main approach of multivariate statistical analysis. In order to display data as single point for each variable and to reveal the correspondence between the principal component and the direction of maximum variance, the data were mean-centered. Pearson correlations ($p < 0.05$ and $p < 0.01$) were used to identify correlations between all variables included in the dataset. All statistical analyzes were performed using Addinsoft XLSTAT software, version 2014.5.03 (Addinsoft Inc., New York, NY, USA).

3. Results and Discussions

3. 1. Phenolic Acids in *Stachys* Extracts

Through their anti-cancer, anti-inflammatory and antimicrobial action^{5,28–31} or through their positive effects on curing neurodegenerative diseases such as Alzheimer's,³ phenolic acids represent bioactive plants secondary metabolites with important preventive and curative acti-

ons. Seven hydroxybenzoic acids and eight hydroxycinnamic acids were identified in *Stachys* flower extracts, with very low (0.01 µg/g trans-cinnamic acid) or generous values (27970.53 µg/g benzoic acid).

The results presented in Table 1 indicate that benzoic acid accumulates significantly especially in flower of *S. sylvatica* (19071.32 µg/g) and *S. palustris* (27970.53 µg/g) and leaves of *S. officinalis* (4564.43 µg/g). The lowest values of benzoic acid were observed in extracts of stems, varying between a minimum of 282.28 µg/g in *S. palustris* and a maximum of 1270.16 µg/g in *S. officinalis*. At a significantly lower detected concentration (3080 µg/g extract), benzoic acid was indicated as one of the most abundant phenolic compound of *S. cretica* subsp. *Mersinaea*.³

The ellagic acid has been identified in the flowers extracts in quantities between 18.02 µg/g for *S. palustris* and 32.01 µg/g for *S. sylvatica*, the obtained values for the stems extracts being below 7 µg/g, and those for the leaves extracts reaching a maximum of 21.12 µg/g in *S. sylvatica*. Uneven amounts of gallic acid were found in the studied extracts. Gallic acid was found in values below 10 µg/g in flower extracts and it was undetected in stems. In comparison, higher content of 16.59 mg gallic acid equiv./g dry matter in *Stachys lavandulifolia* Vahl.³² or 900.61±0.06 mg gallic acid equivalent /100 g in dried herb in *Stachys aleurites* Boiss. & Heldr. was reported.³³ The p-hydroxybenzoic acid was identified at significant values in the flower extracts of *S. sylvatica* (83.15 µg/g) and in the leaves extracts of *S. officinalis* (73.43 µg/g). Salicylic acid was found in trace, with amounts between 0.22 µg/g – 9.42 µg/g in flowers extracts, and with subunit values in extracts of stems and leaves (0.27 µg/g – 0.96 µg/g), irrespectively of the species. Significantly lower amount of p-hydroxybenzoic acid

(0.006 mg g⁻¹ DW) and significantly higher amount of salicylic acid (0.168 mg g⁻¹ DW) were found in methanol extracts of leaves of *S. byzantina*, in comparison with leaves and flower extracts in our study.³⁴ These results suggest a species-specific phenolic acid pattern.

Syringic acid was fluctuated in flower extracts between 389.41 µg/g in *S. officinalis* and 569.78 µg/g in *S. palustris*, in stems extracts between 11.24 µg/g in *S. palustris* and 126.32 µg/g in *S. sylvatica*, and in leaf extracts between 9.29 µg/g in *S. palustris* and 111.11 µg/g in *S. sylvatica*. A syringic acid derivative was found in ethanol extract of dried roots of *Stachys geobombycis* C.Y.Wu.³⁵ Vanillic acid was not detected in the stems and leaves of studied extracts, and was identified only in the flower extracts at values between 266.78 µg/g (*S. officinalis*) and 343.21 µg/g (*S. palustris*).

Among the hydroxycinnamic acids identified, the most significant amounts were found in the case of chlorogenic acid with values varying in the flower extracts between 1011.78 µg/g (*S. officinalis*) and 7132.29 µg/g (*S. palustris*). Chlorogenic acid was also identified in stems (125.37 µg/g – 333.25 µg/g) and in leaves (113.48 µg/g – 452.65 µg/g) in all three species. Chlorogenic acid and vanillic acid were predominant in aerial parts extracts of *Stachys cretica* L. subsp. *vacillans* Rech. Fil.³⁰ Syringic acid and vanillic acid were identified in *Stachys* sp. aff. *Schimperi* whole plant extract.³⁶

Caffeic acid was identified in the flower extracts at values over 100 µg/g, but in leaf and stems extracts the values were only subunit, or undetectable in the stems extracts of *S. officinalis*. Caffeic acid was found as major phenolic compound for *Stachys tmolea* Boiss.³⁷ The p-coumaric acid was detected in all *Stachys* extracts, values being significantly identified in the flower extracts (35.66 µg/g –

Table 1. Phenolic acids identified and quantified in extracts obtained from flowers, stems and leaves of *S. officinalis*, *S. palustris*, *S. sylvatica*

Phenolic acid	<i>S. officinalis</i> (µg/g)			<i>S. palustris</i> (µg/g)			<i>S. sylvatica</i> (µg/g)		
	Flowers	Stems	Leaves	Flowers	Stems	Leaves	Flowers	Stems	Leaves
Hydroxybenzoic acid									
Benzoic acid	12464.34	1270.16	4564.43	27970.53	282.28	2225.44	19071.32	347.79	3447.22
Ellagic acid	24.25	4.56	12.34	18.02	1.27	2.97	32.01	6.96	21.12
Gallic acid	7.33	n.d	0.27	2.48	n.d	0.22	9.34	n.d	n.d
P-hydroxybenzoic acid	25.39	2.11	73.43	49.27	8.54	57.14	83.15	n.d	4.04
Salicylic acid	5.23	0.96	0.35	9.42	0.27	0.22	1.22	0.29	0.77
Syringic acid	389.41	34.12	22.44	569.78	11.24	9.29	487.76	126.32	111.11
Vanillic acid	266.78	n.d	n.d	343.21	n.d	n.d	312.22	n.d	n.d
Hydroxycinnamic acid									
Caffeic acid	102.56	n.d	0.01	176.53	0.02	0.15	149.28	0.04	0.11
Chlorogenic acid	1011.78	125.37	452.65	7132.29	234.23	217.02	2119.69	333.25	113.38
P- coumaric acid	35.66	10.21	12.92	46.22	9.22	16.78	55.19	22.33	24.21
Ferulic acid	821.32	247.77	293.99	916.16	196.78	241.39	441.02	133.44	188.07
M-coumaric acid	5.66	1.21	2.92	4.22	n.d	n.d	5.19	2.33	4.21
Rosmarinic acid	9.56	n.d	n.d	4.93	n.d	n.d	4.55	n.d	n.d
Sinapic acid	7.99	n.d	n.d	3.23	n.d	0.03	7.13	n.d	0.05
Trans-cinnamic acid	0.01	n.d	n.d	n.d	n.d	n.d	n.d	n.d	n.d
Total	15177.27	1696.47	5435.75	37246.29	743.85	2770.65	22779.07	972.75	3914.29

Values are expressed as mean (n = 3), n.d = not detected

55.19 µg/g), and lower in stems and leaves (9.22 µg/g – 24.21 µg/g). In all assessed extracts a significant amount of ferulic acid were quantified. The values determined in the flower extracts varied between 441.02 µg/g and 916.16 µg/g, and in the stem extracts up to a maximum of 247.77 µg/g. Ferulic acid were identified in other species, such as *Stachys germanica* L.,³⁸ *Stachys pumila* Banks & Sol.,³⁹ *S. byzantine*³⁴ and in *Stachys thirkei* K. Koch was found as major phenolic compounds along with chlorogenic acid, caffeic acid and rosmarinic acid.³⁷

In the extracts obtained from flowers have been detected m-coumaric acids (4.22 µg/g – 5.66 µg/g), rosmarinic acid (4.55 µg/g – 9.56 µg/g), sinapic acid (3.23 µg/g – 7.29 µg/g), trans-cinnamic acid (0.01 µg/g for *Stachys Officinalis* L). Other authors analyzed phenolics compounds, respectively PAs from various *Stachys* extracts, results being noted in the case of species *S. officinalis*,^{20,40,41,42} *S. palustris*,^{12,41} *S. sylvatica*,^{12,38} *Stachys cretica* ssp. *anatolica* Rech. Fil.,³¹ *Stachys lavandulifolia* Vahl.,⁴³ *Stachys tmolea* Boiss.⁴⁴

3. 2. Total Flavonoid Content in Flower, Stem and Leaf Extracts

Flavonoids are important bioactive compounds identified in all extracts, irrespective of plant species or organ used. As noted in table 2, the highest value of 51.66 mg QE/g DW were identified in flower extract of *S. palustris*, followed by flower extracts of *S. officinalis* (45.36 mg QE/g DW) and *S. sylvatica* (39.48 mg QE/g DW). TFC was lower in the extracts obtained from the stems and leaves regardless of the species. Similar or lower TFC was identified by other authors in *Stachys* species. Sarikurkcu et al. reported a TFC between 39.24 mg Re/g extract (routine equivalents) and 47.70 mg Re/g for *S. byzantina* extract,⁴⁵ and Ahmadvand et al. referenced a TFC of 17.09 mg QE/g extract and 31.18 mg QE/g for *Stachys inflata* Benth extract.⁴⁶

3. 3. Anthocyanins Content in Flower, Stem and Leaf Extracts

Anthocyanins are water-soluble, colored and bioactive compounds, associated with the red color of the flower petals of the three studied species. In this study, anthocyanins were identified at an average value of 32.61 mg/g extract in *Stachys officinalis* flowers, 19.88 mg/g extract in *Stachys palustris* flowers and 27.72 mg/g extract in *Stachys sylvatica* flowers. Table 2 shows the lack of anthocyanins in the extracts from stems and leaves. Anthocyanins were also detected by Lachowicz-Wisniewska et al.²⁷ in the flowers of the species *Stachys palustris* at an average amount of 20 mg/100 g d.m. or by Bursal et al.⁴⁷ in the extracts of *Stachys annua* at an average value of 34.3 µg/g, but also by other authors who highlighted their antioxidant and anti-inflammatory qualities.⁴⁸

Table 2. Flavonoids, anthocyanins, tannins and antioxidant activity of *S. officinalis*, *S. palustris*, *S. sylvatica*

Species	Aerial part	Total flavonoids (mgQE/g DW)	Anthocyanins (mg/g DW)	Total tannins (mg TAE/g DW)	FRAP (mg TE/g DW)
<i>S. officinalis</i>	Flowers	45.36	32.61	87.55	71.34
	Stems	39.45	n.d	77.39	56.38
	Leaves	31.22	n.d	84.27	83.22
	Total	38.67	10.87	83.07	70.31
<i>S. palustris</i>	Flowers	51.66	19.88	75.54	93.76
	Stems	19.78	n.d	44.97	66.09
	Leaves	32.67	n.d	71.76	76.21
	Total	34.70	19.88	64.09	78.68
<i>S. sylvatica</i>	Flowers	39.48	27.72	101.33	87.54
	Stems	29.07	n.d	56.39	63.27
	Leaves	31.63	n.d	51.15	75.77
	Total	34.70	27.72	69.62	75.52

3. 4. Determination of Total Tannin Content

Tannins are phenolic compounds produced as secondary metabolites by terrestrial and aquatic plants.⁴⁹ Table 2 stands out the fact that tannins vary in the flower extracts from 75.54 mg TAE/g DW to 101.33 mg TAE/g DW, the significantly higher value being attributed to *S. sylvatica*. In the extracts derived from stems, TTC was quantified to a value of 44.97 mg TAE/g DW and 77.39 mg TAE/g DW, the lowest value being defining for the species *S. palustris*. Lachowicz-Wisniewska et al. identified 36 hydrolysable tannins in *S. palustris* flower extracts, 32 in stem extracts and 31 in leaf extracts.²⁷ TTC varied between the level of 1.72% and 2.91% pyrogallol equivalent in *S. officinalis*, depending of the vegetative stage of plant development.²⁰

3. 5. Principal Component Analysis of Flowers, Stems and Leaves Sample of *S. Officinalis*, *S. Palustris* and *S. Sylvatica*

The results obtained through HPLC method were analyzed and interpreted to explain and to identify the relationships and the patterns of chemical compounds characteristic of *S. officinalis*, *S. palustris* and *S. sylvatica* flowers, leaves and stems. The first principal component (PC1) corresponds to 68% of the total variation, while the second principal component (PC2) explains only approximately 11% (Figure 1). The analysis of the PCA from flowers, leaves and stems showed a separation of the samples depending on their chemical composition, leaves and stems of *S. sylvatica*, stems of *S. officinalis* being located on the negative semiaxes. The location of the *S. officinalis* flower sample in quadrant II, away from the other samples, suggests the highest content of anthocyanins, flavonoids, rosmarinic acid, M-coumaric acid, etc. A similar content of

PAs are indicated by the close location of samples from flowers of *S. palustris* and *S. sylvatica* in the first quadrant, on the one hand, and samples from leaves of *S. palustris* and *S. officinalis* in the IV quadrant, on the other side (Figure 1a). The main components of positive side of PC1 were p-coumaric acid, flavonoids, ellagic acid, rosmarinic acid, anthocyanin, salicylic acid, syringic acid, sinapic acid and trans-cinnamic acid, while the positive side of the PC2 is identified with vanillic acid, tannins, caffeic acid, ferulic acid, p-hydroxybenzoic acid (Figure 1b).

The results are confirmed by the Pearson correlation coefficient. In the heatmap presented in Figure 2, a significant positive correlation can be observed between the chemical variables identified in the analyzed samples, very rarely being identified a weak negative correlation between the chemical components, such as between trans-cinnamic acid and p-hydroxybenzoic acid or FRAP.

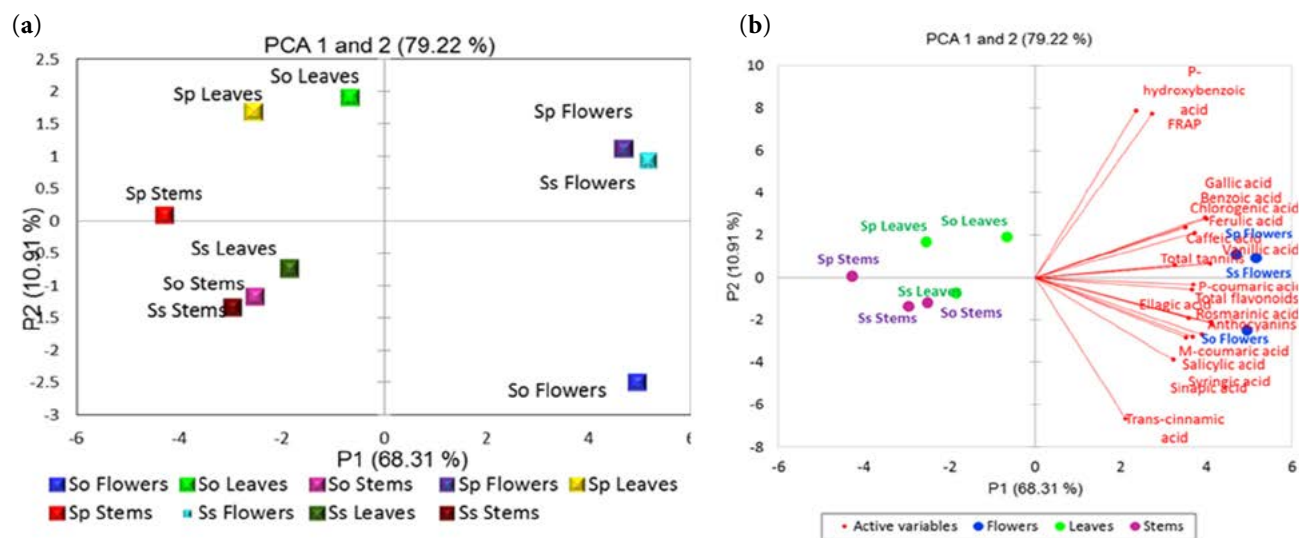


Figure 1. Differentiation of flowers, leaves and stems sources based on the compositional profile; (a) PCA score plot illustrating differentiation of flowers, leaves and stems sources based on the compositional profile. Colored symbols correspond to the flowers, leaves and stems of the three species addressed in this study (So – *S. officinalis*, Sp – *S. palustris* and Ss – *S. sylvatica*). The first two principal axes explained approximately 79% of the variance; (b) PCA loading plot showing the multivariate variation among the flowers, leaves and stems of the three species in terms of chemical compositional variables

3. 6. FRAP of Flower, Stem and Leaves Extracts

In the flower, stem and leaf extracts of *S. officinalis*, *S. palustris*, *S. sylvatica*, FRAP values varied between 56.38 mg TE/g DW and 93.76 mg TE/g DW (Table 2). It is noted that this activity is more significant for flower extracts obtained from *S. palustris*, followed by *S. sylvatica*, and then by *S. officinalis*. Regarding the leaf extracts, a more pronounced activity is on *S. officinalis* (83.22 mg TE/g extract), followed by *S. palustris* (76.21 mg TE/g extract) and *S. sylvatica* (75.77 mg TE/g extract). Significant values were also obtained on *Stachys cretica* L. extract (12.98±0.11 mg TE/g extract, 236.44±2.96 mg TE/g extract, 254.40±8.58 mg TE/g extract, 127.20 mg TE/g extract).^{3,29,30,31,47} Cüce et al. established for micropropagated plants of *Stachys an-*

nua L. that FRAP values varied between 334.5 mg TE/g extract and 1409.5 mg TE/g extract.⁵⁰ Other studies revealed that FRAP values of *Stachys thirkei* K. Koch. and *Stachys turcomanica* Trautv. extracts varied depending on the solvent type and on the concentration of the solvent used for extraction, respectively.^{5,51}

4. Conclusions

Extracts obtained from flowers, leaves and stems of *S. officinalis*, *S. palustris*, *S. sylvatica* have a chemical composition rich in phenolic compounds. The comparative analysis has completed the literature data with new and comprehensive information about the phenolic and antioxidant profile. Compared to stems and leaves, these bioactive compounds are more abundant in flowers, but to-

gether they create a generous profile. Flavonoids, anthocyanins and tannins are found in the most significant amounts in *S. officinalis*, followed by *S. palustris* and *S. sylvatica*. The PCA analysis revealed significant differences in chemical composition of flowers, leaves and stems. Valuable elements such as hydroxybenzoic or hydroxycinnamic acids, the plenteous load of natural antioxidants in the assessed extracts, place them in the recommended list for their further use in pharmaceutical, cosmetic and food industries.

Funding

This work was supported by the grant POCU/993/6/13 -153178, co-financed by the European Social Fund within

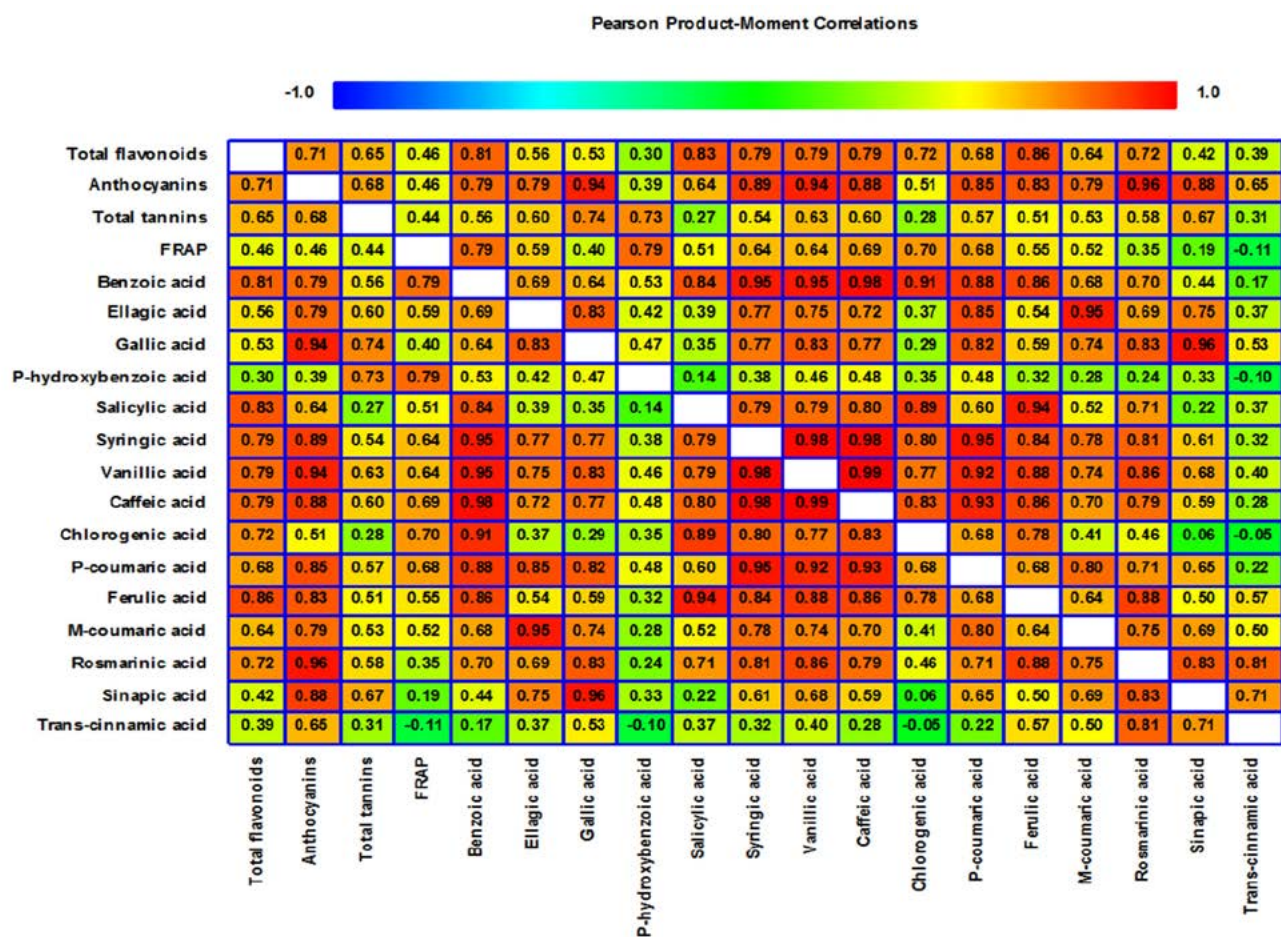


Figure 2. Heatmap of Pearson correlation coefficient obtained from chemical compositional variables analyzed from flowers, leaves and stems of *S. officinalis*, *S. palustris* and *S. sylvatica*

the Sectorial Operational Program Human Capital 2014 – 2020, PN 23150301 (The implementation of integrated isotopic-chemical-nuclear analytical method-ologies for the authentication of traditional Romanian food product-s).N.A.Ş. gratefully acknowledges the support obtained through project number PN-III-P4-ID-PCE-2020-0620, within PNCDI III, a grant from the Romanian Ministry of of Education and Research, CNCS–UEFISCDI.

5. References

- M.S. Kocak, M.C. Uren, M. Calapoglu, A. Sihoglu Tepe, A. Mocan, K.R.R. Rengasamy, C. Sarikurkc, *S. Afr. J. Bot.* **2017**, *113*, 128–1321. DOI:10.1016/j.sajb.2017.08.005
- E.M.Tomou, C. Barda, H. Skaltsa, *Medicines* **2020**, *7*, 63. DOI:10.3390/medicines7100063
- M.B. Bahadori, B. Kirkan, C.Sarikurkc, *Ind. Crop Prod.* **2019**, *127*, 82–87. DOI:10.1016/j.indcrop.2018.10.066
- A.Shakeri, G. D’Urso, S.F. Taghizadeh, S. Piacente, S.Norouzi, V.Sohaili, J.Asili, D. Salarbashi, *J. Pharm. Biomed. Anal.* **2019**, *168*, 209–216. DOI:10.1016/j.jpba.2019.02.018
- G. Gülsoy Toplan, T. Taşkın, E. Mataracı Kara, G.E. Genç, *Istanbul J. Pharm.* **2021**, *51*, 341–347. DOI:10.26650/IstanbulJPharm.2021.974035
- D.I. Stegăruş, E. Lengyel, G.F. Apostolescu, O.R. Botoran, C. Tanase, *Plants* **2021**, *10*, 2710. DOI:10.3390/plants10122710
- H. Sadeghi, D. Rostamzadeh, E. Panahi Kokhdan, A. Asfaram, A.H. Doustimotlagh, N. Hamidi, S. Hossein, *Evid. Based Complement. Alternat. Med.* **2022**, 7621599. DOI:10.1155/2022/7621599
- H. Sadeghi, M. Mansourian, E.P. Kokhdan, Z. Salehpour, I. Sadati, K. Abbaszadeh-Goudarzi, A. Asfaram, AH. Doustimotlagh, *J. Food Biochem.* **2020**, *44*, e13190. DOI:10.1111/jfbc.13190
- E. Háznagy-Radnai, Á. Balogh, S. Czigle, I. Máthé, J. Hohmann, G. Blazsó, *Phytother. Res.* **2012**, *26*, 505–509. DOI:10.1002/ptr.3582
- R. Jahani, D. Khaledyan, A. Jahani, E. Jamshidi, M. Kamalnejad, M. Khoramjouy, M. Faizi, *Res. Pharm. Sci.* **2019**, *14*, 544–553. DOI:10.4103/1735-5362.272563
- E. Panahi Kokhdan, H. Sadeghi, H. Ghafoori, H. Sadeghi, N. Danaei, S. Salaminia, M.R. Aghamaali, *Armaghane Danesh* **2019**, *24*, 17–30.

12. A. Venditti, C. Frezza, D. Celona, A. Bianco, M. Serafini, K. Cianfaglione, D. Fiorini, S. Ferraro, F. Maggi, A.R. Lizzi, G. Celenza, **2017**, *Food Chem.* **221**, 473–481. DOI:10.1016/j.foodchem.2016.10.096
13. M. Tunçturk, R. Tunçturk, U. Karik, T. Eryigit, *Int. J. Agric. Environ. Food Sci.* **2019**, **3**, 5–8. DOI:10.31015/jaefs.2019.1.2
14. J.K. Lee, J.-J. Lee, Y.-K. Kim, Y. Lee, J.-H. Ha, *Nutrients* **2020**, **12**, 2063. DOI:10.3390/nu12072063
15. K. Namvar, E.A. Salehi, N. Mokhtarian, *Bioscience Journal* **2018**, **34**, 1349–1356. DOI:10.14393/BJ-v34n5a2018-41517
16. C. Georgescu, A. Frum, L.I. Virchea, A. Sumacheva, M. Shamtsyan, F.G. Gligor, N.K. Olah, E. Mathe, M. Mironescu, *Molecules* **2022**, **27**, 4986. DOI:10.3390/molecules27154986
17. V.B. Vundać, A.H. Brantner, M. Plazibat, *Food Chem.* **2007**, **104**, 1277–1281. DOI:10.1016/j.foodchem.2007.01.036
18. C. Popescu, C. Popescu, B. Popescu, D. Daas, C. Morgovan, N.K. Olah, *Farmacia* **2014**, **62**, 743–752. DOI:10.1016/j.foodchem.2007.01.036
19. C. Drăgulescu (Ed.), „Lucian Blaga” University Sibiu, **2010**, pp.450–452.
20. K. Bączek, O. Kosakowska, J.L. Przybył, Z. Węglar, *Herba Pol.* **2016**, **62**, 7–16. DOI:10.1515/hepo-2016-0007
21. F.G. Gligor, A. Frum, L.G. Vicas, M. Totan, C. Roman-Filip, C.M. Dobrea, *Anal. Lett.* **2020**, **53**, 1391–1406. DOI:10.1080/00032719.2019.1708373
22. V.I. Craciun, F.G. Gligor, A.M. Juncan, A.A. Chis, L.L. Rus, *Rev. Chim.* **2019**, **70**, 3202–3205. DOI:10.37358/RC.19.9.7516
23. D.I. Popescu, E. Lengyel, F.G. Apostolescu, L.C. Sun, O.R. Botoran, N.A. Şuţan, *Horticulturae* **2022**, **8**, 952. DOI:10.3390/horticulturae8100952
24. J. Lee, R.W. Durst, R.E. Wrolstad, *J. AOAC Int.* **2005**, **88**, 1269–1278. DOI:10.1093/jaoac/88.5.1269
25. E.L.C. Amorim, J.E. Nascimento, J.M. Monteiro, T.J.S.P. Sobrinho, T.A.S. Araujo, U.P. Albuquerque, *Functional Ecosystems and Communities* **2008**, 88–94.
26. C.L. Gomes, C.C.A.R. Silva, C.G. De Melo, M.R.A. Ferreira, L.A.L. Soares, R.M.F. Da Silva, L.A. Rolim, P.J. Rolim Neto, *An. Acad. Bras. Cienc.* **2021**, **93**, e20190373. DOI:10.1590/0001-3765202120190373
27. S. Lachowicz-Wisniewska, A. Pratap-Singh, I. Kapusta, A. Kruszynska, A. Rapak, I. Ochmian, T. Cebulak, W. Zukiwicz-Sobczak, P. Rubinski, *Pharmaceuticals* **2022**, **15**, 785. DOI:10.3390/ph15070785
28. V. Amalan, V. Natesan, I. Dhananjayan, R. Arumugam, *Bio-med. Pharmacother.* **2016**, **84**, 230–236. DOI:10.1016/j.biopha.2016.09.039
29. M.B. Bahadori, B. Kirkan, C. Sarikurkcü, O. Ceylan, *Ind. Crops Prod.* **2019**, **131**, 85–89. DOI:10.1016/j.indcrop.2019.01.038
30. B. Kirkan, C. Sarikurkcü, O. Ceylan, *Ind. Crop and Prod.* **2019**, **131**, 85–89. DOI:10.1016/j.indcrop.2019.01.038
31. I. Carev, C. Sarikurkcü, *Plants* **2021**, **10**, 1054. DOI:10.3390/plants10061054
32. S. Rahimi Khoigani, A. Rajaei, S.A.Goli, *Nat. Prod. Res.* **2017**, **31**, 355–358. DOI:10.1080/14786419.2016.1233410
33. G. Ozkan, R.S. Gokturk, O. Unal, S. Celik, *Chem. Nat. Comp.* **2006**, **42**, 172–174. DOI:10.1007/s10600-006-0070-1
34. O. Sytar, I. Hemmerich, M. Zivcak, C. Rauh, M. Brestic, *Saudi J Biol.* **2018**, **25**(4), 631–641. DOI:10.1016/j.sjbs.2016.01.036
35. X. Zhou, S. Huang, P. Wang, Q. Luo, X. Huang, Q. Xu, X. Qin, J. Qin, C. Liang, X. Chen, *Nat. Prod. Res.* **2017**, 1–6. DOI:10.1080/14786419.2017.1405413
36. M. Abdel-Mogib, H.S.M. Al-Zahrani, *JKAU: Sci.* **2005**, **17**, 77–82. DOI:10.4197/Sci.17-1.8
37. T. Askun, E.M. Tekwu, F. Satil, S. Modanlioglu, H. Aydeniz, *BMC Complement. Altern. Med.* **2013**, **13**, 365. DOI:10.1186/1472-6882-13-365
38. S.S. Mitic, M. Stojkovic, J.L. Pavlović, M. Mitić, B.T. Stojanović, *Oxid. Commun.* **2012**, **35**, 1011–1021.
39. R.A. Kepekçi, S. Polat, G. Çoşkun, A. Çelik, A.S. Bozkurt, Ö. Yumrutaş, M. Pehlivan, *J. Food Biochem.* **2017**, **41**, 12286. DOI:10.1111/jfbc.12286
40. I. Şliumpaite, P. Venskutonis, M. Murkovic, O. Ragažinskienė, *Ind. Crop Prod.* **2013**, **50**, 715–722. DOI:10.1016/j.indcrop.2013.08.024
41. V. B. Vundać, **2019**, *Plants (Basel)*, **8**, 32. DOI:10.3390/plants8020032
42. J.S. Lazarević, A.S. Đorđević, D.V. Kitić, B.K. Zlatković, G.S. Stojanović, *Chem. Biodivers.* **2013**, **10**, 1335–1349. DOI:10.1002/cbdv.201200332
43. M.N. Bingol, E. Bursal, *Int. Lett. Nat. Sci.* **2018**, **72**, 28–36. DOI:10.18052/www.scipress.com/ILNS.72.28
44. W. Elfalleh, B. Kirkan, C. Sarikurkcü, *Ind. Crop Prod.* **2019**, **127**, 212–216. DOI:10.1016/j.indcrop.2018.10.078
45. C. Sarikurkcü, M.S. Kocak, M.C. Uren, M. Calapoglu, A.S. Tepe, *Eur. J. Integr. Med.* **2016**, **8**, 631–637. DOI:10.1016/j.eujim.2016.04.010
46. H. Ahmadvand, S. Farajollahi, H. Amiri, A. Amiri, *Herb. Med. J.* **2017**, **2**, 97–104. DOI: 10.22087/hmj.v0i0.623
47. S.E. Bursal, P. Taslimi, A.C. Gören, I. Gülçin, *Biocatal. Agric. Biotechnol.* **2020**, **28**, 101711. DOI:10.1016/j.bcab.2020.101711
48. G. Paun, E. Neagu, V. Moroceanu, C. Albu, T.-M. Ursu, A. Zanfrescu, S. Negres, C. Chirita, G.L. Radu, *Rev. Bras. Farmacogn.* **2018**, **28**, 57–64. DOI:10.1016/j.bjp.2017.10.008
49. M. Fraga-Corral, P. Otero, J. Echave, P. Garcia-Oliveira, M. Carpena, A. Jarboui, B. Nuñez-Estevéz, J. Simal-Gandara, M.A. Prieto, *Foods* **2021**, **10**, 137. DOI:10.3390/foods10010137
50. M. Khanavi, M. Hajimahmoodi, M. Cheraghi-Niroomand, Z. Kargar, Y. Ajani, A. Hadjiakhoondi, M. R. Oveisi, *Afr. J. Biotechnol.* **2009**, **8**, 1143–1147. DOI:10.5897/AJB2009.000-9182
51. M. Cüce, T. Bekircan, A.H. Laghari, M. Sökmen, A. Sökmen, E.Ö. Uçar, A.O. Kılıç, *Indian J. Tradit. Knowl.* **2017**, **16**, 407–416.
52. K. Namvar, A. Mohammadi, E.A. Salehi, P. Feyzi, *Pharm. Sci.* **2017**, **23**, 244–248. DOI:10.15171/PS.2017.36

Povzetek

Stachys officinalis L., *Stachys palustris* L., *Stachys sylvatica* L. (Lamiaceae) se pogosto uporabljajo kot zdravila rastlinskega izvora. V tej raziskavi je bila opravljena primerjalna ocena vsebnosti fenolnih kislin, flavonoidov, antocianinov in taninov ter antioksidativne aktivnosti izvlečkov, pridobljenih iz cvetov, listov in stebel. Fenolne kisline, določene z metodo HPLC, so dosegle najvišje vrednosti v izvlečku cvetov *S. palustris*, izvlečku stebela *S. officinalis* in izvlečku listov *S. sylvatica*. Na podlagi spektrofotometrične metode so bile pri vseh treh vrstah ugotovljene vrednosti flavonoidov, ki so presegale 100 mg ekvivalentov kvercetina (QE)/g suhe snovi. Antocianini so bili zaznani le v izvlečkih iz cvetov. *S. officinalis* se je odlikoval z najvišjo vsebnostjo antocianinov in taninov. Antioksidativna aktivnost je bila prisotna pri vseh treh proučevanih vrstah, pri čemer se je vrsta *S. palustris* odlikovala z najintenzivnejšo antioksidativno sposobnostjo reduciranja železovih ionov. Dobljeni rezultati so zaradi raznolikosti in bogastva bioaktivnih spojin in antioksidantov pripeljali do potrditve uporabnosti teh rastlin v zdravilne in prehrabene namene.



Except when otherwise noted, articles in this journal are published under the terms and conditions of the Creative Commons Attribution 4.0 International License

Synthesis, Spectroscopic Characterization, Crystal Structures and Antibacterial Activity of Benzohydrazones Derived from 4-Pyridinecarboxaldehyde with Various Benzohydrazides

Yi-Xuan Zhou¹, Wei Li^{1,*} and Zhonglu You²

¹ Department of Radiology, The Second Hospital of Dalian Medical University, Dalian 116023, P.R. China

² Department of Chemistry and Chemical Engineering, Liaoning Normal University, Dalian 116029, P.R. China

* Corresponding author: E-mail: liwei_dlm@126.com

Received: 03-08-2023

Abstract

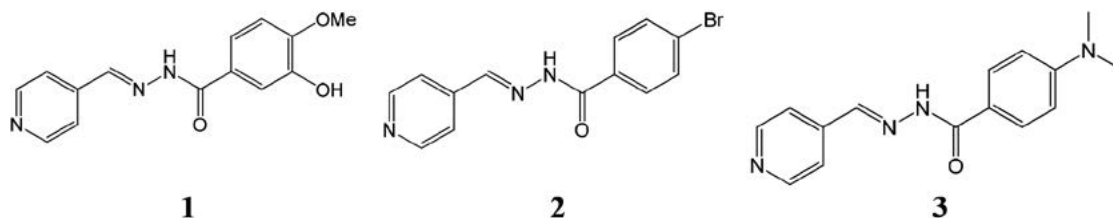
Reaction of 4-pyridinecarboxaldehyde with 3-hydroxy-4-methoxybenzohydrazide, 4-bromobenzohydrazide and 4-dimethylaminobenzohydrazide, respectively in methanol afforded three new benzohydrazones. They are 3-hydroxy-4-methoxy-*N*'-(pyridin-4-ylmethylene)benzohydrazide (1), 4-bromo-*N*'-(pyridin-4-ylmethylene)benzohydrazide (2), and 4-(dimethylamino)-*N*'-(pyridin-4-ylmethylene)benzohydrazide (3). The compounds have been characterized by elemental analysis, ¹H and ¹³C NMR and IR spectroscopy, as well as single crystal X-ray diffraction. The antibacterial activities of the compounds against *E. coli*, *P. aeruginosa*, *B. subtilis*, and *S. aureus* were investigated and gave interesting results.

Keywords: Benzohydrazones; 4-pyridinecarboxaldehyde; synthesis; crystal structure; antibacterial activity.

1. Introduction

Hydrazones are a class of compounds containing –C(O)–NH–N=CH– groups, which can be facile synthesized from the condensation reactions of aldehydes with hydrazides. The compounds have wide application in biological fields like antibacterial,¹ antifungal,² antitumor,³ anti-inflammatory,⁴ and cytotoxic.⁵ It was reported that the compounds containing halide groups on the aromatic rings usually show improved biological activities especially the antibacterial and antifungal activities.⁶ Rai and

co-workers reported a series of fluoro, chloro, bromo, and iodo-substituted compounds, and found that they have significant antimicrobial activities.⁷ In addition, nicotinic hydrazide has remarkable antituberculous activity. As a continuation of work on the exploration of novel antibacterial drugs, in the present paper, three new benzohydrazones, 3-hydroxy-4-methoxy-*N*'-(pyridin-4-ylmethylene)benzohydrazide (1), 4-bromo-*N*'-(pyridin-4-ylmethylene)benzohydrazide (2), and 4-(dimethylamino)-*N*'-(pyridin-4-ylmethylene)benzohydrazide (3) were prepared and evaluated for their antibacterial activities.



Scheme 1. The benzohydrazones

2. Experimental

2. 1. Materials and Measurements

Commercially available 4-pyridinecarboxaldehyde, 3-hydroxy-4-methoxybenzohydrazide, 4-bromobenzohydrazide and 4-dimethylaminobenzohydrazide were purchased from Sigma-Aldrich and used without further purification. Other solvents and reagents were made in China and used as received. C, H and N elemental analyses were performed with a Perkin-Elmer elemental analyzer. Infrared spectra were recorded on a Nicolet AVATAR 360 spectrometer as KBr pellets in the 4000–400 cm^{-1} region. ^1H NMR spectra were recorded on a Bruker 500 MHz instrument. Single crystal X-ray diffraction was carried out on a Bruker D8 VENTURE PHOTON diffractometer equipped with MoK_α radiation.

2. 2. Synthesis of the Compounds

The three compounds were synthesized according to the same method as described. 4-Pyridinecarboxaldehyde (1.0 mmol, 11 mg) dissolved in methanol (20 mL) was added to the methanolic solution (20 mL) of 3-hydroxy-4-methoxybenzohydrazide (1.0 mmol, 18 mg), 4-bromobenzohydrazide or 4-dimethylaminobenzohydrazide aroylhydrazine, and were stirred at room temperature for 30 min to give clear solution. X-ray quality single crystals were formed by slow evaporation of the solution in air for a few days.

2. 2. 1. 3-Hydroxy-4-methoxy-*N'*-(pyridin-4-ylmethylene)benzohydrazide (1)

Colorless crystals. Yield: 76%. Anal. calcd. for $\text{C}_{29}\text{H}_{32}\text{N}_6\text{O}_8$: C, 58.78; H, 5.44; N, 14.18; found C, 58.63; H, 5.55; N, 14.06%. Characteristic IR data (cm^{-1}): 3484 (w), 3409 (w), 3205 (w), 1657 (s), 1604 (s), 1560 (m), 1510 (s), 1445 (w), 1361 (w), 1289 (s), 1221 (m), 1141 (m), 1069 (m), 1018 (w), 947 (w), 853 (m), 752 (w), 532 (m). ^1H NMR (500 MHz, d_6 -DMSO): δ : 11.87 (s, 1H, NH), 9.76 (s, 1H, OH), 8.65 (s, 2H, PyH), 8.43 (s, 1H, CH=N), 7.65 (s, 2H, PyH), 7.50 (s, 1H, ArH), 7.47 (d, 1H, ArH), 6.90 (d, 1H, ArH), 3.85 (s, 3H, CH_3). ^{13}C NMR (126 MHz, d_6 -DMSO): δ : 162.91, 150.38, 150.19, 147.29, 144.36, 141.64, 123.72, 121.56, 120.85, 114.96, 111.79, 55.73.

2. 2. 2. 4-Bromo-*N'*-(pyridin-4-ylmethylene)benzohydrazide (2)

Colorless crystals. Yield: 82%. 1–173 °C. Anal. calcd. for $\text{C}_{15}\text{H}_{18}\text{N}_4\text{O}_2$: C, 62.92; H, 6.34; N, 19.57; found C, 63.11; H, 6.26; N, 19.43%. Characteristic IR data (cm^{-1}): 3188 (w), 1645 (s), 1602 (s), 1517 (s), 1353 (w), 1281 (s), 1196 (m), 1128 (m), 1065 (w), 938 (w), 820 (w), 756 (w), 672 (w), 506 (w). ^1H NMR (500 MHz, d_6 -DMSO): δ : 11.93 (s, 1H, NH), 8.65 (s, 2H, PyH), 8.45 (s, 1H, CH=N), 7.72

(s, 2H, PyH), 7.81 (d, 2H, ArH), 7.72 (d, 2H, ArH). ^{13}C NMR (126 MHz, d_6 -DMSO): δ : 162.83, 150.17, 146.85, 144.22, 132.33, 131.53, 128.76, 125.83, 120.12.

2. 2. 3. 4-(Dimethylamino)-*N'*-(pyridin-4-ylmethylene)benzohydrazide (3)

Colorless crystals. Yield: 73%. Anal. calcd. for $\text{C}_{13}\text{H}_{10}\text{BrN}_3\text{O}$: C, 51.34; H, 3.31; N, 13.82; found C, 51.19; H, 3.22; N, 13.75%. Characteristic IR data (cm^{-1}): 3396 (w), 3243 (w), 1650 (s), 1603 (s), 1590 (w), 1539 (s), 1466 (m), 1436 (w), 1342 (w), 1280 (m), 1141 (m), 1073 (w), 1062 (w), 1011 (w), 957 (w), 915 (m), 851 (w), 780 (w), 745 (w), 658 (w), 618 (w), 526 (w). ^1H NMR (500 MHz, d_6 -DMSO): δ : 12.16 (s, 1H, NH), 8.65 (s, 2H, PyH), 8.45 (s, 1H, CH=N), 7.88 (d, 2H, PyH), 7.76 (d, 2H, ArH), 7.67 (d, 2H, ArH), 3.13 (s, 6H, CH_3). ^{13}C NMR (126 MHz, d_6 -DMSO): δ : 162.43, 153.73, 150.23, 145.65, 141.33, 132.08, 131.52, 129.76, 120.95, 42.7.

2. 3. Single Crystal X-ray Crystallography

Diffraction intensities for the compounds were collected at 298(2) K using a Bruker D8 VENTURE PHOTON diffractometer with MoK_α radiation ($\lambda = 0.71073 \text{ \AA}$). The collected data were reduced using the SAINT program,⁸ and multi-scan absorption corrections were performed using the SADABS program.⁹ The structures were solved by direct method, and refined against F^2 by full-matrix least-squares method using the SHELXTL.¹⁰ All of the non-hydrogen atoms were refined anisotropically. The water and amino hydrogen atoms were located from difference Fourier maps and refined isotropically, with O–H, H...H and N–H distances restrained to 0.85(1), 1.37(2) and 0.90(1) \AA , respectively. All other hydrogen atoms were placed in idealized positions and constrained to ride on their parent atoms. The crystallographic data for the complexes are summarized in Table 1.

3. Results and Discussion

3. 1. Chemistry

The benzohydrazones were prepared by the condensation reaction of equimolar quantities of 4-pyridinecarboxaldehyde with 3-hydroxy-4-methoxybenzohydrazide, 4-bromobenzohydrazide and 4-dimethylaminobenzohydrazide, respectively, in methanol. The compounds have been characterized by elemental analysis, IR, ^1H and ^{13}C NMR spectra. Structures of the compounds were further confirmed by single crystal X-ray diffraction.

The three compounds were crystallized as well-shaped single crystals. They are soluble in MeOH, EtOH, MeCN, CHCl_3 , DMF and DMSO. The characteristic intense bands in the range 1645–1657 cm^{-1} are generated by the $\nu(\text{C}=\text{O})$ vibrations, whereas the bands in the range 1602–1604 cm^{-1} are assigned to the $\nu(\text{C}=\text{N})$ vibrations.¹¹

Table 1. Crystallographic data and refinement parameters for the compounds

	1·0.5MeOH·0.5H ₂ O	2·H ₂ O	3
Chemical formula	C ₂₉ H ₃₂ N ₆ O ₈	C ₁₅ H ₁₈ N ₄ O ₂	C ₁₃ H ₁₀ BrN ₃ O
<i>Mr</i>	592.60	286.33	304.15
Crystal color, habit	Colorless, block	Colorless, block	Colorless, block
Crystal system	Monoclinic	Orthorhombic	Orthorhombic
Space group	<i>P</i> 2 ₁ / <i>n</i>	<i>P</i> 2 ₁ 2 ₁ 2 ₁	<i>Pbca</i>
Unit cell parameters			
<i>a</i> (Å)	12.2635(15)	7.2634(5)	10.183(2)
<i>b</i> (Å)	12.3785(15)	11.7864(9)	7.949(1)
<i>c</i> (Å)	19.569(2)	17.1102(12)	30.863(2)
β (°)	97.977(1)		
<i>V</i> (Å ³)	2942.0(6)	1464.8(2)	2498.3(5)
<i>Z</i>	4	4	8
<i>D</i> _{calc} (g cm ⁻³)	1.338	1.298	1.617
μ (mm ⁻¹)	0.099	0.089	3.281
<i>F</i> (000)	1248	608	1216
Collected data	17255	10810	13785
Number of unique data	5469	3625	2330
Number of observed data [<i>I</i> > 2 σ (<i>I</i>)]	4119	2839	1759
Number of parameters	406	201	167
Number of restraints	5	4	1
<i>R</i> ₁ , <i>wR</i> ₂ [<i>I</i> > 2 σ (<i>I</i>)]	0.0415, 0.1028	0.0423, 0.0902	0.0355, 0.0758
<i>R</i> ₁ , <i>wR</i> ₂ (all data)	0.0586, 0.1165	0.0611, 0.1015	0.0563, 0.0840
Goodness of fit on <i>F</i> ²	1.013	1.035	1.019

In the spectrum of **1**, there are broad absorptions centered at 3484 and 3409 cm⁻¹, which can be attributed to the hydrogen-bonded phenol and hydroxyl groups. The sharp and weak bands in the range 3188–3243 cm⁻¹ are assigned to the ν (N–H) vibrations. The C, H, N analyses were in accordance with the chemical formulae proposed by the single crystal X-ray crystallography.

3. 2. Crystal Structure Description

The molecular structures of compounds **1–3** are shown in Figures 1–3, respectively. Selected bond lengths are listed in Table 2. The asymmetric unit of compound **1** contains two benzohydrazone molecules, one methanol molecule and one water molecule. The asymmetric unit of compound **2** contains one benzohydrazone molecule and one water molecule. There is only one benzohydrazone molecule in compound **3**. The benzohydrazone molecules of the compounds adopt *E* configuration with respect to the methyldene units. The distances (1.270–1.273 Å) of the methyldene bonds in the compounds are comparable to each other, which confirm them as typical double bonds. The shorter distances of the C–N bonds and the longer distances of the C=O bonds for the –C(O)–NH– units than usual, suggest the presence of conjugation effects in the molecules. All the bond lengths in the three compounds are within normal values.¹² The dihedral angles between the benzene ring and the pyridine ring in the benzohydrazone molecules are 17.3(2) and 22.8(2)° for **1**, 44.8(2)° for **2**, and 19.1(3)° for **3**.

In the crystal structure of compound **1**, the benzohydrazone molecules are linked by water molecules through O–H...O hydrogen bonds to form a dimer. The dimers are further linked through O–H...N hydrogen bonds to form chains. The methanol molecules are linked to the benzohydrazone molecules through O–H...N and O–H...O hydrogen bonds (Table 3, Figure 4). In the crystal structure of compound **2**, the benzohydrazone molecules are linked by water molecules through O–H...O, O–H...N, N–H...O and C–H...O hydrogen bonds to form a three-dimensional network (Figure 5). In the crystal structure of compound **3**, the benzohydrazone molecules are linked through N–H...O hydrogen bonds to form chains (Figure 6).

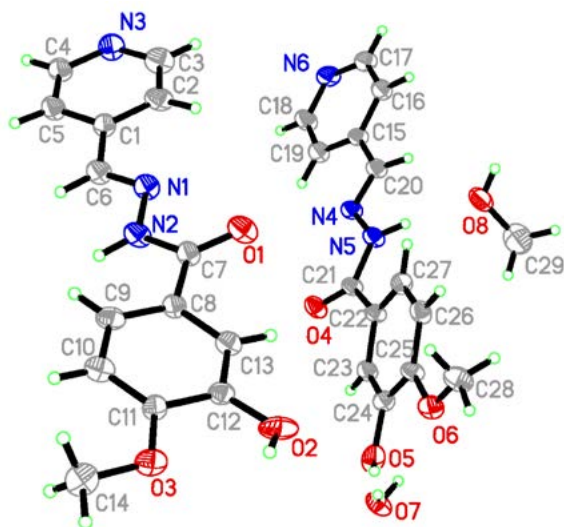
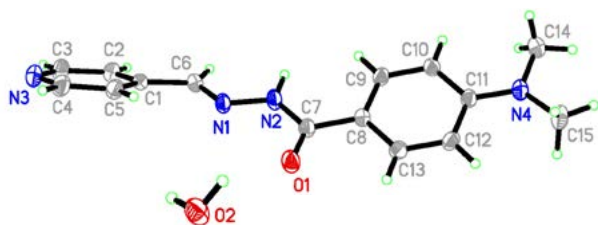
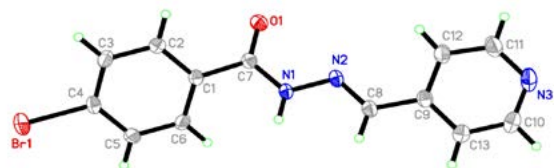
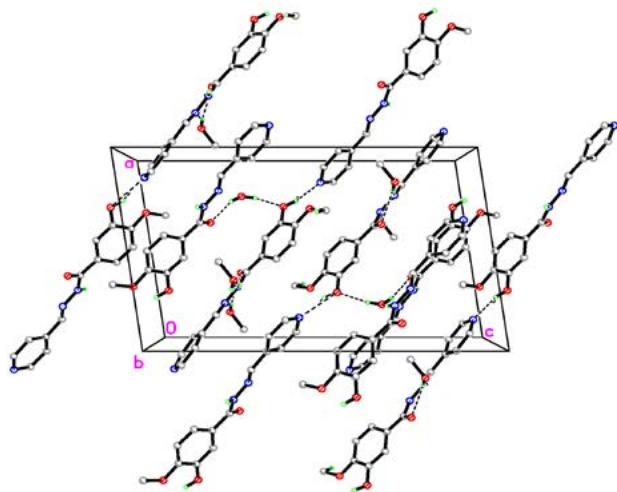
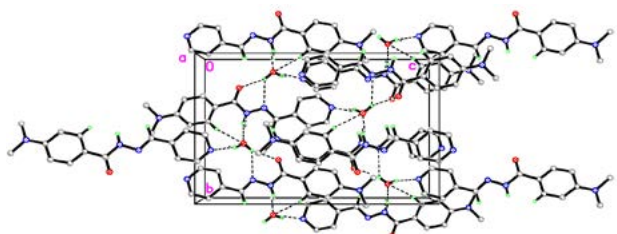
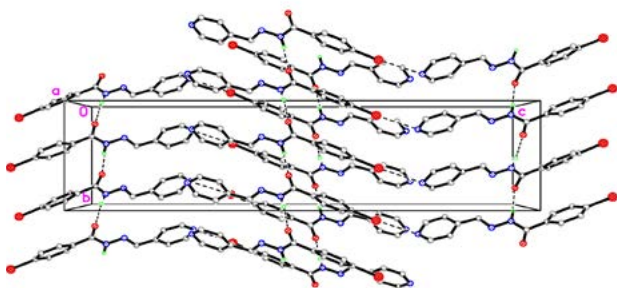
Table 2. Selected bond distances (Å) for the compounds

1 · 0.5MeOH·0.5H ₂ O			
N1–C6	1.273(2)	N1–N2	1.3683(17)
N2–C7	1.358(2)	N4–C20	1.270(2)
N4–N5	1.3727(17)	N5–C21	1.356(2)
O1–C7	1.2236(19)	O4–C21	1.2242(19)
2 · H ₂ O			
N1–C6	1.270(3)	N1–N2	1.379(2)
N2–C7	1.366(3)	O1–C7	1.226(3)
3			
N1–C7	1.359(3)	N1–N2	1.376(3)
N2–C8	1.272(3)	O1–C7	1.229(3)

Table 3. Hydrogen bond distances (Å) and bond angles (°) for the compounds

<i>D</i> – <i>H</i> ... <i>A</i>	<i>d</i> (<i>D</i> – <i>H</i>), Å	<i>d</i> (<i>H</i> ... <i>A</i>), Å	<i>d</i> (<i>D</i> ... <i>A</i>), Å	Angle (<i>D</i> – <i>H</i> ... <i>A</i>), °
1·0.5MeOH·0.5H₂O				
O2–H2B...N6 ⁱ	0.82	1.96	2.727(2)	156(3)
O5–H5B...N3 ⁱⁱ	0.82	1.91	2.687(2)	157(3)
O8–H8...O4 ⁱⁱⁱ	0.82	2.27	2.985(2)	146(3)
O8–H8...N4 ⁱⁱⁱ	0.82	2.38	3.079(2)	144(3)
N2–H2...O7	0.90(1)	1.95(1)	2.846(2)	171(2)
N5–H5...O8	0.90(1)	1.96(1)	2.839(2)	167(2)
O7–H7A...O1 ^{iv}	0.85(1)	2.01(1)	2.823(2)	158(2)
O7–H7A...N1 ^{iv}	0.85(1)	2.66(2)	3.282(2)	131(2)
O7–H7B...O5	0.85(1)	1.98(1)	2.826(2)	170(2)
C28–H28A...O3 ^v	0.96	2.58(2)	3.371(3)	140(3)
2·H₂O				
N2–H2...O2 ^{vi}	0.90(1)	1.98(2)	2.844(2)	159(3)
O2–H2A...N3 ^{vii}	0.85(1)	2.02(1)	2.848(3)	164(3)
O2–H2B...O1	0.85(1)	2.05(2)	2.854(2)	159(3)
O2–H2B...N1	0.85(1)	2.53(2)	3.146(3)	131(2)
C6–H6...O2 ^{vi}	0.93	2.59(2)	3.226(3)	126(3)
C9–H9...O2 ^{vi}	0.93	2.52(2)	3.427(3)	166(3)
3				
N1–H1...O1 ^{viii}	0.90(1)	1.98(1)	2.877(3)	174(4)

Symmetry codes: i) $2 - x, -y, 1 - z$; ii) $-x, -y, -z$; iii) $\frac{1}{2} - x, \frac{1}{2} + y, \frac{1}{2} - z$; iv) $\frac{3}{2} - x, \frac{1}{2} + y, \frac{1}{2} - z$; v) $-\frac{3}{2} + x, \frac{1}{2} - y, -\frac{1}{2} + z$; vi) $1 - x, \frac{1}{2} + y, \frac{1}{2} - z$; vii) $-\frac{1}{2} + x, \frac{1}{2} - y, 1 - z$; viii) $\frac{1}{2} - x, \frac{1}{2} + y, z$.

**Figure 1.** ORTEP plot of the crystal structure of 1. Displacement ellipsoids of non-hydrogen atoms are drawn at the 30% probability level.**Figure 2.** ORTEP plot of the crystal structure of 2. Displacement ellipsoids of non-hydrogen atoms are drawn at the 30% probability level.**Figure 3.** ORTEP plot of the crystal structure of 3. Displacement ellipsoids of non-hydrogen atoms are drawn at the 30% probability level.**Figure 4.** Molecular packing diagram of 1. Viewed along the *b* axis. Hydrogen atoms not related to hydrogen bonding are omitted. Hydrogen bonds are shown as dashed lines.**Figure 5.** Molecular packing diagram of 2. Viewed along the *a* axis. Hydrogen atoms not related to hydrogen bonding are omitted. Hydrogen bonds are shown as dashed lines.**Figure 6.** Molecular packing diagram of 3. Viewed along the *a* axis. Hydrogen atoms not related to hydrogen bonding are omitted. Hydrogen bonds are shown as dashed lines.

3. 3. Antibacterial Activity

The antibacterial assay was performed according to the literature method.¹³ Penicillin G was used as a standard drug. DMSO was used as solvent and the solutions were further diluted by distilled water. The DMSO at the tested concentration has no activity on the bacteria. The zone of inhibition for the 5000 $\mu\text{g mL}^{-1}$ test solutions on the four bacteria *Escherichia coli*, *Pseudomonas aeruginosa*, *Salmonella typhi* and *Staphylococcus aureus* is given in Table 4. The MIC values are given in Table 5. The results indicated that the compounds have from weak to strong activities against the four bacteria. Compound **1** has medium activity on *E. coli* and *P. aeruginosa*, and weak activity on *B. subtilis* and *S. aureus*. Compound **2** has strong activity on *E. coli* and *P. aeruginosa*, and medium activity on *B. subtilis* and *S. aureus*. Compound **3** has medium activity on *E. coli* and *P. aeruginosa*, strong activity on *B. subtilis*, and weak activity on *S. aureus*. Among the compounds, compound **2** has the most activity on *E. coli* and *P. aeruginosa* with MIC values of 3.13 $\mu\text{g mL}^{-1}$, which is even comparable to Penicillin G. The four compounds have better activities against *E. coli*, *B. subtilis* and *S. aureus* than the pyrroles bearing thiazole moiety.¹⁴ Compounds **2** and **3** have stronger activity against *E. coli*, weak activity against *B. subtilis*, and similar activity against *S. aureus* when compared with the fluoro-substituted aroylhydrazones.¹⁵

After careful comparison we noticed that the Br substituent group in compound **2** might contribute to the activity on *E. coli* and *P. aeruginosa*, and the NMe_2 group in compound **3** may contribute to the activity on *B. subtilis*.

Table 4 Antibacterial screening results

Compound	Zone of inhibition (mm)			
	<i>E. coli</i>	<i>P. aeruginosa</i>	<i>B. subtilis</i>	<i>S. aureus</i>
1	17 ± 1.9	14 ± 1.7	5.3 ± 1.4	7.2 ± 1.6
2	25 ± 2.8	23 ± 2.5	18 ± 2.6	15 ± 1.7
3	21 ± 2.3	18 ± 2.0	22 ± 2.5	11 ± 1.4
Penicillin G	30 ± 2.8	26 ± 3.1	30 ± 3.2	24 ± 2.9

Table 5 Antibacterial activities as MIC values ($\mu\text{g mL}^{-1}$)

Compound	<i>E. coli</i>	<i>P. aeruginosa</i>	<i>B. subtilis</i>	<i>S. aureus</i>
1	12.5	12.5	25	25
2	3.13	3.13	6.25	6.25
3	6.25	6.25	3.13	12.5
Penicillin G	3.13	6.25	1.56	6.25

4. Conclusions

In summary, three new benzohydrazone compounds were prepared and structurally characterized. The antibacterial activities against the bacteria *E. coli*, *P. aeruginosa*,

B. subtilis, and *S. aureus* were evaluated. Among the compounds, 4-bromo-*N'*-(pyridin-4-ylmethylene)benzohydrazide has strong activity on *E. coli* and *P. aeruginosa*, and 4-(dimethylamino)-*N'*-(pyridin-4-ylmethylene)benzohydrazide has strong activity on *B. subtilis*, with MIC values of 3.13 $\mu\text{g mL}^{-1}$. The compounds could be useful as templates for future development through modification to explore more effective antibacterial agents.

Supplementary Material

CCDC–2246870 (**1**), 2246872 (**2**), and 2246873 (**3**) contain the supplementary crystallographic data for this paper. These data can be obtained free of charge at <http://www.ccdc.cam.ac.uk/const/retrieving.html> or from the Cambridge Crystallographic Data Centre (CCDC), 12 Union Road, Cambridge CB2 1EZ, UK; fax: +44(0)1223-336033 or e-mail: deposit@ccdc.cam.ac.uk.

5. References

- (a) S. Verma, S. Lal, R. Narang, K. Sudhakar, *ChemMedChem* **2023**, DOI:10.1002/cmcd.202200571
(b) M. A. Shah, A. Uddin, M. R. Shah, I. Ali, R. Ullah, P. A. Hannan, H. Hussain, *Molecules* **2022**, 27, 6770;
(c) M. Nabizadeh, M. R. Naimi-Jamal, M. Rohani, P. Azerang, A. Tahghighi, *Lett. Appl. Microbiol.* **2022**, 75, 667–679
DOI:10.1111/lam.13692 DOI:10.3390/molecules27196770
(d) G.-X. He, L.-W. Xue, *Acta Chim. Slov.* **2021**, 68, 567–574
DOI:10.17344/acsi.2020.6333
(e) K. Pyta, A. Janas, M. Szukowska, P. Pecyna, M. Jaworska, M. Gajęcka, F. Bartl, P. Przybylski, *Eur. J. Med. Chem.* **2019**, 167, 96–104 DOI:10.1016/j.ejmech.2019.02.009
(f) I. Shabeeb, L. Al-Essa, M. Shtaiwi, E. Al-Shalabi, E. Younes, R. Okasha, M. Abu Sini, *Lett. Org. Chem.* **2019**, 16, 430–436. DOI:10.2174/1570178616666181227122326
- (a) M. Aydin, A. Ozturk, T. Duran, U. O. Ozmen, E. Sumlu, E. B. Ayan, E. N. Korucu, *J. Mycologie Medicale* **2023**, 33, 101327
DOI:10.1016/j.mycmed.2022.101327
(b) I. R. Silva, T. Kronenberger, E. C. L. Gomes, I. C. Cesar, R. B. Oliveira, V. G. Maltarollo, *Eur. J. Pharm. Sci.* **2021**, 156, 105575 DOI:10.1016/j.ejps.2020.105575
(c) I. A. Khodja, H. Boulebd, C. Bensouici, A. Belfaitah, *J. Mol. Struct.* **2020**, 1218, 128527
DOI:10.1016/j.molstruc.2020.128527
(d) A. E. Dascalu, A. Ghinet, E. Lipka, C. Furman, B. Rigo, A. Fayeulle, M. Billamboz, *Bioorg. Med. Chem. Lett.* **2020**, 30, 127220 DOI:10.1016/j.bmcl.2020.127220
(e) N. R. Appna, R. K. Nagiri, R. B. Korupolu, S. Kanugala, G. K. Chityal, G. Thipparapu, N. Banda, *Med. Chem. Res.* **2019**, 28, 1509–1528 DOI:10.1007/s00044-019-02390-w
(f) A. Erguc, M. D. Altintop, O. Atli, B. Sever, G. Iscan, G. Gormus, A. Ozdemir, *Lett. Drug Des. Discov.* **2018**, 15, 193–202; DOI:10.2174/1570180814666171003145227
(g) N. J. P. Subhashini, P. Janaki, B. Bhadrachari, *Russ. J. Gen.*

- Chem.* **2017**, *87*, 2021–2026.
DOI:10.1134/S1070363217090183
3. (a) M. S. A. Abdelrahman, F. M. Omar, A. A. Saleh, M. A. Elghamry, *J. Mol. Struct.* **2022**, *1251*, 131947
DOI:10.1016/j.molstruc.2021.131947
(b) B. Ay, O. Sahin, B. S. Demir, Y. Saygideger, J. M. Lopez-de-Luzuriaga, G. Mahmoudi, D. A. Safin, *New J. Chem.* **2020**, *44*, 9064–9072 DOI:10.1039/D0NJ00921K
(c) E. M. Gungor, M. D. Altintop, B. Sever, G. A. Ciftci, *Let. Drug Des. Discov.* **2020**, *17*, 1380–1392
DOI:10.2174/1570180817999200618163507
(d) H. M. A. Abumelha, *J. Heterocycl. Chem.* **2018**, *55*, 1738–1745 DOI:10.1002/jhet.3211
(e) H. F. He, X. Y. Wang, L. Q. Shi, W. Y. Yin, Z. W. Yang, H. W. He, Y. Liang, *Bioorg. Med. Chem. Lett.* **2016**, *26*, 3263–3270.
DOI:10.1016/j.bmcl.2016.05.059
 4. (a) M. A. M. B. Medeiros, M. G. E. Silva, J. D. Barbosa, E. M. de Lavor, T. F. Ribeiro, C. A. F. Macedo, L. A. M. D. Duarte-Filho, T. A. Feitosa, J. D. Silva, H. H. Fokoue, C. R. M. Araujo, A. D. Gonsalves, L. A. D. Ribeiro, J. R. G. D. Almeida, *Plos One* **2021**, *16*, e0258094 DOI:10.1371/journal.pone.0258094
(b) M. X. Song, B. Liu, S. W. Yu, S. H. He, Y. Q. Liang, S. F. Li, Q. Y. Chen, X. Q. Deng, *Let. Drug. Des. Discov.* **2020**, *17*, 502–511 DOI:10.2174/1570180816666190731113441
(c) U. Debnath, S. Mukherjee, N. Joardar, S. P. S. Babu, K. Jana, A. K. Misra, *Eur. J. Pharm. Sci.* **2019**, *134*, 102–115
DOI:10.1016/j.ejps.2019.04.016
(d) U. Kendur, G. H. Chimmalagi, S. M. Patil, K. B. Gudasi, C. S. Frampton, C. V. Mangannavar, I. S. Muchchandi, *J. Mol. Struct.* **2018**, *1153*, 299–310
DOI:10.1016/j.molstruc.2017.10.022
(e) V. Gorantla, R. Gundla, S. S. Jadav, S. R. Anugu, J. Chimakurthy, S. K. Nidasanametla, R. Korupolu, *New J. Chem.* **2017**, *41*, 13516–13532 DOI:10.1039/C7NJ03332J
(f) M. A. Abdelgawad, M. B. Labib, M. Abdel-Latif, *Bioorg. Chem.* **2017**, *74*, 212–220. DOI:10.1016/j.bioorg.2017.08.014
 5. (a) E. Aydin, A. M. Senturk, H. B. Kucuk, M. Guzel, *Molecules* **2022**, *27*, 7309
(b) M. A. Shah, A. Uddin, M. R. Shah, I. Ali, R. Ullah, P. A. Hannan, H. Hussain, *Molecules* **2022**, *27*, 6770
DOI:10.3390/molecules27196770
(c) F. Beygi, A. Mostoufi, A. Mojaddami, *Chem. Biodivers.* **2022**, *19*, e202100754 DOI:10.1002/cbdv.202100754
(d) Z. Ozdemir, N. Basak-Turkmen, I. Ayhan, O. Ciftci, M. Uysal, *Pharm. Chem. J.* **2019**, *52*, 923–929
DOI:10.1007/s11094-019-01927-y
(e) J. C. Coa, W. Castrillon, W. Cardona, M. Carda, V. Ospina, J. A. Munoz, I. D. Velez, S. M. Robledo, *Eur. J. Med. Chem.* **2015**, *101*, 746–753. DOI:10.1016/j.ejmech.2015.07.018
 6. (a) L. C. Felton, J. H. Brewer, *Science* **1947**, *105*, 409–410
DOI:10.1126/science.105.2729.409
(b) M. Gopalakrishnan, J. Thanusu, V. Kanagarajan, R. Govindaraju, *J. Enzym. Inhib. Med. Chem.* **2009**, *24*, 52–58
DOI:10.1080/14756360801906632
(c) L. Shi, H.-M. Ge, S.-H. Tan, H.-Q. Li, Y.-C. Song, H.-L. Zhu, R.-X. Tan, *Eur. J. Med. Chem.* **2007**, *42*, 558–564
DOI:10.1016/j.ejmech.2006.11.010
 - (d) M. Zhang, D.-M. Xian, H.-H. Li, J.-C. Zhang, Z.-L. You, *Aust. J. Chem.* **2012**, *65*, 343–350. DOI:10.1071/CH11424
 7. (a) N. P. Rai, V. K. Narayanaswamy, T. Govender, B. K. Manuprasad, S. Shashikanth, P. N. Arunachalam, *Eur. J. Med. Chem.* **2010**, *45*, 2677–2682 DOI:10.1016/j.ejmech.2010.02.021
(b) N. P. Rai, V. K. Narayanaswamy, S. Shashikanth, P. N. Arunachalam, *Eur. J. Med. Chem.* **2009**, *44*, 4522–4527.
 8. Bruker, SMART and SAINT, Bruker AXS Inc., Madison, Wisconsin, USA, **2012**.
 9. G. M. Sheldrick, SADABS Program for Empirical Absorption Correction of Area Detector, University of Göttingen, Germany, **1996**.
 10. G. M. Sheldrick, *Acta Crystallogr.* **2008**, *A64*, 112–122.
DOI:10.1107/S0108767307043930
 11. W. J. Geary, *Coord. Chem. Rev.* **1971**, *7*, 81–122.
DOI:10.1016/S0010-8545(00)80009-0
 12. (a) M. Kuriakose, M. R. P. Kurup, E. Suresh, *Spectrochim. Acta A* **2007**, *66*, 353–358 DOI:10.1016/j.saa.2006.03.003
(b) L.-W. Xue, S.-T. Li, Y.-J. Han, X.-Q. Luo, *Acta Chim. Slov.* **2022**, *69*, 385–392 DOI:10.17344/acsi.2021.7252
(c) G.-X. He, L.-W. Xue, *Acta Chim. Slov.* **2021**, *68*, 567–574.
DOI:10.17344/acsi.2020.6333
 13. (a) Y. M. Chumakov, B. Y. Antosyak, V. I. Tsapkov, N. M. Samus, *J. Struct. Chem.* **2001**, *42*, 335–339
DOI:10.1023/A:1010587923496
(b) Y.-J. Han, X.-Y. Guo, L.-W. Xue, *Acta Chim. Slov.* **2022**, *69*, 928–936 DOI:10.17344/acsi.2022.7817
(c) H.-Y. Zhu, *Acta Chim. Slov.* **2021**, *68*, 65–71.
DOI:10.17344/acsi2020.6138
 14. M. A. Salem, S. Y. Abbas, M. A. M. Sh. El-Sharief, M. H. Helal, M. A. Gouda, M. A. Assiri, T. E. Ali, *Acta Chim. Slov.* **2021**, *68*, 990–996. DOI:10.17344/acsi.2021.6980
 15. F.-M. Wang, L.-J. Li, G.-W. Zang, T.-T. Deng, Z.-L. You, *Acta Chim. Slov.* **2021**, *68*, 541–547. DOI:10.17344/acsi.2020.6051

Povzetek

Reakcija 4-piridinkarboksaldehida s 3-hidroksi-4-metoksibenzohidrazidom, 4-bromobenzohidrazidom in 4-dimetilaminobenzohidrazidom v metanolu je dala tri nove benzohidrazone. To so 3-hidroksi-4-metoksi-*N'*-(piridin-4-ilmetilen) benzohidrazid (**1**), 4-bromo-*N'*-(piridin-4-ilmetilen)benzohidrazid (**2**) in 4-(dimetilamino)-*N'*-(piridin-4-ilmetilen) benzohidrazid (**3**). Spojine smo okarakterizirali z elementno analizo, ^1H in ^{13}C NMR in IR spektroskopijo ter monokristalno rentgensko difrakcijo. Preučevali smo antibakterijske aktivnosti spojin proti *E. coli*, *P. aeruginosa*, *B. subtilis* in *S. aureus* ter dobili zanimive rezultate.



Except when otherwise noted, articles in this journal are published under the terms and conditions of the Creative Commons Attribution 4.0 International License

Scientific paper

New Bis-1,3,4-Thiadiazoles Based on Fumaric Acid: Preparation, Structure Elucidation, Antibacterial Activities, and Quantum-Chemical Studies

Halit Muğlu,^{1,*} Hasan Yakan,² Ghaith Alabed Ibrayke Elefkhakry,¹
Ergin Murat Altuner,^{3,*} and M. Serdar Çavuş⁴

¹ Department of Chemistry, Kastamonu University, Kastamonu, Turkey

² Department of Chemistry Education, Ondokuz Mayıs University, Samsun, Turkey

³ Department of Biology, Kastamonu University, Kastamonu, Turkey

⁴ Biomedical Engineering Department, Kastamonu University, Kastamonu, Turkey

* Corresponding author: E-mail: hmuglu@kastamonu.edu.tr
ergin.murat.altuner@gmail.com

Received: 09-24-2022

Abstract

New bis-1,3,4-thiadiazoles 1–7 were obtained by the reaction of fumaric acid and *N*-(alkyl/aryl/cyclic)thiosemicarbazides in the presence of phosphorous oxychloride. The structures of all compounds were elucidated by FT-IR, ¹H NMR, and ¹³C NMR and elemental analysis. Antibacterial activity of the compounds was studied for eight selected bacteria. Compounds 2–7 exhibited effect on *Klebsiella pneumoniae*. However, none of the compounds effect on *Pseudomonas aeruginosa*, *Staphylococcus epidermidis*, *Salmonella enterica* serovar *Kentucky*, *Serratia marcescens*. Self-consistent reaction force (SCRFF) calculations were performed in DMSO medium to examine solvent energies using CPCM and SMD models. 6-31G(d) and 6-311++G(2d,2p) basis sets were used for DFT calculations. Besides electronic parameters such as electronegativity, electrophilicity and spectroscopic examinations of the compounds, QTAIM, local electron affinities, and Fukui analyses were also performed. Theoretical approaches supporting the experimental observations revealed that compounds containing aromatic and cyclic groups exhibit stronger antibacterial behavior than compounds containing aliphatic groups.

Keywords: Bis-1,3,4-thiadiazoles; fumaric acid; antibacterial activity; spectroscopic methods; DFT calculations.

1. Introduction

Heterocyclic compounds represent a very significant part of organic chemistry. They have an extensive scope of medicinal, biological, and synthetic applications.¹ Thiadiazoles have both one sulphur and two nitrogen atoms which form aromatic five-membered heterocyclic ring compounds. Thiadiazoles have four isomeric forms, 1,3,4-thiadiazole is one of them, being thermally the most stable among these isomers.^{1h}

1,3,4-Thiadiazoles exhibit various applications in medicinal, biological, agricultural, and materials chemistry such as antioxidant,² antiviral,³ antifungal,⁴ antimicrobial,⁵ analgesic,⁶ antidepressant,⁷ antileishmanial,⁸ anticonvulsant,⁹ anti-inflammatory,¹⁰ antitubercular,¹¹ anticancer,¹² and antiproliferative activities.¹³

Despite the fact that an extensive number of chemotherapeutics and antibiotics exist, the appearance of new and old antibiotic-resistant bacterial strains have shown a need to consider both the synthesis and exploration of novel more harmless, powerful, and confident antimicrobial agents.¹⁴

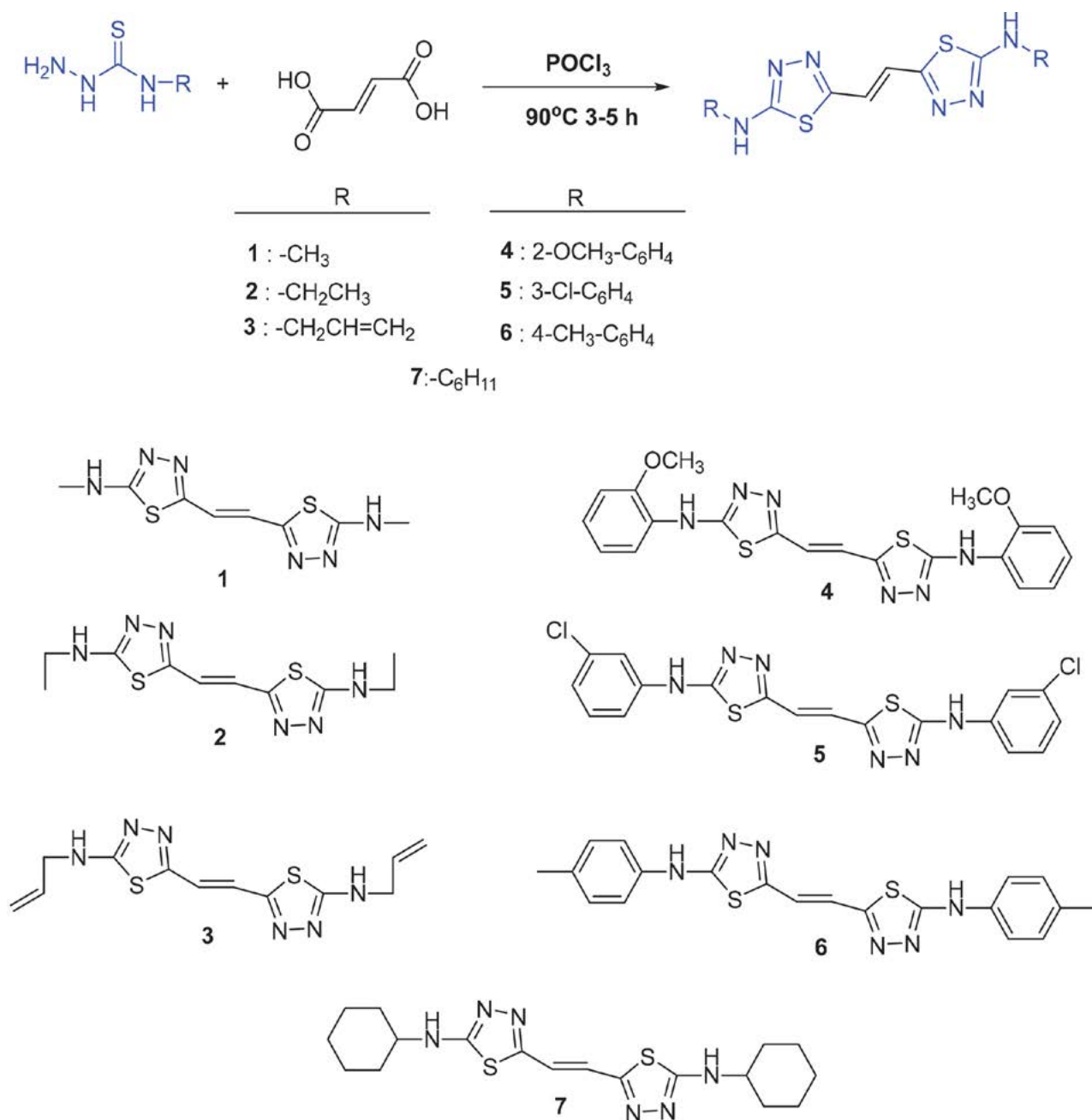
In the paper, new bis-1,3,4-thiadiazole derivatives were obtained from the reaction of fumaric acid, *N*-(alkyl/aryl/cyclic)thiosemicarbazides, and phosphorous oxychloride (POCl₃). The structures of the compounds were determined by using FTIR, ¹H NMR, and ¹³C NMR spectroscopic methods and elemental analysis. The antibacterial activity of the compounds was investigated against several Gram-positive bacteria (*Bacillus subtilis*, *Staphylococcus epidermidis*, and *Enterococcus*

faecium) and Gram-negative bacteria (*Escherichia coli*, *Salmonella enterica* serovar *Kentucky*, *Serratia marcescens*, *Klebsiella pneumoniae*, and *Pseudomonas aeruginosa*) by minimum inhibition concentration (MIC) and minimum bactericidal concentration (MBC) tests. Moreover, optimized molecular structures and spatial conformations of the compounds were investigated by theoretical studies using the DFT method; experimental spectroscopic data were also supported by the calculation results. Some electronic parameters of the compounds were calculated and used to establish the structure-activity relationship.

2. Experimental

2. 1. Measurement and Reagents

Melting points were determined on a Stuart SMP 30 electrothermal apparatus. Eurovector EA3000-Single device was utilized for elemental analysis. A Bruker Alpha FT-IR spectrophotometer were used to obtain Fourier transform infrared (FT-IR) spectra. ^1H NMR and ^{13}C NMR spectra were taken in $\text{DMSO}-d_6$ on a Bruker Avance DPX-400 spectrophotometer (400 MHz and 101 MHz, respectively) spectrometer using tetramethylsilane as an internal standard. The splitting patterns are indicated as



Scheme 1. Structures of compounds 1–7 and synthetic route to them.

s (singlet), d (doublet), dd (doublet of doublet), t (triplet), dt (doublet of triplet), td (triplet of doublet) and m (multiplet). All chemical reagents were purchased from Aldrich, Carlo Erba, Acros Organics, or Merck Chemical Company and used without further purification.

2. 2. Synthesis of the Compounds 1–7

The mixture of fumaric acid (n mol) and N -(alkyl/aryl/cyclic)thiosemicarbazide derivatives ($2n$ mol) was chilled in a refrigerator and phosphorous oxychloride ($3n$ mol) was added drop-wise during stirring. Then, refluxing was continued at 90 °C for 3–5 h. After completion of the reaction, the mixture was cooled to room temperature, poured into ice-cold water with stirring, and then neutralized with ammonia. The precipitated product was filtered, washed with water, and crystallized in a suitable solvent. These new bis-1,3,4-thiadiazoles were prepared according to the procedure described in the literature.^{1b} They were obtained in good yield (61–93%) as shown in Scheme 1.

2. 3. Antibacterial Activity Testing

Bacteria Strains

The antibacterial activities of the synthesized compounds were determined against three Gram-positive (*Bacillus subtilis* DSMZ 1971, *Enterococcus faecium* (food isolate), and *Staphylococcus epidermidis* DSMZ 20044) bacteria, and five Gram-negative (*Escherichia coli* (food isolate), *Klebsiella pneumoniae* (food isolate), *Pseudomonas aeruginosa* DSMZ 50071, *Salmonella enterica* serovar *Kentucky* (food isolate), and *Serratia marcescens* (clinical isolate)). All the bacteria were obtained from the culture collection of Kastamonu University, Department of Biology, Microbiology Laboratory.

Preparation of Chemical Compounds

The stock solutions were prepared by dissolving 24 mg of each compound 1–7 in 1 mL of dimethyl sulfoxide (DMSO) (Merck). Since DMSO is toxic for living cells, the in-test DMSO concentration was adjusted as 1%.¹⁵

Preparation of the Inocula

The bacteria used in the study were incubated at 37 °C for 24 hours and similar colonies were collected by a sterile loop, transferred into 0.9% sterile saline solution, and the turbidities were adjusted to 0.5 McFarland standard.¹⁶

Minimum Inhibition Concentration (MIC) Test

MIC test was applied as a broth dilution test as previously defined in previous studies.¹⁷ Serial 2-fold dilutions were done in a 96-well plate and a concentration range of

0.234–120 µg/mL was obtained. The MIC value was determined as the lowest concentration of extract inhibiting any visible bacterial growth.¹⁸ All tests were studied in triplicate.

Minimum Bactericidal Concentration (MBC) Test

The MBC test is complementary to the MIC test, where the MIC test demonstrates the lowest level of antimicrobial agent that inhibits growth, and the MBC demonstrates the lowest level of antimicrobial agent that causes microbial death. The MBC values were determined by sub-culturing the contents of non-turbid MIC test wells to agar plates. The MBC is identified as the lowest concentration of antibacterial agent that reduces the viability of the initial bacterial inoculum by $\geq 99.9\%$.¹⁹

Controls

1% DMSO was used as a negative control, where gentamicin (GEN), tobramycin (TOB), and ciprofloxacin (CPFX) were used as positive controls.

2. 4. Computational Procedure

The molecular structure of the compound in the ground state (in vacuum) was obtained from the optimization calculations performed using the B3LYP/6-311++g(2d,2p) level of theory by the Kohn–Sham density functional theory (KS-DFT).²⁰ All calculations were performed using Gaussian 09 software²¹ without any symmetry restrictions. The optimized state geometries of the compounds with minimum energy correspond to the global minimum energy points on the potential energy surface, that is, no imaginary frequencies are present in the IR calculations. Moreover, solvent effects were studied using solvation model based on density (SMD) and conductor-like polarizable continuum model (CPCM), at the same level of theory, to calculate the properties of compounds in solution.

¹H and ¹³C NMR chemical shifts calculations were performed using Gauge-independent atomic orbital (GIAO) method in dimethyl sulfoxide (DMSO) phase, in accordance with the experiments. Relative chemical shift values were obtained by subtracting (31.8149 and 183.737 ppm for ¹H and ¹³C NMR, respectively) from the absolute chemical shielding of tetramethylsilane (TMS), which was also calculated at B3LYP/6-311++g(2d,2p) level of theory.

The electronic parameters of the compounds were obtained from the calculations performed at the level of B3LYP/6-311++g(2d,2p) in the gas phase. Global chemical reactivity parameters such as HOMO–LUMO energy gap (E_g), Chemical hardness (η), electronegativity (χ), and electrophilic index (ω) were calculated using frontier molecular orbital (FMO) energy eigenvalues. The calculations of the Fukui functions were performed at the B3LY-

P/6-31g(d) level, and the electrophilic and nucleophilic attack regions were analyzed by visualizing the data. In addition, the reactivity and behavior of the compounds in different environments were estimated by FMO calculations and prominent descriptors were reported. Besides the population analysis of natural bond orbitals (NBOs), intramolecular interactions were studied through topological properties using Bader's quantum theory of atoms in molecules (QTAIM) approach²² and were also used to calculate electron charge distributions on compounds. Ring critical points (RCPs) of charge density distribution and bond critical points (BCPs) of bonded atoms were de-

termined by QTAIM analyses performed using Multiwfn software,²³ and interaction region indicator (IRI) calculations were performed to visualize intramolecular interactions.

3. Results and Discussion

3.1. Physical Data

All the compounds are new. In Table 1, the physical data, melting points, yields, and elemental analysis of these compounds are presented.

Table 1. Physical data and elemental analysis results of the compounds

Comp.	Compound's Names	M. P. (°C)	Yields% (Mass, g)	Colour	Calculated/Found		
					C%	H%	N%
1	(<i>E</i>)- <i>N</i> -methy-5-(2-(5-(methylamino)-1,3,4-thiadiazol-2-yl)vinyl)-1,3,4-thiadiazol-2-amine	65 240–241	Brown (0.206)	37.78/	3.96/ 37.69	33.04/ 4.05	32.89
2	(<i>E</i>)- <i>N</i> -ethyl-5-(2-(5-(ethylamino)-1,3,4-thiadiazol-2-yl)vinyl)-1,3,4-thiadiazol-2-amine	>300	61 (0.296)	Dark Brown	42.53/ 42.45	5.00/ 4.90	29.76/ 29.67
3	(<i>E</i>)- <i>N</i> -allyl-5-(2-(5-(allylamino)-1,3,4-thiadiazol-2-yl)vinyl)-1,3,4-thiadiazol-2-amine	>300	73 (0.289)	Cream	47.04/ 46.94	4.61/ 4.71	27.43/ 27.35
4	(<i>E</i>)- <i>N</i> -(2-methoxyphenyl)-5-(2-(5-(2-methoxyphenylamino)-1,3,4-thiadiazol-2-yl)vinyl)-1,3,4-thiadiazol-2-amine	175–176 (0.404)	87	Dark Yellow 54.72	54.78/ 4.08	4.14/ 19.21	19.16/
5	(<i>E</i>)- <i>N</i> -(3-chlorophenyl)-5-(2-(5-(3-chlorophenylamino)-1,3,4-thiadiazol-2-yl)vinyl)-1,3,4-thiadiazol-2-amine	168–169	75 (0.289)	Dark Cream	48.33/ 48.26	2.70/ 2.75	18.79 18.64
6	(<i>E</i>)-5-(2-(5-(<i>p</i> -toluidin)-1,3,4-thiadiazol-2-yl)vinyl)- <i>N</i> - <i>p</i> -tolyl-1,3,4-thiadiazol-2-amine	198–199	88 (0.462)	Dark Yellow	59.09/ 59.17	4.46/ 4.41	20.67/ 20.88
7	(<i>E</i>)- <i>N</i> -cyclohexyl-5-(2-(5-(cyclohexylamino)-1,3,4-thiadiazol-2-yl)vinyl)-1,3,4-thiadiazol-2-amine	>300	93 (0.457)	Cream	55.35/ 55.43	6.71/ 6.59	21.52/ 21.46

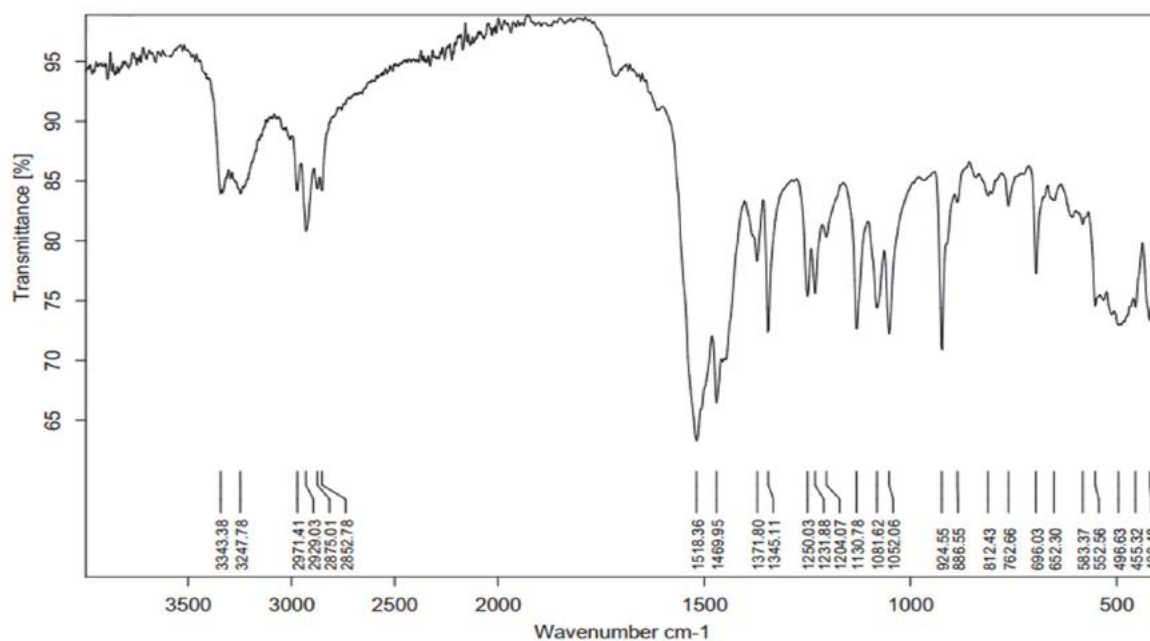


Figure 1. IR spectrum of compound 2

3. 2. Vibrational Frequencies

In the FT-IR spectrum of the synthesized compounds, the fumaric acid ($-\text{COOH}$) signal of the starting material was not observed near $3500\text{--}2700\text{ cm}^{-1}$. Furthermore, the asymmetric and symmetric stretching bands of the amino group ($-\text{NH}_2$) were not observed at $3450\text{--}3200\text{ cm}^{-1}$. These results pointed out a successful reaction, as expected. For all compounds, the peaks of the amino group ($-\text{NH}$) were showed between at $3248\text{--}3195\text{ cm}^{-1}$; the $-\text{C}=\text{N}$ stretching vibrations of thiadiazole ring were observed between at 1635 and 1518 cm^{-1} ; the $-\text{C}-\text{N}$ stretching vibrations were shown between $1174\text{--}1083\text{ cm}^{-1}$; the $-\text{C}-\text{S}$ signals were observed between $721\text{--}634\text{ cm}^{-1}$. For compound **2**, the band of the amino group ($-\text{NH}$) was shown at 3248 cm^{-1}

as shown in Figure 1. The aliphatic CH stretching vibrations were observed at $2929\text{--}2853\text{ cm}^{-1}$. The $-\text{C}=\text{N}$ stretching vibrations of thiadiazole ring appeared at 1518 cm^{-1} . The $-\text{C}-\text{N}$ stretching vibration appeared at 1131 cm^{-1} ; the $-\text{C}-\text{S}$ signal was observed at 696 cm^{-1} . These values provided significant proofs for the products formation. These observations are consistent with values published previously for similar compounds.^{1b,5b,24} IR vibrations for the synthesized compounds are presented in Table 2.

3. 3. ^1H NMR Spectral Interpretations

The ^1H NMR spectra of the synthesized compounds were measured in $\text{DMSO}-d_6$ as the solvent and the chemi-

Table 2. Experimental and calculated FT-IR values of the compounds 1–7 (cm^{-1}).

	C.	$-\text{NH}$	Ar. CH	$\text{C}=\text{N}$	$\text{C}-\text{N}$	$\text{C}-\text{S}$	Spec. Vib.
Experimental	1	3199	–	1586–1555	1153	634	$\text{CH}^{(*)}$: 2924–2847
	2	3248	–	1518	1131	696	$\text{CH}^{(*)}$: 2929–2853
	3	3219	–	1591–1532	1142	697	$\text{CH}^{(*)}$: 2928–2871
	4	3248	3075–3002	1635–1601	1174	654	$\text{CH}^{(*)}$: 2939–2837 –C–O: 1114
	5	3247	3092–3061	1631–1585	1170	721	–C–Cl: 994
	6	3195	3061–2992	1635–1604	1083	714	$\text{CH}^{(*)}$: 2920–2874
	7	3230	–	1611–1560	1120	696	$\text{CH}^{(*)}$: 2926–2852
Calculated	1	3645.81	–	1518.64, 1510.03	1040.41	685.41	$\text{CH}^{(*)}$: 3140.07–3030.96
	2	3622.25	–	1511.22, 1506.33	1060.03	685.91	$\text{CH}^{(*)}$: 3113.31–3016.33
	3	3619.58	–	1508.94, 1498.25	1054.43	686.96	$\text{CH}^{(*)}$: 3222.01–3019.94
	4	3622.59	3239.37–3195.42	1513.02, 1500.08	1266.40	689.77	$\text{CH}^{(*)}$: 3142.48–3024.14 –C–O: 1051.00
	5	3642.73	3250.32–3166.74	1513.73, 1500.88	1256.08	688.46	–C–Cl: 907.16
	6	3642.51	3239.59–3151.08	1512.38, 1501.75	1252.28	687.50	$\text{CH}^{(*)}$: 3106.15–3028.97
	7	3625.36	–	1511.35, 1509.87	1087.40	684.87	$\text{CH}^{(*)}$: 3097.13–3011.82

C.: Compounds, (*) : Aliphatic CH.

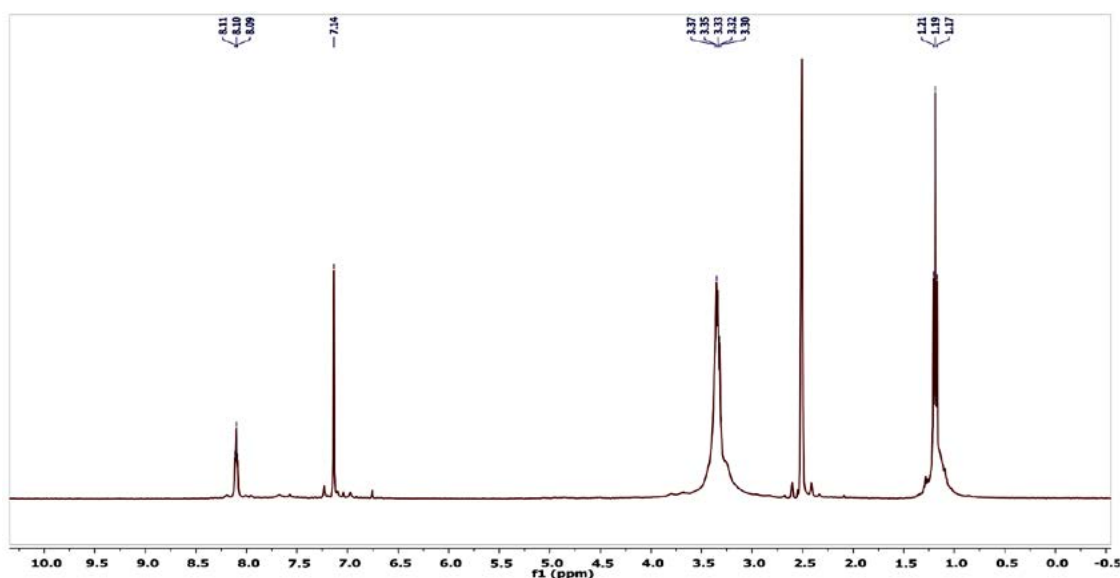


Figure 2. ^1H NMR spectrum of compound **2**.

Table 3. Experimental and calculated ^1H NMR values of the compounds (δ , ppm, in $\text{DMSO}-d_6$)

R: CH_3 , CH_3CH_2 , $\text{CH}_2=\text{CH}-\text{CH}_2$

R: 2-O CH_3 , 3-Cl, 4- CH_3 , C_6H_{11}

	C.	NH	H1	H2	H3	H4	H5	H6
Experimental	1	8.06–8.03 (q)	7.15 (s)	2.93–2.92 (d)	–	–	–	–
	2	8.11–8.09 (t)	7.14 (s)	3.97–3.28 (p)	1.21–1.17 (t)	–	–	–
	3	8.33–8.30 (t)	7.14 (s)	3.97–3.88 (t)	5.97–5.87 (m)	5.29–5.15 (dd)	–	–
	4	10.05 (s)	7.36 (s)	OCH $_3$: 3.89 (s)	8.31–8.29 (m)	7.09–7.04 (m)	–	7.01–6.97 (m)
	5	10.52 (s)	7.50–7.48 (d)	7.94 (s)	–	7.41–7.37 (dd)	–	7.10–7.08 (d)
	6	10.22 (s)	7.46 (s)	6.84–6.80 (d)	7.14–6.99 (d)	CH $_3$: 2.51 (s)	7.14–6.99 (d)	6.84–6.80 (d)
	7	7.93–7.91 (d)	6.74 (s)	–	–	1.95–1.03, (m), Cyclic 11H	–	–
Calculated	1	5.09	7.76	3.29–3.02	–	–	–	–
	2	4.79	7.76	3.68–3.41	1.41–1.26	–	–	–
	3	4.66	7.79	4.69, 3.79	6.51	5.82–5.63	–	–
	4	8.19	7.99	4.38, 3.97	7.30	7.46	7.42	9.03
	5	7.37	8.05	9.18	–	7.38	7.71	7.16
	6	7.25	7.98	8.94	7.61	CH $_3$: 2.63–2.15	7.70	7.25
	7	4.66	7.72	–	–	2.14–1.29, Cyclic 11H	–	–

C.: Compounds, s (singlet), d (doublet), dd (doublet of doublet), t (triplet), td (triplet of doublet) and m (multiplet).

cal shifts are shown in Table 3. For compound **2**, the proton signal of $-\text{NH}$ coupled to the CH_2 proton was detected as a triplet at 8.11–8.09 ppm. The alkyenic ($\text{CH}=\text{C}$) H1 proton was shown as a singlet at 7.14 ppm. The H2 (CH_2) proton coupled to the H3 and NH protons was observed as a pentet at 3.37–3.30 ppm. The H3 (CH_3) proton coupled to the H2 protons was observed as a triplet at 1.21–1.17 ppm as shown in Figure 2. $\text{DMSO}-d_6$ and water in DMSO (HOD, H_2O) signals are shown around at 2.00, 2.50 (quintet) and 3.30 (variable, based on the solvent and its concentration) ppm, respectively.²⁵ These data are consistent with the values of those reported earlier for similar compounds.^{5b,26}

3. 4. ^{13}C NMR Spectral Interpretations

The ^{13}C NMR spectra of all compounds were measured in $\text{DMSO}-d_6$ and the chemical shifts are shown in Table 4. The ^{13}C NMR spectrum of the compound **2** showed 5 different resonances in good agreement with the proposed structure as shown in Figure 3. In compound **2**, the carbon signals of thiadiazole ring (C2 and C3) were detected at 155.4 and 169.0 ppm, respectively. The C3 carbon atom is shifted down-field (high values, δ) due to the presence of electron-negative nitrogen atom (NH group). The alkyenic C1 carbon atom ($\text{CH}=\text{C}$) was observed at 124.6 ppm. While the C4 (CH_2) carbon atom was detected at 40.1 ppm, the C5 (CH_3) resonated at 14.6 ppm. The C4 (CH_2) carbon atom is shifted down-field (high values, δ) as

does the C3 carbon atom due to the presence of electron-negative nitrogen atom (NH group).

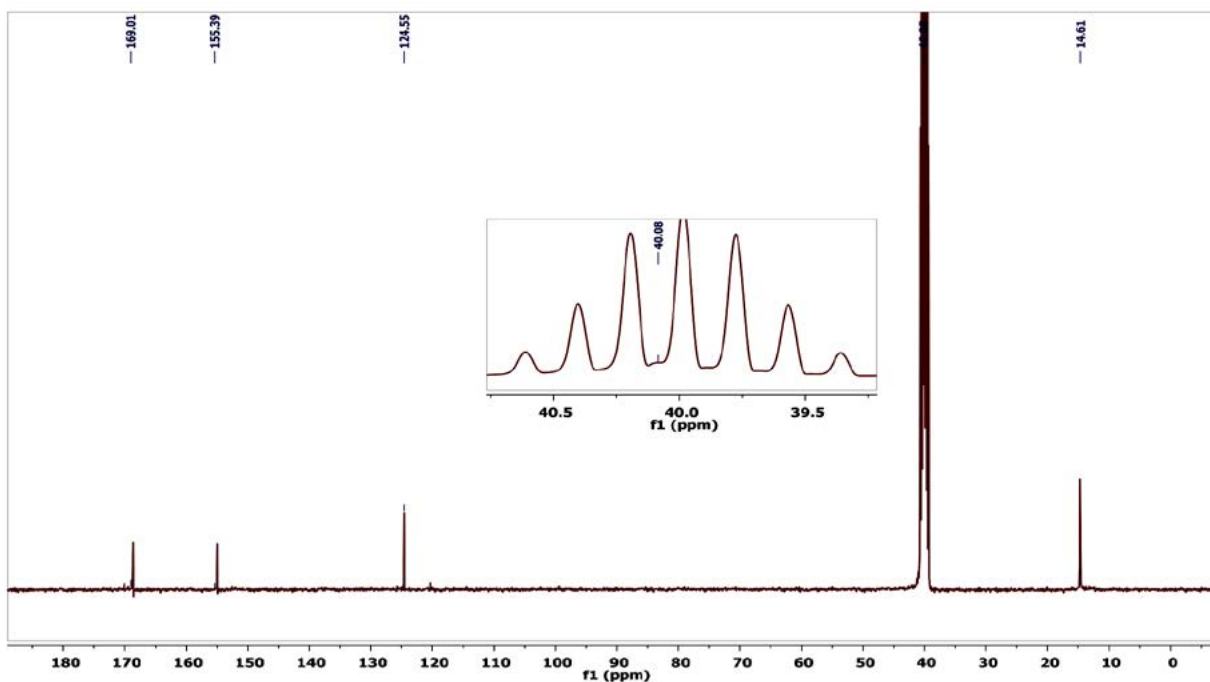
For compounds **1–7**, the alkyenic C1 carbon atom ($\text{CH}=\text{C}$) was observed between 125.7 and 120.8 ppm. While the C2 carbon signals of thiadiazole ring resonated a between 157.2 and 152.4 ppm, the C3 resonated between 169.6 and 164.3 ppm. For compound **3**, the C4 carbon atom (CH_2) was observed at 47.8 ppm. The alkyenic C5 and C6 carbon atoms ($\text{CH}=\text{CH}_2$) were detected at 134.6 and 117.3 ppm, respectively. In compounds **4–6**, the aromatic carbons (C4–C9) were observed at 149.1–111.7, 142.0–116.7, and 138.8–117.9 ppm, respectively. The methoxy ($-\text{OCH}_3$) signal was detected at 56.4 ppm for compound **4**, the methyl (CH_3) group was observed at 20.8 ppm for compound **6**. In compound **7**, the cyclic carbons (C4–C9) were observed between 53.9 and 24.7 ppm. These spectroscopic data are consistent with the values reported previously for similar compounds in the literature.^{5b,26a,b,27}

3. 5. Antibacterial Activity Assessments

In vitro antibacterial activity results for the synthesized 1,3,4-thiadiazole compounds are given in Table 5. The antibacterial activities of bis-1,3,4-thiadiazole compounds **1–7** were determined against three Gram-positive (*S. epidermidis*, *B. subtilis*, and *E. faecium*) and Gram-negative (*S. enterica* serovar *Kentucky*, *E. coli*, *K. pneumoniae*, *S. macrescens*, and *P. aeruginosa*) bacteria by two sequen-

Table 4. Experimental and calculated ^{13}C NMR values of the compounds (δ , ppm, in DMSO- d_6)

		1-3				4-7					
		R: CH_3 , CH_3CH_2 , $\text{CH}_2=\text{CH}-\text{CH}_2$				R: 2-OCH ₃ , 3-Cl, 4-CH ₃ , C ₆ H ₁₁					
		C1	C2	C3	C4	C5	C6	C7	C8	C9	R ₁
Experimental	1	124.9	155.7	169.6	32.2	–	–	–	–	–	–
	2	124.6	155.4	169.0	40.1	14.6	–	–	–	–	–
	3	124.9	155.8	168.5	47.8	134.6	117.3	–	–	–	–
	4	125.2	157.1	165.3	129.7	149.1	111.7	123.7	121.0	120.0	56.4
	5	125.7	157.2	164.3	142.0	117.6	133.9	122.5	131.2	116.7	–
	6	121.2	154.8	165.4	138.8	117.9	129.9	130.2	130.2	117.9	20.8
	7	120.8	152.4	169.4	53.9	32.5	24.7	25.7	24.7	32.5	–
Calculated	1	122.7	164.4	178.7	32.6	–	–	–	–	–	–
	2	122.8	164.3	178.2	44.1	14.8	–	–	–	–	–
	3	123.1	164.9	178.3	52.6	143.9	125.6	–	–	–	–
	4	123.3	165.0	173.3	134.9	154.0	113.4	127.2	125.4	121.8	57.6
	5	123.7	165.7	173.8	147.6	122.0	149.4	127.5	136.2	120.6	–
	6	123.1	164.8	173.5	144.1	121.9	136.2	140.0	135.6	122.5	22.3
	7	122.1	163.6	177.6	53.6	29.0	23.8	22.5	23.6	33.2	–

Figure 3. ^{13}C NMR spectrum of compound 2.

tial tests, the first being the minimum inhibitory concentration (MIC) and the second the minimum bactericidal concentration (MBC) test.

The results of the antibacterial screening given in Table 5 show that none of the compounds 1–7 had activity against *P. aeruginosa*, *S. epidermidis*, *S. enterica* se-

rovar *Kentucky*, and *S. macrescens*. All compounds except 1 showed an effect on Gram-negative *K. pneumoniae*. Compounds 2 and 3 showed antibacterial activity at MIC concentrations of 2.75 mg/L. The rest of compounds 4, 5, 6, and 7 presented antibacterial activity with MIC concentrations of 1.375 mg/L.

Table 5. MIC and MBC values of the synthesized compounds (mg/L).

Bacteria	Activity	1	2	3	4	5	6	7	GEN	TOB	CPFX
<i>S. enterica</i> serovar <i>Kentucky</i>	MIC	–	–	–	–	–	–	–	2.500	2.500	0.078
	MBC	–	–	–	–	–	–	–			
<i>E. coli</i>	MIC	–	–	5.5	–	–	–	5.5	10.00	10.00	–
	MBC	–	–	5.5	–	–	–	–			
<i>K. pneumoniae</i>	MIC	–	2.75	2.75	1.375	1.375	1.375	1.375	0.078	0.078	–
	MBC	–	5.5	5.5	5.5	5.5	5.5	5.5			
<i>S. macrescens</i>	MIC	–	–	–	–	–	–	–	–	–	–
	MBC	–	–	–	–	–	–	–			
<i>P. aeruginosa</i>	MIC	–	–	–	–	–	–	–	10.00	10.00	1.250
	MBC	–	–	–	–	–	–	–			
<i>S. epidermidis</i>	MIC	–	–	–	–	–	–	–	–	–	–
	MBC	–	–	–	–	–	–	–			
<i>B. subtilis</i>	MIC	–	–	–	2.75	5.5	2.75	2.75	1.250	2.500	–
	MBC	–	–	–	5.5	–	–	5.5			
<i>E. faecium</i>	MIC	–	–	5.5	–	5.5	5.5	5.5	–	0.625	0.156
	MBC	–	–	–	–	5.5	5.5	–			

GEN: gentamycin, TOB: tobramycin, CPFX: ciprofloxacin.

The activity type of any compound is decided by looking at the MBC/MIC ratio. If the MBC/MIC ratio is lower than 4 the activity of this compound is accepted as bactericidal, otherwise the activity is decided to be bacteriostatic.²⁸

The MBC test applied after the MIC test for *K. pneumoniae* shows that compounds 2 and 3 presented a bactericidal activity because MBC/MIC is lower than 4. Compounds 4, 5, 6 and 7 showed bacteriostatic activity because MBC/MIC is equal to 4.

MIC test results demonstrated that compounds 3 and 7 have antibacterial activity on Gram-negative *E. coli* at concentrations of 5.5 mg/L. According to the MBC test, compound 3 exhibited a bactericidal activity, but it is not possible to conclude whether the activity of compound 7 is bactericidal or bacteriostatic. Because the MBC of the compound could not be determined, thus MBC/MIC ratio cannot be calculated.

Compounds 4, 6, and 7 show antibacterial activity on Gram-negative *B. subtilis* at 2.75 mg/L, and 5.5 mg/L for compound 5. MBC test shows that compounds 4 and 7 possess bactericidal activity because MBC/MIC ratio is lower than 4. On the other hand, since the MBC of compounds 5 and 6 could not be determined, it is not possible to conclude whether the activities of these two compounds are bactericidal or bacteriostatic.

Compounds 3, 5, 6, and 7 exhibited antibacterial activity on Gram-negative *E. faecium* at concentrations of 5.5 mg/L for each. MBC test shows that compounds 5 and 6 have bactericidal activities because MBC/MIC ratios are lower than 4. On the other hand, since the MBC of compounds 3 and 7 could not be determined, it is not possible

to conclude whether the activities of these two compounds are bactericidal or bacteriostatic.

Rauckyte *et al.*²⁹ synthesized some 1,3,4-thiadiazole derivatives and investigated 12.5, 25.0, 50.0, and 100 g/L concentrations of these compounds for their antibacterial activity against selected bacterial strains. As a result, they observed that the MIC value against *E. coli* for 2-acetamide-1,3,4-thiadiazol-5-sulfonamide was 12.5 g/L. In our study, 1,3,4-thiadiazole derivatives (compounds 3 and 7) showed antibacterial activity against *E. coli* with MIC values of 0.0055 g/L. It was seen that our compounds showed higher antibacterial activity against *E. coli*, compared to the compounds synthesized by Rauckyte *et al.*²⁹ But these two results cannot be compared since the *E. coli* strains were not the same.

The MIC value against *E. faecium* for 2-acetamide-1,3,4-thiadiazol-5-sulfonamide was 12.5 g/L as determined by Rauckyte *et al.*²⁹ In our study, compounds 3, 5, 6, and 7 demonstrated antibacterial activities with MIC values of 0.0055 g/L. This shows that our compounds have higher antibacterial activity against *E. faecium*, but since the strains used in these studies were different it is not suitable to compare these results.

The MIC value against *B. subtilis* for 2-acetamide-1,3,4-thiadiazol-5-sulfonamide has shown no activity as determined by Rauckyte *et al.*²⁹ In the study conducted for *B. subtilis*, compounds 4, 5, 6, and 7 showed antibacterial activity with MIC values either 0.00275 or 0.0055 g/L. This indicates that the compounds show higher antibacterial activity against *B. subtilis*, again it is not convenient to compare the results as the *B. subtilis* strains used in these studies were different.

Moshafi *et al.*³⁰ synthesized 5-nitro-2-furyl and 5-nitro-2-imidazolyl derivatives of 1,3,4-thiadiazole and tested their antibacterial activity against *S. epidermidis* PTCC 1114, *B. subtilis* PTCC 1023, *Streptococcus pyogenes* PTCC 1447, *Micrococcus luteus* PTCC 1110, *E. coli* PTCC 1330, *P. aeruginosa* PTCC 1074, *K. pneumoniae* PTCC 1053, *S. marcescens* PTCC 1621 with a concentration range of 0.5, 1, 2, 4, 8, 16, 32 and 64 mg/L. As a result, they observed that the activity of the compounds were ranging between 0.50 and 64.0 mg/L. For example, the MIC for 2-(1-methyl-5-nitro-H1-imidazol-2-yl)-5-(*n*-pentylsulfinyl)-1,3,4-thiadiazole against *K. pneumoniae* was obtained to be 0.50–64.0 mg/L. In addition, the same MIC value was observed for 2-(5-nitro-2-furyl)-5-(*n*-butylthio)-1,3,4-thiadiazole against *E. coli*. Also, 2-(5-nitro-2-furyl)-5-(*n*-butylsulfonyl)-1,3,4-thiadiazole presented a MIC value of 0.50–16.0 mg/L against *B. subtilis*. In our study, compounds 2, 3, 4, 5, 6, and 7 showed antibacterial activity against *K. pneumoniae* with MIC values of 2.75 and 1.375 mg/L. Again, compounds 3 and 7 presented MIC values of 5.5 mg/L against *E. coli*. In addition, compounds 4, 5, 6, and 7 showed antibacterial activity with MIC values either 2.75 or 5.5 g/L against *B. subtilis*. These results indicate that our compounds usually showed higher antibacterial activity against *K. pneumoniae*, *E. coli*, and *B. subtilis*. However, these differences may be due to the use of different strains.

3. 6. Theoretical Analysis

Although electronic parameters such as the kinetic stability or chemical hardness of a molecule, hence its E_g ,

have a role on the probability of a chemical reaction to take place, the unpredictability of the steps of the reactions with living organisms such as bacteria causes these electronic parameters to be interpreted with hypothetical approaches specific to the relevant experiment in a way that supports the experimental data. It is known that HOMOs are the parameters that determine the capacity to donate electrons and LUMOs to accept electrons. The HOMO-LUMO gap represents the range in the binding energy spectrum in which the most probable excitations can occur, and indeed there is an inverse relationship between the HOMO-LUMO energy gap and the probability of excitations, i.e. the smaller the E_g means that the excitation will occur more easily. Furthermore, E_g can be a useful tool to study (or predict) the stability and chemical reactivity of a molecule, taking into account its sensitive dependence on many factors such as environment (reaction medium), molecular conformation, temperature, conjugation effects, intra- and intermolecular interactions. The small HOMO-LUMO gap of a molecule results in a lower kinetic stability, meaning higher chemical reactivity or lower chemical hardness. In this context, although not a very strong approximation, among synthesized compounds, compounds 4–7 can be expected to exhibit higher chemical reactivity than compounds 1–3 (see Figure 4b). The calculations show that the compounds can be classified in three groups: the first group, compounds 1–3 containing aliphatic structures attached to –NH; the second group, compounds 4–6 containing aromatic structures attached to –NH; and the third group, compound 7 with cyclic structure. The antibacterial ac-

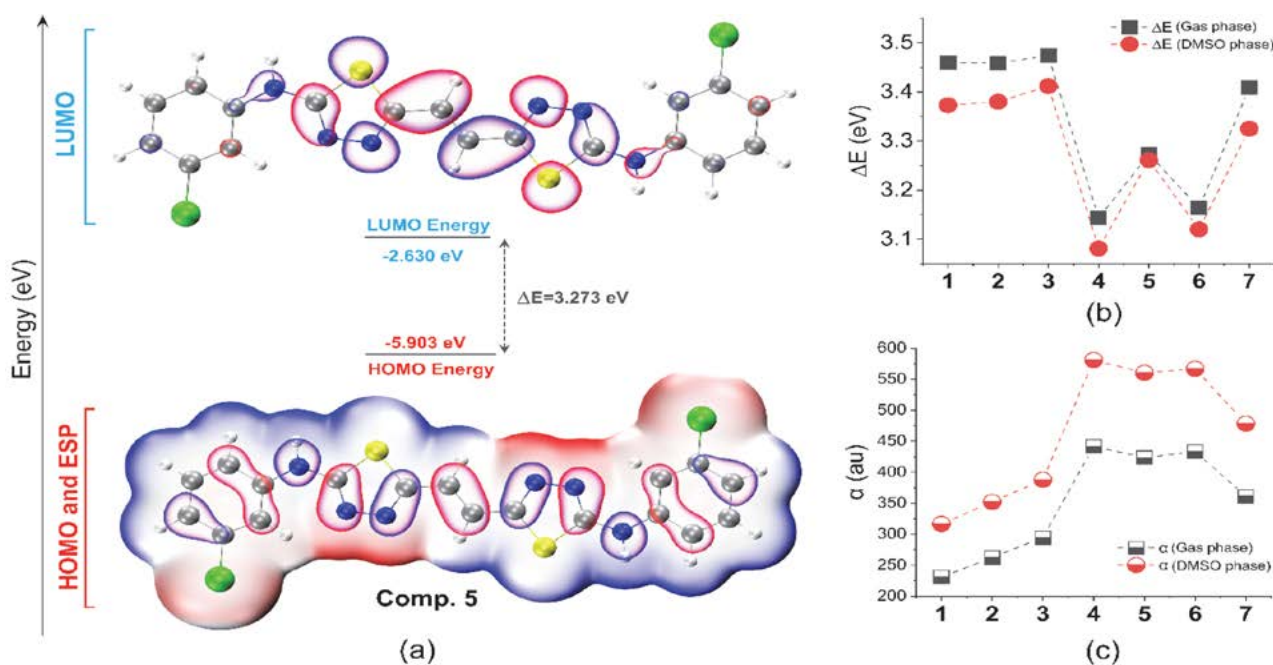


Figure 4. (a) HOMO-ESP and LUMO maps of compound 5; (b) HOMO-LUMO energy gap values of the compounds calculated in gas and DMSO phase; (c) Polarizability values of the compounds calculated in gas phase and DMSO phase (by 6-311++g(2d,2p) basis set).

tivities of the first group compounds appear to be weak, where compound 1 shows no activity, but in this group, the antibacterial activity increases partially as the aliphatic component grows, but aliphatic components do not seem to have a significant effect on the E_g values of the compounds (see Figure 4b). It can be said that aromatic and cyclic structures reduce the E_g values of the compounds and increase the antibacterial activity. On the other hand, the fact that compound 7 has a higher E_g value (3.409 eV) than the compounds in the second group (3.143, 3.273, and 3.164 eV for compounds 4–6, respectively), but is more sensitive to bacterial diversity, strengthens the opinion that cyclic group is a stronger factor for antibacterial activity than aromatic structures. In addition, the fact that the E_g values obtained from the calculations in the DMSO phase are lower than those in the gas phase (see Figure 4b) leads to the expectation that the compounds will show higher activity in the solution. At this point, the solubility of the compounds in DMSO is another parameter that affects the reactions. As it is known, the solvation energy is the difference of the total energies of the compound in the solvent and vacuum environment and depends on the nature of both the solvent and the compound (and the substituted groups). Solvation energies of the first group compounds were calculated to be lower than for those in the other groups (–16.40, –17.54, and –16.42 kcal/mol for compounds 1–3, respectively), which indicates that the first group compounds have poor solubility in DMSO. It was observed that the antibacterial properties of the second and third group compounds with high solubility or high solvation energies (between –18.76 kcal/mol and –22.82 kcal/mol) were higher (see Supplementary file, Tables S1, S2 for all calculated electronic data).

The interactions of the compounds with bacteria occur electrostatically in the first place, and in the later stages, the intramolecular interactions are involved in determining the coordination of the reaction. At this point, although molecular polarizability is defined as

the response of electron distribution on a molecule to an external static electric field, it is an important parameter because the intermolecular interaction energy can be expressed in terms of polarization and dispersion contributions. The polarizability of the first group compounds to which the aliphatic groups are attached was calculated to be lower (230.778, 262.483, and 294.367 a.u. for compounds 1–3, respectively) than that of the other compounds containing aromatic (441.604, 423.492, and 433.128 a.u. for compounds 4–6, respectively) and cyclic (361.137 a.u. for compound 7) structures (see Figure 4c). In addition, compound 1, which does not exhibit antibacterial properties, has the lowest polarizability. It was observed that the compounds with the highest polarizability were those with aromatic rings. Calculations performed in the DMSO phase show that the polarizability values of the compounds increase proportionally in this phase. Although the dipole moments and polarizabilities of the compounds contribute to the activation of reactive sites in intermolecular interactions, the conformational degrees of freedom of the compounds are another strong factor. π -Conjugation between thiadiazole groups reduces the conformational degrees of freedom of the compounds, and the reduction of the effect of intramolecular interactions on conformations increases the probability of the compounds to be exposed to steric effects during the reaction. Moreover, intramolecular interactions of aliphatic, aromatic or cyclic structures become a variable of the degree of freedom as a limiting parameter of the conformational orientations of the compounds. Since intramolecular interactions change the electron density distributions of the reactive sites, they can cause the reaction to occur easily and quickly, and vice versa. The average root mean square (RMS) errors of the superimpositions of the gas and DMSO phase conformations of the compounds were 0.057, 0.042, and 0.044 Å for the first group compounds, respectively; 0.019, 0.016, and 0.019 Å for the second group of compounds, respectively; for com-

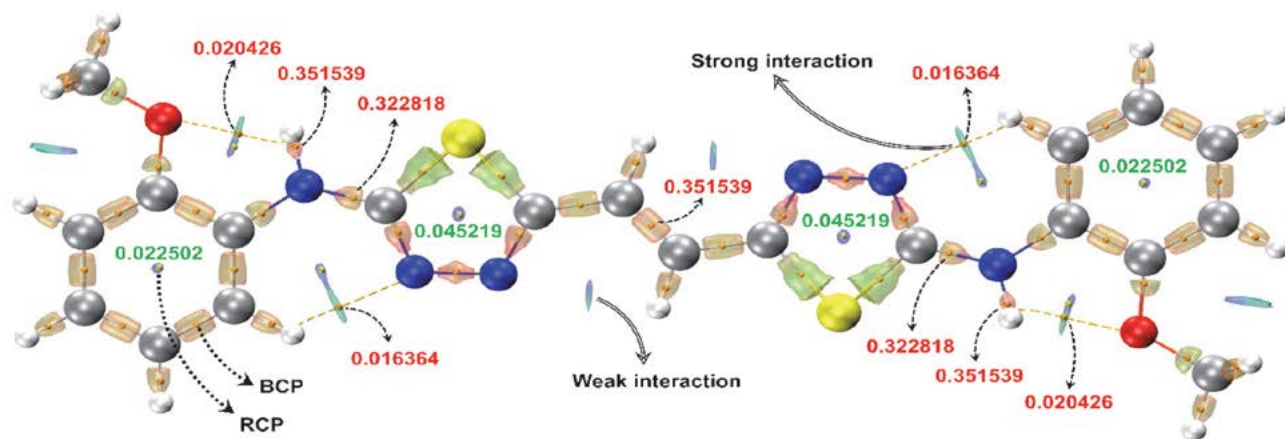


Figure 5. IRI surfaces of compound 5 and QTAIM data: Electron density (e/bohr^3) in BCP and RCP; RCP: Ring critical point, BCP: Bond critical point.

pound 7 with a cyclic group, it was calculated as 0.175 Å. Cyclohexyl group does not show resonance effects due to its absence of π -conjugation, and the larger RMS error of interaction with DMSO than that of other compounds indicates a higher conformational freedom than in the other compounds. This property of cyclohexyl ring may mean that compound 7 can perform a high electrophilic attack as well as less exposure to the steric effect. Moreover, the cyclohexyl group pumps electrons to the thiadiazole region, and in addition to being exposed to nucleophilic attacks by molecular structures (or atoms) with high electronegativity, it also supports the electrophilic attack of the thiadiazole region. The IRI surfaces and QTAIM data of compound 4 are given in Figure 5 as a quantitative visualization of intramolecular interactions (see Supplementary Figure S19 for all compounds).

The growth of electron donor aliphatic groups in the first group compounds caused an increase in electron density towards the central thiadiazole structures. In addition, in terms of the change of electron distribution on the compounds, both the conformational and electronic properties of aliphatic, aromatic and cyclic groups are among the factors that determine the degree of electrophilic attack (or nucleophilic attack) of the compounds. Figure 6 shows the electrophilic and nucleophilic attack region maps of compound 6 (see Supplementary Figure S20 for all compounds). The methyl group pumps electrons to the phenyl ring inductively and exhibits *ortho-para* directing behavior. An increase in electron density is observed both on the carbon atom to which it is attached and on the *para* carbon atom of the phenyl ring. A similar situation is observed in the methoxy substituted compound 4 exhibiting both strong mesomeric and weak inductive

effect. In compound 5, which has an electron-withdrawing chlorine substituent from the ring with an inductive effect, a result close to the effect of the methoxy group was observed. In addition, intramolecular interaction of $-NH$ with phenolic groups and electron donation to the phenyl ring with strong mesomeric effect strengthens the electrophilic attacks of compounds 4–6. In this context, it can be said that the second group compounds can perform electrophilic attack, which is partially stronger than the cyclic compound 7, but much stronger than the first group compounds. The nucleophilic attack regions of the compounds are predominantly concentrated around the alkenylic group ($-C=C-$) and the thiadiazole carbon atom to which this group is attached.

Considering whether the compounds show anti-bacterial action properties in terms of electrophilic and nucleophilic attacks, we can say that the reaction with *K. pneumoniae*, *B. subtilis*, and *E. faecium* bacteria occurs through electrophilic attacks, because for all of the compounds, the nucleophilic attack sites are on the thiadiazole and alkenylic groups; if the reactions had occurred through nucleophilic attacks, similar reaction rates would be expected for each bacterial species, but this was not observed for other bacterial species. At this point, the inability of the nucleophilic attack regions to perform the desired reaction may be due to the π -conjugation of these regions forcing the molecular structure to be planar and the aliphatic, aromatic and cyclic groups creating a steric effect. Moreover, the inability of the compounds to show activity on *S. enterica* serovar *Kentucky*, *S. macrescens*, *P. aeruginosa*, and *S. epidermidis* species may be due to the fact that these bacterial species react with nucleophilic rather than electrophilic attacks.

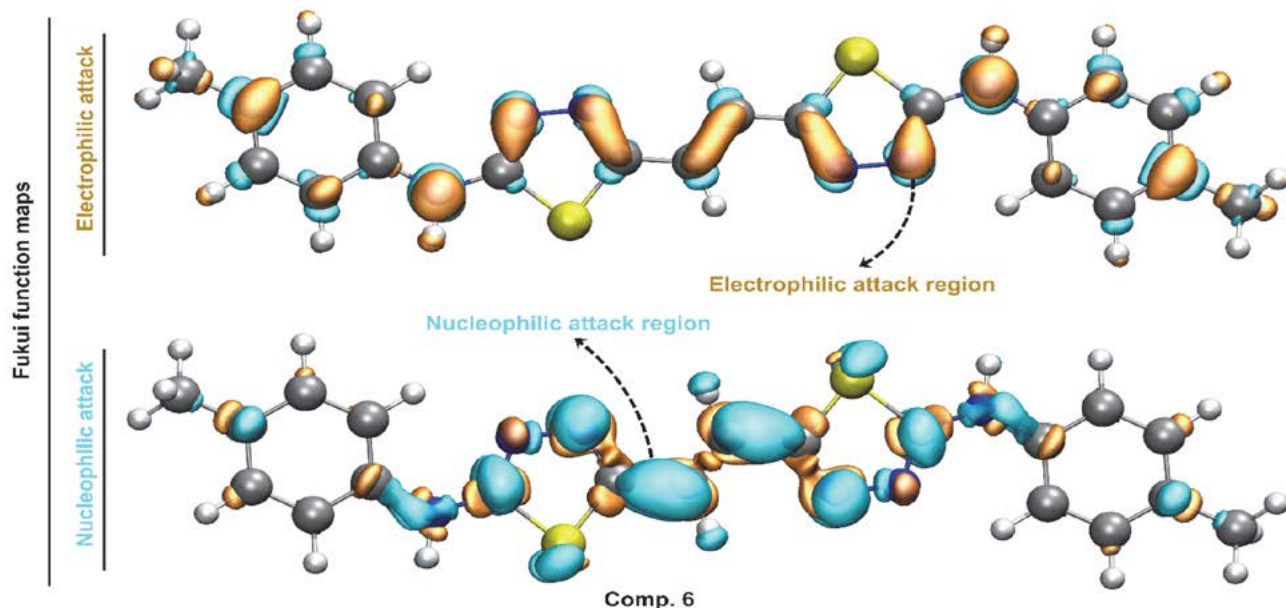


Figure 6. Electrophilic and nucleophilic attack sites maps of compound 6 (by 6-31g(d) basis set).

4. Conclusions

In this study, seven new bis-1,3,4-thiadiazoles 1–7 were obtained in excellent yields (61–93%) starting from fumaric acid. The synthesized compounds were characterized with FT-IR, ^1H NMR and ^{13}C NMR spectroscopic methods and elemental analysis. The conformations of the compounds and some electronic parameters were calculated. Experimental spectroscopic data were supported by DFT calculations.

As a result of experimental MIC procedures, thiadiazoles were found to have antimicrobial activity against *K. pneumoniae*, *E. coli*, *B. subtilis*, and *E. faecium*. We also evaluated the antibacterial activity of newly synthesized compounds with the MBC test. As a result of the MBC test, it was observed that the activity of compounds 2–7 on *K. pneumoniae*, compounds 5 and 6 on *E. faecium*, compounds 4 and 7 on *B. subtilis*, and compound 3 on *E. coli* were bactericidal. None of the compounds was found to have activity against *P. aeruginosa*, *S. epidermidis*, *S. enterica* serovar *Kentucky*, and *S. macrescens*.

Although the calculations cannot give definite answers in determining the antibacterial properties of the compounds, the fact that the antibacterial experiments give very close results each time reveals the existence of dominant variables that determine the results of the reactions. In this study, it was investigated whether there is a relationship between the antibacterial properties of the compounds and electronic data, electrophilic and nucleophilic attack sites. Although the HOMO-LUMO gap is a quantity related to the reactivity of the compounds, single molecular calculations cannot determine the conformational orientations caused by intermolecular interactions in the reaction medium of the compounds and the changes in electronic data caused by these orientations, that is, the E_g values change directly depending on the intermolecular interactions (hence their conformation) of the compounds during the reaction process, which prevents E_g from being a quantitative determinant of the reactions. However, it is also possible to make some predictions, albeit rough, for compounds that are similar derivatives of each other and in which only the substituents change. Especially in molecules with less conformational freedom, the effect of substituted groups can be analyzed with more accurate results. In this context, electronic data such as E_g , polarizability, solvent effects and Fukui function maps calculated for compounds 1–7 can be helpful in determining the reactivity and possible electrophilic/nucleophilic attack properties of the compounds, albeit partially. Although it is undeniable that more data is needed for the results of unknown variables in the reaction environment with bacteria, it was also observed in calculations that compounds with aromatic and cyclic groups are more reactive than compounds containing aliphatic groups, in accordance with experimental data.

Acknowledgements

We are grateful to the Scientific Research Centre for Industrial and Technological Applications and Research Centre (Gubitam) and Dr. Ömer Faruk Ensari for taking the NMR spectra. This study's synthesis, characterization, and antibacterial parts are belong to Ghaith Alabed Ibrayke Elefkhakry's master thesis.

Author contribution statement

Halit Muğlu: Supervision, Methodology, Synthesis, Writing-Review. **Hasan Yakan:** Conceptualization, Methodology, Structure Characterization, Writing-Review. **Ghaith Alabed Ibrayke Elefkhakry:** Synthesis, Investigation, Methodology. **Ergin Murat Altuner:** Antibacterial Activities Assay, Methodology, Writing-Review. **M. Serdar Çavuş:** Theoretical Calculations, Writing-Review.

Declaration of competing interest

The authors declare that they have no conflict of interest. This study was not supported by any organization.

Supplementary Material

All spectra (FT-IR, ^1H NMR and ^{13}C NMR) of the compounds are presented in the supporting information.

Data availability

The datasets generated and/or analyzed during the current study are available from the corresponding author on reasonable request.

5. References

- (a) K. Gowda, H. A. Swarup, S. C. Nagarakere, S. Rangappa, R. S. Kanchugarkoppal, M. Kempegowda, *Synth. Commun.* **2020**, *50*, 1528–1544; DOI:10.1080/00397911.2020.1745843
- (b) H. Muğlu, N. Şener, H. A. M. Emsaed, S. Özkinalı, O. E. Özkan, M. Gür, *J. Mol. Struct.* **2018**, *1174*, 151–159; DOI:10.1016/j.molstruc.2018.03.116
- (c) H. Tahtaci, M. Er, T. Karakurt, K. Sancak, *Tetrahedron* **2017**, *73*, 4418–4425; DOI:10.1016/j.tet.2017.06.006
- (d) A. Al-Mulla, *Der Pharma Chem.* **2017**, *9*, 141–147;
- (e) M. A. Al-Omair, A. R. Sayed, M. M. Youssef, *Molecules* **2015**, *20*, 2591–2610; DOI:10.3390/molecules20022591
- (f) J. K. Gupta, R. K. Yadav, R. Dudhe, P. K. Sharma, *Int. J. Pharmtech Res.* **2010**, *2*, 1493–1507;
- (g) M. Hanif, M. Saleem, M. T. Hussain, N. H. Rama, S. Zaib, M. A. M. Aslam, P. G. Jones, J. Iqbal, *J. Braz. Chem. Soc.* **2012**, *23*, 854–860;
- (h) K. Shrivastava, S. Purohit, S. Singhal, *Asian J. Biomed. Pharm. Sci* **2013**, *3*, 6–23;
- (i) B. Ardan, Y. Slyvka, E. Goresnik, M. Mys'kiv, *Acta Chim. Slov.* **2013**, *60*, 484–490.

2. I. Khan, S. Ali, S. Hameed, N. H. Rama, M. T. Hussain, A. Wadood, R. Uddin, Z. Ul-Haq, A. Khan, S. Ali, *Eur. J. Med. Chem.* **2010**, *45*, 5200–5207. DOI:10.1016/j.ejmech.2010.08.034
3. L. Yu, X. Gan, D. Zhou, F. He, S. Zeng, D. Hu, *Molecules* **2017**, *22*, 658.
4. X. Wang, W.-G. Duan, G.-S. Lin, M. Chen, F.-H. Lei, *Res. Chem. Intermed.* **2021**, *47*, 4029–4049. DOI:10.1007/s11164-021-04510-x
5. (a) W. S. Hamama, M. E. Ibrahim, H. A. Raoof, H. H. Zoorob, *J. Heterocycl. Chem.* **2017**, *54*, 2360–2366; DOI:10.1002/jhet.2826
(b) H. Muğlu, H. Yakan, H. A. Shouaib, *J. Mol. Struct.* **2020**, *1203*, 127470; DOI:10.1016/j.molstruc.2019.127470
(c) A. H. Moustafa, D. H. Ahmed, M. T. El-Wassimy, M. F. Mohamed, *Synth. Commun.* **2021**, *51*, 570–584; DOI:10.1080/00397911.2020.1843179
(d) Y. Liu, G. Liang, D. Yin, *Res. Chem. Intermed.* **2015**, *41*, 2019–2024; DOI:10.1007/s11164-013-1328-4
(e) A. Aly, R. El-Sayed, *Chem. Pap.* **2006**, *60*, 56–60. DOI:10.1016/S8756-5005(08)70230-0
6. S. Schenone, C. Brullo, O. Bruno, F. Bondavalli, A. Ranise, W. Filippelli, B. Rinaldi, A. Capuano, G. Falcone, *Biorg. Med. Chem.* **2006**, *14*, 1698–1705. DOI:10.1016/j.bmc.2005.10.064
7. N. Siddiqui, S. B. Andalip, R. Ali, O. Afzal, M. J. Akhtar, B. Azad, R. Kumar, *J. Pharm. Bioallied Sci.* **2011**, *3*, 194–212. DOI:10.4103/0975-7406.80765
8. F. Poorrajab, S. K. Ardestani, S. Emami, M. Behrouzi-Fardmoghadam, A. Shafiee, A. Foroumadi, *Eur. J. Med. Chem.* **2009**, *44*, 1758–1762. DOI:10.1016/j.ejmech.2008.03.039
9. J. J. Luszczki, M. Karpińska, J. Matysiak, A. Niewiadomy, *Pharmacol. Rep.* **2015**, *67*, 588–592. DOI:10.1016/j.pharep.2014.12.008
10. S. M. Gomha, Z. A. Muhammad, H. M. Gaber, M. M. Amin, *J. Heterocycl. Chem.* **2017**, *54*, 2708–2716. DOI:10.1002/jhet.2872
11. B. Kasetti Ashok, I. Singhvi, N. Ravindra, A. B. Shaik, *Rev. Roum. Chim* **2020**, *65*, 771–776. DOI:10.33224/rrch.2020.65.9.01
12. (a) I. Singh, L. H. Al-Wahaibi, R. Srivastava, O. Prasad, S. K. Pathak, S. Kumar, S. Parveen, M. Banerjee, A. A. El-Emam, L. Sinha, *ACS Omega* **2020**, *5*, 30073–30087; DOI:10.1021/acsomega.0c04474
(b) U. A. Çevik, D. Osmaniye, S. Levent, B. N. Sağlık, B. K. Çavuşoğlu, A. B. Karaduman, Y. Özkay, Z. A. Kaplancikli, *Acta Pharm.* **2020**, *70*, 499–513. DOI:10.2478/acph-2020-0034
13. M. M. Wassel, Y. A. Ammar, G. A. E. Ali, A. Belal, A. B. Mehany, A. Ragab, *Bioorg. Chem.* **2021**, *110*, 104794. DOI:10.1016/j.bioorg.2021.104794
14. F. Prestinaci, P. Pezzotti, A. Pantosti, *Pathog. Glob. Health* **2015**, *109*, 309–318. DOI:10.1179/2047773215Y.0000000030
15. P. Cos, A. J. Vlietinck, D. V. Berghe, L. Maes, *J. Ethnopharmacol.* **2006**, *106*, 290–302. DOI:10.1016/j.jep.2006.04.003
16. K. Canli, Ö. Şimşek, A. Yetgin, E. M. Altuner, *Bangladesh J. Pharmacol.* **2017**, *12*, 463–469. DOI:10.3329/bjp.v12i4.33652
17. (a) I. Wiegand, K. Hilpert, R. E. Hancock, *Nat. Protoc.* **2008**, *3*, 163–175; DOI:10.1038/nprot.2007.521
(b) B. Baldas, E. M. Altuner, *Communications Faculty of Sciences University of Ankara Series C Biology* **2018**, *27*, 1–10.
18. (a) A. Vollekova, D. Košťálová, R. Sochorova, *Folia Microbiologica* **2001**, *46*, 107–111; DOI:10.1007/BF02873586
(b) H. Usman, A. Haruna, I. Akpulu, M. Ilyas, A. Ahmadu, Y. Musa, *J. Trop. Biosci* **2005**, *5*, 72–76.
19. E. M. Altuner, B. Çetin, *Kastamonu Üniversitesi Orman Fakültesi Dergisi* **2018**, *18*, 126–137. DOI:10.17475/kastorman.315779
20. (a) P. Hohenberg, W. Kohn, *Phys. Rev.* **1964**, *136*, B864–B871; DOI:10.1103/PhysRev.136.B864
(b) W. Kohn, L. J. Sham, *Phys. Rev.* **1965**, *140*, A1133–A1138; DOI:10.1103/PhysRev.140.A1133
(c) N. A. Sánchez-Bojorge, L. M. Rodríguez-Valdez, N. Flores-Holguín, *J. Mol. Model.* **2013**, *19*, 3537–3542. DOI:10.1007/s00894-013-1878-9
21. M. J. Frisch, G. W. Trucks, H. B. Schlegel, G. E. Scuseria, M. A. Robb, J. R. Cheeseman, G. Scalmani, V. Barone, B. Mennucci, G. A. Petersson, H. Nakatsuji, M. Caricato, X. Li, H. P. Hratchian, A. F. Izmaylov, J. Bloino, G. Zheng, J. L. Sonnenberg, M. Hada, M. Ehara, K. Toyota, R. Fukuda, J. Hasegawa, M. Ishida, T. Nakajima, Y. Honda, O. Kitao, H. Nakai, T. Vreven, J. A. Montgomery, Jr., J. E. Peralta, F. Ogliaro, M. Bearpark, J. J. Heyd, E. Brothers, K. N. Kudin, V. N. Staroverov, R. Kobayashi, J. Normand, K. Raghavachari, A. Rendell, J. C. Burant, S. S. Iyengar, J. Tomasi, M. Cossi, N. Rega, J. M. Millam, M. Klene, J. E. Knox, J. B. Cross, V. Bakken, C. Adamo, J. Jaramillo, R. Gomperts, R. E. Stratmann, O. Yazyev, A. J. Austin, R. Cammi, C. Pomelli, J. W. Ochterski, R. L. Martin, K. Morokuma, V. G. Zakrzewski, G. A. Voth, P. Salvador, J. J. Dannenberg, S. Dapprich, A. D. Daniels, Ö. Farkas, J. B. Foresman, J. V. Ortiz, J. Cioslowski, D. J. Fox, M. J. Frisch, G. W. Trucks, H. B. Schlegel, G. E. Scuseria, M. A. Robb, J. R. Cheeseman, G. Scalmani, V. Barone, B. Mennucci, G. A. Petersson, H. Nakatsuji, M. Caricato, X. Li, H. P. Hratchian, A. F. Izmaylov, J. Bloino, G. Zheng, J. L. Sonnenberg, M. Hada, M. Ehara, K. Toyota, R. Fukuda, J. Hasegawa, M. Ishida, T. Nakajima, Y. Honda, O. Kitao, H. Nakai, T. Vreven, J. A. Montgomery, Jr., J. E. Peralta, F. Ogliaro, M. Bearpark, J. J. Heyd, E. Brothers, K. N. Kudin, V. N. Staroverov, R. Kobayashi, J. Normand, K. Raghavachari, A. Rendell, J. C. Burant, S. S. Iyengar, J. Tomasi, M. Cossi, N. Rega, J. M. Millam, M. Klene, J. E. Knox, J. B. Cross, V. Bakken, C. Adamo, J. Jaramillo, R. Gomperts, R. E. Stratmann, O. Yazyev, A. J. Austin, R. Cammi, C. Pomelli, J. W. Ochterski, R. L. Martin, K. Morokuma, V. G. Zakrzewski, G. A. Voth, P. Salvador, J. J. Dannenberg, S. Dapprich, A. D. Daniels, Ö. Farkas, J. B. Foresman, J. V. Ortiz, J. Cioslowski, D. J. Fox, Gaussian 09, Revision B.01, Gaussian, Inc., Wallingford CT, **2009**.
22. (a) R. F. Bader, *Acc. Chem. Res.* **1985**, *18*, 9–15; DOI:10.1021/ar00109a003
(b) R. F. Bader, *Chem. Rev.* **1991**, *91*, 893–928; DOI:10.1021/cr00005a013

- (c) V. S. Duarte, G. D. D'Oliveira, J. M. Custodio, S. S. Oliveira, C. N. Perez, H. B. Napolitano, *J. Mol. Model.* **2019**, *25*, 1–14; DOI:10.1007/s00894-019-4082-8
- (d) A. S. Abo Dena, Z. A. Muhammad, W. M. Hassan, *Chem. Pap.* **2019**, *73*, 2803–2812. DOI:10.1007/s11696-019-00833-7
23. T. Lu, F. Chen, *J. Comput. Chem.* **2012**, *33*, 580–592. DOI:10.1002/jcc.22885
24. (a) A. Ç. Karaburun, U. Acar Çevik, D. Osmaniye, B. N. Sağlık, B. Kaya Çavuşoğlu, S. Levent, Y. Özkay, A. S. Koparal, M. Behçet, Z. A. Kaplancıklı, *Molecules* **2018**, *23*, 3129; DOI:10.3390/molecules23123129
- (b) M. Gür, N. Şener, H. Muğlu, M. S. Çavuş, O. E. Özkan, F. Kandemirli, İ. Şener, *J. Mol. Struct.* **2017**, *1139*, 111–118; DOI:10.1016/j.molstruc.2017.03.019
- (c) Y.-T. Liu, L. Feng, D.-W. Yin, B.-J. Su, *Res. Chem. Intermed.* **2014**, *40*, 1607–1612. DOI:10.1007/s11164-013-1065-8
25. W. Kemp, *Nuclear Magnetic Resonance Spectroscopy*. In: *Organic Spectroscopy*, Palgrave, London, **1991**, pp. 101–241. DOI:10.1007/978-1-349-15203-2_3
26. (a) S. Ningaiah, U. K. Bhadraiah, A. Sobha, D. Shridevi, *Polycycl. Aromat. Compd.* **2020**, 1–11;
- (b) N. Kerru, L. Gummidi, S. V. Bhaskaruni, S. N. Maddila, S. B. Jonnalagadda, *Monatsh. Chem.* **2020**, *151*, 981–990; DOI:10.1007/s00706-020-02625-2
- (c) H. Muğlu, M. Akın, M. S. Çavuş, H. Yakan, N. Şaki, E. Güzel, *Comput. Biol. Chem.* **2022**, *96*, 107618. DOI:10.1016/j.compbiolchem.2021.107618
27. H. Yakan, *El-Cezeri Journal of Science and Engineering* **2021**, *8*, 155–163.
28. T. R. Keepers, M. Gomez, C. Celeri, W. W. Nichols, K. M. Krause, *Antimicrob. Agents Chemother.* **2014**, *58*, 5297–5305. DOI:10.1128/AAC.02894-14
29. T. Rauckyte-Žak, B. Szejniuk, *Ecol. Chem. Eng., A* **2011**, *18*, 1691–1704.
30. M. H. Moshafi, A. Peymani, A. Foroumadi, M. R. Zabihi, F. Doostishoar, *Intern. Med. Med. Investig. J.* **2019**, *4*, 1–8. DOI:10.24200/imminv.v4i2.213

Povzetek

Serijo novih bis-1,3,4-tiadiazolov **1–7** smo pripravili z reakcijo med fumarno kislino in *N*-(alkil/aril/ciklo)tiosemikarbazidi v prisotnosti fosforjevega oksiklorida. Strukture vseh spojin smo določili z FT-IR, ¹H NMR in ¹³C NMR ter z elementno analizo. Antibakterijsko aktivnost vseh spojin smo proučili na osmih izbranih bakterijah. Spojine **2–7** izkazujejo učinek na *Klebsiella pneumoniae*. Vendar pa nobena izmed spojin ni učinkovala na *Pseudomonas aeruginosa*, *Staphylococcus epidermidis*, *Salmonella enterica* serovar *Kentucky*, in *Serratia marcescens*. SCRF ("self-consistent reaction force") izračune smo izvajali v DMSO kot mediju z namenom ugotoviti energije solvatacij s pomočjo CPCM in SMD modelov. Pri DFT izračunih smo uporabili bazne sete 6-31G(d) and 6-311++G(2d,2p). Poleg elektronskih parametrov smo raziskali tudi elektronegativnost, elektrofilnost in spektroskopske lastnosti spojin, QTAIM, lokalne elektronske afinitete ter izvedli Fukuijevo analizo. Teoretični rezultati podpirajo eksperimentalna opažanja ter nakazujejo, da spojine, ki vsebujejo aromatske ali ciklične skupine, izkazujejo močnejše antibakterijsko delovanje kot spojine, ki vsebujejo alifatske skupine.



Except when otherwise noted, articles in this journal are published under the terms and conditions of the Creative Commons Attribution 4.0 International License

Scientific paper

Novel 5,6,7,8-tetrahydrobenzo[*b*]pyran Derivatives: Synthesis and Anticancer Activity

Amira E. M. Abdallah,^{1*} Rafat M. Mohareb,² Maher H. E. Helal¹
and Mariam M. Abd Elkader¹

¹ Department of Chemistry, Faculty of Science, Helwan University, Ain Helwan, Cairo, 11795, A. R. Egypt

² Department of Chemistry, Faculty of Science, Cairo University, Giza 12614, A. R. Egypt

* Corresponding author: E-mail: amiraelsayed135@yahoo.com

Tel: +2 01091769838

Received: 11-19-2022

Abstract

Many new cyclized pyran systems with a potential anti-cancer activity were designed and prepared. Pyran systems showed high reactivity to various chemical reagents. 24 products of the prepared compounds were chosen and tested in (mM) as respectable anticancer factors. The findings revealed that compounds **3b**, **6b**, and **8** were the widely effective compounds against the three cancer cell lines including A-549 (lung carcinoma), HC-29 (colorectal adenocarcinoma), and MKN-45 (gastric cancer) compared to the standard reference control foretinib.

Keywords: Tetrahydrobenzo[*b*]pyran, thiophene, pyridine, anti-proliferative activity.

1. Introduction

Pyran as a six-membered heterocyclic ring system was considered one of the most important rings in the synthesis of numerous bioactive fused systems with carbocyclic or heterocyclic ring systems. Figure 1 displays some important pyran-based synthetic marketed drugs. Moreover, Figure 2 shows some natural product compounds which have the pyran ring in their structures and are found in different food sources such as fruits, trees, and olive oil in addition to pigments in leaves.¹

Due to the continuous need to prepare novel poly-functionalized heterocyclic compounds used in a variety of applications in industry and medicine, tetrahydrobenzo[*b*]pyrans were selected as important bioactive scaffolds widely utilized in such fields. For drug and pharmaceutical applications, tetrahydrobenzo[*b*]pyran derivatives were used as antiviral,^{2,3} antioxidant,⁴ anticancer,^{5–7} anticoagulant,⁸ diuretic,^{9,10} antimicrobial,^{11–13} anti-inflammatory,¹⁴ and anti-anaphylactic agents.¹⁵ In the area of industrial application, they were used as a raw material in laser dyes, food additives, hand soaps, detergents, lotions and perfume.

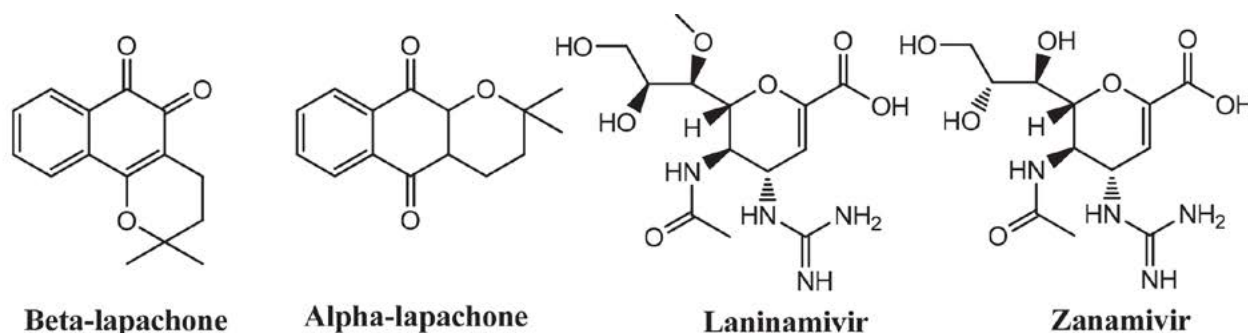


Figure 1. Some important pyran-based synthetic marketed drugs.

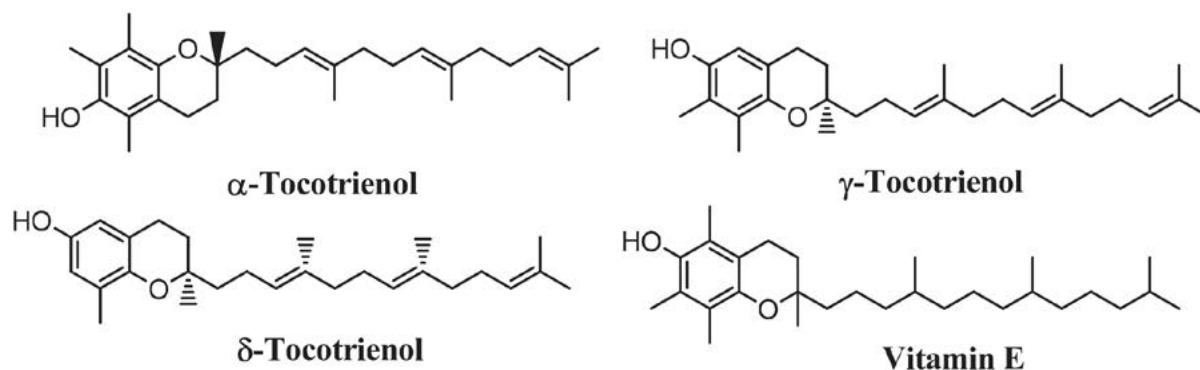


Figure 2. Pyran-containing natural product compounds.

Multi-component reactions were widely used to prepare tetrahydrobenzo[*b*]pyran systems in the presence of different catalysts,^{16–20} and reaction conditions such as microwave, ultrasonic, or electrochemical synthesis conditions in deep eutectic solvents.^{21–25} These methods mostly introduce green synthesis for the production of tetrahydrobenzo[*b*]pyrans obtained in pure form with good yields and shorter reaction times than the other traditional methods.

The current study constitutes a further thread in green organic chemistry and one-pot multi-component reactions (MCRs); it aims to improve the synthetic procedures of various prepared compounds.^{26–30} Herein preparations of many 5,6,7,8-tetrahydrobenzo[*b*]pyrans are described through multi-component reactions and via other simple methods. The obtained products were tested on three human tumor cell lines, including A-549 (lung carcinoma), HC-29 (colorectal adenocarcinoma), and MKN-45 (gastric cancer).

2. Experimental Section

On a digital thermoelectric melting point instrument, the melting points were measured and are not calibrated. By using Pye Unicam SP-1000 spectrophotometer, the infrared spectra (KBr disc) were determined. The Varian Gemini-300 (300 MHz) (Cairo University) instrument was utilized in the measurement of the ¹H NMR spectra by using DMSO-*d*₆ as solvent and TMS as the internal standard; chemical shifts (δ) are given in ppm. The mass spectrometry was carried out using a GCMS-QP2010 Shimadzu instrument. The analytical data were recorded at Cairo University, by using a Vario El III Elemental CHNS analyzer.

2. 1. Synthetic Procedures

2. 1. 1. General Method for the Preparation of 2-Amino-4-phenyl-5,6,7,8-tetrahydro-4H-chromene-3-carbonitrile Derivatives 1a,b

To a solution of compound cyclohexanone (0.98 g, 0.01 mol) in absolute ethanol (25 mL), either benzaldehyde

(1.06 g, 0.01 mol) or *para*-methoxybenzaldehyde (1.08 g, 0.01 mol) was added with malononitrile (0.66 g, 0.01 mol) in triethylamine (0.50 mL). Under reflux, the reaction was heated for 1 h. The resultant products were treated by adding them onto ice/water mixture with a few drops of HCl added. The precipitated product was collected by filtration, and recrystallize from ethanol.

2-Amino-4-phenyl-5,6,7,8-tetrahydro-4H-chromene-3-carbonitrile (1a). Brown crystals, yield: 1.66 g (66%), m.p. 257–260 °C. IR (ν , cm⁻¹): 3417, 3340 (NH₂), 3031 (CH-aromatic), 2932–2831 (CH₂), 2209 (CN), 1645, 1599 (C=C). ¹H NMR (δ , ppm): 1.66–1.71 (m, 4H, 2CH₂), 2.16–2.81 (m, 4H, 2CH₂), 5.73 (s, 1H, CH pyran), 7.14–7.89 (m, 7H, C₆H₅, NH₂). ¹³C NMR (δ , ppm): 21.0, 24.9, 27.0, 42.9, 112.4, 116.2, 126.9, 128.6, 128.8, 128.9, 129.3, 132.4, 134.6, 143.5. Anal. Calcd for C₁₆H₁₆N₂O (252.31): C, 76.16; H, 6.39; N, 11.10. Found: C, 76.21; H, 6.40; N, 11.12

2-Amino-4-(4-methoxyphenyl)-5,6,7,8-tetrahydro-4H-chromene-3-carbonitrile (1b). Pale brown crystals, yield: 1.98 g (70%), m.p. 269–272 °C. IR (ν , cm⁻¹): 3419, 3340 (NH₂), 3013 (CH aromatic), 2943–2836 (CH₂, CH₃), 2211 (CN), 1645, 1602 (C=C). ¹H NMR (δ , ppm): 1.46–1.48 (m, 4H, 2CH₂), 2.16–2.51 (m, 4H, 2CH₂), 3.87 (s, 3H, OCH₃), 5.72 (s, 1H, CH pyran), 6.99–7.89 (m, 6H, C₆H₄, NH₂). Anal. Calcd for C₁₇H₁₈N₂O₂ (282.34): C, 72.32; H, 6.43; N, 9.92. Found: C, 72.55; H, 6.65; N, 10.29.

2. 1. 2. General Method for the Preparation of Ethyl N-(3-cyano-4-phenyl-5,6,7,8-tetrahydro-4H-chromen-2-yl)formimidate Derivatives 2a,b

To form a mixture of an equimolar amount of **1a** (2.52 g, 0.01 mol) or **1b** (2.82 g, 0.01 mol) in acetic acid (20 mL), triethyl orthoformate (1.45 g, 0.01 mol) was added. The reaction was refluxed for 2 h and then added to a mixture of ice/water with a few drops of HCl added. The obtained products were filtered and recrystallized by using acetic acid.

Ethyl *N*-(3-cyano-4-phenyl-5,6,7,8-tetrahydro-4*H*-chromen-2-yl)formimidate (2a). Green crystals, yield: 2.00 g (65%), m.p. 212–215 °C. IR (ν , cm^{-1}): 3061 (CH-aromatic), 2937, 2868 (CH_2 , CH_3), 2191 (CN), 1639, 1491 (C=C), 1580 (C=N). ^1H NMR (δ , ppm): 1.20 (t, 3H, CH_3), 1.56–1.91 (m, 4H, 2CH_2), 2.49–2.51 (m, 4H, 2CH_2), 4.25 (q, 2H, CH_2), 6.35 (s, 1H, CH-pyran), 6.95 (s, 1H, CH), 7.19–7.52 (m, 5H, C_6H_5). MS m/z (%): 310 [$\text{M}^+ + 2$] (1.51), 309 [$\text{M}^+ + 1$] (1.51), 308 [M^+] (1.28), 275 (100.00), 77 [C_6H_5] $^+$ (14.10). Anal. Calcd for $\text{C}_{19}\text{H}_{20}\text{N}_2\text{O}_2$ (308.37): C, 74.00; H, 6.54; N, 9.08. Found: C, 74.29; H, 6.67; N, 9.40.

Ethyl *N*-(3-cyano-4-(4-methoxyphenyl)-5,6,7,8-tetrahydro-4*H*-chromen-2-yl)formimidate (2b). Redish brown crystals, yield: 2.40 g (71%), m.p. 82–85 °C. IR (ν , cm^{-1}): 3010 (CH-aromatic), 2935 (CH, CH_2 , CH_3), 2200 (CN), 1637, 1510 (C=C), 1602 (C=N). ^1H NMR (δ , ppm): 1.10 (t, 3H, CH_3), 1.66–1.91 (m, 4H, 2CH_2), 2.49–2.50 (m, 4H, 2CH_2), 3.81 (s, 3H, OCH_3), 4.30 (q, 2H, CH_2), 5.43 (s, 1H, CH-pyran), 6.85 (s, 1H, CH), 6.88–7.89 (m, 4H, C_6H_4). ^{13}C NMR (δ , ppm): 21.4, 22.0, 22.4, 24.9, 26.6, 55.1, 55.4, 113.8, 114.1, 141.5, 118.0, 129.3, 129.7, 131.8, 146.7, 149.2, 158.6, 159.2, 159.7. Anal. Calcd for $\text{C}_{20}\text{H}_{22}\text{N}_2\text{O}_3$ (338.40): C, 70.99; H, 6.55; N, 8.28. Found: C, 71.32; H, 6.90; N, 8.49.

2. 1. 3. General Method for the Preparation of *N*'-(3-Cyano-4-phenyl-5,6,7,8-tetrahydro-4*H*-chromen-2-yl)formimidohydrazide derivatives 3a–d

To an equimolar amount of **2a** (3.08 g, 0.01 mol) or **2b** (3.38 g, 0.01 mol) in absolute ethanol (25 mL), hydrazine hydrate (0.50 g, 0.01 mol) or phenyl hydrazine (1.08 g, 0.01 mol) were added. By using the reflux heating, the reaction lasted for 3 h. The resultant products were treated by adding them to ice/water mixture with a few HCl drops added. The resultant products were collected and filtered; then ethanol was used to recrystallize them.

***N*'-(3-Cyano-4-phenyl-5,6,7,8-tetrahydro-4*H*-chromen-2-yl)formimidohydrazide (3a).** Yellow crystals, yield: 2.79 g (95%), m.p. 157–160 °C. IR (ν , cm^{-1}): 3444, 3355 (NH_2), 3243 (NH), 3070 (CH-aromatic), 2934, 2865 (CH_2), 2197 (CN), 1639, 1448 (C=C), 1596 (C=N). ^1H NMR (δ , ppm): 1.58–1.74 (m, 4H, 2CH_2), 2.13–2.15 (m, 4H, 2CH_2), 6.40 (s, 1H, CH-pyran), 6.96 (s, 1H, CH), 7.20–7.54 (m, 7H, C_6H_5 , NH_2), 10.80 (s, 1H, NH). ^{13}C NMR (δ , ppm): 22.0, 22.3, 24.9, 26.7, 45.7, 95.4, 115.4, 115.7, 124.6, 127.6, 128.2, 128.5, 128.6, 143.6, 146.8, 150.1, 150.7. Anal. Calcd for $\text{C}_{17}\text{H}_{18}\text{N}_4\text{O}$ (294.35): C, 69.37; H, 6.16; N, 19.03. Found: C, 69.71; H, 6.30; N, 19.12. MS m/z (%): 295 [$\text{M}^+ + 1$] (27.04), 294 [M^+] (66.09), 293 [$\text{M}^+ - 1$] (100.00).

***N*'-(3-Cyano-4-phenyl-5,6,7,8-tetrahydro-4*H*-chromen-2-yl)-*N*'-phenylformimidohydrazide (3b).** Dark

brown crystals, yield: 2.82 g (75%), m.p. 107–110 °C. IR (ν , cm^{-1}): 3442–3244 (2NH), 3075 (CH-aromatic), 2936, 2865 (CH_2), 2211 (CN), 1638, 1492 (C=C), 1598 (C=N). ^1H NMR (δ , ppm): 1.56–1.74 (m, 4H, 2CH_2), 2.13–2.17 (m, 4H, 2CH_2), 6.37 (s, 1H, CH-pyran), 6.60 (s, 1H, CH), 7.19–7.86 (m, 10H, $2\text{C}_6\text{H}_5$), 10.30 (s, 1H, NH), 10.90 (s, 1H, NH). MS m/z (%): 378 [$\text{M}^+ + 2$] (4.24), 377 [$\text{M}^+ + 1$] (6.47), 376 [M^+] (8.13), 273 (100.00), 77 [C_6H_5] $^+$ (20.56). Anal. Calcd for $\text{C}_{23}\text{H}_{28}\text{N}_4\text{O}$ (376.49): C, 69.37; H, 6.16; N, 19.03. Found: C, 69.39; H, 6.20; N, 19.04.

***N*'-(3-Cyano-4-(4-methoxyphenyl)-5,6,7,8-tetrahydro-4*H*-chromen-2-yl)formimidohydrazide (3c).** Redish brown crystals, yield: 2.76 g (85%), m.p. 97–100 °C. IR (ν , cm^{-1}): 3437, 3348 (NH_2), 3225 (NH), 3080 (CH-aromatic), 2934, 2862 (CH_2), 2197 (CN), 1639, 1511 (C=C), 1605 (C=N). ^1H NMR (δ , ppm): 1.63–1.70 (m, 4H, 2CH_2), 2.16–2.20 (m, 4H, 2CH_2), 3.60 (s, 3H, OCH_3), 6.30 (s, 1H, CH-pyran), 6.86 (s, 1H, CH), 6.89–7.32 (m, 6H, C_6H_4 , NH_2), 10.90 (s, 1H, NH). ^{13}C NMR (δ , ppm): 22.3, 24.9, 25.6, 26.6, 44.7, 55.1, 113.9, 114.1, 115.9, 119.0, 129.6, 129.7, 130.5, 149.2, 158.6. MS m/z (%): 322 [$\text{M}^+ - 2$] (6.18), 305 (100.00), 76 [C_6H_4] $^+$ (4.89). Anal. Calcd for $\text{C}_{18}\text{H}_{20}\text{N}_4\text{O}_2$ (324.38): C, 66.65; H, 6.21; N, 17.27. Found: C, 70.01; H, 6.30; N, 17.29.

***N*'-(3-Cyano-4-(4-methoxyphenyl)-5,6,7,8-tetrahydro-4*H*-chromen-2-yl)formimidohydrazide (3d).** Dark brown crystals, yield: 4.04 g (99%), m.p. 82–85 °C. IR (ν , cm^{-1}): 3435–3225 (NH), 3005 (CH-aromatic), 2861, 2838 (CH, CH_2 , CH_3), 2207 (CN), 1639, 1510 (C=C), 1602 (C=N). ^1H NMR (δ , ppm): 1.56–1.71 (m, 4H, 2CH_2), 2.16–2.20 (m, 4H, 2CH_2), 3.86 (s, 3H, OCH_3), 6.31 (s, 1H, CH-pyran), 6.96 (s, 1H, CH), 7.03–7.88 (m, 9H, C_6H_4 , C_6H_5), 9.87 (s, 1H, NH), 10.10 (s, 1H, NH). MS m/z (%): 408 [$\text{M}^+ + 2$] (38.22), 407 [$\text{M}^+ + 1$] (35.80), 406 [M^+] (26.39), 405 [$\text{M}^+ - 1$] (12.85), 404 [$\text{M}^+ - 2$] (7.92), 303 (100.00), 77 [C_6H_5] $^+$ (35.65), 76 [C_6H_4] $^+$ (5.20). Anal. Calcd for $\text{C}_{24}\text{H}_{30}\text{N}_4\text{O}_2$ (406.52): C, 71.98; H, 6.04; N, 13.99. Found: C, 72.12; H, 6.30; N, 13.99.

2. 1. 4. Synthesis of *N*'-(3-Cyano-4-phenyl-5,6,7,8-tetrahydro-4*H*-chromen-2-yl)-*N*-phenylformimidamide (4).

For an equimolar amount of **2a** (3.08 g, 0.01 mol) in absolute ethanol (25 mL), aniline (0.93 g, 0.01 mol) was added. The reaction was refluxed for 3 h and then the mixture was added to an ice/water mixture with a few HCl drops added. The obtained product was filtered and recrystallized by using ethanol.

Brown crystals, yield: 2.84 g (80%), m.p. 97–100 °C. IR (ν , cm^{-1}): 3417–3242 (NH), 3058 (CH-aromatic), 2935, 2862 (CH, CH_2), 2210 (CN), 1640, 1495 (C=C), 1596 (C=N). ^1H NMR (δ , ppm): 1.54–1.79 (m, 4H, CH_2), 2.13–2.39 (m, 4H, CH_2), 5.73 (s, 1H, CH-pyran), 6.80–7.58 (m,

11H, 2C₆H₅, CH), 10.01 (s, 1H, NH). ¹³C NMR (δ, ppm): 21.4, 22.0, 24.9, 26.9, 42.9, 66.4, 112.6, 115.4, 115.8, 116.2, 124.3, 128.0, 128.2, 128.3, 128.5, 128.6, 129.3, 129.4, 137.3, 143.6, 146.9, 150.1, 150.7. MS *m/z* (%): 357 [M⁺ + 2] (31.33), 356 [M⁺ + 1] (40.77), 355 [M⁺] (23.18), 300 (100.00), 77 [C₆H₅]⁺ (36.91). Anal. Calcd for C₂₃H₂₁N₃O (355.43): C, 77.72; H, 5.96; N, 11.82. Found: C, 77.94; H, 6.17; N, 12.20.

2. 1. 5. General Method for the Preparation of 2-(((3-Cyano-4-phenyl-5,6,7,8-tetrahydro-4H-chromen-2-yl)imino)methyl)malononitrile derivatives 5a–d

To compound **2a** (3.08 g, 0.01 mol) or **2b** (3.38 g, 0.01 mol) in absolute ethanol (25 mL), malononitrile (0.66 g, 0.01 mol) and ethyl cyanoacetate (1.13 g, 0.01 mol) were added. On the reflux system, the reaction was heated for 3 h. The resultant products were poured onto the ice/water mixture with a few drops of HCl added. The precipitated products were collected by filtration and then recrystallized from ethanol.

2-(((3-Cyano-4-phenyl-5,6,7,8-tetrahydro-4H-chromen-2-yl)imino)methyl)malononitrile (5a). Yellow crystals, yield: 3.12 g (95%), m.p. 95–98 °C. IR (ν, cm⁻¹): 3100 (CH-aromatic), 2936, 2865 (CH, CH₂), 2260, 2220, 2208 (3CN), 1639, 1448 (C=C), 1597 (C=N). ¹H NMR (δ, ppm): 1.49–1.72 (m, 4H, CH₂), 2.13–2.18 (m, 4H, CH₂), 5.80 (s, 1H, CH-pyran), 6.37, 6.93, (2d, 2H, 2CH), 7.10–7.53 (m, 5H, C₆H₅). ¹³C NMR (δ, ppm): 21.1, 22.4, 24.4, 24.9, 26.9, 66.4, 112.4, 115.4, 115.8, 116.2, 124.3, 127.9, 128.2, 128.5, 128.6, 137.3, 143.6, 146.7, 150.1, 150.7. MS *m/z* (%): 330 [M⁺ + 2] (17.26), 329 [M⁺ + 1] (13.72), 328 [M⁺] (17.92), 327 [M⁺ – 1] (12.17), 300 (100.00), 77 [C₆H₅]⁺ (19.91). Anal. Calcd for C₂₀H₁₆N₄O (328.42): C, 73.15; H, 4.91; N, 17.06. Found: C, 73.34; H, 4.95; N, 17.28.

Ethyl-2-cyano-3-((3-cyano-4-phenyl-5,6,7,8-tetrahydro-4H-chromen-2-yl)imino)propanoate (5b). Brown crystals, yield: 2.48 g (66%), m.p. 147–150 °C. IR (ν, cm⁻¹): 3061 (CH-aromatic), 2937, 2865 (CH, CH₂, CH₃), 2260, 2213 (2CN), 1697 (C=O), 1644, 1448 (C=C), 1595 (C=N). ¹H NMR (δ, ppm): 1.19–1.21 (t, 3H, CH₃), 1.54–1.74 (m, 4H, 2CH₂), 2.13–2.17 (m, 4H, 2CH₂), 4.19–4.21 (q, 2H, CH₂), 5.75 (s, 1H, CH-pyran), 6.37, 6.80 (2d, 2H, 2CH), 7.20–7.53 (m, 5H, C₆H₅). MS *m/z* (%): 377 [M⁺ + 2] (4.15), 375 [M⁺] (2.60), 273 (100.00), 77 [C₆H₅]⁺ (9.84). Anal. Calcd for C₂₂H₂₁N₃O₃ (375.42): C, 70.38; H, 5.64; N, 11.19. Found: C, 70.58; H, 5.67; N, 11.29.

2-(((3-Cyano-4-(4-methoxyphenyl)-5,6,7,8-tetrahydro-4H-chromen-2-yl)imino)methyl)malononitrile (5c). Red crystals, yield: 1.97 g (55%), m.p. 82–85 °C. IR (ν, cm⁻¹): 3006 (CH-aromatic), 2936 (CH, CH₂, CH₃), 2260, 2203, 2190 (3CN), 1639, 1450 (C=C), 1604 (C=N). ¹H

NMR (δ, ppm): 1.46–1.73 (m, 4H, 2CH₂), 2.16–2.25 (m, 4H, 2CH₂), 3.84 (s, 3H, OCH₃), 5.03 (s, 1H, CH-pyran), 6.32–6.70 (2d, 2H, 2CH), 6.85–7.99 (m, 4H, C₆H₄). Anal. Calcd for C₂₁H₁₈N₄O₂ (358.39): C, 70.38; H, 5.06; N, 15.63. Found: C, 70.39; H, 5.17; N, 15.70.

Ethyl-2-cyano-3-(3-cyano-4-(4-methoxyphenyl)-5,6,7,8-tetrahydro-4H-chromen-2-yl)imino)propanoate (5d). Yellow crystals, yield: 2.03 g (50%), m.p. 102–105 °C. IR (ν, cm⁻¹): 3100 (CH-aromatic), 2935, 2862 (CH, CH₂, CH₃), 2260, 2202 (2CN), 1701 (C=O), 1639, 1451 (C=C), 1600 (C=N). ¹H NMR (δ, ppm): 1.06–1.08 (t, 3H, CH₃), 1.67–1.70 (m, 4H, 2CH₂), 2.18–2.22 (m, 4H, 2CH₂), 3.84 (s, 3H, OCH₃), 4.22–4.24 (q, 2H, CH₂), 5.70 (s, 1H, CH-pyran), 6.30, 6.67 (2d, 2H, 2CH), 6.86–7.32 (m, 4H, C₆H₄). MS *m/z* (%): 407 [M⁺ + 2] (4.56), 406 [M⁺ + 1] (4.27), 405 [M⁺] (2.99), 404 [M⁺ – 1] (2.63), 305 (100.00), 76 [C₆H₄]⁺ (6.13). Anal. Calcd for C₂₃H₂₃N₃O₄ (405.45): C, 68.13; H, 5.72; N, 10.36. Found: C, 68.33; H, 5.78; N, 10.69.

2. 1. 6. General Method for the Preparation of 2-Cyano-N-(3-cyano-4-phenyl-5,6,7,8-tetrahydro-4H-chromen-2-yl)acetamide derivatives 6a,b

To form a mixture of equimolar amounts of **1a** (2.52 g, 0.01 mol) or **1b** (2.82 g, 0.01 mol) in *N,N*-dimethylformamide (15 mL), ethyl cyanoacetate (1.13 g, 0.01 mol) was added. The chemical reaction was refluxed for 3 h and then added into a beaker containing a mixture of ice and water. The precipitated products were collected by filtration and recrystallized from *N,N*-dimethylformamide.

2-Cyano-N-(3-cyano-4-phenyl-5,6,7,8-tetrahydro-4H-chromen-2-yl)acetamide (6a). Pale brown crystals, yield: 3.18 g (99%), m.p. 250–253 °C. IR (ν, cm⁻¹): 3417–3227 (NH), 3033 (CH-aromatic), 2932–2861 (CH₂), 2260, 2209 (2CN), 1647 (C=O), 1600, 1448 (C=C). ¹H NMR (δ, ppm): 1.45–1.49 (m, 4H, 2CH₂), 2.16–2.20 (m, 4H, 2CH₂), 3.80 (s, 2H, CH₂), 5.73 (s, 1H, CH-pyran), 7.33–7.43 (m, 5H, C₆H₅), 10.01 (s, 1H, NH). ¹³C NMR (δ, ppm): 21.0, 24.8, 27.0, 42.9, 81.5, 112.3, 116.2, 126.9, 128.6, 128.8, 128.9, 129.3, 132.4, 134.6, 143.6. MS *m/z* (%): 317 [M⁺ – 2] (0.31), 300 (100.00), 77 [C₆H₅]⁺ (2.82). Anal. Calcd for C₁₉H₁₇N₃O₂ (319.36): C, 71.46; H, 5.37; N, 13.16. Found: C, 71.83; H, 5.38; N, 13.19.

2-Cyano-N-(3-cyano-4-(4-methoxyphenyl)-5,6,7,8-tetrahydro-4H-chromen-2-yl)acetamide (6b). Reddish brown crystals, yield: 1.74 g (50%), m.p. 122–125 °C. IR (ν, cm⁻¹): 3426–3242 (NH), 3100 (CH-aromatic), 2936 (CH₂, CH₃), 2260, 2208 (2CN), 1714 (C=O), 1593, 1439 (C=C). ¹H NMR (δ, ppm): 1.66–1.71 (m, 4H, 2CH₂), 2.10–2.20 (m, 4H, 2CH₂), 3.73 (s, 3H, OCH₃), 4.34 (s, 2H, CH₂), 5.70 (s, 1H, CH-pyran), 6.91–7.90 (m, 4H, C₆H₄), 8.31 (s, 1H,

NH). MS m/z (%): 347 [$M^+ - 2$] (15.34), 330 (100.00). Anal. Calcd for $C_{20}H_{19}N_3O_3$ (349.38): C, 68.75; H, 5.48; N, 12.03. Found: C, 69.03; H, 5.49; N, 12.27

2. 1. 7. General Method for the Preparation of 3, 5-Diamino-4-cyano-*N*-(3-cyano-4-phenyl-5,6,7,8-tetrahydro-4*H*-chromen-2-yl)thiophene-2-carboxamide derivatives 7a,b

To an equimolar amounts of **6a** (3.19 g, 0.01 mol) in absolute ethanol (25 mL) and triethylamine (0.50 mL), and either malononitrile (0.66 g, 0.01 mol) or ethyl cyanoacetate (1.13 g, 0.01 mol) was added with elemental sulfur (0.32 g, 0.01 mol). The reaction was refluxed for 3 h and then added onto the mixture of ice, water and HCl (a few drops). The precipitated products were collected by filtration and then recrystallized from ethanol.

3,5-Diamino-4-cyano-*N*-(3-cyano-4-phenyl-5,6,7,8-tetrahydro-4*H*-chromen-2-yl)thiophene-2-carboxamide (7a). Reddish brown crystals, yield: 2.97 g (71%), m.p. 201–204 °C. IR (ν , cm^{-1}): 3417, 3340 (2NH₂), 3244 (NH), 3034 (CH-aromatic), 2932, 2864 (CH₂), 2260, 2209 (2CN), 1644 (C=O), 1601, 1448 (C=C). ¹H NMR (δ , ppm): 1.45–1.71 (m, 4H, 2CH₂), 2.01–2.24 (m, 4H, 2CH₂), 5.73 (s, 1H, CH-pyran), 7.28–7.62 (m, 9H, C₆H₅, 2NH₂), 8.50 (s, 1H, NH). ¹³C NMR (δ , ppm): 21.0, 22.0, 24.8, 26.5, 42.8, 81.5, 112.3, 113.7, 116.2, 124.2, 128.2, 128.6, 128.7, 128.8, 132.3, 133.4, 134.6, 143.5. MS m/z (%): 418 [$M^+ + 1$] (4.38), 417 [M^+] (6.65), 300 (100.00). Anal. Calcd for $C_{22}H_{19}N_5O_2S$ (417.48): C, 63.29; H, 4.59; N, 16.78; S, 7.68. Found: C, 63.30; H, 4.70; N, 16.98; S, 7.86.

Ethyl 2,4-diamino-5-((3-cyano-4-phenyl-5,6,7,8-tetrahydro-4*H*-chromen-2-yl)carbamide)thiophene-3-carboxylate (7b). Brown crystals, yield: 2.78 g (60%), m.p. 232–235 °C. IR (ν , cm^{-1}): 3418, 3340 (2NH₂), 3251 (NH), 3035 (CH-aromatic), 2933–2831 (CH₂, CH₃), 2209 (CN), 1709 (C=O), 1645, 1450 (C=C). ¹H NMR (δ , ppm): 1.29–1.31 (t, 3H, CH₃), 1.66–1.71 (m, 4H, 2CH₂), 2.15–2.20 (m, 4H, 2CH₂), 4.31–4.34 (q, 2H, CH₂), 5.73 (s, 1H, CH-pyran), 7.03–7.63 (m, 9H, C₆H₅, 2NH₂), 8.41 (s, 1H, NH). Anal. Calcd for $C_{24}H_{24}N_4O_4S$ (464.54): C, 62.05; H, 5.21; N, 12.06; S, 6.90. Found: C, 62.16; H, 5.23; N, 12.25; S, 7.11.

2. 1. 8. Synthesis of *N*-(3-Cyano-4-phenyl-5,6,7,8-tetrahydro-4*H*-chromen-2-yl)-2-oxo-2*H*-chromene-3-carboxamide (8)

A solution of compound **6a** (3.19 g, 0.01 mol) is made by adding absolute ethanol (25 mL) and piperidine (0.50 mL) with salicylaldehyde (1.22 g, 0.01 mol). The chemical reaction was refluxed for 3 h and then added into a beaker containing a mixture of ice and water. The precipitated product was filtered and then recrystallized from ethanol.

Brown crystals, yield: 2.13 g (50%), m.p. 91–94 °C. IR (ν , cm^{-1}): 3434, 3245 (NH), 3054 (CH-aromatic), 2932, 2855 (CH₂), 2215 (CN), 1738, 1696 (2C=O), 1598, 1441 (C=C). ¹H NMR (δ , ppm): 1.69–1.71 (m, 4H, 2CH₂), 2.10–2.20 (m, 4H, 2CH₂), 6.30 (s, 1H, CH-pyran), 6.89 (s, 1H, CH-coumarin), 6.92–7.37 (m, 9H, C₆H₄, C₆H₅), 8.25 (s, 1H, NH). ¹³C NMR (δ , ppm): 22.1, 22.3, 23.6, 25.6, 43.8, 87.9, 113.6, 114.6, 116.4, 118.2, 119.2, 125.2, 125.9, 127.2, 127.7, 128.1, 128.3, 128.6, 128.7, 129.1, 146.9, 148.3, 150.8, 153.2, 158.7, 163.2. MS m/z (%): 426 [$M^+ + 2$] (0.45), 425 [$M^+ + 1$] (1.54), 424 [M^+] (4.77), 423 [$M^+ - 1$] (17.73), 422 [$M^+ - 2$] (31.09), 77 [C₆H₅]⁺ (1.97), 76 [C₆H₄]⁺ (0.83). Anal. Calcd for $C_{26}H_{20}N_2O_4$ (424.45): C, 73.57; H, 4.75; N, 6.60. Found: C, 73.60; H, 4.89; N, 6.98.

2. 1. 9. General Method for the Preparation of 1-(3-Cyano-4-phenyl-5,6,7,8-tetrahydro-4*H*-chromen-2-yl)-4,6-dimethyl-2-oxo-1,2-dihydropyridine-3-carbonitrile derivatives 9a,b

To a solution of compound **6a** (3.19 g, 0.01 mol) in absolute ethanol (25 mL) and piperidine (0.50 mL), either acetylacetone (1.00 g, 0.01 mol) or ethyl acetoacetate (1.30 g, 0.01 mol) was added. The reaction was carried out for 3 h. Thereafter, the reaction mixture was poured onto the mixture of ice/water with a few drops of HCl added. The precipitated products were collected by filtration and then recrystallized from ethanol.

1-(3-Cyano-4-phenyl-5,6,7,8-tetrahydro-4*H*-chromen-2-yl)-4,6-dimethyl-2-oxo-1,2-dihydropyridine-3-carbonitrile (9a). Reddish brown crystals, yield: 1.91 g (50%), m.p. 71–74 °C. IR (ν , cm^{-1}): 3034 (CH-aromatic), 2943, 2866 (CH₂, CH₃), 2258, 2218 (2CN), 1751 (C=O), 1636, 1447 (C=C). ¹H NMR (δ , ppm): 1.02–1.06 (s, 3H, CH₃), 1.08–1.29 (s, 3H, CH₃), 1.60–1.70 (m, 4H, 2CH₂), 2.10–2.20 (m, 4H, 2CH₂), 5.70 (s, 1H, CH-pyran), 6.30 (s, 1H, CH-pyridine), 6.96–7.53 (m, 5H, C₆H₅). ¹³C NMR (δ , ppm): 21.5, 22.1, 22.3, 26.9, 27.1, 28.2, 40.5, 53.3, 113.6, 115.1, 115.5, 115.8, 120.6, 125.9, 127.0, 127.7, 128.6, 128.7, 143.5, 146.9, 150.1, 150.7, 158.7, 166.0. Anal. Calcd for $C_{24}H_{21}N_3O_2$ (383.44): C, 75.18; H, 5.52; N, 10.96. Found: C, 75.19; H, 5.81; N, 11.15.

1-(3-Cyano-4-phenyl-5,6,7,8-tetrahydro-4*H*-chromen-2-yl)-6-hydroxy-4-methyl-2-oxo-1,2-dihydropyridine-3-carbonitrile (9b). Brown crystals, yield: 2.76 g (72%), m.p. 56–58 °C. IR (ν , cm^{-1}): 3442–3245 (OH), 3100 (CH-aromatic), 2940, 2869 (CH₂), 2260, 2219 (2CN), 1745 (C=O), 1635, 1447 (C=C). ¹H NMR (δ , ppm): 1.24–1.29 (s, 3H, CH₃), 1.60–1.70 (m, 4H, 2CH₂), 2.10–2.27 (m, 4H, 2CH₂), 5.71 (s, 1H, CH-pyran), 6.26 (s, 1H, CH-pyridine), 7.26–7.53 (m, 5H, C₆H₅), 8.40 (s, 1H, OH). MS m/z (%): 387 [$M^+ + 2$] (32.13), 386 [$M^+ + 1$] (26.38), 385 [M^+] (15.59), 384 [$M^+ - 1$] (13.19), 383 [$M^+ - 2$] (19.66), 346

(100.00). Anal. Calcd for $C_{23}H_{19}N_3O_3$ (385.42): C, 71.67; H, 4.97; N, 10.90. Found: C, 71.76; H, 5.24; N, 11.02.

2. 1. 10. Synthesis of 2-Cyano-*N*-(3-cyano-4-phenyl-5,6,7,8-tetrahydro-4*H*-chromen-2-yl)-3-ethoxyacrylamide (10)

To a mixture of equimolar amounts of **6a** (3.19 g, 0.01 mol) in acetic acid (25 mL), triethyl orthoformate (1.45 g, 0.01 mol) was added. The chemical reaction was refluxed for 1 h and then added into a beaker containing a mixture of ice and water. The resultant product was filtered and then recrystallized from acetic acid.

Yellow powder, yield: 2.25 g (60%), m.p. 172–175 °C. IR (ν , cm^{-1}): 3427–3245 (NH), 3100 (CH-aromatic), 2934, 2864 (CH₂, CH₃), 2260–2199 (2CN), 1701 (C=O), 1638–1490 (C=C). ¹H NMR (δ , ppm): 1.05–1.10 (t, 3H, CH₃), 1.50–1.99 (m, 4H, 2CH₂), 2.06–2.27 (m, 4H, 2CH₂), 4.22–4.24 (q, 2H, CH₂), 5.80 (s, 1H, CH-pyran), 6.80–7.53 (m, 6H, C₆H₅, CH), 11.10 (s, 1H, NH). MS m/z (%): 377 [$M^+ + 2$] (10.63), 376 [$M^+ + 1$] (7.20), 375 [M^+] (12.60), 374 [$M^+ - 1$] (6.39), 373 [$M^+ - 2$] (7.67), 329 (100.00), 77 [C₆H₅]⁺ (21.72). Anal. Calcd for $C_{22}H_{21}N_3O_3$ (375.42): C, 70.38; H, 5.64; N, 12.79. Found: C, 70.62; H, 5.82; N, 12.96.

2. 1. 11. Synthesis of 2-Cyano-*N*-(3-cyano-phenyl-5,6,7,8-tetrahydro-4*H*-chromen-2-yl)-3-(phenyl amino) acrylamide (11)

To a solution of compound **10** (3.75 g, 0.01 mol) in absolute ethanol (25 mL), aniline (0.93 g, 0.01 mol) was added. The reaction was refluxed for 3 h and then poured onto an ice/water mixture with a few drops of HCl added. The obtained product was filtered and recrystallized from ethanol.

Yellow crystals, yield: 2.78 g (65%), m.p. 210–213 °C. IR (ν , cm^{-1}): 3422–3244 (2NH), 3061 (CH-aromatic), 2934–2864 (CH, CH₂), 2260, 2211 (2CN), 1696 (C=O), 1638, 1490 (C=C). ¹H NMR (δ , ppm): 1.56–1.74 (m, 4H, 2CH₂), 2.13–2.17 (m, 4H, 2CH₂), 5.80 (s, 1H, CH-pyran), 6.96–7.50 (m, 11H, 2C₆H₅, CH), 8.50, 10.10 (2s, 2H, 2NH). MS m/z (%): 424 [$M^+ + 2$] (33.57), 423 [$M^+ + 1$] (20.37), 422 [M^+] (14.63), 273 (100.00), 77 [C₆H₅]⁺ (42.32). Anal. Calcd for $C_{26}H_{22}N_4O_2$ (422.48): C, 73.92; H, 5.25; N, 13.26. Found: C, 74.09; H, 5.29; N, 13.28.

2. 1. 12. General Method for the Preparation of 6-Amino-1-(3-cyano-4-phenyl-5,6,7,8-tetrahydro-4*H*-chromen-2-yl)-2-oxo-1,2-dihydropyridine-3,5-dicarbonitrile derivatives 12a,b

To a solution of **10** (3.75 g, 0.01 mol) in absolute ethanol (25 mL), either malononitrile (0.66 g, 0.01 mol) or ethyl cyanoacetate (1.13 g, 0.01 mol) was added. On the reflux system, the reaction was heated for 3 h. The resultant product was poured onto the ice/water mixture with a few

drops of HCl added. The precipitated products were collected by filtration and then recrystallized from ethanol.

6-Amino-1-(3-cyano-4-phenyl-5,6,7,8-tetrahydro-4*H*-chromen-2-yl)-2-oxo-1,2-dihydropyridine-3,5-dicarbonitrile (12a). Brown crystals, yield: 3.00 g (76%), m.p. 112–115 °C. IR (ν , cm^{-1}): 3442, 3351 (NH₂), 3242 (NH), 3100 (CH-aromatic), 2935, 2865 (CH₂), 2260, 2220, 2199 (3CN), 1699 (C=O), 1638, 1449 (C=C). ¹H NMR (δ , ppm): 1.54–1.74 (m, 4H, 2CH₂), 2.13–2.17 (m, 4H, 2CH₂), 5.80 (s, 1H, CH-pyran), 6.37 (s, 1H, CH-pyridine), 6.95–7.53 (m, 7H, C₆H₅, NH₂). ¹³C NMR (δ , ppm): 21.4, 22.0, 22.4, 26.9, 42.9, 95.7, 115.4, 115.8, 124.2, 127.6, 127.9, 128.5, 128.7, 137.3, 146.9, 150.1, 150.7. MS m/z (%): 397 [$M^+ + 2$] (2.57), 396 [$M^+ + 1$] (2.71), 395 [M^+] (3.46), 394 [$M^+ - 1$] (4.29), 393 [$M^+ - 2$] (10.61), 391 (100.00), 77 [C₆H₅]⁺ (5.32). Anal. Calcd for $C_{23}H_{17}N_5O_2$ (395.41): C, 69.86; H, 4.33; N, 17.71. Found: C, 70.01; H, 4.49; N, 17.98.

6-Amino-1-(3-cyano-4-phenyl-5,6,7,8-tetrahydro-4*H*-chromen-2-yl)-2-oxo-1,2-dihydropyridine-3,5-dicarbonitrile (12b). Yellowish brown crystals, yield: 3.75 g (95%), m.p. 87–90 °C. IR (ν , cm^{-1}): 3419–3240 (OH), 3100 (CH-aromatic), 2935, 2864 (CH₂), 2260, 2240, 2209 (3CN), 1696 (C=O), 1640, 1448 (C=C). ¹H NMR (δ , ppm): 1.54–1.73 (m, 4H, 2CH₂), 2.13–2.17 (m, 4H, 2CH₂), 5.70 (s, 1H, CH-pyran), 6.36 (s, 1H, CH-pyridine), 7.20–7.52 (m, 5H, C₆H₅), 8.40 (s, 1H, OH). MS m/z (%): 397 [$M^+ + 1$] (4.82), 396 [M^+] (8.26), 300 (100.00), 77 [C₆H₅]⁺ (13.12). Anal. Calcd for $C_{23}H_{16}N_4O_3$ (396.40): C, 69.69; H, 4.07; N, 14.13. Found: C, 69.93; H, 4.29; N, 14.39.

2. 2. Biological Evaluations

2. 2. 1. Materials and Methods

- Gibco Invitrogen Company (Scotland, UK): Provide fetal bovine serum (FBS) and L-glutamine.
- Cambrex (New Jersey, USA): Provide RPMI-1640 medium
- Sigma Chemical Company. (Saint Louis, MO, USA): Provide dimethyl sulfoxide (DMSO), foretinib, penicillin, streptomycin, and sulforhodamine B (SRB).

2. 2. 2. Samples

Tumor Cell Proliferation Assay: The effects of **1a,b** to **12a,b** on the *in vitro* proliferation of human cancer cell lines were tested. The method were obtained from the National Cancer Institute (NCI, USA) in the *In vitro Anticancer Drug Discovery Screen* using the protein-binding dye sulforhodamine B to assess cell proliferation.

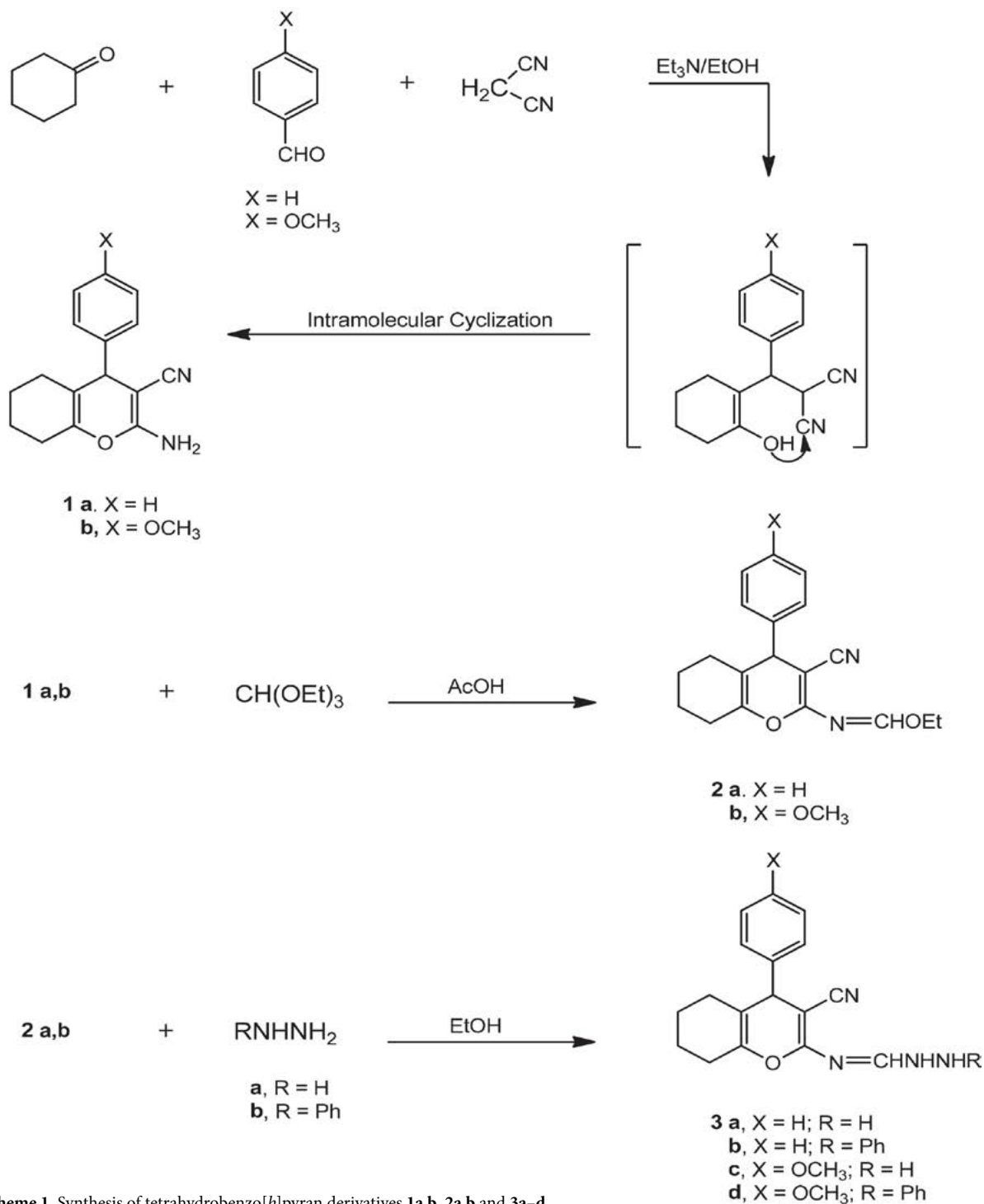
2. 2. 3. Cell Cultures

The three human cancer cell lines were A-549 (lung carcinoma), HC-29 (colorectal adenocarcinoma),

and MKN-45 (gastric cancer). The later cells were obtained from the National Cancer Institute (NCI), Cairo, Egypt.

The cell cultures were prepared as the following: They were grown as monolayers and plated in RPMI 1640 medium supplemented with 5% heat-inactivated FBS, 2 mM glutamine and antibiotics (penicillin 100 U/mL and streptomycin 100 µg/mL) in a humidified atmosphere at

37 °C. Permanently maintained at 5% CO₂, exponentially growing cells were plated at 0.75×10^4 cells/mL followed by 1.5×10^5 cells/mL for MCF-7 and SF-268 and 0.75×10^4 cells/mL for three-cell line and maintained the incubation for 48 h. The effect of carrier solvent (DMSO) on the growth of these cell lines was examined in all experiments by exposing untreated control cells to the highest concentration of DMSO used in each assay (0.5%).



Scheme 1. Synthesis of tetrahydrobenzo[*b*]pyran derivatives **1a,b**, **2a,b** and **3a–d**.

3. Results and Discussion

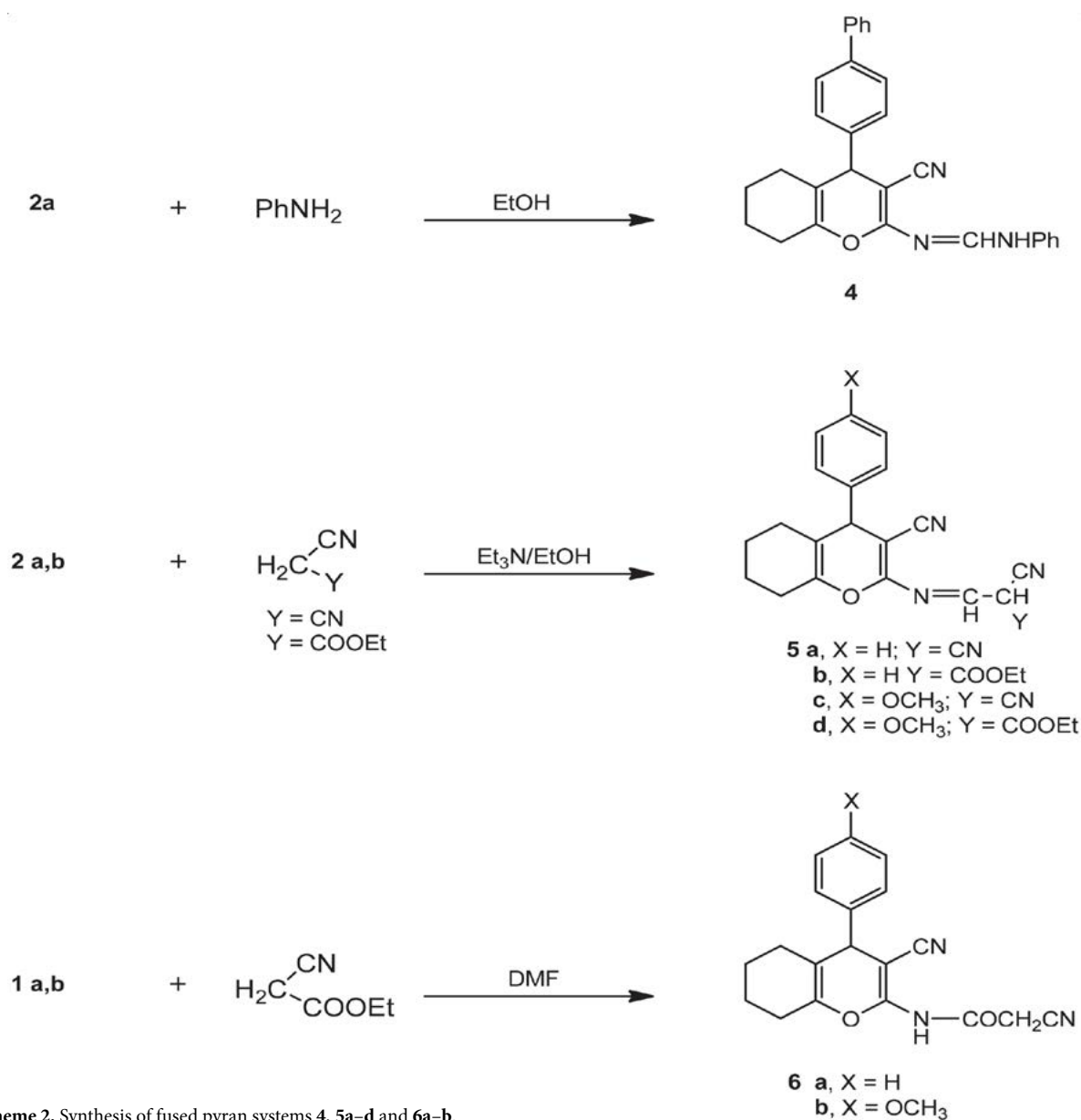
3. 1. Chemistry

The reaction of cyclohexanone with malononitrile and either of benzaldehyde or 4-methoxybenzaldehyde gave the pyran derivatives **1a** and **1b**,³¹ respectively (Scheme 1). According to the data obtained from the spectroscopic analysis methods, the structures of the resultant products were indicated. The obtained structures were confirmed by ¹H NMR and IR spectroscopy. Thus, for ¹H NMR spectrum of the compound **1a**, a multiplet at δ 1.66–1.71 ppm for 2CH₂ cyclohexene, a multiplet at 2.16–2.81 ppm for the other 2CH₂ of cyclohexene ring and a singlet at 5.73 ppm for CH pyran were observed. Moreover, the presence of a multiplet at δ 7.14–7.89 ppm for phenyl moiety and NH₂ group and cyano group in the IR spectrum in

the range of 2209 cm⁻¹ supported the proposed structure. Besides, for compound **1b**, the presence of the methoxy group in the ¹H NMR in the range of 3.87 ppm confirmed its structure.

The reaction of compound **1a** or **1b** with triethylorthoformate in acetic acid gave the 2-*N*-ethoxymethino derivatives **2a** and **2b**, respectively (Scheme 1). The disappearance of the NH₂ group signal in the ¹H NMR and IR spectrum of the compounds **2a** and **2b**, confirmed the structures. The appearance of the ethoxy group in the range between 1.10–1.20 ppm for the CH₃ group and 4.25–4.30 ppm for the CH₂ confirmed the structures.

Previously obtained products **2a** or **2b** were reacted with either of hydrazine hydrate or phenylhydrazine to give hydrazino derivatives **3a–d**, respectively (Scheme 1). The ¹H NMR spectrum of **3a** indicated a multiplet at δ



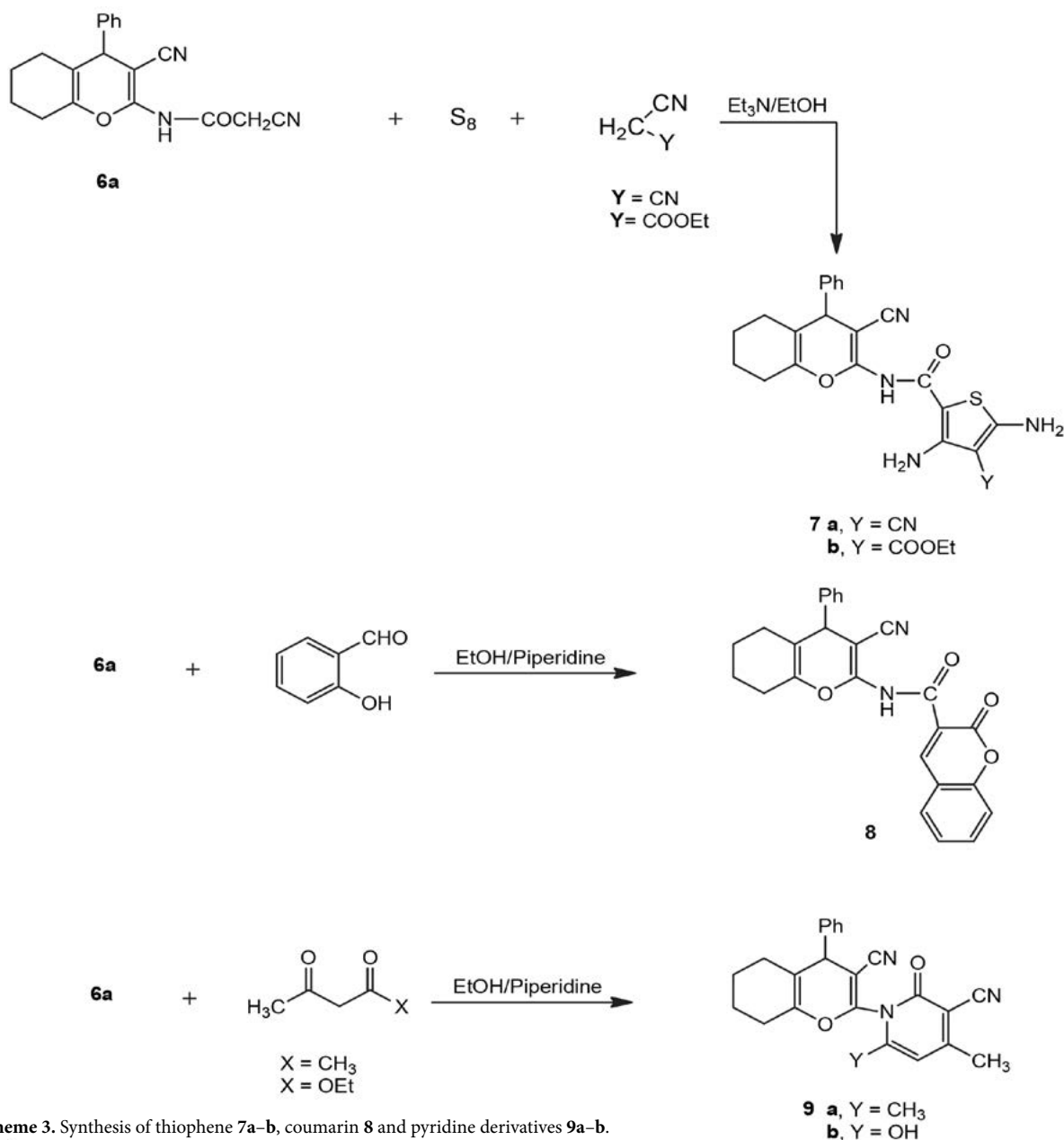
Scheme 2. Synthesis of fused pyran systems **4**, **5a–d** and **6a–b**.

1.58–1.74 ppm for 2CH₂ cyclohexene moiety, a multiplet at δ 2.13–2.15 ppm for the other 2CH₂, a singlet at δ 6.40 ppm for CH-pyran ring, a singlet at δ 6.96 ppm for CH group, a multiplet at δ 7.20–7.54 ppm for NH₂ group and phenyl ring. Moreover, the appearance of the singlet at δ 10.80 ppm for NH group elucidated the chemical structure of compound **3a**.

Compound **2a** upon reaction with aniline in ethanol gave the aniline derivative **4** (Scheme 2). The reaction of compound **2a** or **2b** with either of malononitrile or ethyl cyanoacetate gave 2-*N*-alkyl products **5a–d**, respectively (Scheme 2). The structures of these products were confirmed by the presence of the ethoxy groups in the ¹H NMR spectra for compounds **5b** and **5d** in the range at δ 1.06–1.21 ppm for CH₃ group and 4.19–4.24 ppm for CH₂

group. On the other hand, the appearance in the IR spectra of compounds **5a** and **5c** of the three cyano moieties in the range at ν 2190–2260 cm⁻¹ elucidated the proposed structures.

Compounds **1a** and **1b** showed interesting reactivity towards amide formation. Thus, the reaction of either of compound **1a** or **1b** with ethyl cyanoacetate gave the cyanoacetamide derivatives **6a** and **6b**, respectively (Scheme 2). The analytical and spectral data of **6a** and **6b** elucidated their structures. Thus, the ¹H NMR of **6a** contains a multiplet at δ 1.45–1.49 ppm for 2CH₂ cyclohexene ring, a multiplet at δ 2.16–2.20 ppm for the second 2CH₂ cyclohexene moiety, a singlet at δ 5.73 ppm CH-pyran ring, a multiplet at δ 7.33–7.43 ppm for phenyl ring and a singlet at δ 10.01 ppm for NH group; also spectrum of **6b** revealed a multi-



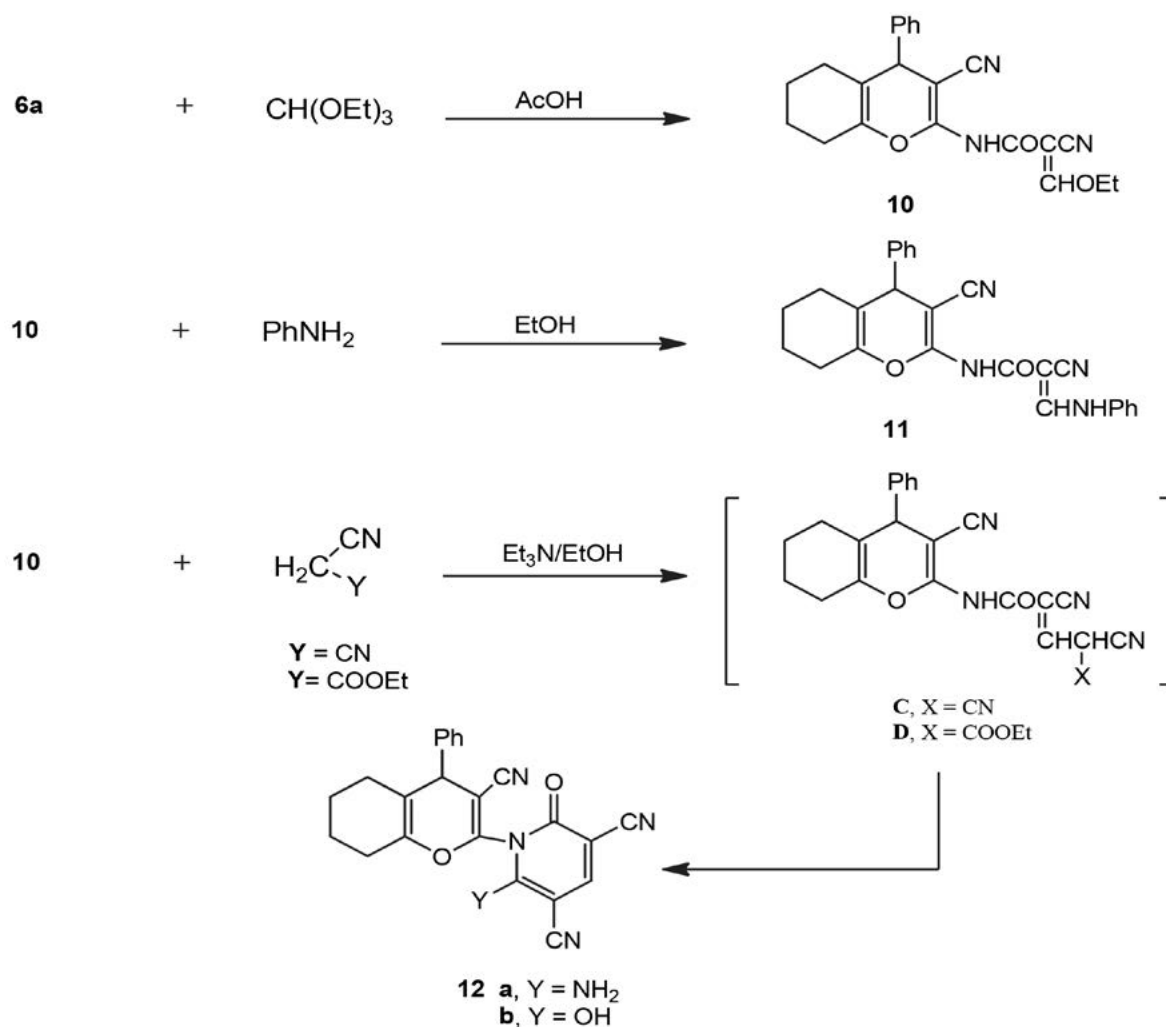
Scheme 3. Synthesis of thiophene **7a–b**, coumarin **8** and pyridine derivatives **9a–b**.

plet at δ 1.66–1.71 ppm for 2CH_2 groups, a multiplet at δ 2.10–2.20 ppm for the other 2CH_2 cyclohexene moiety, a singlet at δ 3.73 ppm for OCH_3 group, a singlet at δ 4.34 ppm for CH_2 group, a singlet at δ 5.70 ppm for CH -pyran ring, a multiplet at δ 6.91–7.90 ppm for C_6H_4 moiety and a singlet at δ 8.31 ppm for NH group.

Compound **6a** underwent the Gewald's thiophene synthesis^{32–34} by the reaction of either of malononitrile or ethyl cyanoacetate with elemental sulfur in ethanol and triethylamine to give the thiophene derivatives **7a** and **7b**, respectively (Scheme 3). The formation of the latter products was confirmed by the ^1H NMR spectrum via the presence of the two NH_2 moieties in the range between δ 7.19–7.63 ppm with the phenyl groups. In addition, the IR spectrum of compounds **7a** and **7b** showed two bands in the range between ν 3417–3340 cm^{-1} due to the presence of the two NH_2 groups. Moreover, compound **6a** upon the reaction with salicylaldehyde in ethanol and piperidine gave the coumarin derivative **8** (Scheme 3). Mass spectrum of **8** exhibited molecular ion at m/z 424 corresponding to the molecular formula $\text{C}_{26}\text{H}_{20}\text{N}_2\text{O}_4$, which confirmed the assign-

ment for coumarin structure **8**. The other resulting peaks which confirmed the molecular ion peak were observed at m/z 426, 425, 423, 422, 77 and 76 which correspond to $[\text{M}^+ + 2]$, $[\text{M}^+ + 1]$, $[\text{M}^+ - 1]$, $[\text{M}^+ - 2]$, $[\text{C}_6\text{H}_5]^+$ and $[\text{C}_6\text{H}_4]^+$, respectively. In addition, the structure of **8** was elucidated via the ^{13}C NMR which confirmed the presence of two carbonyl groups at δ 158.7 and 163.2 ppm.

The reactivity of compound **6a** towards 1,3-dicarbonyl compounds was studied to give bioactive pyridine derivatives. Compound **6a** reacted with either of acetylacetone or ethyl acetoacetate to afford the pyridine derivatives **9a** and **9b**, respectively (Scheme 3). The structures of the latter products were confirmed according to the results of the spectral data. Thus, the ^{13}C NMR spectrum of **9a** showed the carbonyl carbon signal at δ 166.00 ppm. Moreover, the mass spectrum of **9b** exhibited a molecular ion peak $[\text{M}^+]$ at m/z 385 corresponding to the molecular formula $\text{C}_{23}\text{H}_{19}\text{N}_3\text{O}_3$. Many other peaks were observed to confirm the final chemical structure of **9b**, such as the peak at m/z 387, 386, 384 and 383 which corresponds to $[\text{M}^+ + 2]$, $[\text{M}^+ + 1]$, $[\text{M}^+ - 1]$ and $[\text{M}^+ - 2]$, respectively.



Scheme 4. Synthesis of tetrahydrobenzo[*b*]pyran derivatives **10**, **11** and pyridines **12a,b**.

Compound **6a** upon the reaction with ethyl orthoformate gave ethoxyvinyl product **10** which reacted with aniline to give the aniline derivative **11** (Scheme 4). The structure of **10** was confirmed based on analytical and spectral data. Thus, the IR spectrum revealed absorption bands at ν 1701 cm^{-1} corresponding to C=O. ^1H NMR showed a triplet in the range at δ 1.05–1.10 ppm for the CH_3 group and quartet in the range at δ 4.22–4.24 ppm for the CH_2 moiety which confirmed the presence of the ethyl group in compound **10**. Mass spectra of compounds **10** and **11** revealed molecular ion peaks at m/z 375 and 422, respectively, corresponding to the respective molecular formulas $\text{C}_{22}\text{H}_{21}\text{N}_3\text{O}_3$ and $\text{C}_{26}\text{H}_{22}\text{N}_4\text{O}_2$. Compound **10** was reacted with either of malononitrile or ethyl cyanoacetate in ethanol under reflux to give pyridine derivatives **12a** and **12b**, respectively (Scheme 4). The latter products were formed through the intermediate acyclic products **C** and **D**, respectively. Compounds **12a,b** were confirmed; thus, the ^1H NMR spectrum of **12a** showed a multiplet at δ 1.54–1.74 ppm for 2CH_2 , a multiplet at δ 2.13–2.17 ppm for the other 2CH_2 groups, a singlet at δ 6.37 ppm for CH-pyridine ring, a singlet at δ 5.80 ppm for CH-pyran moiety and a multiplet at δ 6.95–7.53 ppm for NH_2 group and C_6H_5 moiety. In addition, the mass spectrum of **14b** showed molecular ion peak $[\text{M}^+]$ 396 corresponding to its molecular formula $\text{C}_{23}\text{H}_{16}\text{N}_4\text{O}_3$.

3. 2. Biological Activity Evaluations

3. 2. 1. Structure Activity Relationship

Table 1 demonstrates the cytotoxicity of the prepared products on the three cancer cell lines comparing compounds **1a** and **1b**, where compound **1b** has more potency than compound **1a** due to the 4-methoxyphenyl group present in compound **1b**. The same also appears in compound **2b** which has higher cytotoxicity than **2a**. By comparing compound **3a–d**, it can be noticed that compound **3b** has the highest cytotoxic effect among the other compounds **3**. Moreover, in the case of the pyran compounds **5a–d**, compound **5b** with the ethoxy carbonyl group has the highest potency within the four compounds; reaction of compounds **1a** and **1b** with ethyl cyanoacetate gave compounds **6a** and **6b**. Compound **6b** with the 4-methoxyaryl group demonstrated higher potency than compound **6a**. Reaction of compound **6a** with ethyl orthoformate gave the ethoxy metheno derivative **10** possessing moderate cytotoxicity. Besides, compound **11** obtained from the reaction of **10** with aniline has shown the same moderate cytotoxicity.

Comparing compounds **7a** and **7b** explains that compound **7a** with the electronegative cyano group exhibited higher potency than **7b** with the ester group. The coumarine derivative **8** shows a high potency. The pyridine derivatives **9a** and **9b** showed similar cytotoxicity. The cytotoxic effect for the compounds **12a** and **12b** represents moderate activity, but compound **12b** showed a higher ef-

fect than **12a** especially for the A-549 and MKN-45 cell lines. The latter activity is attributed to the presence of the hydroxyl group in compound **12b**.

Finally, the presence of the two phenyl rings, methoxy group and coumarin moiety in the compounds **3b**, **6b** and **8**, respectively, were responsible for the highest effect of these compounds among all the other tested compounds.

Table 1. The cytotoxic effect of the prepared products against three cancer cell lines

Compd. Number	[GI ₅₀ (mM)]		
	A-549	HC-29	MKN-45
1a	29.48±5.43	40.69±4.61	48.90±12.53
1b	18.48±1.84	19.54±2.80	11.85±4.75
2a	49.11±10.42	52.2±10.32	36.59±4.80
2b	0.26±0.08	1.69±0.59	0.86±0.04
3a	45.24±6.55	70.2±10.50	64.21±10.33
3b	0.08±0.002	0.09±0.09	0.1±0.01
3c	48.29±6.81	73.2±12.53	69.31±12.59
3d	14.23±1.80	15.80±2.79	12.64±2.55
4	14.70±1.83	18.11±2.82	20.12±4.15
5a	40.63±8.62	45.60 ± 3.51	37.39± 4.21
5b	4.70±1.93	0.1±0.02	0.02±0.005
5c	28.19±6.73	19.26±2.60	22.80±4.76
5d	38.41±6.80	22.59±6.90	29.30±5.70
6a	4.73±1.69	5.80±0.98	2.66±0.39
6b	0.03±0.002	0.06±0.09	0.2±0.01
7a	8.09±2.70	10.39±4.62	8.39±3.77
7b	12.37±2.75	6.19±1.65	8.62±2.63
8	0.08±0.003	1.20±0.22	0.07±0.01
9a	10.69±2.73	12.70±2.84	12.61±3.74
9b	12.69±2.59	14.72±2.80	8.91±3.76
10	8.33±1.75	6.29±1.39	4.28±1.30
11	10.50±2.65	6.08±1.27	14.59±1.19
12a	4.82±0.27	3.79±0.92	10.55±1.76
12b	4.73±1.69	5.80±0.98	2.66±0.39
Foretinib (mM)	0.18±0.09	0.24±0.023	0.021±0.0016

4. Conclusions

The current research describes a practical synthesis method for 24 novel pyran derivatives. The variety of the final products prepared can be attributed to the various ways of possible attacks of chosen reagents on the reactive points in the pyran system. Moreover, anti-cancer activities of all the compounds were examined on three human cancer cell lines. Some of the tested products were shown to be favorable as anti-proliferative agents. The most promising compounds were **3b**, **6b**, and **8** against the three tumor cell lines such A-549 (lung carcinoma), HC-29 (colorectal adenocarcinoma), and MKN-45 (gastric cancer).

Conflict of Interests

The authors do not report any conflicts of interest in this work.

Compliance with Ethical Standards

Any of the author's experiments involving animals or human subjects are not included in this article.

5. References

1. E. Middleton, C. Kandaswami, T. C. Theoharides, *Pharmacol Rev.* **2000**, *52*, 673–751.
2. H. F. Roaiah, S. S. El-Nakkady, W. S. El-Serwy, M. A. A. Ali, A. H. Abd El-Rahman, Z. El-Bazzad, *Nat Sci.* **2010**, *8*, 20–29. DOI:10.7537/marsnsj080710.04
3. V. R. Rao, P. V. Kumar, V. R. Reddy, K. M. Reddy, *Heterocycl. Commun.* **2005**, *11*, 273–284. DOI:10.1515/HC.2005.11.3-4.273
4. M. Grażul, A. Kufelnicki, M. Wozniczka, I.-P. Lorenz, P. Mayer, A. Józwiak, M. Czyz, E. Budzisz, *Polyhedron.* **2012**, *31*, 150–158. DOI:10.1016/j.poly.2011.09.003
5. D. A. Vasselin, A. D. Westwell, C. S. Matthews, T. D. Bradshaw, M. F. Stevens, *J. Med. Chem.* **2006**, *49*, 3973–3981. DOI:10.1021/jm060359j
6. M. M. F. Ismail, H. S. Rateb, M. M. M. Hussein, *Eur. J. Med. Chem.* **2010**, *45*, 3950–3959. DOI:10.1016/j.ejmech.2010.05.050
7. Z.-F. Wang, X.-L. Nai, Y. Xu, F.-H. Pan, F.-S. Tang, Q.-P. Qin, L. Yang, S.-H. Zhang, *Dalton Trans.* **2022**, *51*, 12866–12875. DOI:10.1039/D2DT01929A
8. D. Ashok, K. Pallavi, *Heterocycl. Commun.* **2006**, *12*, 103–106. DOI:10.1111/j.1355-0691.2006.01241_1.x
9. N. Artizzu, L. Bonsignore, G. Loy, A. Calignano, *Farmaco* **1995**, *50*, 853–856.
10. L. Bonsignore, G. Loy, D. Secci, A. Calignano, *Eur. J. Med. Chem.* **1993**, *28*, 517–520. DOI:10.1016/0223-5234(93)90020-F
11. A. Dutta, N. Rahman, J. E. Kumar, J. Rabha, T. Phukan, R. Nongkhlaw, *Synth. Commun.* **2021**, *51*, 263–278. DOI:10.1080/00397911.2020.1825741
12. M. R. P. Heravi, P. Aghamohammadi, E. Vessally, *J. Mol. Struct.* **2022**, *1249*, 131534. DOI:10.1016/j.molstruc.2021.131534
13. J. Li, C.-W. Lv, X.-J. Li; D. Qu, Z. Hou, M. Jia, X.-X. Luo, X. Li, M.-K. Li, *Molecules* **2015**, *20*, 17469–17482. DOI:10.3390/molecules200917469
14. I. E. Bylov, M. V. Vasylyev, Y. V. Bilokin, *Eur. J. Med. Chem.* **1999**, *34*, 997–1001. DOI:10.1016/S0223-5234(99)00119-1
15. A. Nohara, T. Umetani, Y. Sanno, *Tetrahedron* **1974**, *30*, 3553–3561. DOI:10.1016/S0040-4020(01)97034-6
16. M. Biglari, F. Shirini, N. O. Mahmoodi, M. Zabihzadeh, M. Mashhadinezhad, *J. Mol. Struct.* **2020**, *1205*, 127652. DOI:10.1016/j.molstruc.2019.127652
17. H. R. Saadati-Moshtaghin, F. M. Zonoz, *Mater Chem. Phys.* **2017**, *199*, 159–165. DOI:10.1016/j.matchemphys.2017.06.066
18. A. Thongni, P. T. Phanrang, A. Dutta, R. Nongkhlaw, *Synth. Commun.* **2022**, *52*, 43–62. DOI:10.1080/00397911.2021.1998535
19. J. Yang, S. Liu, H. Hu, S. Ren, A. Ying, *Chin. J. Chem. Eng.* **2015**, *23*, 1416–1420. DOI:10.1016/j.cjche.2015.04.020
20. F. Sepehr, S. Allameh, A. Davoodnia, *Ann. Romanian Soc. Cell Biol.* **2021**, *25*, 19067–19072.
21. F. Mohamadpour, *J. Taiwan Inst. Chem. Eng.* **2021**, *129*, 52–63. DOI:10.1016/j.jtice.2021.09.017
22. F. Mohamadpour, *Polycycl. Aromat. Compd.* **2021**, *42*, 7607–7615. DOI:10.1080/10406638.2021.2006244
23. I. Devi, P. J. Bhuyan, *Tetrahedron Lett.* **2004**, *45*, 8625–8627. DOI:10.1016/j.tetlet.2004.09.158
24. J.-T. Li, W.-Z. Xu, L.-C. Yang, T.-S. Li, *Synth. Commun.* **2004**, *34*, 4565–4571. DOI:10.1081/SCC-200043233
25. D. Elhamifar, Z. Ramazani, M. Norouzi, R. Mirbagheri, *J. Colloid Interface Sci.* **2018**, *511*, 392–401. DOI:10.1016/j.jcis.2017.10.013
26. A. E. M. Abdallah, R. M. Mohareb, *Pigm. Resin Technol.* **2019**, *48*, 89–103. DOI:10.1108/PRT-11-2017-0085
27. A. E. M. Abdallah, R. M. Mohareb, E. A. Ahmed, *J. Heterocycl. Chem.* **2019**, *56*, 3017–3029. DOI:10.1002/jhet.3697
28. R. M. Mohareb, E. M. Khalil, A. E. Mayhoub, A. E. M. Abdallah, *J. Heterocycl. Chem.* **2020**, *57*, 1330–1343. DOI:10.1002/jhet.3870
29. A. E. M. Abdallah, R. M. Mohareb, M. H. E. Helal, G. J. Mo-feed, *Acta Chim. Slov.* **2021**, *68*, 604–616. DOI:10.17344/acsi.2020.6446
30. R. M. Mohareb, M. H. E. Helal, S. S. Mohamed, A. E. M. Abdallah, *Anti-Cancer Agents in Med. Chem.* **2022**, *22*, 2327–2339. DOI:10.2174/1871520622666211224102301
31. F. Javadi, R. Tayebee, *Micropor. Mesopor. Mat.* **2016**, *231*, 100–109. DOI:10.1016/j.micromeso.2016.05.025
32. D. Wang, J. Wu, Q. Cui, *Chin. Chem. Lett.* **2014**, *25*, 1591–1594. DOI:10.1016/j.cclet.2014.07.007
33. Y. Han, W.-Q. Tang, C.-G. Yan, *Tetrahedron Lett.* **2014**, *55*, 1441–1443. DOI:10.1016/j.tetlet.2014.01.043
34. V. D. Dyachenko, A. N. Chernega, *Russ. J. Gen. Chem.* **2005**, *75*, 952–960. DOI:10.1007/s11176-005-0351-6

Povzetek

Doslej so bili načrtovani in pripravljani že mnogi novi ciklični piranski sistemi s potencialnimi delovanjem proti raku. Poleg tega piranski sistemi kažejo tudi visoko reaktivnost do mnogih kemijskih reagentov. Pripravili smo 24 produktov in jih preizkusili kot morebitne protirakave učinkovine (v mM območju). Rezultati kažejo, da so spojine **3b**, **6b** in **8** široko učinkovite proti trem rakavim celičnim linijam in sicer A-549 (pljučni karcinom), HC-29 (kolorektalni adenokarcinom) in MKN-45 (rak želodca) in kažejo primerljivo aktivnost glede na standardno referenčno kontrolno spojino foretinib.



Except when otherwise noted, articles in this journal are published under the terms and conditions of the Creative Commons Attribution 4.0 International License

Direct Determination of Kynurenic Acid with HPLC-MS/MS Method in Honey

Anže Pavlin, Matevž Pompe and Drago Kočar*

Department of Chemistry and Biochemistry, Faculty of Chemistry and Chemical Technology, University of Ljubljana, Večna pot 113, SI-1000 Ljubljana, Slovenia

Faculty of Chemistry and Chemical Technology, University of Ljubljana, Slovenia

* Corresponding author: E-mail: drago.kocar@fkkt.uni-lj.si

Received: 02-16-2023

Abstract

Kynurenic acid (KYNA) has been attributed many beneficial properties, such as antioxidant, antiproliferative, anti-inflammatory, and anti-obesogenic, as it is believed to affect metabolism and weight gain. A rapid and simple HPLC-MS/MS method for the determination of kynurenic acid (KYNA) in honey has been developed. HPLC-MS/MS system allowed us to perform the analyzes without any special extraction or treatment of the samples. The study was carried out on different honeys: Chestnut (C), Linden (L), Acacia (A), Spruce (S), Silver Fir (SF), Forest (Fo) and Flower (F). The highest mean concentration, 682 µg/g, was determined for chestnut honey, making it one of the foods with the highest KYNA content.

Keywords: Kynurenic acid, honey, HPLC-MS/MS, SRM

1. Introduction

4-Hydroxyquinoline-2-carboxylic acid (structural formula shown in Figure 1), also known as kynurenic acid (KYNA), is a tryptophan metabolite, a byproduct of the kynurenine metabolic pathway, and was discovered by Liebig in 1853.¹ The kynurenine metabolic pathway is a process of dietary tryptophan metabolism and production of the cofactor nicotinamide adenine dinucleotide (NAD⁺). It is formed directly from kynurenine in a reaction catalyzed by kynurenine aminotransferases.² Studies and analyzes of KYNA have been performed on various samples. It has been detected in samples ranging from honeybee products, various plants, herbs and spices to cells and human and animal tissues and excretions showing anti-convulsant and neuroprotective activity.^{3–15} In this study, the presence of KYNA in food and honeybee products was investigated. KYNA was found in all 37 tested samples of food and honeybee products. The highest concentration of KYNA was obtained from honeybee products' samples, propolis (9.6 nmol/g). Many properties were attributed to it, such as anti-ulcer, anti-inflammatory and anti-proliferation.^{12,16–18} High antioxidant capacity and regulation of bacterial growth have also been observed along with properties of reducing hypermotility and antagonizing ionotropic glutamate receptors.^{15,18–21}

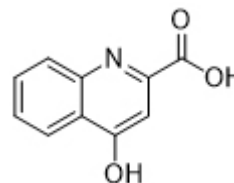


Figure 1: Structural formula of kynurenic acid (KYNA).

It has also been observed that KYNA concentration deviates from normal value if subject suffers from irritable bowel syndrome, Parkinson's disease, Huntington's disease, or multiple sclerosis, resulting in a decrease in concentration, while the opposite phenomenon has been observed in colon lesions such as adenomas or adenocarcinomas and inflammatory bowel disease, in which the concentration of KYNA is increased.^{22–28}

There has also been a suspected association between lower KYNA levels and various types of mood disorders, a phenomenon which occurs primarily in women.²⁹ Consequently tryptophan and its metabolites such as kynurenine and kynurenic acid were investigated in human plasma.³⁰

KYNA plays an important role as antagonist of ionotropic glutamate receptor and an agonist for the orphan G

protein-coupled receptor GPR35, which is found in the gastrointestinal tract and immune cells.^{13,21} Mainly the positive properties in gastrointestinal tract and capability of decreasing hypermotility call for broader investigation of KYNA intake from food.^{18,20} KYNA is found in many herbs, spices, and other remedies used to relieve digestive system problems.^{10,11} For example common nettle or St. John's wort, both KYNA rich substances, are often used as remedies for reducing the symptoms of digestive system diseases.¹⁰ This means that KYNA, among many other beneficial properties, may play an important role in digestion and also weight gain. KYNA has been suggested to be an anti-obesogenic compound which can influence weight gain. The concentration of KYNA has been studied in human breast milk and in baby formula, suggesting that a deficiency of KYNA in baby formula may lead to obesity of infants and children. This was further tested on rats, resulting in lower weight gain in rats postnatally fed with KYNA supplements compared to rats without it.⁷

In general, the methods developed so far require complex preparation of samples. This means mainly homogenization, centrifugation, and various extraction methods (such as Solid Phase Extraction – SPE) which potentially eliminate possible interferences. The method for determination of KYNA in potatoes and flour consisted of homogenization of samples and further centrifugation. KYNA was later extracted from the supernatant by SPE method using a cation exchange resin.⁸ The same SPE method was used to determine KYNA in honey.⁹ However, a RP-SPE cartridge filled with solid phase, was used in NMR and MS study of KYNA in plants.^{4,31} Our goal was to simplify sample preparation.

Selectivity can also be improved in other ways, for example by using a liquid chromatography system coupled to a triple quadrupole mass spectrometry system in Selected Reaction Monitoring (SRM) mode to observe only the molecule of interest.^{30,32,33}

All mentioned positive properties of KYNA and the need to optimize the preparation methods make honey of different botanical sources an interesting target for the study of KYNA content. Our main goal was developing a method avoiding all mentioned complex and not necessary preparations steps which resulted in cheaper and less time-consuming method for analysis of KYNA in honey matrix. Method was developed for HPLC-MS/MS system in SRM mode. An example of the method LC-MS/MS in SRM mode is shown in Figure 2. Newly developed method does not require any centrifugation or special extraction of the analyte and its selectivity does not depend on compounds fluorescence or UV light absorption so no other detector is necessary.^{30,32,34} Analyses were performed on Chestnut (C), Linden (L), Acacia (A), Spruce (S), Silver Fir (SF), Forest (Fo) and Flower (F) honey types.

2. Experimental

Honey

Different honey samples, in total 129, including chestnut (6), linden (14), spruce (2), acacia (20), silver fir (2), flower (59) and forest (26) honey, were obtained from local bee keepers and Medex (Medex d.o.o., Slovenia).

Sample preparation

KYNA (Sigma, USA) standard for calibration curve was dissolved in 0.1% NH₃ (Gram-Mol d.o.o., Republic of Croatia), as were the honey samples. 0.1 g of chestnut honey, 1 g of flower, forest, acacia and linden honey and 3 g of spruce and silver fir honey were separately dissolved in 0.1 % NH₃, mixed thoroughly, and filled to mark in 50 mL volumetric flask. The solution was filtered through nylon filter (pore size 0.45 μm) and transferred to vial.

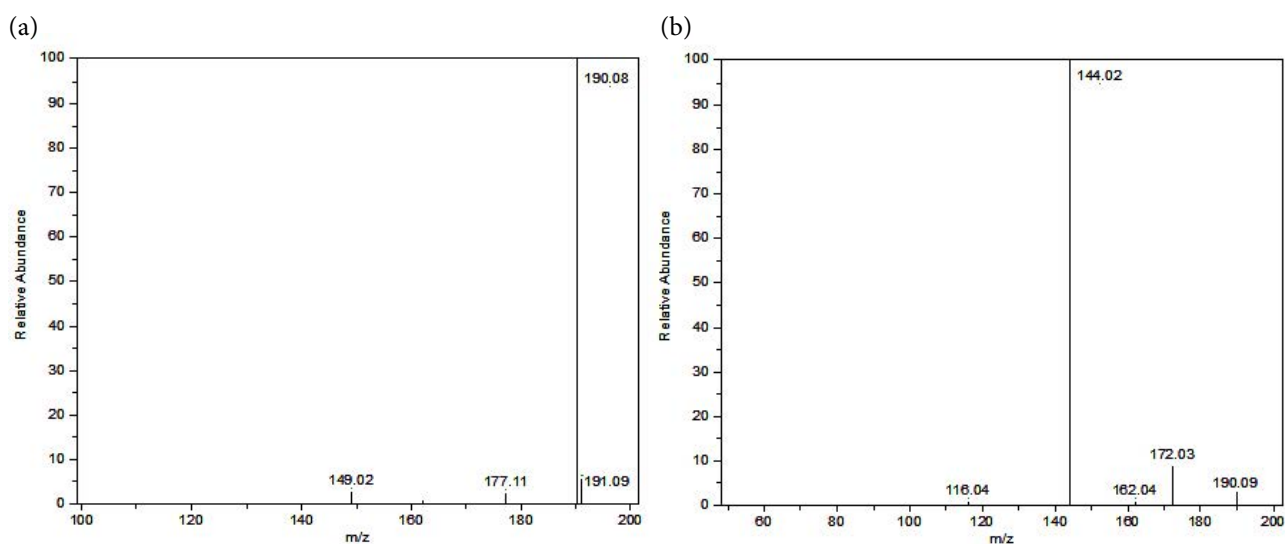


Figure 2: (a) MS spectrum of KYNA precursor ion; (b) MS spectrum of KYNA product ions.

For purposes of recovery determination L 131 and A 15 were prepared the same way and additionally spiked with KYNA standard, 105.5 mg and 9.1 mg, respectively.

HPLC-MS/MS Analysis

Analysis was developed for UHPLC system (Vanquish™ Flex UHPLC, Thermo Scientific™, USA) coupled with H-ESI-MS system (TSQ Quantis™ Triple Quadrupole Mass Spectrometer, Thermo Scientific™, USA).

Chromatographic conditions

Sampler compartment was thermostated at temperature 20 °C. Injection volume was 10 µL. Column (Kinetex® 2.6 µm C18 100 Å, LC Column 150 × 4.6 mm, Phenomenex Inc., USA) was thermostated at temperature 25 °C. Mobile phase A was 0.1% formic acid (Honeywell, USA) in ultrapure MilliQ water (Millipore, USA), mobile phase B was acetonitrile (Fisher Chemical, UK). Gradient method was developed at flow 0.7 mL/min. Elution was used as follows: time 1 min, 10% B; time 8 min, 80% B; time 11 min, 80% B; time 13 min, 10% B; time 18 min, 10% B.

Mass spectrometric conditions

A SRM method for H-ESI-MS was developed. H-ESI-MS was used in positive mode with spray voltage +190 V. Gases were optimized at following values: Sheath gas 8.55 L/min; Auxiliary gas 14.29 L/min; Sweep gas 1.5 L/min. Ion Transfer Tube Temperature was held at 350 °C and Vaporizer Temperature was held at 400 °C. SRM parameters for KYNA were: Precursor ion (m/z) 190.08; Product ion (m/z) 144.02; Collision energy 18 V.^{30,32}

Determination of KYNA

The concentration and content of KYNA in honey was determined using method of calibration curve in concentration range from 0.01 mg/L to 20 mg/L.

3. Results and Discussion

This research was aimed at developing a HPLC-MS/MS method for determination of KYNA in honey matrix with application advantages such as avoiding the use of any special extraction method or other sample pretreatment consistently used laboratory practice so far. 129 honey samples were analyzed. Our study confirmed that KYNA is poorly soluble in acetonitrile and methanol.³⁴ The best MS-compatible solvent was determined to be 0.1 % ammonia; alkaline solvent improves solubility as well as stability of kynurenic acid.

During optimization of MS ion source conditions, we tested different ionization voltages. +190 V turned out

to give the same, if not better, results as some higher voltages, used in experiments described in literature.^{30,32} Easy ionization may be due to free electron pair on nitrogen while formic acid from mobile phase acts like an excellent proton donor.

Calibration curve, LOD, LOQ

Concentrations were determined by a calibration curve. 3 calibration curves, covering the entire linearity range from 0.01 mg/L to 20 mg/L, were used. Equation for calibration curve in range (0.01 – 0.1) mg/L was $y = 2 \cdot 10^7 x + 14246$ with coefficient of determination $R^2 = 0.9987$. Equation for calibration curve in range (0.1–1) mg/L was $y = 2 \cdot 10^7 x + 282943$ with coefficient of determination $R^2 = 0.9994$. Equation for calibration curve in range (1–20) mg/L was $y = 2 \cdot 10^7 + 8 \cdot 10^6$ with coefficient of determination $R^2 = 0.9957$. LOQ and LOD were determined experimentally analyzing low concentration standard solutions. LOQ was determined to be 0.01 mg/L (S/N = 10), while LOD was determined to be 0.001 mg/L (S/N = 3), which would give a KYNA content of 0.5 µg/g and 0.05 µg/g, respectively, given the weight of the honey sample was 1 g.

Repeatability, stability and recovery

Repeatability, shown in Table 1, was investigated for each honey type. Three parallel samples of each representative honey type were prepared. Relative standard deviation (RSD) of the peak area was calculated.

Table 1: Repeatability of each honey type.

SAMPLE	RSD [%]
Chestnut	2.9
Spruce	2.2
Silver Fir	2.8
Linden	1.2
Acacia	2.8
Forest	4.0
Flower	1.0

The stability of three KYNA standard solutions at concentrations of 0.05 mg/L, 0.5 mg/L, and 10 mg/L at 20 °C was studied over a 21-day period. They were all found to be stable over this period with relative standard deviations of instrument response over time of 11.0%, 9.6% and 8.7%, respectively. The stability of the standard solution with a concentration of 0.5 mg/L over time is presented in Figure 3.

For purposes of recovery determination L 131 and A 15 were spiked with KYNA standard. The recoveries for L 131 and A 15 were 106% and 113%, respective-

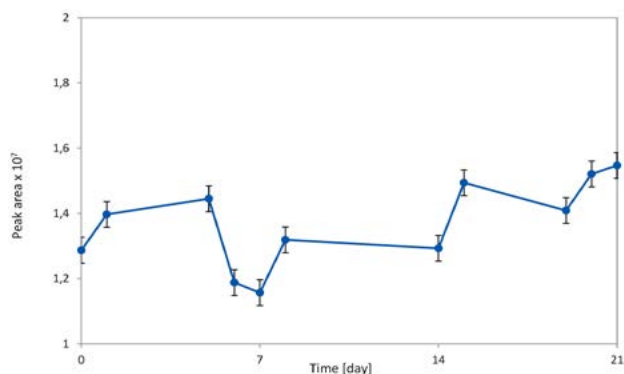


Figure 3: Stability of standard solution with concentration 0.5 mg/L of KYNA. Standard deviations were determined with three consecutive parallel determinations.

L 131 sample and L 131 spiked with KYNA standard can be seen in Figure 4.

Concentration in honey

As shown in Figure 5 concentration of KYNA is the highest in chestnut honey in range (327.8–1015.7) $\mu\text{g/g}$ followed by linden honey in general range (24.6–188.7) $\mu\text{g/g}$. Next, in general order is spruce honey in range (8.0–8.9) $\mu\text{g/g}$ followed by acacia honey in general range (0.7–5.3) $\mu\text{g/g}$. Somewhere in between acacia honey range is silver fir honey with concentration range (1.4–2.2) $\mu\text{g/g}$. Results of spruce, acacia and silver fir honey are presented in Figure 6.

As expected the range of mixed honey samples, such as flower honey and forest honey, varies from low to high concen-

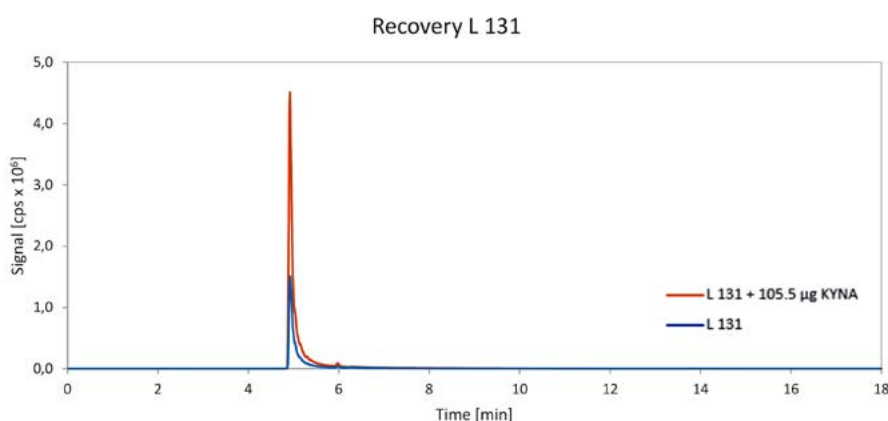


Figure 4: SRM chromatogram of Linden 131 sample and Linden 131 spiked with KYNA standard.

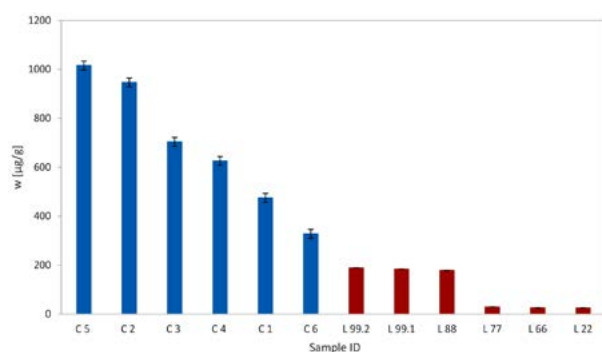


Figure 5: KYNA concentration in all chestnut (C) honeys (samples C 1–6) and three samples of linden (L) honey with maximal concentration (sequence label L 99.2, L 99.1 and L 88) and three samples with minimal concentration (sequence label L 77, L 66 and L 22) of KYNA. Standard deviations were determined on three consecutive parallel determinations.

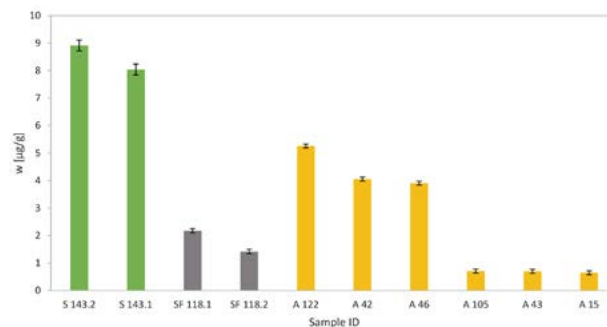


Figure 6: KYNA concentration in both samples of spruce (sequence label S 143.2 and S 143.1) and silver fir (sequence label S 118.1 and S 118.2) honeys and three samples of acacia (A) honey with maximal concentration (sequence label A 122, A 42 and A 46) and three samples with minimal concentration (sequence label A 105, A 43 and A 15) of KYNA. Standard deviations were determined on three consecutive parallel determinations.

ly. These specific samples were selected based on their KYNA content, which was moderate in L 131 (106.2 $\mu\text{g/g}$) and low in A 15 (0.7 $\mu\text{g/g}$), making them perfect for the recovery study. L 131 was spiked with 105.5 μg and A 15 was spiked with 9.1 μg of KYNA. Chromatogram of L

trations with no observable order. Therefore, the concentration of KYNA in forest honey and flower honey samples ranged from (0.8–397.7) $\mu\text{g/g}$ and (1.4–194.2) $\mu\text{g/g}$, respectively.

The content of KYNA is the highest in chestnut honey then followed by linden honey and others. It can

be noticed that concentrations of KYNA in some acacia honey samples are higher than its general range, as the concentration of KYNA in some linden honey samples are lower than its general range which could be explained as presence of some other type of honey which increases or decreases KYNA concentration. Reason for this could be mixing honey with honey of different type, intentional dilution of honey or heterogeneity of honey bee apiary area.^{35,36}

As for flower and forest honey it was expected to have wide concentration range of KYNA. Besides the mentioned reasons, for out of general range concentrations, explanation of this phenomenon, could be wide range of botanical sources of honey as this is not honey from one specific plant. High concentration of KYNA in some forest and flower honey may suggest a greater share of chestnut honey or even linden honey.

Comparison with other KYNA rich substances

Similar study was also conducted on honeys from different countries where it was also evident that chestnut honey has the highest KYNA content. Concentration range was determined to be (103–141) µg/g or in another study (129–601) µg/g for chestnut honey, (0.177–0.391) µg/g for linden honey and (0.093–0.124) µg/g for flower honey.^{9,33} These results somehow overlap with our results for chestnut honey, but are significantly lower in comparison with our results for linden and flower honey. From another set of results containing flower honey it is evident that the determined concentration of KYNA is 0.878 µg/g.³ This may suggest that concentration of KYNA may also be dependent on soil, environment or fertilizer.¹⁰

Concentration of KYNA in honey samples is also high in comparison with other food. In other studies potato was suggested as food with high KYNA content where concentration varies (0.239–3.240) µg/g dry weight which quite coincides with concentration range of KYNA in acacia honeys.⁸ There are also some herbs and spices with high amount of KYNA with basil as one of the most prominent representatives with concentration 14.08 µg/g which positions basil in between linden and spruce honey, but not even close the amount of KYNA in chestnut honey.¹¹

Based on our results we can say that chestnut and linden honey are KYNA rich substances. Since the concentration of KYNA is considerably high in chestnut honey the source of it must be a part of chestnut tree. Research on chestnut tree parts (flower, peeled chestnut, nectar, pollen, ...) suggest that the source of KYNA is nectar of male flowers, since female flowers do not produce nectar.^{9,37} KYNA in chestnut nectar is also observed in another study where the content of honey bee's stomach of honey bee collecting in chestnut wood was investigated.³⁸

4. Conclusions

Our main objective was to develop an optimal method for preparation and analysis of KYNA in honey samples resulting in a fast and simple method with very few steps, avoiding any kind of extraction or other special pretreatment of samples that have been used by most so far. HPLC-MS method, where MS detector was used in SRM mode, was developed. Main focus was the optimization of SRM parameters allowing us to perform a selective analysis of KYNA within the untreated samples (except dilution and filtration). Mainly the spray voltage and collision energy needed to be optimized for better selectivity and flows of sheath, auxiliary and sweep gasses for better limit of detection. Interestingly the spray voltage in positive was determined to be only 190 V, which can be attributed to using the correct mobile phase and other MS parameters. The fragmentation of precursor ion was also investigated, since there is many product ions, and it was determined that the fragmentation to the product ion (*m/z*) 144.02 is the most suitable for selective determination; collision energy for that reaction was optimized and determined at 18 V. Honeys of chestnut and linden botanical species were found to be rich in KYNA, with average contents of 682 mg/g and 85 mg/g, respectively, followed by spruce (8.5 mg/g), acacia (2.2 mg/g), and silver fir (1.8 mg/g) honeys. Forest honey (0.8–397.7 mg/g) and flower honey (1.4–194.2 mg/g) show a very wide range of concentrations, which could be attributed to them being honey of various floral sources or heterogeneity of apiary area; a higher KYNA content could also suggest presence of chestnut or even linden honey. These results could lead chestnut or even linden honey under consideration as food supplement for relieving of digestive problems or influencing digestion and body weight. In addition, the results could as well set values for KYNA content to detect altered honeys.

Acknowledgements

The authors thank Medex d.o.o. for providing honey samples and Mikro+Polo d.o.o., for providing laboratory material. This work was supported by the Slovenian research agency ARRS, grant number P1-153.

5. References

1. J. Liebig, *Justus Liebigs Ann. Chem.* **1853**, 86, 125–126.
DOI:10.1002/jlac.18530860115
2. M. Dehghani, H. Kazemi Shariat Panahi, G. J. Guillemin, *Int. J. Tryptophan Res.* **2019**, 12, 1–10.
DOI:10.1177/1178646919852996
3. M. P. Turski, M. Turska, W. Zgrajka, D. Kuc, W. A. Turski, *Amino Acids*, **2009**, 36, 75–80.
DOI:10.1007/s00726-008-0031-z
4. G. Beretta, E. Caneva, R. M. Facino, *Planta Med.* **2007**, 73,

- 1592–1595. DOI:10.1055/s-2007-993740
5. M. Kaihara, J. M. Price, H. Takahashi, *J. Biol. Chem.* **1956**, 223, 705–708. DOI:10.1016/S0021-9258(18)65070-7
 6. M. Kaihara, J. M. Price, *J. Biol. Chem.* **1962**, 237, 1727–1729. DOI:10.1016/S0021-9258(19)83769-9
 7. P. Milart, P. Paluszkiwicz, P. Dobrowolski, E. Tomaszewska, K. Smolinska, I. Debinska, K. Gawel, K. Walczak, J. Bednarski, M. Turska, M. Raban, T. Kocki, W. A. Turski, *Sci. Rep.* **2019**, 9, 6108–6115. DOI:10.1038/s41598-019-42646-4
 8. M. P. Turski, P. Kamiński, W. Zgrajka, M. Turska, W. A. Turski, *Plant Foods Hum. Nutr.* **2012**, 67, 17–23. DOI:10.1007/s11130-012-0283-3
 9. M. P. Turski, S. Chwil, M. Turska, M. Chwil, T. Kocki, G. Rajtar, J. Palada-Turska, *J. Food Compos. Anal.* **2016**, 48, 67–72. DOI:10.1016/j.jfca.2016.02.003
 10. M. P. Turski, M. Turska, W. Zgrajka, M. Bartnik, T. Kocki, W. A. Turski, *Planta Med.* **2010**, 77, 858–864. DOI:10.1055/s-0030-1250604
 11. M. P. Turski, M. Turska, T. Kocki, W. A. Turski, P. Paluszkiwicz, *J. Chem.* **2015**, 1, 1–6. DOI:10.1155/2015/617571
 12. K. Walczak, W. A. Turski, G. Rajtar, *Amino Acids*, **2014**, 46, 2393–2401. DOI:10.1007/s00726-014-1790-3
 13. J. Wang, N. Simonavicius, X. Wu, G. Swaminath, J. Reagan, H. Tian, L. Ling, *J. Biol. Chem.* **2006**, 281, 22021–22028. DOI:10.1074/jbc.M603503200
 14. W. A. Turski, N. Nakamura, W. P. Todd, B. K. Carpenter, W. O. Whetsell Jr., R. Schwarcz, *Brain Res.* **1988**, 454, 164–169. DOI:10.1016/0006-8993(88)90815-3
 15. R. Lugo-Huitrón, T. Blanco-Ayala, P. Ugalde-Muñoz, P. Carrillo-Mora, J. Pedraza-Chaverri, D. Silva-Adaya, P. D. Maldonado, I. Torres, E. Pinzón, E. Ortiz-Islas, T. López, E. Garcia, B. Pineda, M. Torres-Ramos, A. Santamaría, V. Pérez-De La Cruz, *Neurotoxicol. Teratol.* **2011**, 33, 538–547. DOI:10.1016/j.ntt.2011.07.002
 16. G. B. Glavin, C. Pinsky, *Res. Commun. Chem. Pathol. Pharmacol.* **1989**, 64, 111–119.
 17. G. B. Glavin, R. Bose, C. Pinsky, *Prog. Neuro-Psychopharmacology Biol. Psychiatry*, **1989**, 13, 569–572. DOI:10.1016/0278-5846(89)90148-6
 18. G. Varga, D. Erces, B. Fazekas, M. Fülöp, T. Kovács, J. Kaszaki, F. Fülöp, L. Vécsei, M. Boros, *Neurogastroenterol. Motil.* **2010**, 22, 7–9.
 19. J. Dolecka, T. Urbanik-Sypniewska, B. Skrzydło-Radomańska, J. Parada-Turska, *Pharmacol. Reports*, **2011**, 63, 548–551. DOI:10.1016/S1734-1140(11)70522-9
 20. J. Kaszaki, Z. Palásthy, D. Erczes, A. Rác, C. Torday, G. Varga, L. Vécsei, M. Boros, *Neurogastroenterol. Motil.* **2008**, 20, 53–62.
 21. M. H. S. Mok, A. C. Fricker, A. Weil, J. N. C. Kew, *Neuropharmacology*, **2009**, 57, 242–249. DOI:10.1016/j.neuropharm.2009.06.003
 22. G. Clarke, P. Fitzgerald, J. F. Cryan, E. M. Cassidy, E. M. Quigley, T. G. Dinan, *BMC Gastroenterol.* **2009**, 9, 6–12. DOI:10.1186/1471-230X-9-6
 23. T. Ogawa, W. R. Matson, M. F. Beal, R. H. Myers, E. D. Bird, P. Milbury, S. Saso, *Neurology*, **1992**, 42, 1702 LP – 1706. DOI:10.1212/WNL.42.9.1702
 24. M. F. Beal, W. R. Matson, K. J. Swartz, P. H. Gamache, E. D. Bird, K. J. Neurochem. **1990**, 55, 1327–1339. DOI:10.1111/j.1471-4159.1990.tb03143.x
 25. M. F. Beal, W. R. Matson, E. Storey, P. Milbury, E. A. Ryan, T. Ogawa, E. D. Bird, *J. Neurol. Sci.* **1992**, 108, 80–87. DOI:10.1016/0022-510X(92)90191-M
 26. K. Rejdak, H. Bartosik-Psujek, B. Dobosz, T. Kocki, P. Grieb, G. Giovannoni, W. A. Turski, Z. Stelmasiak, *Neurosci. Lett.* **2002**, 331, 63–65. DOI:10.1016/S0304-3940(02)00710-3
 27. K. Walczak, W. Dąbrowski, E. Langner, W. Zgrajka, J. Piłat, T. Kocki, W. Rzeski, W. A. Turski, *Scand. J. Gastroenterol.* **2011**, 46, 903–912. DOI:10.3109/00365521.2011.579159
 28. C. M. Forrest, S. R. Gould, L. G. Darlington, T. W. Stone, *Adv. Exp. Med. Biol.* **2003**, 527, 395–400. DOI:10.1007/978-1-4615-0135-0_46
 29. T. B. Meier, W. C. Drevets, T. Kent Teague, B. E. Wurfel, S. C. Mueller, J. Bodurka, R. Dantzer, J. Savitz, *Brain. Behav. Immun.* **2018**, 67, 59–64. DOI:10.1016/j.bbi.2017.08.024
 30. L. J. Hu, X. F. Li, J. Q. Hu, X. J. Ni, H. Y. Lu, J. J. Wang, X. N. Huang, C. X. Lin, D. W. Shang, Y. G. Wen, *J. Anal. Toxicol.* **2017**, 41, 37–44. DOI:10.1093/jat/bkw071
 31. G. Beretta, R. Artali, E. Caneva, S. Orlandini, M. Centini, R. M. Facino, *J. Pharm. Biomed. Anal.* **2009**, 50, 432–439. DOI:10.1016/j.jpba.2009.05.029
 32. Q. Tong, J. Song, G. Yang, L. FaN, W. Xiong, J. Fang, *Biomed. Chromatogr.* **2018**, 32. DOI:10.1002/bmc.4156
 33. M. E. Soto, A. M. Ares, J. Bernal, M. J. Nozal, J. L. Bernal, *J. Chromatogr. A*, **2011**, 1218, 7592–7600. DOI:10.1016/j.chroma.2011.06.105
 34. T. Du, T. Cui, H. M. Qiu, N. R. Wang, D. Huang, X. H. Jiang, *J. Pharm. Biomed. Anal.* **2018**, 158, 8–14. DOI:10.1016/j.jpba.2018.05.032
 35. R. Fakhlaei, J. Selamat, A. Khatib, A. F. A. Razi, R. Sukor, S. Ahmad, A. A. Babadi, *Foods*. **2020**, 9, 1538–1558. DOI:10.3390/foods9111538
 36. T. Ždiniaková, C. Lörchner, O. De Rudder, T. Dimitrova, G. Kaklamanos, A. Breidbach, A. Respaldiza, I. Vaz Silva, V. Paiano, F. Ulberth, A. Maquet, *Publications Office of the European Union*, <https://op.europa.eu/en/publication-detail/-/publication/330ee93f-c9fc-11ed-a05c-01aa75ed71a1/language-en>, (accessed: April 16, 2023).
 37. Á. Farkas, E. Zajácz, *Eur. J. Plant Sci. Biotechnol.* **2007**, 1, 125–151.
 38. P. Truchado, I. Martos, L. Bortolotti, A. G. Sabatini, F. Ferreres, F. A. Tomas-Barberan, *J. Agric. Food Chem.* **2009**, 57, 5680–5686. DOI:10.1021/jf900766v

Povzetek

Kinurenski kislini (KYNA) pripisujejo številne koristne lastnosti, kot so antioksidativne, antiproliferativne, protivnetne in anti-obesogene značilnosti. S svojim delovanjem naj bi vplivala na metabolizem in s tem na uravnavanje telesne mase. Razvili smo hitro, enostavno in zanesljivo HPLC-MS/MS metodo za določanje kinurenske kisline (KYNA) v medu. Sistem HPLC-MS/MS nam je omogočil izvedbo analiz brez posebne ekstrakcije ali obdelave vzorcev. V raziskavi smo analizirali med različnih botaničnih vrst, in sicer kostanjev (C), lipov (L), akacijev (A), smrekov (S), hojev (SF), gozdni (Fo) in cvetlični (F) med. Najvišjo povprečno koncentracijo kinurenske kisline (682 µg/g) smo določili v kostanjevem medu, kar ga uvršča med živila z najvišjo vsebnostjo KYNA.



Except when otherwise noted, articles in this journal are published under the terms and conditions of the Creative Commons Attribution 4.0 International License

Scientific paper

Synthesis, SC XRD Based Structure Elucidation, Supramolecular Assembly Exploration Via Hirshfeld Surface Analysis, Computational and QTAIM Study of Functionalized Anilide

Muhammad Nawaz Tahir,¹ Muhammad Ashfaq,^{1*} Akbar Ali,^{2*} Chin Hung Lai,^{3,4} Bojja Rajeshwar Rao,⁵ Khurram Shahzad Munawar^{6,7} and Irshad Ali Shahid¹

¹ Department of Physics, University of Sargodha, Sargodha 40100, Pakistan

² Department of Chemistry, Government College University, Faisalabad, Pakistan

³ Department of Medical Applied Chemistry, Chung Shan Medical University, Taichung 40241, Taiwan

⁴ Department of Medical Education, Chung Shan Medical University Hospital, Taichung 402, Taiwan

⁵ Senior Chemist (Retired), Chemical Division, Kakatiya Thermal Power Project (O&M) Chelpur-506 170, Telangana State, India

⁶ Department of Chemistry, University of Mianwali, 42200, Pakistan

⁷ Department of Chemistry, University of Sargodha, 40100, Pakistan

* Corresponding author: E-mail: ashfaq.muhammad@uos.edu.pk

Received: 03-03-2023

Abstract

The anilide compound named (Z)-4-(2-methoxy-4-nitrophenyl)amino)-4-oxobut-2-enoic acid (MAOA) has been synthesized by the chemical reaction of 2-methoxy-4-nitroaniline and maleic anhydride in ethyl acetate. The synthesized compound was characterized by elemental analysis, FT-IR and UV-Vis spectroscopy, and TGA/DSC technique. Furthermore, the crystal structure was analyzed by the single crystal X-ray diffraction (SC XRD) technique. The supramolecular assembly of MAOA in terms of non-covalent interactions was explored by Hirshfeld surface analysis. Void analysis inferred that MAOA is expected to have good mechanical properties. The crystal packing environment was further investigated by interaction energy between molecular pairs and energy frameworks. Moreover, the result of the gas-phase DFT study showed that there is an intramolecular N–H...O and O–H...O hydrogen bond in MAOA due to the distance between D and A being smaller than the sum of their van der Waals radii. The result of the QTAIM study showed that there should also be an intramolecular CH...O hydrogen bond with a strength of 3.40 kcal/mol in MAOA.

Keywords: Anilide; Crystal structure; Supramolecular assembly; Non-covalent interactions; Gas-phase DFT

1. Introduction

Substituted anilines are very important chemical species that could be used as a starting material for the synthesis of valuable triazole-based medicines like flucanazole, itraconazole, voriconazole, and posaconazole.¹ Another important method of aniline modification is the N-alkylation followed by photochemical radical cyclization reaction for the synthesis of indoles,² as a precursor for the synthesis of the acetaminophen (paracetamol) that

is widely used as a medication to treat the pain and fever,³ and for the photochemical cyclization to accomplish the highly substituted indolines.⁴ Aniline could also be used as a precursor for the synthesis of quinoline which is an important heterocyclic aromatic compound with medicinal and chemical significance.⁵ Acid anhydrides are also valuable chemical building blocks with the speciality of high reactivity that can be used for the synthesis of new chemical architectures that might be used as intermediates or the

final products for utilization in the field of chemical modification specially anilides.

Anilides, mostly produced by the reaction of substituted anilines and anhydrides are well-recognized chemical building blocks in the field of medicinal chemistry because of their broad bioactive spectrum. Anilides such as MAOA having the nitro group and carboxylic acid functionality could be exciting chemical compounds as the hetero atoms might be responsible for non-covalent interactions and could also be used as potential ligands in coordination chemistry. Nitro group containing anilides have shown several biological activities like antidepressants and anticancer,^{6,7} analgesic and antimicrobial,⁷ caspases activators and apoptosis inducers,⁸ and anti-HIV-1 agents⁹ as shown in Figure 1.

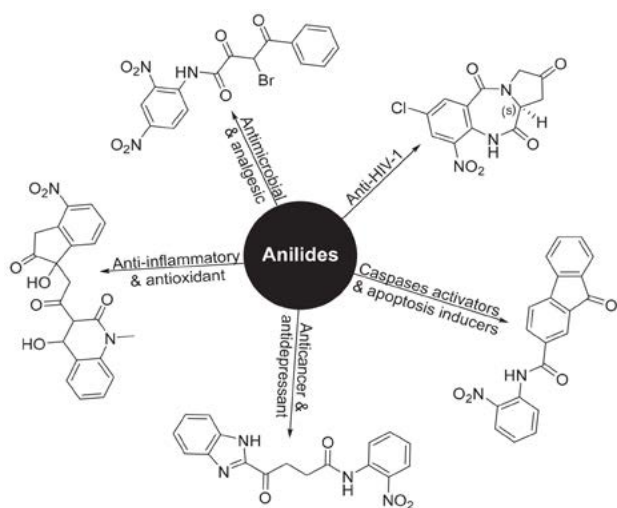


Figure 1. Anilide functionality embedded molecules with their biological potential.

Currently, the synthesis of crystalline organic compounds and their single crystal analysis together with the computational investigation are gaining enormous attention in order to predict various electronic features such as non-linear optical properties,^{10–13} frontier molecular orbitals¹⁴ and non-covalent interactions etc.^{15–17} Maleic anhydride could also be utilized for the N-alkylation of primary amines to produce functionalized anilides. Herein, we are presenting our findings concerning the synthesis, single crystal analysis-based structural investigation and computational exploration of the MAOA.

2. Experimental

2.1. Materials and methods

The 2-methoxy-4-nitroaniline, maleic anhydride, and other reagents used in the current work were of analytical grade and purchased from Sigma-Aldrich, Merck, Daejung, and Alfa Aesar. The combustion analysis for the

estimation of C, H, and N was carried out using a Vario EL elemental analyzer. The melting point of the synthesized compound was measured in an open capillary using the Gallen Kamp electrochemical melting point device. Functional groups present in the sample were analyzed by using Fourier transform infrared spectroscopy from 400 to 4000 cm^{-1} using IRspirit-T equipped with diamond ATR (Shimadzu). The thermal data (TGA/DSC) was collected using Discovery 650 SDT simultaneous thermal analyzer (TA Instruments) with a temperature range from ambient to 400 °C. The heating rate was 10 °C/minute under a 99.999% nitrogen atmosphere with a flow rate of 50 mL/min. The absorption spectra were measured on a CE 7200 double-beam UV-Visible spectrophotometer using DMSO as a solvent. For the sake of thin-layer chromatography, the pre-coated silica was employed to monitor the progress of the chemical reaction and to ensure the purity of the product formed.

2.2. Synthesis of (Z)-4-(2-Methoxy-4-nitroanilino)-4-oxobut-2-enoic acid (MAOA)

Equimolar amounts of 2-methoxy-4-nitroaniline (1.0 mmol, 0.168 g) and maleic anhydride (1.0 mmol, 0.098 g) were dissolved separately in 10 mL of ethyl acetate in 50 mL of beakers. Both solutions were then mixed drop by drop with continuous stirring. After complete addition, the mixture was further stirred for 5 hours. The progress and completion of the reaction and purity of the product were continuously monitored with the help of thin-layer chromatography. The yellow solid product was then obtained by evaporation of solvent *via* a rotary evaporator. Recrystallization of the obtained product was done in methanol to get light yellow crystals (0.213 g) of good quality (Scheme 1).

MAOA: Yield: 80 %; M.P: 171 °C; Color: Light Yellow; Anal. Calc. for $\text{C}_{11}\text{H}_{10}\text{N}_2\text{O}_6$: C, 49.63; H, 3.79; N, 10.52; Found: C, 49.52; H, 3.71; N, 10.55 %; FT-IR (cm^{-1}): 3328 ($\nu\text{N-H}$), 3055 ($\nu\text{CH}_{\text{aromatic}}$), 3001 ($\nu\text{C-H}_{\text{alkene}}$), ~2970 ($\nu\text{C-H}_{\text{aliphatic}}$), 1713 (νCOO), 1615 ($\nu\text{C=O}$), 1582 ($\nu\text{C=C}$), 1552 and 1349 (νNO_2), 1017 ($\nu\text{C-N}$) [Figure S1]; UV-Vis (DMSO); $\lambda_{\text{max}} = 360$ ($\pi-\pi^*$) [Figure S2]; TGA/DSC; 71% weight loss from 130 to 260 °C, Enthalpy (normalized); 1361 J/g, Phase change at 171 °C with heat flow -0.671 W/g, Residue 12.97% [Figure S3].

2.3. X-ray Crystallography Details

Raw data of single crystal by X-ray was collected on Bruker Kappa Apex-II CCD diffractometer with a target made of molybdenum and $\lambda = 0.71073$ Å. APEX-II software was employed for data collection. The structure was solved and refined on SHELXT2014¹⁸ and SHELXL-2019/2,¹⁹ respectively. Refinement of all atoms other than H-atoms was performed by employing aniso-

tropic displacement parameters of atoms whereas refinement of H-atoms was performed with relative isotropic displacement parameters by using the riding model. ORTEP-3,²⁰ PLATON²¹ and Mercury 4.0²² software were employed for the graphical representation of results.

Table 1. Crystal data and refinement parameter for MAOA.

Chemical formula	C ₁₁ H ₁₀ N ₂ O ₆
Molecular weight	266.21
Temperature	296(2) K
Crystal system	Monoclinic
Space group	P2 ₁ /c
<i>a</i> (Å)	3.8664(6)
<i>b</i> (Å)	23.282(4)
<i>c</i> (Å)	11.2114(17)
α (°)	90
β (°)	96.461(9)
γ (°)	90
<i>V</i> (Å ³)	1132.0(3)
<i>Z</i>	4
μ (mm ⁻¹)	0.130
<i>F</i> (000)	552
Reflections collected	8207
Unique reflections	2168
Observed reflections [<i>I</i> > 2 σ (<i>I</i>)]	1388
Data/restraints/parameters	2168/0/174
<i>R</i> _{int}	0.078
<i>S</i>	1.071
<i>R</i> ₁ , <i>wR</i> ₂ [<i>I</i> ≥ 2 σ (<i>I</i>)]	0.0811, 0.1770
<i>R</i> ₁ , <i>wR</i> ₂ (all data)	0.1191, 0.1988

2. 4. Procedure of Hirshfeld Surface Analysis and Interaction Energy Between Molecular Pairs

Hirshfeld surface analysis is a unique way for the exploration of strong as well as weak intermolecular interactions in single crystals. The analysis is done on Crystal Explorer version 21.5.²³ Hirshfeld surfaces providing information about the intermolecular interactions by color coding.²⁴ We further explored the crystal packing environment by finding the interaction energy between molecules. Crystal Explorer version 21.5 is used for interaction energy calculations along with B3LYP/6-31G(d,p) electron density model. The interaction energy is the sum of four

kinds of energies named as electrostatic (*E*_{ele}), polarization (*E*_{pol}), dispersion (*E*_{dis}) and exchange repulsion (*E*_{rep}).²⁵ Electrostatic energy can be attractive or repulsive whereas polarization and dispersion energy are always attractive.

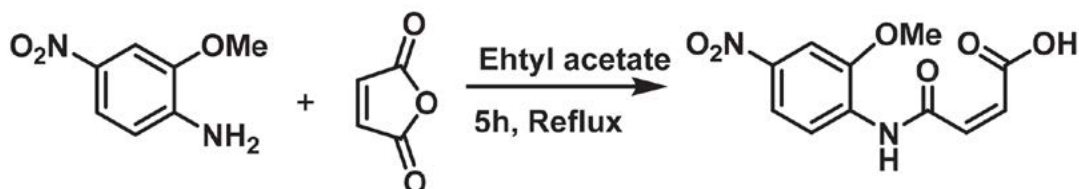
2. 5. Computational Details

2. 5. 1. DFT and NBO Studies

The DFT study is utilized to examine the title compound's gas-phase structures. The DFT calculations were done using the hybrid B3LYP approach, which is a combination of the exact exchange (HF) and Becke functionals, as well as the LYP correlation functional, and is based on Becke's notion.^{26–28} A B3LYP calculation was performed with the basis set 6-311++G**.²⁹ After obtaining the converged geometry, the vibrational harmonic frequencies are calculated at the same theoretical level to ensure that the imaginary frequency number is zero for the saddle point. For the study of the intrinsic electronic properties of the studied compound, the NBO analysis on the studied compound is performed at the same theoretical level. All mentioned calculations are performed by Gaussian 16.³⁰ Moreover, the molecular conformation is acquired by Austin Model method and compared with the molecular conformation by SC XRD. The details and findings of Austin Model method are given in the supplementary information file.

2. 5. 2. QTAIM Study

The quantum theory of atoms in molecules (QTAIM) also called atoms in molecules (AIM) is a model of molecules and condensed matters. In this model, the major objects of molecules and condensed matters, i.e., atoms and bonds are naturally expressed by the distribution function of the observable electronic density of a molecule. The electron density distribution of a molecule is a probability distribution and describes the average distribution of the electronic charge in the field of attraction exerted by the nuclei. According to QTAIM, the molecular structure is revealed by the stationary points and the gradient paths of electron density. The gradient paths of a molecule's electron density are originated and terminated from the stationary points. In this study, the QTAIM analysis is performed using the multiwfn program.³¹



Scheme 1. Synthetic scheme for the (Z)-4-(2-methoxy-4-nitroanilino)-4-oxobut-2-enoic acid (MAOA).

3. Results and Discussion

3. 1. Synthesis and Analysis

A new functionalized anilide (**MAOA**) was synthesized by reacting 2-methoxy-4-nitroaniline with maleic anhydride in ethyl acetate under stirring conditions. The obtained yellow solid product was recrystallized in methanol to get pure crystals suitable for X-ray diffraction analysis and spectroscopic characterizations (Scheme 1).

3. 2. Single Crystal X-ray Diffraction Analysis of MAOA

The Cambridge structure database search confirmed that the crystal structure of **MAOA** is novel. The search provides a lot of crystal structures that have some similar-

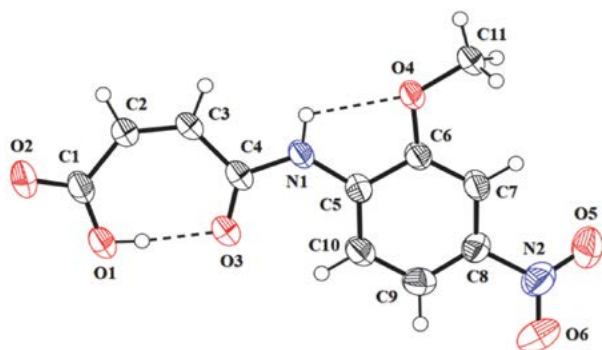


Figure 2. ORTEP diagram of **MAOA** that is drawn at the probability level of 50% with H-atoms are displayed by small circles of arbitrary radii.

ities with the crystal structure of **MAOA**. The crystal structure of **MAOA** is compared with the closely related crystal structures.

The molecular configuration of **MAOA** (Figure 2, Table 2) is stabilized by intramolecular N-H...O and O-H...O bonding. S(5) and S(7) H-bonded loops are formed by the intramolecular N-H...O and O-H...O bonding, respectively.³² The (*Z*)-4-oxobut-2-enoic acid group A (C1–C4/O1–O3) and 2-methoxyanilinic group B (C5–C11/N1/O4) are roughly planar with root mean square (r.m.s.) deviations of 0.0694 and 0.0159 Å, respectively. The corresponding dihedral angle A/B is 6.73(14)°. The nitro group C (N2/O5/O6) is twisted at the dihedral angle of 10.3(4)° with respect to group B. The substitutions on the phenyl ring make the molecule non-planar. The molecules are connected in the form of dimers through N-H...O and C-H...O bonding to form R₂¹(6) loop (Figure 3, Table 2). In both H-bonding, the acceptor O-atom is from the carbonyl O-atom (O2) of the carboxylate group (C1/O1/O2). In C-H...O bonding, the H-bond donor is from group A. The phenyl ring, carbonyl O-atoms (O3/O4) and nitro group are not involved in any intermolecular H-bonding. Due to the intermolecular bonding, a monophasic infinite chain of molecules is formed with a base vector [2 0 1]. Moreover, solid-state packing is further stabilized by π...π stacking. The phenyl rings of the molecule present in the asymmetric unit are involved in off-set π...π stacking interactions with the phenyl rings of the symmetry-related molecules (1 - x, y, z and 1 + x, y, z). Inter-centroid separation of this interaction is 3.866 Å and the ring off-set range is from 1.527 to 3.866 Å as displayed

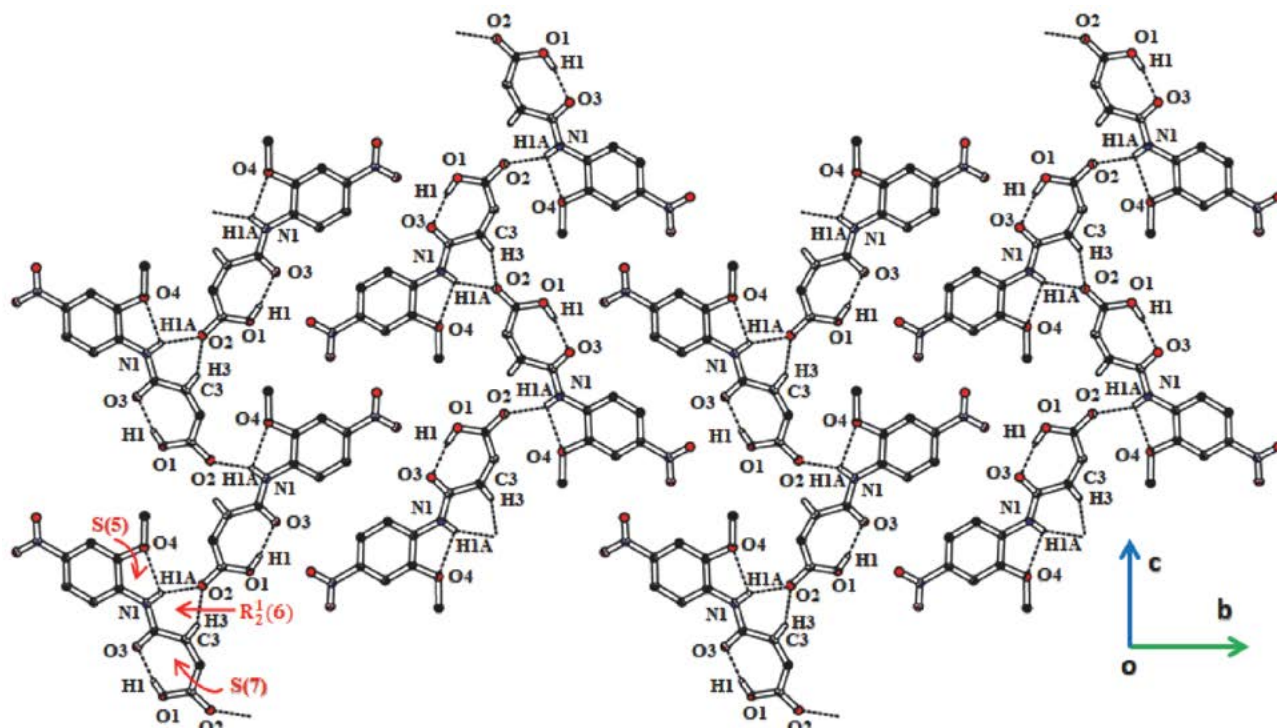


Figure 3. Packing diagram of **MAOA** showing dimerization of molecules.

in Figure 4. The other weak interactions such as C–H... π , N–O... π and C–O... π are not found in the crystal packing of MAOA. The Cambridge structure database search provides more than 50 crystal structures that have some similarity with the crystal structure of MAOA. The close inspection of these structures inferred that 5 out of 50 have close similarity with the crystal structure of MAOA. Two structures with reference code JAYGEW³³ and MNP-MAL01³⁴ have nitro-substituted phenyl rings whereas, the other two structures with reference code LAQJEU³⁵ and SAGFIR³⁶ have disubstituted phenyl rings (nitro and chloro). The molecular configuration of JAYGEW and MNP-MAL01 is stabilized by intramolecular O–H...O and C–H...O bonding along with intermolecular N–H...O and C–H...O bonding. O–H...O intramolecular H-bonding is found in LAQJEU and SAGFIR along with N–H...Cl bond-

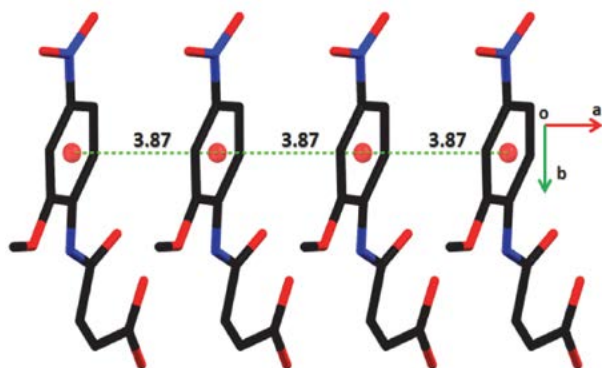


Figure 4. Graphical representation of chain along a-axis that is formed by off-set π ... π stacking interactions. H-atoms are not shown for clarity. Distances are measured in Å.

ing which is present in SAGFIR. π ... π stacking interaction is found in these four selected literature crystal structures.

Table 2. Hydrogen-bond geometry (Å, °) for MAOA.

<i>D</i> –H... <i>A</i>	<i>D</i> –H	H... <i>A</i>	<i>D</i> ... <i>A</i>	$\angle(D-H...A)^\circ$
N1–H1A...O4	0.86	2.22	2.621 (3)	108
O1–H1...O3	0.82	1.74	2.545 (3)	167
N1–H1A...O ² _i	0.86	2.39	3.198 (4)	156
C3–H3...O ² _i	0.93	2.31	3.176 (4)	154

Symmetry codes: (i) $x - 1, -y + \frac{1}{2}, z - \frac{1}{2}$.

3. 3. Hirshfeld Surface Analysis

Hirshfeld surface (HS) mapped over d_{norm} is displayed in Figure 5a. The surface uses three colors, red, white and blue to classify interatomic contacts by their strength. Red and blue spots stand for short and long contacts, respectively. The contacts for which the distance between the interacting atoms is equal to the sum of the van der Waal radii are shown by white spots on the surface. The most dominant interactions in the crystal packing are indicated by red spots on the HS whereas nearly negligible and intermediate intermolecular interactions are indicated by blue and white color, respectively. The red spot around the NH group, one of the CH of group A and the carbonyl O-atom of the carboxylate group indicate that these atoms are involved in short contacts or H-bonding. The H-bonding is represented by the green dotted line in Figure 5a. π ... π stacking interactions can be visualized by plotting HS over the shape index. The presence of consecutive red and

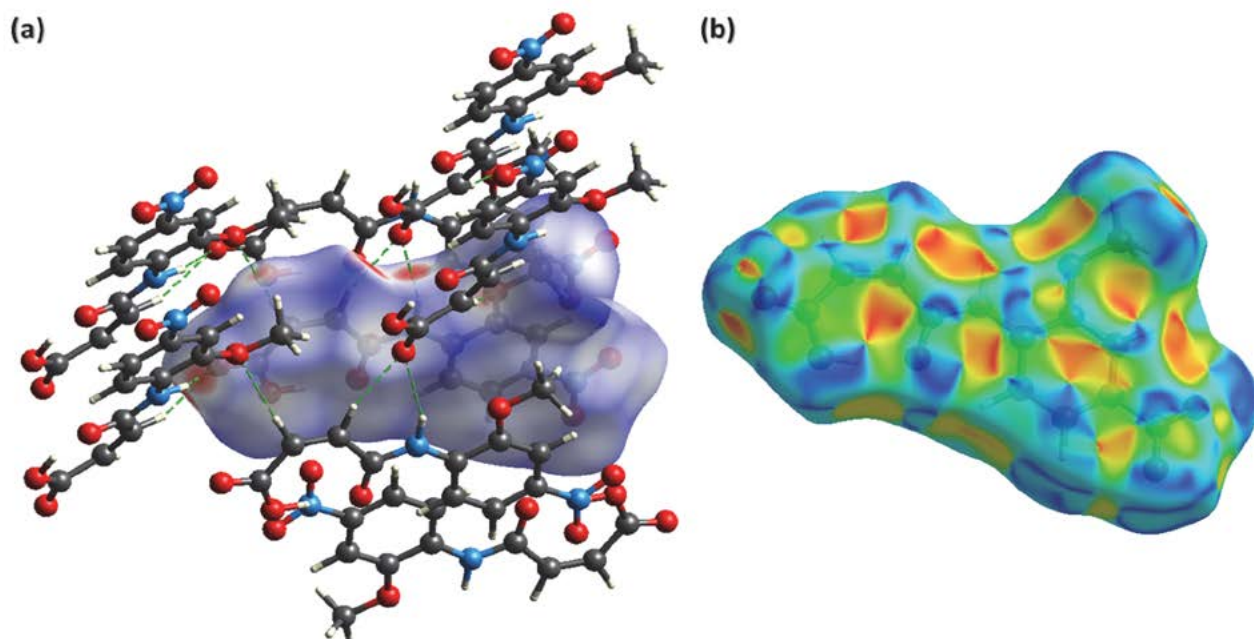


Figure 5. Hirshfeld surface plotted over (a) d_{norm} , (b) shape index.

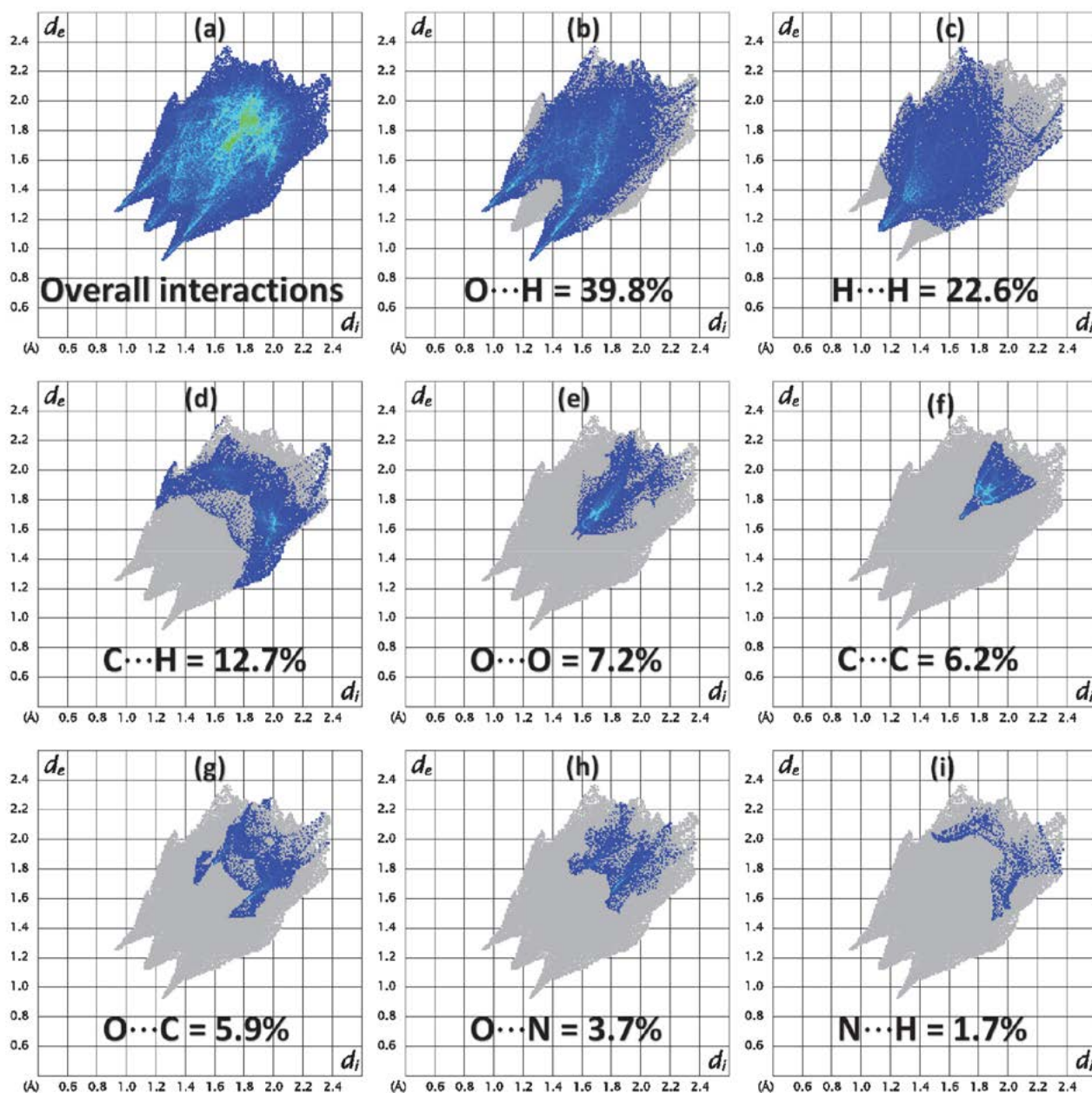


Figure 6. Two-dimensional fingerprint plots in MAOA for (a) overall interactions and (b-i) individual interatomic contacts.

blue triangular-shaped regions around phenyl rings in Figure 5b indicates that stacking interactions are present in MAOA.

The intermolecular interactions can be further explored with the utilization of two-dimensional fingerprint plots which is a key analysis to separately identify and quantify the interatomic contacts.^{37–40} Figure 6a is the 2D fingerprint plot for overall interactions on which short interactions contacts are shown by large spikes. In most crystal structures of organic compounds, H...H contacts are the most significant contributors in the crystal packing but in our case, the O...H contacts are the most significant contributors in the crystal packing with

a percentage contribution of 39.8% (Figure 6b). The other significant interatomic contributors responsible for the overall packing of molecules are H...H, C...H, O...O, C...C and O...C with percentage contributions of 22.6%, 12.7%, 7.2%, 6.2%, and 5.9% (Figure 6c–g), respectively. The enrichment ratio provides the tendency of the pair of chemical species in the single crystal to form crystal-packing interactions. Each pair of chemical species has a unique ability to be involved in the crystal packing. Some pairs have a higher tendency to be involved in the crystal packing interactions than others. The enrichment ratio for a pair (X, Y) is acquired by dividing the proportion of the actual contact by the proportion of the ran-

dom contact calculated theoretically.⁴¹ The results of this study are summarized in Table S1. Although the O...H contacts are the most significant contributors to the crystal packing but the contact which has the highest tendency to form crystal packing is C...C with an enrichment ratio of 2.58. The other higher tendency contacts are O...N and O...H with enrichment ratios of 2.15 and 1.26, respectively. The H...H contacts are not favorable as the enrichment ratio for this contact is less than 1.

For the sake of further exploration of the crystal packing in MAOA, the interaction of an atom of a molecule with all other atoms present in its surrounding is calculated.⁴² Figure 7a gives a quantitative description of the interaction of an atom present inside the HS to the atoms present in the surrounding HS. The H-atoms present inside the HS interact strongly with atoms present in the surrounding HS with a percentage contribution of 46.6%. The quantitative contribution of other such interactions O-ALL, C-ALL and N-ALL is 33.2%, 17% and 3.2%, respectively. Figure 7b gives a quantitative description of the interaction of an atom present outside the HS with all the atoms present inside the HS. The H-atoms present outside the HS interact strongly with atoms present inside the HS with a percentage contribution of 53%. The quantitative contribution of other such interactions ALL-O, ALL-C and ALL-N is 30.6%, 14.1%, and 2.3%, respectively.

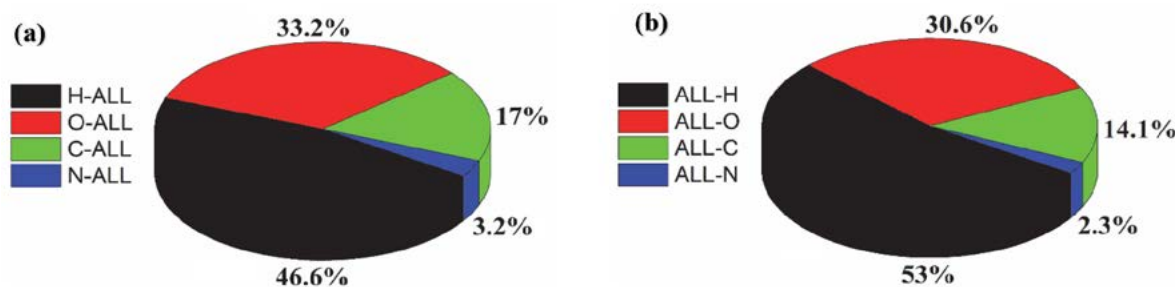


Figure 7. Graphical summary of the (a) Interaction of an atom present inside the HS to atoms present in the surrounding of HS, (b) Interaction of an atom present outside the HS to atoms present in the HS.

Table 3. Intermolecular interaction energies in kJ mol^{-1} calculated at B3LYP/6-31G(d,p) electron density model for MAOA.

Colour	Symmetry codes	N	R	E_{ele}	E_{pol}	E_{dis}	E_{rep}	E_{tot}	%E_attract contribution			
									%E_attract	%E_ele	%E_pol	%E_dis
	(i)	1	6.07	1.9	-1.6	-23.1	10	-12.8	-24.7	0	6.48	93.5
	(ii)	2	3.87	15.8	-6	-62	28	-24.2	-68	0	8.82	91.2
	(i)	1	11.07	-26.9	-5.1	-14.6	18.4	-28.2	-46.6	57.7	10.9	31.3
	(ii)	2	11.44	-14.8	-2.8	-6.7	5	-19.3	-24.3	60.9	11.5	27.6
	(iii)	2	9.91	-30.2	-9.1	-15.9	30.7	-24.5	-55.2	54.7	16.5	28.8
	(i)	1	10.57	-21	-3.9	-17.2	11.3	-30.8	-42.1	49.9	9.26	40.9
	(iii)	2	9.39	-0.8	-5.6	-18.4	13.4	-11.4	-24.8	3.23	22.6	74.2
	(i)	1	6.80	13.8	-2.5	-17.4	7.9	4.2	-19.9	0	12.6	87.4

Symmetry codes: (i) $-x, -y, -z$; (ii) x, y, z ; (iii) $-x, -y + \frac{1}{2}, z + \frac{1}{2}$.

3. 4. Interaction Energy and Energy Frames Analysis

The molecule present in the asymmetric unit is taken as a reference molecule and molecules present in the vicinity of the reference molecule (3.8 Å) are taken in calculations. The results of interaction energy calculations are given in Table 3. The total energy is maximum for the molecular pairs with the center-to-center separation of 11.07 Å that are related to each other by inversion symmetry and for this pair, the hydrogen-bonded contacts are the major controller of the interaction energy as compared to the π ... π stacking interaction. The net attractive energy is maximum for the molecular pairs with the center-to-center separation of 9.91 Å that is related to each other by symmetry ($-x, -y + \frac{1}{2}, z + \frac{1}{2}$). The electrostatic energy is repulsive for two molecular pairs with the center-to-center separation of 3.87 and 6.07 Å. For the molecular pair with an intermolecular distance of 3.87 Å, hydrogen-bonded contacts and π ... π stacking interaction both are the significant controller of the interaction energy. For all other pairs, the hydrogen-bonded contacts are the significant controller of the interaction energy. The strength of a particular type of interaction energy can be visualized by energy frameworks that contained cylinders whose width is directly proportional to the strength of the interaction.⁴³ Figure 8 represents energy frames of the electrostatic and dispersion energy, respectively. Energy

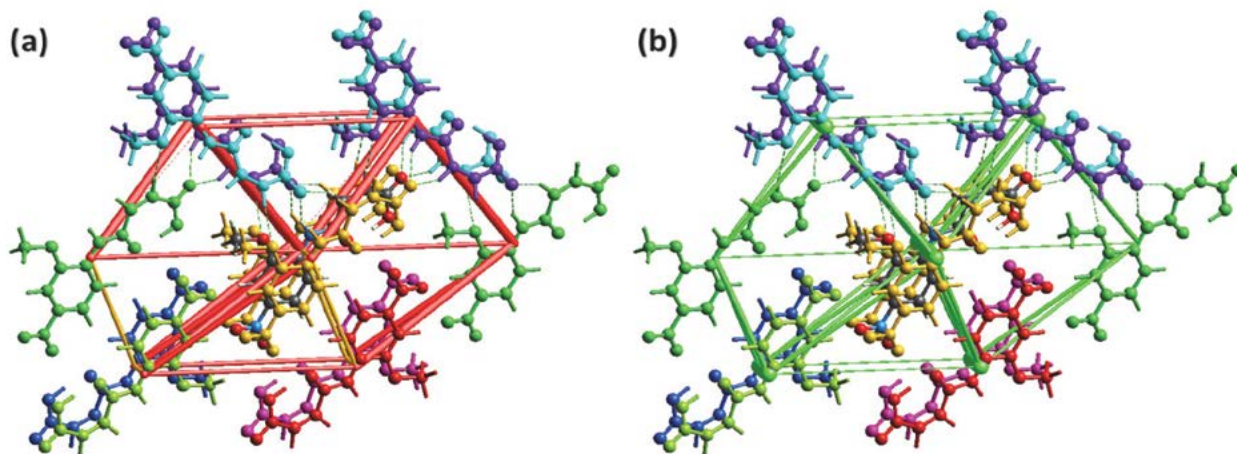


Figure 8. Energy frames for (a) electrostatic energy, (b) dispersion energy.

frames show that the contribution of the dispersion energy in defining the total interaction energy is greater than the contribution of the electrostatic energy.

3. 5. Void Analysis

The percentage of void volume in the unit cell of a compound is the demonstration of how strongly the molecules are packed with each other. Figure S4 is a graphical view of voids that is obtained by summation of electron densities of spherically symmetric atoms at the pertinent nuclear positions.^{44–47} The computations of the crystal void infer that the void volume is of the order of 80.53 Å³. It is found that the calculated void volume of the entitled compound is nearly equal to 7% indicating that the crystal has a high packing factor without a large cavity in the crystal packing.

3. 6. DFT Exploration

A gas-phase DFT study was performed utilizing the B3LYP functional to rationalize the relationship between

the intrinsic electronic properties, the chemical reactivity, and the biological activities of the title compound. The B3LYP-optimized geometry of the title compound is depicted in Figure 9. Moreover, the detailed comparison between the optimized geometry and the crystallographical one could be seen in the Supporting information (Table S2). Accordingly, the B3LYP/6-311+G** theoretical level which was utilized in this study is proved to be a suitable one to investigate anilide derivatives.

According to the frontier molecular orbital theory, one can determine a molecule's nucleophilicity or electrophilicity by focusing on the highest occupied and lowest unoccupied molecular orbitals (HOMO and LUMO).⁴⁸ Instead of considering the total electron density as a nucleophile, evaluate the localization of the HOMO orbital since electrons from this orbital have the best probability of participating in the nucleophilic attack, whereas a site with the lowest empty orbital is a suitable electrophilic site. The title compound's frontier molecular orbital is thus studied further in this work. As depicted in Figure 10, in the studied chemical, the orbital

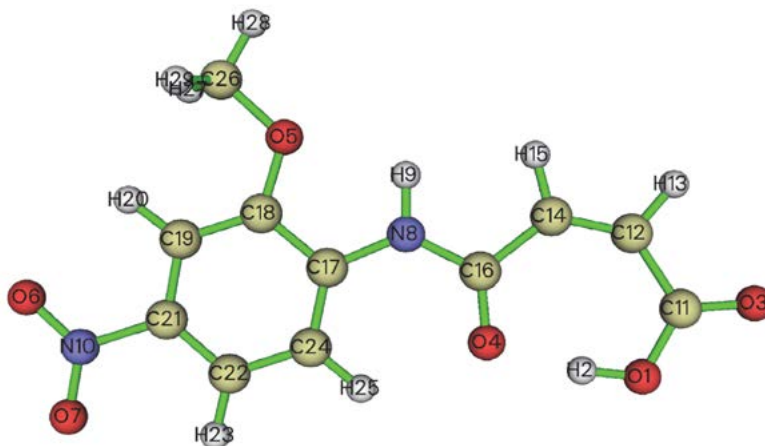


Figure 9. The B3LYP-optimized geometry of the title compound.

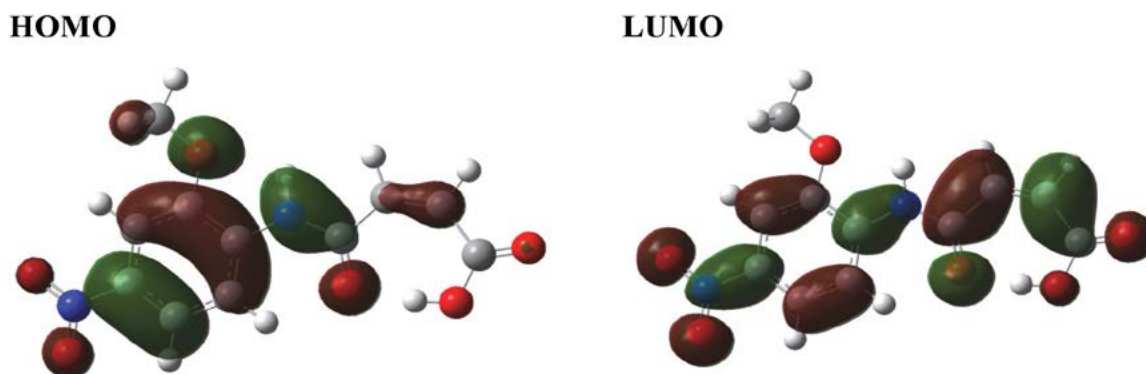


Figure 10. The HOMOs and LUMOs of the studied compound (the isovalue = 0.02 a.u.).

transfer from HOMO to LUMO belongs to a π - π^* transition.

Molecular electrostatic potentials (MEPs) are essential assessments of the strength of interactions between neighboring charges, nuclei, and electrons at a specific point, allowing us to examine charge distribution and charge-related features of molecules. A graphic depiction with different colors is utilized to make the electrostatic potential data easier to understand. Electrophiles may be attracted to red since it reflects the lowest electrostatic potential value. Blue, on the other hand, has the largest electrical potential and may be attractive to nucleophiles. The entire density of the title compound is calculated using the whole density matrix, and the resulting MEP is mapped on its surface. As depicted in Figure 11, the oxygen atoms are the most sensitive site for the attack by an electrophile among the title compound.

3. 6. 1. NBO Analysis

The second-order perturbation theory is used to analyze the relative strength of the intramolecular hydro-

gen bonds in the tested molecule in this study. When a hydrogen bond occurs, there should be an orbital interaction between the nonbonding orbital of the hydrogen-bonded acceptor (n_A) and the antibonding orbital of the H-donor bond (σ_{H-D}^*). As a result of this orbital interaction, the H-D bond's bond strength and bond order should be reduced and decreased, respectively. Therefore, the interaction between a lone pair and the X-H antibonding orbital is summarized in Table 4. It is noteworthy that such orbital interactions with interaction energies larger than 1 kcal/mol in the whole studied chemical are only listed in Table 4. As expected, the oxygen atom has two lone pairs (LPs) whereas the nitrogen atom has only one LP. The two LPs on the oxygen atom are represented as LP, and LP', respectively. The LPs on the oxygen atom of the methoxy group in the title chemical have three orbital interactions by interaction energies larger than 1 kcal/mol with respect to the antibonding orbitals of the C-H bond in the methyl group. However, the LPs on the oxygen atom of the methoxy group in the title chemical don't form orbital interactions by interaction energies larger than 1 kcal/mol (about 0.8 kcal/mol) with respect to the antibonding orbital of the

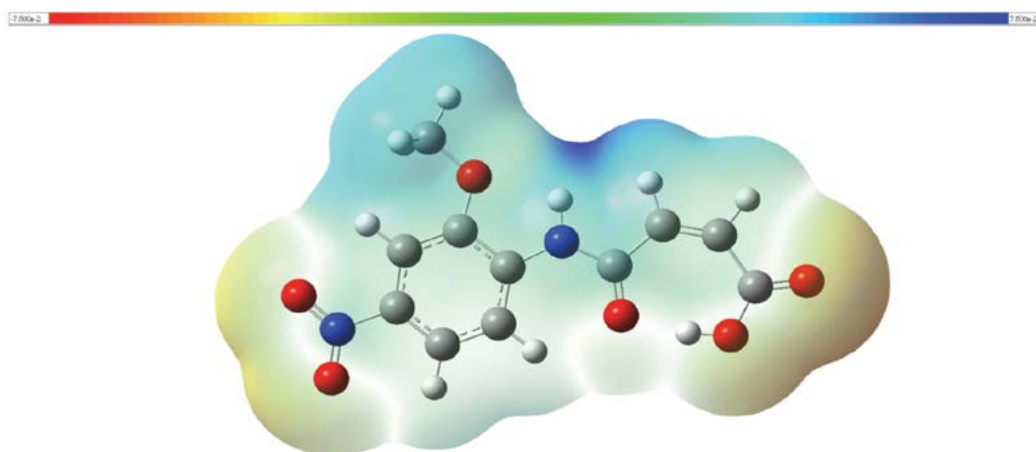


Figure 11. The MEP of the studied compound (the isovalue = 0.0004 a.u.).

Table 4. The NBO results of the title compound.

The type of n_A	The electron configuration of n_A	The orbital interaction	The interaction energy (in kcal/mol) ^b	The occupancy of σ_{H-D}^*	The bond order of σ_{H-D}^c
LP(O4) ^a	s(56.05%) p(43.92%) d(0.02%)	LP(O4)... $\sigma^*(O1-H2)^a$	7.44	0.06057	0.5873
LP'(O4) ^a	s(3.32%) p(96.62%) d(0.06%)	LP'(O4)... $\sigma^*(O1-H2)^a$	25.67	0.06057	0.5873
LP(O5) ^a	s(36.50%) p(63.47%) d(0.03%)	LP(O5)... $\sigma^*(C26-H27)^a$	1.06	0.01534	0.7942
LP(O5) ^a	s(36.50%) p(63.47%) d(0.03%)	LP(O5)... $\sigma^*(C26-H28)^a$	3.23	0.00770	0.7942
LP'(O5) ^a	s(0.00%) p(99.96%) d(0.04%)	LP'(O5)... $\sigma^*(C26-H27)^a$	4.11	0.01534	0.7942

a) Please see the atomic designations in Figure 9.

b) The interaction energy was calculated based on the second-order perturbation theory.

c) The listed values were the atom-atom overlap-weighted NAO bond order.

neighboring N–H bond. Moreover, the lone pair on the nitrogen atom in the title compound doesn't show orbital interactions by interaction energies larger than 1 kcal/mol with respect to any antibonding orbitals.

3. 7. QTAIM Study

The aforementioned results of the NBO analysis which show that the LPs of the oxygen atom in the methoxy group do not form orbital interactions by more than 1 kcal/mol with the antibonding orbital of the neighboring N–H bond motivated us to investigate whether there is no

intramolecular N–H...O hydrogen bond in the studied compound. The QTAIM study is thus performed using the Multiwfn program. Under the condition that the Poincaré-Hopf relationship is satisfied, the calculated critical points (CPs) have a total of 65 (in Figure 13). There are 29, 32, 4, and 0 for the (3,–3), (3,–1), (3,+1) and (3,+3) CP, respectively. As depicted in Figure S5, the (3,–1) CP designated as points 32, 34, 61 may indicate that there is an intramolecular O1–H2...O4, C24–H25...O4, and N8–H9...O5 hydrogen bond, respectively. The QTAIM study has already been used as a powerful tool to investigate intra- or intermolecular hydrogen bonding of several sys-

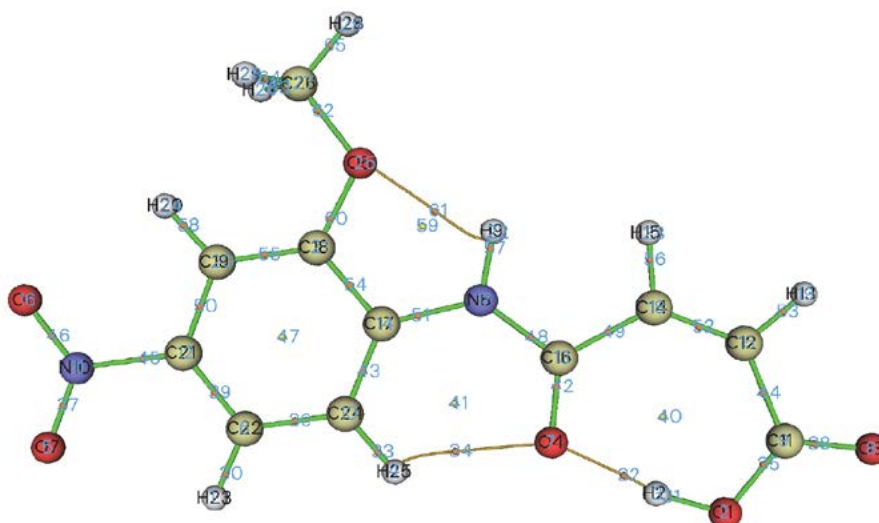


Figure 12. All the critical points of MAOA.

tems.^{49–56} According to QTAIM, if D-H forms a hydrogen bond with A, there should be a CP between H and A. In addition, criteria about the electron density (ρ_b) and the Laplacian of electron density ($\nabla^2\rho_b$) at BCPs have been established by Koch and Popelier to distinguish hydrogen bonding from van der Waals interactions. Moreover, Liu and coworkers have established a relationship between the hydrogen bonding strength (BE) and the electron density (ρ) at the CP corresponding to the hydrogen bond. The relationship could be described as Eq. (1) shows

$$\text{BE (in kcal/mol)} \approx -223.08 \times \rho + 0.7423 \quad (1)$$

Accordingly, the strength of the aforementioned intramolecular O1–H2...O4, C24–H25...O4, and N8–H9...O5 hydrogen bonds is calculated as –11.43, –3.40, and –3.99 kcal/mol, respectively.

4. Conclusion

The (Z)-4-(2-methoxy-4-nitrophenyl)amino)-4-oxobut-2-enoic acid is synthesized and characterized by single crystal X-ray diffraction (SC XRD), UV-Vis, FT-IR, TGA/DSC techniques. SC-XRD analysis inferred that the strong intermolecular H-bonding of type O–H...O, N–H...O and comparatively weak C–H...O bonding and π ... π stacking interactions are responsible for crystal packing. UV-Vis spectrum showed λ_{max} at 360 nm due to π - π^* transitions. FT-IR result confirms the formation of the compound by showing characteristics carboxylic acid peak at 1713 cm^{-1} . TGA/DSC results represent the major weight loss (71%) in a single step from 130 to 260 °C with the loss of main fragments leaving behind residue comprised of carbon in the form of coke. It is evident from heat flow that the sample changed its phase from solid to liquid around 171 °C. Hirshfeld surface analysis shows that O–H/H...O inter-atomic contact is the most significant contributor to the overall strengthening of packing of molecules with a percentage contribution of 39.8%. The void analysis predicted that MAOA will have good mechanical properties. The interaction energy between molecular pairs and energy framework analysis showed that for the stabilization of the supramolecular assembly in MAOA, the dispersion energy is the dominant energy as compared to other types of energies. According to the results of the DFT and QTAIM studies, MAOA could be stabilized by the intramolecular O–H...O, N–H...O, and C–H... hydrogen bonds in the gas phase.

Supplementary data

CCDC 2009600 contains the supplementary crystallographic data for (MAOA). The data can be obtained free of charge via <http://www.ccdc.cam.ac.uk/conts/retrieving.html>, or from the Cambridge Crystallographic Data Cen-

tre, 12 Union Road, Cambridge CB2 1EZ, UK; fax: (+44) 1223-336-033; or e-mail: deposit@ccdc.cam.ac.uk.

Acknowledgement

Akbar Ali greatly acknowledges the support of HEC Pakistan and Khurram Shahzad Munawar is highly thankful to the University of Mianwali for characterization.

Conflict of interest: The authors declare that they have no conflict of interest.

5. References

1. A. Ali, A. G. Corrêa, D. Alves, J. Zukerman-Schpector, B. Westermann, M. A. Ferreira, M. W. Paixão, *ChemComm.* **2014**, 50, 11926–11929. DOI:10.1039/C4CC04678A
2. G. P. da Silva, A. Ali, R. C. da Silva, H. Jiang, M. W. Paixao, *ChemComm.* **2015**, 51, 15110–15113. DOI:10.1039/C5CC06329A
3. W. M. Lee, *J. Hepatol.* **2017**, 67, 1324–1331. DOI:10.1016/j.jhep.2017.07.005
4. C. A. Caiuby, A. Ali, V. T. Santana, F. W. d. S. Lucas, M. S. Santos, A. G. Corrêa, O. R. Nascimento, H. Jiang, M. W. Paixão, *RSC Adv.* **2018**, 8, 12879–12886. DOI:10.1039/C8RA01787E
5. S. M. Prajapati, K. D. Patel, R. H. Vekariya, S. N. Panchal, H. D. Patel, *RSC Adv.* **2014**, 4, 24463–24476. DOI:10.1039/C4RA01814A
6. P. Theivendren, A. Subramanian, I. Murugan, S. D. Joshi, U. A. More, *Chem. Biol. Drug Des.* **2017**, 89, 714–722. DOI:10.1111/cbdd.12894
7. T. Panneerselvam, S. Arumugam, M. A. Ali, K. Selvaraj, M. Indhumathy, A. Sivakumar, S. D. Joshi, *ChemistrySelect* **2017**, 2, 2341–2347. DOI:10.1002/slct.201601763
8. W. Kemnitzer, S. Cai, J. Drewe, N. Sirisoma, Substituted N-Aryl-9-Oxo-9H-Fluorene-1-Carboxamides and Analogs as Activators of Caspases and Inducers of Apoptosis, Patent Number WO2006039356A3, date of patent April 13, **2006**.
9. H. J. Breslin, M. J. Kukla, D. W. Ludovici, R. Mohrbacher, W. Ho, M. Miranda, J. D. Rodgers, T. K. Hitchens, G. Leo, *J. Med. Chem.* **1995**, 38, 771–793. DOI:10.1021/jm00005a005
10. A. Ali, M. Khalid, M. F. u. Rehman, S. Haq, A. Ali, M. N. Tahir, M. Ashfaq, F. Rasool, A. A. C. Braga, *ACS Omega* **2020**, 5, 15115–15128. DOI:10.1021/acsomega.0c00975
11. B. Khan, M. Khalid, M. R. Shah, M. N. Tahir, M. U. Khan, A. Ali, S. Muhammad, *ChemistrySelect* **2019**, 4, 9274–9284. DOI:10.1002/slct.201901422
12. M. Khalid, A. Ali, M. Adeel, Z. U. Din, M. N. Tahir, E. Rodrigues-Filho, J. Iqbal, M. U. Khan, *J. Mol. Struct.* **2020**, 1206, 127755. DOI:10.1016/j.molstruc.2020.127755
13. M. Khalid, A. Ali, J. Tariq, M. N. Tahir, H. A. R. Aliabad, I. Hussain, M. Ashfaq, M. U. Khan, *ChemistrySelect* **2020**, 5, 10618–10631. DOI:10.1002/slct.202002653
14. A. Ali, Z. U. Din, M. Khalid, M. N. Tahir, E. Rodrigues-Fil-

- ho, B. Ali, S. Asim, S. Muhammad, *ChemistrySelect* **2020**, *5*, 3735–3745. DOI:10.1002/slct.201904757
15. A. Ali, M. Khalid, S. Abid, M. N. Tahir, J. Iqbal, M. Ashfaq, F. Kanwal, C. Lu, *Crystals* **2020**, *10*, 778. DOI:10.3390/cryst10090778
16. M. Khalid, A. Ali, S. Asim, M. N. Tahir, M. U. Khan, L. C. Curcino Vieira, A. F. de la Torre, M. Usman, *J. Phys. Chem. Solids* **2021**, *148*, 109679. DOI:10.1016/j.jpcs.2020.109679
17. M. Khalid, A. Ali, S. Haq, M. N. Tahir, J. Iqbal, A. A. C. Braga, M. Ashfaq, S. U. H. Akhtar, *J. Mol. Struct.* **2021**, *1224*, 129308. DOI:10.1016/j.molstruc.2020.129308
18. G. M. Sheldrick, *Acta Crystallogr., Sect. A: Found. Adv.* **2015**, *71*, 3–8. DOI:10.1107/S2053273314026370
19. G. M. Sheldrick, *Acta Crystallogr. C Struct. Chem.* **2015**, *71*, 3–8. DOI:10.1107/S2053229614024218
20. L. J. Farrugia, *J. Appl. Crystallogr.* **2012**, *45*, 849–854. DOI:10.1107/S0021889812029111
21. A. L. Spek, *Acta Crystallogr. D Biol. Crystallogr.* **2009**, *65*, 148–155. DOI:10.1107/S090744490804362X
22. C. F. Macrae, I. Sovago, S. J. Cottrell, P. T. Galek, P. McCabe, E. Pidcock, M. Platings, G. P. Shields, J. S. Stevens, M. Towler, *J. Appl. Crystallogr.* **2020**, *53*, 226–235. DOI:10.1107/S1600576719014092
23. P. R. Spackman, M. J. Turner, J. J. McKinnon, S. K. Wolff, D. J. Grimwood, D. Jayatilaka, M. A. Spackman, *J. Appl. Crystallogr.* **2021**, *54*, 1006–1011. DOI:10.1107/S1600576721002910
24. M. A. Spackman, D. Jayatilaka, *CrystEngComm* **2009**, *11*, 19–32. DOI:10.1039/B818330A
25. M. J. Turner, S. Grabowsky, D. Jayatilaka, M. A. Spackman, *J. Phys. Chem. Lett.* **2014**, *5*, 4249–4255. DOI:10.1021/jz502271c
26. A. D. Becke, *Phys. Rev. A* **1988**, *38*, 3098–3100. DOI:10.1103/PhysRevA.38.3098
27. B. Miehlich, A. Savin, H. Stoll, H. Preuss, *Chem. Phys. Lett.* **1989**, *157*, 200–206. DOI:10.1016/0009-2614(89)87234-3
28. C. Lee, W. Yang, R. G. Parr, *Phys. Rev. B* **1988**, *37*, 785–789. DOI:10.1103/PhysRevB.37.785
29. A. McLean, G. Chandler, *J. Chem. Phys.* **1980**, *72*, 5639–5648. DOI:10.1063/1.438980
30. M. J. Frisch, G. Trucks, H. Schlegel, G. Scuseria, M. Robb, J. Cheeseman, G. Scalmani, V. Barone, G. Petersson, H. Nakatsuji, Gaussian 16, Gaussian, Inc. Wallingford, CT, 2016.
31. T. Lu, F. Chen, *J. Comput. Chem.* **2012**, *33*, 580–592. DOI:10.1002/jcc.22885
32. J. Bernstein, R. E. Davis, L. Shimon, N. L. Chang, *Angew Chem. Int. Ed. Engl.* **1995**, *34*, 1555–1573. DOI:10.1002/anie.199515551
33. J. L. Wardell, J. M. Skakle, J. N. Low, C. Glidewell, *Acta Crystallogr., Sect. E: Struct. Rep. Online* **2005**, *61*, o3849–o3851. DOI:10.1107/S160053680503374X
34. B. T. Gowda, M. Tokarčík, K. Shakuntala, J. Kožíšek, H. Fuess, *Acta Crystallogr., Sect. E: Struct. Rep. Online* **2010**, *66*, o1671–o1672. DOI:10.1107/S1600536810022245
35. U. Chaithanya, S. Foro, B. T. Gowda, *Acta Crystallogr., Sect. E: Struct. Rep. Online* **2012**, *68*, o873–o873. DOI:10.1107/S1600536812008021
36. K. Shakuntala, M. Fronc, B. T. Gowda, J. Kožíšek, *Acta Crystallogr., Sect. E: Struct. Rep. Online* **2012**, *68*, o99–o100. DOI:10.1107/S1600536811052573
37. J. J. McKinnon, D. Jayatilaka, M. A. Spackman, *ChemComm.* **2007**, 3814–3816. DOI:10.1039/b704980c
38. N. Kitanovski, M. Počkaj, *Acta Chim. Slov.* **2021**, *68*, 475–482. DOI:10.17344/acsi.2020.6634
39. T. Topal, *Acta Chim. Slov.* **2021**, *68*, 88–101. DOI:10.17344/acsi.2020.6183
40. J.-J. Wang, L.-N. Dun, B.-S. Zhang, Z.-H. Wang, H. Wang, C.-B. Li, W. Liang, *Acta Chim. Slov.* **2021**, *68*, 239–246. DOI:10.17344/acsi.2020.6438
41. C. Jelsch, K. Ejsmont, L. Huder, *IUCrJ* **2014**, *1*, 119–128. DOI:10.1107/S2052252514003327
42. H. Kargar, M. Fallah-Mehrjardi, R. Behjatmanesh-Ardakani, K. S. Munawar, M. Ashfaq, M. N. Tahir, *Inorg. Chim. Acta.* **2021**, *526*, 120535. DOI:10.1016/j.ica.2021.120535
43. C. F. Mackenzie, P. R. Spackman, D. Jayatilaka, M. A. Spackman, *IUCrJ* **2017**, *4*, 575–587. DOI:10.1107/S205225251700848X
44. M. J. Turner, J. J. McKinnon, D. Jayatilaka, M. A. Spackman, *CrystEngComm* **2011**, *13*, 1804–1813. DOI:10.1039/C0CE00683A
45. M. Ashfaq, M. Khalid, M. N. Tahir, A. Ali, M. N. Arshad, A. M. Asiri, *ACS Omega* **2022**, *7*, 9867–9878. DOI:10.1021/acsomega.2c00288
46. H. Kargar, M. Ashfaq, M. Fallah-Mehrjardi, R. Behjatmanesh-Ardakani, K. S. Munawar, M. N. Tahir, *J. Mol. Struct.* **2022**, *1253*, 132264. DOI:10.1016/j.molstruc.2021.132264
47. M. Ashfaq, M. N. Tahir, S. Muhammad, K. S. Munawar, A. Ali, G. Bogdanov, S. S. Alarfaji, *ACS Omega* **2021**, *6*, 31211–31225. DOI:10.1021/acsomega.1c04884
48. K. O. Ali, H. A. Mohamad, T. Gerber, E. Hosten, *Acta Chim. Slov.* **2022**, *69*, 905–912. DOI:10.17344/acsi.2022.7682
49. U. Koch, P. L. Popelier, *J. Phys. Chem.* **1995**, *99*, 9747–9754. DOI:10.1021/j100024a016
50. A. Saeed, M. Bolte, M. F. Erben, H. Pérez, *CrystEngComm* **2015**, *17*, 7551–7563. DOI:10.1039/C5CE01373A
51. M. Xu, B. Zhang, Q. Wang, Y. Yuan, L. Sun, Z. Huang, *J. Chil. Chem. Soc.* **2018**, *63*, 3788–3794. DOI:10.4067/s0717-97072018000103788
52. M. J. Javan, *Comput. Theor. Chem.* **2021**, *1205*, 113440. DOI:10.1016/j.comptc.2021.113440
53. M. K. Chaudhary, T. Karthick, B. D. Joshi, P. Prajapati, M. S. A. de Santana, A. P. Ayala, V. J. Reeda, P. Tandon, *Spectrochim. Acta A Mol. Biomol. Spectrosc.* **2021**, *246*, 118976. DOI:10.1016/j.saa.2020.118976
54. I. N. Kolesnikova, N. A. Chegodaev, P. Y. Sharanov, I. F. Shishkov, *Chem. Phys. Lett.* **2022**, *793*, 139447. DOI:10.1016/j.cplett.2022.139447
55. A. Jezierska, J. J. Panek, K. Błaziak, K. Raczynski, A. Koll, *Molecules* **2022**, *27*, 792–810. DOI:10.3390/molecules27030792
56. S. Emamian, T. Lu, H. Kruse, H. Emamian, *J. Comput. Chem.* **2019**, *40*, 2868–2881. DOI:10.1002/jcc.26068

Povzetek

(Z)-4-(2-metoksi-4-nitrofenil)amino)-4-oksobut-2-enojsko kislino (**MAOA**) smo sintetizirali z reakcijo 2-metoksi-4-nitroanilina in maleinskega anhidrida v etil acetatu. Sintetizirano spojino smo okarakterizirali z elementarno analizo, FT-IR in UV-Vis spektroskopijo in TGA/DSC analizo. Kristalno strukturo smo določili z monokristalno rentgensko difrakcijo (SC XRD). Supramolekularno strukturo **MAOA** glede na nekovalentne interakcije smo raziskali z analizo Hirshfeldove površine. Analiza praznin je pokazala, da naj bi imela **MAOA** dobre mehanske lastnosti. Okolje kristalnega pakiranja smo nadalje raziskali z interakcijsko energijo med molekularnimi pari in energijskimi mrežami. Poleg tega je rezultat DFT študije v plinski fazi pokazal, da v **MAOA** obstajata N–H...O in O–H...O intramolekularni vodikovi vezi, ker je razdalja med D in A manjša od vsote njunih van der Waalsovih radijev. Rezultat študije QTAİM je pokazal, da bi morala v **MAOA** obstajati tudi intramolekularna vodikova vez CH...O z močjo 3,40 kcal/mol.



Except when otherwise noted, articles in this journal are published under the terms and conditions of the Creative Commons Attribution 4.0 International License

DRUŠTVENE VESTI IN DRUGE AKTIVNOSTI SOCIETY NEWS, ANNOUNCEMENTS, ACTIVITIES

Vsebina

Poročilo o delu v letu 2022	S41
Koledar važnejših znanstvenih srečanj s področja kemije in kemijske tehnologije	S48
Navodila za avtorje	S50

Contents

Report for 2022	S41
Scientific meetings – Chemistry and chemical engineering.....	S48
Instructions for authors	S50

POROČILO PREDSEDNIKA SLOVENSKEGA KEMIJSKEGA DRUŠTVA O DELU DRUŠTVA V LETU 2022

Tudi v letu 2022 je bilo društvo aktivno na številnih področjih. Izvajali smo redne letne aktivnosti, pri katerih je bil glavni poudarek na rednem izdajanju društvene revije *Acta Chimica Slovenica* (ACSi) ter organizaciji največjega letnega dogodka društva, konference »Slovenski kemijski dnevi 2022«.

V letu 2021 je društvo praznovalo 70-letnico. Slovesnost ob jubileju je bila zaradi Covida 19 prestavljena v leto 2022 in je potekala v sklopu konference Slovenski kemijski dnevi v Grand Hotelu Bernardin v Portorožu. Dogodka se je udeležilo več kot 310 povabljenih gostov iz 13 držav, med drugim tudi predsednika hrvaškega in slovaškega kemijskega društva ter predstavniki ECTN in EuChemS. Slavnostni govorci so bili prof. dr. Tamara Lah Turnšek, akad. prof. dr. Branko Stanovnik in prof. dr. Venčeslav Kaučič, Slovensko kemijsko društvo pa je podelilo priznanja 8 častnim članom, 9 zaslužnim članom, 11 zaslužnim inštitucijam; priznanja za sodelovanje pri uredništvu znanstvene revije *Acta Chimica Slovenica* je prejelo 30 sodelavcev. Zahvala gre tudi sponzorjem Slavnostne akademije, ki so omogočili proslavo ob tako pomembni obletnici - hvala torej podjetjem Cinkarna Celje, Salonit Anhovo, Knauf Insulation, Melamin, Aquafil, Novartis, Belinka Perkemija, Krka, Kemomed, Mettler Toledo, Belinka Prkemija in Primalab za podporo in sodelovanje.

21. septembra smo prav tako v sklopu omenjene konference izvedli redni občni zbor društva, kjer smo uradno ustanovili Sekcijo za okolje ter sklenili, da elektorje za volitve v Državni svet izbere Glavni odbor med svojimi člani.

Slovenski kemijski dnevi 2022 so bili organizirani v Portorožu, v Kongresnem centru Grand hotela Bernardin, in sicer v dneh od 21. do 23. septembra 2022. Programskemu in organizacijskemu odboru je predsedoval znan. svet. dr. Albin Pintar, skupaj s člani odbora v zasedbi prof. dr. Romana Cerc-Korošec, prof. dr. Zorka Novak Pintarič, prof. dr. Darja Lisjak, doc. dr. Matic Lozinšek, prof. dr. Matjaž Valant, dr. Silvo Zupančič in Marjana Gantar Albreht ter Eva Mihalinec, ki se je društvu priključila v drugi polovici leta.

Na konferenci je bilo predstavljenih preko 180 prispevkov v obliki predavanj in posterjev. Delo je potekalo plenarno in v treh vzporednih sekcijah. Udeleženci konference, bilo jih je 279 iz Slovenije in dvanajstih drugih držav, so bili zelo zadovoljni s kakovostjo znanstvenih in strokovnih prispevkov ter družabnim programom srečanja. Na konferenci je sodelovalo tudi 21 razstavljalcev laboratorijske in procesne opreme. Sponzorji dogodka so bili Mikro+Polo, Analysis Adria, Chemass, Donau Lab, Hiden Analytical, Kemomed, Labtim, Merck, Mettler Toledo, Optik Instruments, Primalab in Vigor ter MDPI. Objavili smo zbornik povzetkov konference, ki je dostopen na USB ključu ter na voljo v NUK-u in strokovnih knjižnicah po Sloveniji.

Plenarni predavatelji na konferenci so bili prof. dr. Goran Dražić (**Kemijski inštitut, Ljubljana**), prof. dr. Doris Vollmer (Max Planck Institute for Polymer Research, Mainz, Nemčija) in prof. dr. Ioannis Katsoyiannis (Aristotle University of Thessalo-

niki, Grčija). Poleg treh plenarnih predavanj so udeleženci poslušali šest »keynote« vabljenih predavanj, ki so jih izvedli dr. Slavko Kralj (Institut Jožef Stefan in Fakulteta za farmacijo UL), prof. dr. Nataša Novak Tušar (Kemijski inštitut in Univerza v Novi Gorici), prof. dr. Layla Martin-Samos (Italian National Research Council (CNR-IOM Democritos), Trst, Italija), dr. Dinesh Shetty (Khalifa University, Abu Dhabi, UAE), dr. Nataša Kovačević (Kolektor Mobility) in prof. dr. Robin A. Hutchinson (Queen's University, Kingston (ON), Kanada).

Podelili smo tudi nagrade za najboljša študijska dela s področja trajnostne kemije. Strokovno komisijo za izbor najboljših del so sestavljali dr. Vid Margon, dr. Ema Žagar, izr. prof. dr. Romana Cerc Korošec in prof. dr. Marjan Veber, ki so se odločili, da nagrado za najboljšo diplomsko delo prejme Martin Ciringar, za najboljšo magistrsko delo Ana Rebeka Kamšek, za najboljšo doktorsko delo pa dr. Maja Čolnik. Sponzor nagrad je bilo podjetje AquafilSLO.

Ob zaključku konference smo že tradicionalno podelili nagrade doktorskim študentom za najboljša predavanja in posterske predstavitve.

V letu 2022 smo v reviji *Acta Chimica Slovenica* (ACSi) izdali 4 številke revije, v katerih je bilo skupaj objavljenih 92 originalnih znanstvenih člankov na skupno 943 straneh z dvokolonskim tiskom. Članki pokrivajo vsa področja kemije, kemije materialov in kemijskega in biokemijskega inženirstva. Vseh člankov, ki so bili leta 2022 oddani v uredniški sistem, je bilo 469, kar pomeni, da jih je bilo na koncu sprejetih okoli 19 %. Vsi članki so objavljeni na spletu in so prosto dostopni. Poleg tega so objavljeni tudi v več podatkovnih bazah. Faktor vpliva revije za leto 2021 je bil 1,524. Od objavljenih člankov sta bila dva tako imenovana »Feature Articles« (FA). Med FA je bil tudi prispevek raziskovalne skupine iz tujine, ki raziskuje na področju polimerne kemije pod vodstvom Prof. Heikkija Tenhuja z Univerze v Helsinkih.

Z letom 2022 delo odgovorne urednice ACSi in področne urednice za področje Physical Chemistry zaključuje Ksenija Kogej.

V društvenih vesteh smo objavili seznam diplomskih, magistrskih in doktorskih del FKKT UL, FKKT UM, podiplomskega študijskega programa »Znanosti o okolju« in Fakultete za znanosti okolju, UNG v letu 2020. Objavili smo tudi letna poročila sekcij. V letu 2022 so društvene vesti obsegale 120 strani. Na društvenih straneh je bila poleg ostalih novic objavljena tudi novica o Slavnostni akademiji ob 70. letnici društva.

Zahvaljujem se tudi vsem inštitucijam, ki so v letu 2022 finančno podprle izdajanje revije *Acta Chimica Slovenica*. Te so Fakulteta za kemijo in kemijsko tehnologijo Univerze v Ljubljani, Fakulteta za kemijo in kemijsko tehnologijo Univerze v Mariboru, Univerza v Novi Gorici, Kemijski inštitut, Inštitut »Jožef Stefan« in Belinka Perkemija. Sponzorji revije so bili z objavo oglasa Krka d.d., Novo mesto, Donau Lab d.o.o. Ljubljana in Helios Domžale, d.o.o.

V letu 2022 smo nadaljevali z aktivnostmi za pridobivanje novih članov. Medse smo jih privabili 48, od tega 30 študentov. Za komunikacijo s člani smo pogosteje uporabljali Facebook, Twitter in LinkedIn ter jih obveščali o dogodkih po elektronski pošti.

V društvu smo prvič objavili razpis za povezovanje dijakov s strokovnjaki kemijske stroke, pripravili pa smo 5 tem raziskovalnih nalog na različnih institucijah. Kot mentorji dijakom so se predstavili prof. dr. Darja Lisjak (Institut Jožef Stefan), asist. Miha Slapničar in Tim Prezelj (Univerza v Ljubljani, Pedagoška fakulteta), red. prof. Urban Bren in Veronika Furlan (Univerza v Mariboru in Fakulteta za kemijo in kemijsko tehnologijo), dr. Annamaria Vujanovic in izr. Prof. Lidija Čuček (Univerza v Mariboru in Fakulteta za kemijo in kemijsko tehnologijo) in dr. Jan Bitenc (Kemijski inštitut).

Člani Slovenskega kemijskega društva so bili aktivni tudi na področju mednarodnega sodelovanja. Predvsem je potrebno omeniti članstvo društva v mednarodnih združenjih IUPAC, ECTN, IUCr, EURACHEM, EuChemS, EFCE, EPF, ECA in EFCATS. Društvo se je v letu 2022 prijavilo na Javni razpis ARRS za sofinanciranje delovanja v mednarodnih znanstvenih združenjih v letu 2022, kjer smo bili uspešni pri vseh oddanih vlogah. Konec leta smo oddali tudi prijavo na Javni razpis ARRS za sofinanciranje izdajanja domačih periodičnih znanstvenih publikacij v letih 2023 in 2024, rezultati pa bodo znani v 2023.

dr. Peter Venturini, predsednik društva
dr. Albin Pintar, predsednik organizacijskega odbora
konference Slovenski kemijski dnevi
prof. dr. Ksenija Kogej, glavna urednica ACSi

Poročilo o delovanju in aktivnostih Mariborske podružnice za leto 2022

Mariborska podružnica se je v letu 2022 usmerila v izpolnitev ciljev, ki si jih je zastavila v preteklem letu.

Kot vsako leto smo se tudi letos v Portorožu udeležili konference Slovenski kemijski dnevi, kjer smo predsedovali različnim sekcijam, sodelovali kot predavatelji in kot predstavniki prispevkov na posterjih ter v komisiji za ocenjevanje študentskih del. Skrb Mariborske podružnice je tudi stalno izobraževanje članov. V ta namen smo organizirali strokovna predavanja in razne seminarje, na katerih so predavali priznani tuji in domači strokovnjaki. Predavanja so pokrivala pomembna področja teoretične in uporabne kemije, kemijske in procesne tehnike ter kemijskega izobraževanja.

V letu 2022 smo gostili predstavnike številnih podjetij (Kansai Helios, Lek, Etol, Krka, Microinnova ...) z namenom sodelovanja fakultete z industrijskimi partnerji. Izvedli smo promocijo kemijskih znanosti na 14. srednjih šolah po Sloveniji. Organizirali smo razpravo s srednješolskimi učitelji na FKKT UM o načinu poučevanja. Z dijaki smo izvedli delavnici z naslovom angl. *Belle 2 master clas-*

ses. Dvakrat smo se udeležili tudi kariernega sejma.

Pojavljamo se v medijih kot so RTV Slovenija, Delo, Večer, dijaški.net, FAX VPISNIK, kjer predstavljamo obnovo naše fakultete, novo raziskovalno opremo in dosežke najuspešnejših raziskovalcev (npr. uvrstitev sodelavcev na Stanfordovo lestvico najuspešnejših raziskovalcev na svetu).

Prvič do sedaj smo v avgustu 2022 organizirali poletno šolo kemije in kemijskega inženirstva za dijake srednjih šol. Aktivno smo sodelovali tudi pri mednarodnih poletnih šolah.

Na naši fakulteti je v sodelovanju s fakulteto iz Gradca potekala mednarodna poletna šola na temo visokotlačnih tehnologij: 'ESS-HPT 2022' The European Summer school in High Pressure Technology, ki jo je organiziral Laboratorij za separacijske procese in produktno tehniko v sodelovanju s Tehnološko fakulteto v Gradcu.

izr. prof. dr. Matjaž Finšgar

Poročilo Komisije za slovensko kemijsko terminologijo in nomenklaturu za leto 2022

Komisija za slovensko kemijsko terminologijo in nomenklaturu je tudi v preteklem letu sodelovala pri delu Tehniške komisije Sekcije za terminološke slovarje pri Inštitutu za slovenski jezik ZRC SAZU. Člana tehniške komisije za področje kemije in kemijske tehnologije sta Andrej Šmalc iz ljubljanske ter Peter Glavič iz mariborske podružnice Slovenskega kemijskega društva.

V letu 2022 je potekala končna redakcija gradiva s področja kemije, kemijske tehnologije in kemijske tehnike za novo izdajo splošnega tehniškega slovarja, ki bo predvidoma končana v letu 2023

Obenem s tem je potekalo nadaljnje zbiranje gradiva za novi Kemijski slovar, ki je že nekaj let na spletu in predstavlja pomembno dopolnitev bodočega Splošnega tehni-

škega slovarja. Prednost spletne oblike slovarja je prav v tem, da ga je mogoče ves čas dopolnjevati in po potrebi tudi popravljati. V letu 2022 je bilo obdelanih 688 gesel, ki bodo v naslednjem letu vnesena v slovar.

Za leto 2023 je predvideno nadaljnje sodelovanje pri končni redakciji Slovenskega tehniškega slovarja, kot tudi nadaljnje zbiranje gradiva za nova gesla ter njihova obdelava in vnašanje v Kemijski slovar.

Poleg dela v zvez s Kemijskim slovarjem bomo še nadalje sodelovali pri prevodu mednarodnega standarda ISO 80000: Veličine in enote s strokovnim pregledom novih prevodov, ki bo nadomestil sedanji standard SIST ISO 31.

prof. dr. Andrej Šmalc

Poročilo Sekcije za polimere za leto 2022

Sekcija za polimere je članica Evropske polimerne federacije (EPF), kateri je v letu 2022 predsedoval prof. dr. Jiri Kotek (Inštitut za makromolekularno kemijo, Češka). Zaradi COVID-19 epidemije je prof. dr. Jiri Kotek z eno letno zamudo lani organiziral največji evropski polimerni kongres, EPF 2022, pri katerem predstavniki nacionalnih polimernih sekcij in društev iz 28 držav delujemo kot mednarodni svetovni odbor. Na generalni skupščini EPF, ki smo jo imeli Februarja v Pragi, Češka, smo izvolili novo predsednico EPF prof. dr. Katjo Loos (Univerza v Groningu, Nizozemska), ki bo predsedovala do leta 2025, ko bo organizirala naslednji EPF kongres v Groningu, Nizo-

zemska. Na sestanku smo med drugim potrdili drugega prejemnika EPF nagrade, ki jo je prejel prof. dr. Christopher Barner-Kowollik (Centre for Materials Science, Avstralija) za pionirsko delo na področju makromolekularne fotokemije.

Člani sekcije so bili v juniju povabljeni na predavanje prof. dr. Michael S. Silversteina, ki je v sklopu Preglovihih predavateljev na Kemijskem inštitutu imel predavanje z naslovom: „Accessing Innovative Polymers through Emulsion Templating“.

dr. David Pahovnik

Poročilo Sekcije mladih SKD za leto 2022

Sekcija mladih je v letu 2022 izvedla sledeče dogodke in projekte:

Razpis raziskovalnih nalog za dijake

V februarju 2022 smo pričeli z razpisom za povezovanje dijakov s strokovnjaki kemijske stroke, ki bi jim bili mentorji pri raziskovalnih nalogah.

Razpis skupaj s seznamom in opisom tem (4 teme) smo poslali po slovenskih srednjih šolah. Dijaki so imeli čas za prijavo do sredine aprila, strokovna komisija SKD je pregledala prijave in povezala dijake z izbranimi mentorji.

Ekскурzija v KRKO (v sodelovanju s Študentsko organizacijo FKKT)

V aprilu 2022 smo organizirali v sodelovanju s študentsko organizacijo UL FKKT strokovno ekscurzijo v

farmacevtsko podjetje Krka. Ekscurzijo smo kombinirali z ogledom vinske kleti. V sklopu ekscurzije so se lahko študenti včlanili v društvo, za člane je bila cena prevoza nižja. Na tak način smo uspeli privabiti nove člane.

Javni razpis: nagrade za najboljša študijska dela s področja trajnostne kemije

Poleti smo v sodelovanju s podjetjem Aquafil objavili razpis za nagrade za najboljša diplomsko, magistrsko in doktorsko delo iz trajnostne kemije. Strokovna komisija SKD je pregledala prijave in ocenila dela. Nagrada je obsegala plaketo in denarno nagrado. Nagrade smo podelili na konferenci Slovenski Kemijski dnevi 2022.

dr. Tina Paljk

Poročilo Sekcije za katalizo za leto 2022

Članice in člani sekcije za katalizo smo bili angažirani pri organizaciji mednarodnega znanstvenega srečanja, tj. 6th International Conference on New Photocatalytic Materials for Environment, Energy and Sustainability (NPM-6) & 7th International Conference on Photocatalytic and Advanced Oxidation Technologies for the Treatment of Water, Air, Soil and Surface (PAOT-7), ki je potekal na Kemijskem inštitutu v Ljubljani od 4. do 6. aprila 2022.

Prav tako smo leta 2022 pridobili organizacijo mednarodne znanstvene konference z naslovom “4th International Conference on Fundamentals and Applications of Cerium Dioxide in Catalysis”, ki bo potekala od 17. do 20. septembra 2024 v kongresnem centru Grand hotela Bernardin v Portorožu. Več informacij o dogodku je na voljo na konferenčni spletni strani: <https://ceria2024.chem-soc.si/>.

Izvajamo tudi aktivnosti za pridobitev organizacije mednarodne znanstvene konference “13th European Conference on Solar Chemistry and Photocatalysis: Environmental Applications (SPEA)”, ki jo bomo v primeru potrditve kandidature organizirali leta 2026.

Nataša Novak Tušar in Albin Pintar sta kot nacionalna predstavnika sodelovala pri izvajanju aktivnosti pri Evropski federaciji katalitskih združenj (EFCATS).

V sekciji za katalizo smo v lanskem letu sodelovali pri organizaciji predavanj vabljenih tujih raziskovalcev, ki smo jih pripravili v sodelovanju z raziskovalnimi in akademskimi institucijami, zelo angažirani pa smo bili pri organizaciji konference “Slovenski kemijski dnevi 2022”, kakor tudi pri sodelovanju na dogodku s predstavitvami velikega števila prispevkov.

dr. Albin Pintar

Poročilo Sekcije za kristalografijo pri Slovenskem kemijskem društvu za leto 2022

V letu 2022 smo člani kristalografske sekcije aktivno sodelovali pri organizaciji dveh mednarodnih konferenc. Obe bi morali biti izvedeni že v predhodnih letih, pa sta bili zaradi pandemije COVID-19 preloženi na primernejši čas.

Prvi od teh dveh dogodkov je bila Evropska konferenca o praškovni difrakciji (EPDIC17), ki je bila izvedena v Šibeniku od 31. maja do 3. junija 2022. Kot svetovalec organizacijskega odbora je bil v delo pri organizaciji zaradi izkušenj večletnega članstva v Evropskem odboru za praškovno difrakcijo vključen tudi vodja sekcije za kristalografijo pri SKD Anton Meden. Konferenca je bila zelo uspešna in na njej je aktivno sodelovala tudi osmerica slovenskih udeležencev. Program je obsegal pet plenarnih predavanj in 12 mikrosimpozijev, udeležilo se ga je več kot 20 sponzorjev/razstavljalcev. Dobro sta bili obiskani tudi dve delavnici pred začetkom konference (za delo s programom Topas za Rietveldovo analizo in za uporabo zbirke podatkov PDF).

Drugi dogodek je bilo tradicionalno 28. Hrvaško-slovensko kristalografsko srečanje od 8. do 11. septembra v Poreču. V organizacijskem odboru tega srečanja je sodelovalo pet članov iz Slovenije, pet iz Hrvaške in eden iz

Poljske. Tudi tokrat je uspelo pridobiti dovolj sponzorskih sredstev, da kotizacija ni bila potrebna. Lahko smo celo podelili nekaj nagrad za najboljše predstavitve v različnih kategorijah raziskovalcev. Tako brezplačna udeležba kot kandidiranje za nagrade je za udeležbo mladih raziskovalcev dobra spodbuda in odlična priložnost za pridobivanje kompetenc, saj so vsi prispevki v obliki kratkih predavanj.

Udeležba je bila zelo dobra, program pa kakovosten. Plenarna predavanja so bila štiri, kratkih predavanj 66, od tega 21 iz Slovenije. Plenarna predavanja so bila na različne teme: materiali za sproščanje tekočih sestavin (Alessina Bacchi, Parma, Italija), strukturna analiza nanomaterialov z elektronsko difrakcijo (Mariana Klementova, Praga, Češka), strukturni vpogled v pripravo in molekularno delovanje bioaktivnih kovinskih spojin (Jakob Kljun Ljubljana, Slovenija) in kristalografija kot zmogljiva metoda v nanosti o materialih (Anna Moliterni, Bari, Italija).

Že v letu 2022 so stekle tudi priprave na 29. slovensko-hrvaško kristalografsko srečanje, ki bo od 14. do 18. junija 2023 v Topolšici (<https://scm2023.fkkt.uni-lj.si/>). Pridobili smo že 10 sponzorjev in 4 vabljeni predavatelji, kar obeta, da bo tudi ta znanstveni dogodek uspešen.

prof. dr. Anton Meden

Poročilo o delu Sekcije za okolje SKD za leto 2022

Sekcija za okolje SKD je bila ustanovljena v letu 2022 na pobudo Darje Lisjak. 18.1.2022 smo organizirali uvodni sestanek sekcije, na katerem smo izbrali predsednika sekcije (Marko Štrok) ter podpredsednico in tajnico sekcije (Janja Vidmar). Po sestanku je Janja Vidmar vzpostavila oblak, na katerem se zbirajo dokumenti in zapisniki sestankov, vezani na delo sekcije (https://1drv.ms/u/s!AgGv2g6_iqYaxFGqYul2Qt2xwvMK?e=OKiqEx). Prav tako je bila pripravljena novica o ustanavljanju sekcije in objavljena na različnih internetnih straneh in socialnih medijih z namenom seznaniti zainteresirane o ustanavljanju sekcije in pritegniti čim večje število članov SKD k članstvu v sekciji.

Na podlagi sestanka smo pripravili tudi vizijo, poslanstvo in program dela sekcije. Poslanstvo sekcije je združevanje članov SKD, ki jih zanimajo tematike s področja kemije okolja z namenom izboljšati razumevanje in percepcijo kemije okolja med različnimi deležniki, ter tako vplivati na kvaliteto življenja. Vizija sekcije je postati eno izmed vodilnih združenj strokovnjakov v Sloveniji na po-

dročju tematik, povezanih s kemijo okolja z namenom ozaveščanja, razširjanja, izobraževanja in svetovanja različnim deležnikom na tem področju. Cilji sekcije pa so sledeči:

- Povezovanje članov Slovenskega kemijskega društva, ki delujejo na področju kemije okolja
- Postati stičišče različnih deležnikov na področju kemije okolja z namenom povezovanja in skupnega sodelovanja na področjih aktualnih za kemijo okolja
- Izboljšati ozaveščenost splošne in strokovne javnosti o tematikah povezanih s kemijo okolja

Sekcija pa bo delovala predvsem na naslednjih področjih:

- Ozaveščanje in razširjanje spoznanj, povezanih s kemijo okolja
- Izobraževanje
- Mednarodno sodelovanje

Program sekcije je bil predstavljen in sprejet na 3. seji glavnega odbora društva 6.6.2022.

Z namenom, da bi pripravili kratkoročni program dela sekcije za leti 2022-2023, smo 27.5.2022 organizirali drugi sestanek članov sekcije.

Na podlagi tega programa smo v letu 2022 na področju ozaveščanja in razširjanja spoznanj, povezanih s kemijo okolja in izobraževanja, na pobudo Andree Oarga-Mulec in Vesne Mislej začeli s projektom snemanja izobraževalnih / promocijskih videov na tematiko ponovne uporabe blata iz čistilnih naprav. Projekt je večplasten in vključuje študente Akademije umetnosti UNG, ki se pod mentorstvom Jasne Hribernik učijo snemati promocijske filme, strokovnjake na področju čiščenja odpadnih vod, kot sta Vesna Mislej iz CČN Ljubljana in Mojca Müller iz CČN Škofja Loka, ter učitelje in učence osnovnih in srednjih šol. Pri izvedbi projekta pa aktivno sodelujejo s svojo podporo tudi Andreea Oarga-Mulec, Janja Vidmar in Marko Štok. Ideja projekta je, da bi študenti Akademije umetnosti v sklopu svojega izobraževanja posneli izobraževalne / promocijske filme na tematiko blata iz čistilnih naprav in pomembnosti čistilnih naprav za okolje. Ti videi pa bodo podlaga za pripravo učnega paketa za osnovne in srednje šole, ki bi ga bodo učitelji uporabili pri poučevanju v šolah. V letu 2022 nam je Vesna Mislej pomagala pri iskanju lokacije za snemanje. Na koncu smo dobili zeleno luč za snemanje CČN Škofje Loke, ki jo strokovno vodi Mojca Müller. 20.9.2022 smo si tako ogledali lokacijo snemanja, 12.11.2022 pa je Jasna Hribernik s svojimi študenti izvedla snemalni dan na CČN Škofja Loka. Material, ki so ga študentje posneli, je sedaj v post produkciji, tako da se izvedba projekta nadaljuje v letu 2023. V letu 2022 smo s

pomočjo Iztoka Devetaka poslali vabilo učiteljem osnovnih in srednjih šol, ki bi se želeli priključiti projektu. In na podlagi vabila so pripravljenost izrazile štiri osnovnošolske in ena srednješolska učiteljica.

25.8.2022 smo se člani sekcije (Andreea Oarga-Mulec, Janja Vidmar in Marko Štok) na pobudo Andree Oarga-Mulec udeležili sestanka z Izobraževalnim centrom za zaščito in reševanje Ig. Jože Pogačar in njegovi sodelavci so nam predstavili delovanje centra, pogovarjali smo se tudi o morebitnem sodelovanju med sekcijo in centrom. Tako smo se dogovorili, da bi lahko v letu 2023 organizirali ogled centra in njegovih aktivnosti oz. študijo primera nesreče Kemis za člane sekcije oz. društva.

Sekcija je tudi sodelovala pri pripravi javnega razpisa za nagrade za najboljša študijska dela s področja trajnostne kemije, kjer je Marko Štok podal pripombe na osnutek razpisa in predlagal članico komisije za izbor.

V letu 2022 so se člani sekcije aktivno udeležili tudi Slovenskih kemijskih dnevov v Portorožu med 21.-23.9.2022, kjer je na podlagi našega predloga imel tudi predavanje plenarni predavatelj prof. dr. Ioannis Katsoyannis, ki je predsednik EuChemS Division of Chemistry and the Environment. Na Slovenskih kemijskih dnevih je potekal tudi izredni občni zbor SKD, kjer je bila Sekcija za kemijo okolja tudi formalno ustanovljena.

Po podatkih tajništva SKD znaša število članov sekcije 27 na dan 23.2.2023, od tega se jih je približno tretjina aktivno udeleževala in prispevala k aktivnostim sekcije v letu 2022.

dr. Marko Štok

Poročilo Analizne sekcije za leto 2022

Osnovna dejavnost sekcije za Analizno kemijo v okviru Slovenskega kemijskega društva je organiziranje mednarodnih in domačih znanstvenih ter strokovnih srečanj, predavanj domačih in tujih strokovnjakov ter izvedba različnih delavnic, seminarjev in simpozijev. Člani sekcije so aktivni tudi znotraj delovnih skupin Eurachem in drugih združenj v evropskem prostoru (DAC, FECS) in tako dodatno prispevajo k prepoznavnosti Slovenskega kemijskega društva.

Po letih 2020 in 2021, na kateri je ključno vplivala epidemija Sars-Covid 19 in so bile planirane aktivnosti sekcije praviloma odpovedane ali prestavljene, je leto 2022 potekalo brez tovrstnih omejitev. Med 4. in 7. 7. 2022 smo izvedli tradicionalno 27. mednarodno srečanje podiplomskih študentov in njihovih mentorjev YISAC (Young Investigators Seminar on Analytical Chemistry) na Univerzi v

Lodzu na Poljskem. Med aktivnostmi sekcije v Sloveniji velja izpostaviti 28. jubilejno konferenco »Slovenski kemijski dnevi 2022«, ki se je odvijala septembra 2022 v Portorožu. Področje analizne kemije je bilo dobro zastopano, konference se je udeležilo veliko kolegov iz različnih institucij, ki so predstavili številne zanimive raziskave s področij spektroskopije, kromatografije, elektrokemije, materialov in okolja.

V prihodnje želimo v sekcijo aktivno vključiti mlajše kolege in nadaljevati z organizacijo domačih ter tujih srečanj, predavanj in konferenc. Posebej želimo okrepiti povezovanje in prenos znanja iz univerzitetnih in raziskovalnih laboratorijev v industrijo.

prof. dr. Mitja Kolar

Poročilo sekcije EURACHEM Slovenija za leto 2022

V Sloveniji je do sedaj večina preskusnih laboratorijev akreditiranih v skladu z ISO 17025, tako da večjih potreb po izobraževanjih za preskusne laboratorije s področja, ki ga pokriva Eurachem, ni več. Izjema so medicinski laboratoriji, za katere velja ISO 15189, ki se vsebinsko ne razlikuje bistveno od 17025.

Za tiste, ki želijo pridobiti znanja s področja kakovosti merjenj v kemijskih/biokemijskih laboratorijih, je tudi v letu 2022 organiziral SIQ tako Šolo kakovosti za analitske laboratorije, kot tudi celodnevna izobraževanja za posamezne vsebine (meroslovna sledljivost, validacija meril-

nih postopkov, ovrednotenje merilne negotovosti). Predavateljici sva dr. Monika Inkret in jaz. V lanskem letu je bilo vzpodbudno predvsem to, da so se za udeležbo na SIQ izobraževanju odločili tudi raziskovalni laboratoriji, ki se nimajo namena akreditirati. To bi vsekakor veljalo vzpodbujati in razširiti na druge raziskovalne laboratorije.

Tudi v okviru Eurachem-a ni bilo večjih novosti, kar je pričakovano, saj so koncepti, ki so se intenzivno oblikovali v začetku tega tisočletja, do sedaj definirani in so v pretežni meri „zgolj“ stvar implementacije, poleg seveda širitve na biopodročja.

dr. Nina Hrastelj

Poročilo Sekcije za živilsko kemijo za leto 2022

Člani Sekcije za živilsko kemijo (SŽK) smo se aktivno udeležili različnih znanstvenih in strokovnih srečanj, kjer so predstavili svoje raziskovalne dosežke. Aktivni pa so bili tudi na delavnicah in na področju izobraževanja in popularizacije kemije in še posebej živilske kemije. Člani SŽK so sodelovali pri organizacijah mednarodnih znanstvenih srečanj, katerih organizacijo je podprlo tudi Slovensko kemijsko društvo:

- 26th International Symposium on Separation Sciences (ISSS 2022, www.iss2020.si),
- 25th International Symposium for High-Performance Thin-Layer Chromatography (HPTLC 2022, www.hptlc2020.si),
- 11th Central European Congress on Food and Nutrition: “Food, Technology and Nutrition for Healthy People in a Healthy Environment“ (CE-Food 2022, www.cefood2022.si).

Aktivno smo sodelovali tudi pri različnih dejavnostih Sekcije za živilsko kemijo (Food Chemistry Division, FCD) Evropskega kemijskega združenja (European Chemical Society - EuChemS), kjer predstavljamo Slovensko kemijsko društvo. Prvič smo organizirali letni sestanek FCD v Sloveniji (30. 9. 2022). V okviru FCD smo sodelovali pri izboru tematik mednarodnega kongresa »XXII EuroFoodChem Congress«, ki bo leta 2023. Med te aktualne tematike spadajo: kakovost in varnost hrane; hrana in trajnostni razvoj (vključno z valorizacijo stranskih proizvodov); nova živila; hrana in zdravje, funkcionalna živila in sestavine s funkcionalnimi lastnostmi; kemijske reakcije in interakcije med sestavinami v živilih; kemijske spremembe v hrani med predelavo in skladiščenjem; ponarejanje živil,

avtentičnost in sledljivost; nove metode analize živil; kontaminanti v hrani. V okviru Skupine za organizacijo in izvedbo webinarjev, ki od leta 2021 deluje v okviru FCD, smo tudi leta 2022 sodelovali tudi pri izboru tematik in organizaciji webinarjev:

- »Fighting global food crime with analytical chemistry«, prof. dr. Chris Elliott z Institute for Global Food Security, Queen's University, Belfast;
- »Interpreting the gut microbiota function by employing LC/GC-MS metabolomic approaches« by Dr. Josep Rubert z Wageningen University, Wageningen.

V okviru FCD je potekalo tudi sodelovanje pri pripravi razpisa za mednarodno nagrado »The EuChemS Food Chemistry Division Young Researcher Award 2023«, ki bo podeljena mladi raziskovalki ali mlademu raziskovalcu za raziskave izvedene v okviru doktorske disertacije na področju živilske kemije in sorodnih področij. (<https://www.euchems.eu/divisions/food-chemistry-2/news/>).

V planu za leto 2023 smo predvideli aktivno udeležbo na mednarodnih simpozijih. Načrtujemo večjo udeležbo na »XXII EuroFoodChem Congress«, ki bo od 14. do 16. 6. 2023 v Beogradu, saj gre za dogodek iz najpomembnejše serije kongresov in simpozijev, ki jih organizira FCD. Udeležili se bomo tudi sestanka FCD, kjer bomo predstavili naše delo in z ostalimi člani FCD naredili načrt dela za prihodnje leto.

dr. Irena Vovk

KOLENDAR VAŽNEJŠIH ZNANSTVENIH SREČANJ S PODROČJA KEMIJE IN KEMIJSKE TEHNOLOGIJE

SCIENTIFIC MEETINGS – CHEMISTRY AND CHEMICAL ENGINEERING

2023

June 2023

- 14 – 16 XXII EUROFOODCHEM CONGRESS
Belgrade, Serbia
Information: <https://xxiieurofoodchem.com/>
- 18 – 21 33RD EUROPEAN SYMPOSIUM ON COMPUTER-AIDED PROCESS ENGINEERING
(ESCAPE-33)
Athens, Greece
Information: <https://escape33-ath.gr/>
- 28 – 30 MASS SPECTROMETRY CONGRESS IN ITALY – MASSA 2023
Torino, Italy
Information: <https://torino2023.spettrometriadimassa.it/>

July 2023

- 2 – 5 17TH EUROPEAN CONFERENCE ON MIXING
Porto, Portugal
Information: <http://mixing17.eu/>
- 2 – 6 FEZA 2023 – 9TH CONFERENCE OF THE FEDERATION OF THE EUROPEAN ZEOLITE
ASSOCIATIONS
Portorož-Portorose, Slovenia
Information: <https://feza2023.org/en/>
- 2 – 7 XV POSTGRADUATE SUMMER SCHOOL ON GREEN CHEMISTRY
Venice, Italy
Information: <https://www.greenchemistry.school/>
- 3 – 7 SCIENCE, TECHNOLOGY, SOCIETY AND WIKIPEDIA
Milano, Italy
Information: <https://iupac.org/project/2018-038-1-400/>
- 4 – 7 EURODRYING 2023
Lodz, Poland
Information: <https://www.eurodrying2023.p.lodz.pl/>
- 7 – 11 9TH EUCHEMS CHEMISTRY CONGRESS (ECC9)
Dublin, Ireland
- 9 – 14 38TH INTERNATIONAL CONFERENCE ON SOLUTION CHEMISTRY
Belgrade, Serbia
Information: <https://icsc2023.pmf.uns.ac.rs/>

August 2023

- 7 – 11 CHEMISTRY AND INTERDISCIPLINARY RESEARCH TOWARDS SDGS
Online/ Virtual
Information: <https://sites.google.com/uom.ac.mu/vcca-2023>
- 18 – 25 52ND IUPAC GENERAL ASSEMBLY
The Hague, Netherlands
Information: <https://iupac.org/event/ga2023/>
- 20 – 27 IUPAC WORLD CHEMISTRY CONGRESS 2023
The Hague, Netherlands
Information: <https://iupac2023.org/>
- 27 – 31 EUROANALYSIS 2023
Geneva, Switzerland
Information: <https://www.euroanalysis2023.ch/>
- 30 – Sept 1 28TH INTERNATIONAL WORKSHOP ON INDUSTRIAL CRYSTALLIZATION - BIWIC 2023
Stockholm, Sweden
Information: <https://www.biwic2023.se/>

September 2023

- 4 – 7 POLYMER MEETING 15 IN BRATISLAVA (PM15)
Bratislava, Slovakia
Information: <https://pm15.sav.sk/>
- 5 – 8 22ND INTERNATIONAL SYMPOSIUM ON INDUSTRIAL CRYSTALLIZATION - ISIC 2023
Glasgow, Scotland
Information: <https://www.isic2023.com/>
- 5 – 8 12TH INTERNATIONAL WORKSHOP ON POLYMER REACTION ENGINEERING (PRE)
Potsdam, Germany
Information: <https://dechema.de/en/PRE2023.html>
- 12 – 14 8TH INTERNATIONAL FAPS POLYMER CONGRESS
Istanbul, Turkey
Information: <https://www.faps2023.com/home>
- 13 – 15 SCS ANNUAL MEETING 2023
Portorose, Slovenia
Information: <https://skd2023.chem-soc.si/en/>
- 17 – 21 14TH EUROPEAN CONGRESS OF CHEMICAL ENGINEERING AND
7TH EUROPEAN CONGRESS OF APPLIED BIOTECHNOLOGY
Berlin, Germany
Information: <https://ecce-ecab2023.eu/>
- 17 – 22 6TH INTERNATIONAL MASS SPECTROMETRY SCHOOL
Cagliari, Italy
Information: <https://www.spettrometriadimassa.it/imss2023/>

October 2023

- 15 – 19 31ST INTERNATIONAL SYMPOSIUM ON THE CHEMISTRY OF NATURAL PRODUCTS
AND 11TH INTERNATIONAL CONGRESS ON BIODIVERSITY
Naples, Italy
Information: <https://www.iscnp31-icob11.org/>
- 22 – 25 2ND INTERNATIONAL CONFERENCE ON ENERGY, ENVIRONMENT & DIGITAL
TRANSITION – E2DT 2023
Palermo, Italy
Information: <https://www.aidic.it/e2dt2023/>

Acta Chimica Slovenica

Author Guidelines

Submissions

Submission to ACSi is made with the implicit understanding that neither the manuscript nor the essence of its content has been published in whole or in part and that it is not being considered for publication elsewhere. All the listed authors should have agreed on the content and the corresponding (submitting) author is responsible for having ensured that this agreement has been reached. The acceptance of an article is based entirely on its scientific merit, as judged by peer review. There are no page charges for publishing articles in ACSi. The authors are asked to read the Author Guidelines carefully to gain an overview and assess if their manuscript is suitable for ACSi.

Additional information

- Citing spectral and analytical data
- Depositing X-ray data

Submission material

Typical submission consists of:

- full manuscript (PDF file, with title, authors, abstract, keywords, figures and tables embedded, and references)
- supplementary files
 - **Full manuscript** (original Word file)
 - **Statement of novelty** (Word file)
 - **List of suggested reviewers** (Word file)
 - **ZIP file containing graphics** (figures, illustrations, images, photographs)
 - **Graphical abstract** (single graphics file)
 - **Proposed cover picture** (optional, single graphics file)
 - **Appendices** (optional, Word files, graphics files)

Incomplete or not properly prepared submissions will be rejected.

Submission process

Before submission, authors should go through the checklist at the bottom of the page and prepare for submission.

Submission process consists of 5 steps.

Step 1: Starting the submission

- Choose one of the journal sections.
- Confirm all the requirements of the **checklist**.
- Additional plain text comments for the editor can be provided in the relevant text field.

Step 2: Upload submission

- Upload full manuscript in the form of a Word file (with title, authors, abstract, keywords, figures and tables embedded, and references).

Step 3: Enter metadata

- First name, last name, contact email and affiliation for all authors, in relevant order, must be provided. Corresponding author has to be selected. Full postal address and phone number of the corresponding author has to be provided.

- **Title and abstract** must be provided in plain text.
- Keywords must be provided (max. 6, separated by semicolons).
- Data about contributors and supporting agencies may be entered.
- **References** in plain text must be provided in the relevant text filed.

Step 4: Upload supplementary files

- Original Word file (original of the PDF uploaded in the step 2)
- **List of suggested reviewers** with at least five reviewers with two recent references from the field of submitted manuscript must be uploaded as a Word file. At the same time, authors should declare (i) that they have no conflict of interest with suggested reviewers and (ii) that suggested reviewers are experts in the field of the submitted manuscript.
- All **graphics** have to be uploaded in a single ZIP file. Graphics should be named Figure 1.jpg, Figure 2.eps, etc.
- **Graphical abstract image** must be uploaded separately
- **Proposed cover picture** (optional) should be uploaded separately.
- Any additional **appendices** (optional) to the paper may be uploaded. Appendices may be published as a supplementary material to the paper, if accepted.
- For each uploaded file the author is asked for additional metadata which may be provided. Depending of the type of the file please provide the relevant title (Statement of novelty, List of suggested reviewers, Figures, Graphical abstract, Proposed cover picture, Appendix).

Step 5: Confirmation

- Final confirmation is required.

Article Types

Feature Articles are contributions that are written on Editor's invitation. They should be clear and concise summaries of the author's most recent work written with the broad scope of ACSi in mind. They are intended to be general overviews of the authors' subfield of research but should be written in a way that engages and informs scientists in other areas. They should contain the following (see also general guidelines for article structure below): (1) an introduction that acquaints readers with the authors' research field and outlines the important questions for which answers are being sought; (2) interesting, novel, and recent contributions of the author(s) to the field; and (3) a summary that presents possible future directions. Manuscripts should normally not exceed 40 pages of one column format (font size 12, 33 lines per page). Generally, experts who have made an important contribution to a specific field in recent years will be invited by the Editor to contribute a **Feature Article**. Individuals may, however, send a proposal (of no more than one page) for a **Feature Article** to the Editor-in-Chief for consideration.

Scientific articles should report significant and innovative achievements in chemistry and related sciences and should exhibit a high level of originality. They should have the following structure:

1. Title (max. 150 characters),
2. Authors and affiliations,
3. Abstract (max. 1000 characters),
4. Keywords (max. 6),
5. Introduction,
6. Experimental,
7. Results and Discussion,
8. Conclusions,
9. Acknowledgements,
10. References.

The sections should be arranged in the sequence generally accepted for publications in the respective fields and should be successively numbered.

Short communications generally follow the same order of sections as Scientific articles, but should be short (max. 2500 words) and report a significant aspect of research work meriting separate publication. Editors may decide that a Scientific paper is categorized as a Short Communication if its length is short.

Technical articles report applications of an already described innovation. Typically, technical articles are not based on new experiments.

Preparation of Submissions

Text of the submitted articles must be prepared with Microsoft Word. Normal style set to single column, 1.5 line spacing, and 12 pt Times New Roman font is recommended. Line numbering (continuous, for the whole document) must be enabled to simplify the reviewing process. For any other format, please consult the editor. Articles should be written in English. Correct spelling and grammar are the sole responsibility of the author(s). Papers should be written in a concise and succinct manner. The authors shall respect the ISO 80000 standard [1], and IUPAC Green Book [2] rules on the names and symbols of quantities and units. The Système International d'Unités (SI) must be used for all dimensional quantities.

Graphics (figures, graphs, illustrations, digital images, photographs) should be inserted in the text where appropriate. The captions should be self-explanatory. Lettering should be readable (suggested 8 point Arial font) with equal size in all figures. Use common programs such as MS Excel or similar to prepare figures (graphs) and ChemDraw to prepare structures in their final size. Width of graphs in the manuscript should be 8 cm. Only in special cases (in case of numerous data, visibility issues) graphs can be 17 cm wide. All graphs in the manuscript should be inserted in relevant places and **aligned left**. The same graphs should be provided separately as images of appropriate resolution (see below) and submitted together in a ZIP file (Graphics ZIP). Please do not submit figures as a Word file. In **graphs**, only the graph area determined by both axes should be in the frame, while a frame around the whole graph should be omitted. The graph area should be white. The legend should be inside the graph area. The style of all graphs should be the same. **Figures and illustrations** should be of sufficient quality for the printed version, i.e. 300 dpi minimum. **Digital images and photographs** should be of high quality (minimum

250 dpi resolution). On submission, figures should be of good enough resolution to be assessed by the referees, ideally as JPEGs. High-resolution figures (in JPEG, TIFF, or EPS format) might be required if the paper is accepted for publication.

Tables should be prepared in the Word file of the paper as usual Word tables. The captions should appear above the table and should be self-explanatory.

References should be numbered and ordered sequentially as they appear in the text, likewise methods, tables, figure captions. When cited in the text, reference numbers should be superscripted, following punctuation marks. It is the sole responsibility of authors to cite articles that have been submitted to a journal or were in print at the time of submission to ACSi. Formatting of references to published work should follow the journal style; please also consult a recent issue:

1. J. W. Smith, A. G. White, *Acta Chim. Slov.* **2008**, *55*, 1055–1059.
2. M. F. Kemmere, T. F. Keurentjes, in: S. P. Nunes, K. V. Peinemann (Ed.): *Membrane Technology in the Chemical Industry*, Wiley-VCH, Weinheim, Germany, **2008**, pp. 229–255.
3. J. Levec, Arrangement and process for oxidizing an aqueous medium, US Patent Number 5,928,521, date of patent July 27, **1999**.
4. L. A. Bursill, J. M. Thomas, in: R. Sersale, C. Collola, R. Aiello (Eds.), *Recent Progress Report and Discussions: 5th International Zeolite Conference*, Naples, Italy, 1980, Gianini, Naples, **1981**, pp. 25–30.
5. J. Szegezdi, F. Csizmadia, Prediction of dissociation constant using microconstants, http://www.chemaxon.com/conf/Prediction_of_dissociation_constant_using_microconstants.pdf, (assessed: March 31, 2008)

Titles of journals should be abbreviated according to Chemical Abstracts Service Source Index (CASSI).

Special Notes

- Complete characterization, **including crystal structure**, should be given when the synthesis of new compounds in crystal form is reported.
- Numerical **data should be reported with the number of significant digits corresponding to the magnitude** of experimental uncertainty.
- **The SI system of units and IUPAC recommendations** for nomenclature, symbols and abbreviations should be followed closely. Additionally, the authors should follow the general guidelines when citing spectral and analytical data, and depositing crystallographic data.
- **Characters** should be correctly represented throughout the manuscript: for example, 1 (one) and l (ell), 0 (zero) and O (oh), x (ex), D7 (times sign), B0 (degree sign). Use Symbol font for all Greek letters and mathematical symbols.
- The rules and recommendations of the **IUBMB** and the **International Union of Pure and Applied Chemistry (IUPAC)** should be used for abbreviation of chemical names, nomenclature of chemical compounds, enzyme nomenclature, isotopic compounds, optically active isomers, and spectroscopic data.
- **A conflict of interest** occurs when an individual (author, reviewer, editor) or its organization is in-

volved in multiple interests, one of which could possibly corrupt the motivation for an act in the other. Financial relationships are the most easily identifiable conflicts of interest, while conflicts can occur also as personal relationships, academic competition, etc. **The Editors** will make effort to ensure that conflicts of interest will not compromise the evaluation process; potential editors and reviewers will be asked to exempt themselves from review process when such conflict of interest exists. When the manuscript is submitted for publication, **the authors** are expected to disclose any relationships that might pose potential conflict of interest with respect to results reported in that manuscript. In the Acknowledgement section the source of funding support should be mentioned. The statement of disclosure must be provided as Comments to Editor during the submission process.

- **Published statement of Informed Consent.** Research described in papers submitted to ACSi must adhere to the principles of the Declaration of Helsinki (<http://www.wma.net/e/policy/b3.htm>). These studies must be approved by an appropriate institutional review board or committee, and informed consent must be obtained from subjects. The Methods section of the paper must include: 1) a statement of protocol approval from an institutional review board or committee and 2), a statement that informed consent was obtained from the human subjects or their representatives.
- **Published Statement of Human and Animal Rights.** When reporting experiments on human subjects, authors should indicate whether the procedures followed were in accordance with the ethical standards of the responsible committee on human experimentation (institutional and national) and with the Helsinki Declaration of 1975, as revised in 2008. If doubt exists whether the research was conducted in accordance with the Helsinki Declaration, the authors must explain the rationale for their approach and demonstrate that the institutional review body explicitly approved the doubtful aspects of the study. When reporting experiments on animals, authors should indicate whether the institutional and national guide for the care and use of laboratory animals was followed.
- To avoid conflict of interest between authors and referees we expect that not more than one referee is from the same country as the corresponding author(s), however, not from the same institution.
- Contributions authored by **Slovenian scientists** are evaluated by non-Slovenian referees.
- Papers describing **microwave-assisted reactions** performed in domestic microwave ovens are not considered for publication in *Acta Chimica Slovenica*.
- *Manuscripts that are **not prepared and submitted** in accord with the instructions for authors are not considered for publication.*

Appendices

Authors are encouraged to make use of supporting information for publication, which is supplementary material (appendices) that is submitted at the same time as the manuscript. It is made available on the Journal's

web site and is linked to the article in the Journal's Web edition. The use of supporting information is particularly appropriate for presenting additional graphs, spectra, tables and discussion and is more likely to be of interest to specialists than to general readers. When preparing supporting information, authors should keep in mind that the supporting information files will not be edited by the editorial staff. In addition, the files should be not too large (upper limit 10 MB) and should be provided in common widely known file formats to be accessible to readers without difficulty. All files of supplementary materials are loaded separately during the submission process as supplementary files.

Proposed Cover Picture and Graphical Abstract Image

Graphical content: an ideally full-colour illustration of resolution 300 dpi from the manuscript must be proposed with the submission. Graphical abstract pictures are printed in size 6.5 x 4 cm (hence minimal resolution of 770 x 470 pixels). Cover picture is printed in size 11 x 9.5 cm (hence minimal resolution of 1300 x 1130 pixels)

Authors are encouraged to submit illustrations as candidates for the journal Cover Picture*. The illustration must be related to the subject matter of the paper. Usually both proposed cover picture and graphical abstract are the same, but authors may provide different pictures as well.

* The authors will be asked to contribute to the costs of the cover picture production.

Statement of novelty

Statement of novelty is provided in a Word file and submitted as a supplementary file in step 4 of submission process. Authors should in no more than 100 words emphasize the scientific novelty of the presented research. Do not repeat for this purpose the content of your abstract.

List of suggested reviewers

List of suggested reviewers is a Word file submitted as a supplementary file in step 4 of submission process. Authors should propose the names, full affiliation (department, institution, city and country) and e-mail addresses of five potential referees. Field of expertise and at least two references relevant to the scientific field of the submitted manuscript must be provided for each of the suggested reviewers. The referees should be knowledgeable about the subject but have no close connection with any of the authors. In addition, referees should be from institutions other than (and countries other than) those of any of the authors. Authors declare no conflict of interest with suggested reviewers. Authors declare that suggested reviewers are experts in the field of submitted manuscript.

How to Submit

Users registered in the role of author can start submission by choosing USER HOME link on the top of the page, then choosing the role of the Author and follow the relevant link for starting the submission process.

Prior to submission we strongly recommend that you familiarize yourself with the ACSi style by browsing the journal, particularly if you have not submitted to the ACSi before or recently.

Correspondence

All correspondence with the ACSi editor regarding the paper goes through this web site and emails. Emails are sent and recorded in the web site database. In the correspondence with the editorial office please provide ID number of your manuscript. All emails you receive from the system contain relevant links. **Please do not answer the emails directly but use the embedded links in the emails for carrying out relevant actions.** Alternatively, you can carry out all the actions and correspondence through the online system by logging in and selecting relevant options.

Proofs

Proofs will be dispatched via e-mail and corrections should be returned to the editor by e-mail as quickly as possible, normally within 48 hours of receipt. Typing errors should be corrected; other changes of contents will be treated as new submissions.

Submission Preparation Checklist

As part of the submission process, authors are required to check off their submission's compliance with all of the following items, and submissions may be returned to authors that do not adhere to these guidelines.

1. The submission has not been previously published, nor is it under consideration for publication in any other journal (or an explanation has been provided in Comments to the Editor).
2. All the listed authors have agreed on the content and the corresponding (submitting) author is responsible for having ensured that this agreement has been reached.
3. The submission files are in the correct format: manuscript is created in MS Word but will be **submitted in PDF** (for reviewers) as well as in original MS Word format (as a supplementary file for technical editing); diagrams and graphs are created in Excel and saved in one of the file formats: TIFF, EPS or JPG; illustrations are also saved in one of these formats. The preferred position of graphic files in a document is to embed them close to the place where they are mentioned in the text (See **Author guidelines** for details).
4. The manuscript has been examined for spelling and grammar (spell checked).
5. The **title** (maximum 150 characters) briefly explains the contents of the manuscript.
6. Full names (first and last) of all authors together with the affiliation address are provided. Name of author(s) denoted as the corresponding author(s), together with their e-mail address, full postal address and telephone/fax numbers are given.
7. The **abstract** states the objective and conclusions of the research concisely in no more than 150 words.
8. Keywords (minimum three, maximum six) are provided.
9. **Statement of novelty** (maximum 100 words) clearly explaining new findings reported in the manuscript should be prepared as a separate Word file.
10. The text adheres to the stylistic and bibliographic requirements outlined in the **Author guidelines**.
11. Text in normal style is set to single column, 1.5 line spacing, and 12 pt. Times New Roman font is

recommended. All tables, figures and illustrations have appropriate captions and are placed within the text at the appropriate points.

12. Mathematical and chemical equations are provided in separate lines and numbered (Arabic numbers) consecutively in parenthesis at the end of the line. All equation numbers are (if necessary) appropriately included in the text. Corresponding numbers are checked.
13. Tables, Figures, illustrations, are prepared in correct format and resolution (see **Author guidelines**).
14. The lettering used in the figures and graphs do not vary greatly in size. The recommended lettering size is 8 point Arial.
15. Separate files for each figure and illustration are prepared. The names (numbers) of the separate files are the same as they appear in the text. All the figure files are packed for uploading in a single ZIP file.
16. Authors have read **special notes** and have accordingly prepared their manuscript (if necessary).
17. References in the text and in the References are correctly cited. (see **Author guidelines**). All references mentioned in the Reference list are cited in the text, and vice versa.
18. Permission has been obtained for use of copyrighted material from other sources (including the Web).
19. The names, full affiliation (department, institution, city and country), e-mail addresses and references of five potential referees from institutions other than (and countries other than) those of any of the authors are prepared in the word file. At least two relevant references (important recent papers with high impact factor, head positions of departments, labs, research groups, etc.) for each suggested reviewer must be provided. Authors declare no conflict of interest with suggested reviewers. Authors declare that suggested reviewers are experts in the field of submitted manuscript.
20. Full-colour illustration or graph from the manuscript is proposed for graphical abstract.
21. **Appendices** (if appropriate) as supplementary material are prepared and will be submitted at the same time as the manuscript.

Privacy Statement

The names and email addresses entered in this journal site will be used exclusively for the stated purposes of this journal and will not be made available for any other purpose or to any other party.

ISSN: 1580-3155

Koristni naslovi

Slovensko kemijsko društvo
Slovenian Chemical Society



Slovensko kemijsko društvo

www.chem-soc.si

e-mail: chem.soc@ki.si



Wessex Institute of Technology

www.wessex.ac.uk



SETAC

www.setac.org



European Water Association

<http://www.ewa-online.eu/>



European Science Foundation

www.esf.org



European Federation of Chemical Engineering

<https://efce.info/>



IUPAC

INTERNATIONAL UNION OF
PURE AND APPLIED CHEMISTRY

International Union of Pure and Applied Chemistry

<https://iupac.org/>

Novice evropske zveze kemijskih društev EuChemS najdete na:

 **EuChemS**
European Chemical Society

Brussels News Updates

<http://www.euchems.eu/newsletters/>



Komore za testiranje baterij

Vakuumski sušilniki

Klimatske komore



Donau Lab d.o.o., Ljubljana
Tbilisijska 85
SI-1000 Ljubljana
www.donaulab.si
office-si@donaulab.com

Razvojna usmerjenost

- Nove formulacije na bazi vodikovega peroksida
- Širjenje uporab vodikovega peroksida na različnih področjih

V svoje vrste vabimo mlade raziskovalce, diplomante in post diplomante, ki bodo skupaj z nami reševali nove izzive.

 **belinka perkemija**

Belinka Perkemija, d. o. o., Zasavska cesta 95, Ljubljana
perkemija@belinka.si, www.belinka-perkemija.com
Contact person: mag. Ivan Grčar; igo@belinka.si

Member of KANSAI HELIOS. Part of KANSAI PAINT.

Področja uporabe



Razvoj in inovacije za globalno uspešnost

Znanje, kreativnost zaposlenih in inovacije so ključnega pomena v okolju, kjer nastajajo pametni premazi skupine KANSAI HELIOS. Z rešitvami, ki zadostijo široki paleti potreb, kontinuiranim razvojem ter s kakovostnimi izdelki, Helios predstavlja evropski center za inovacije in poslovni razvoj skupine Kansai Paint.



Part of  **KANSAI
PAINT**



www.helios-group.eu

 **KANSAI
HELIOS**
Designing Excellence

Dasselta[®]

CONTROL



Odpihnite alergijo!

- Lajša simptome alergijskega rinitisa oz. **senenega nahoda**.
- Deluje 24 ur.
- Ne povzroča zaspanosti.



www.dasselta.si

 KRKA

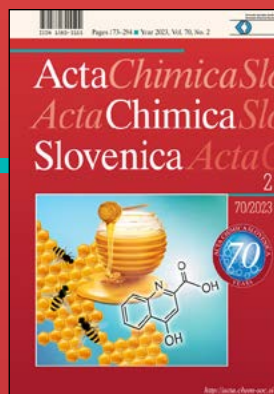
Dasselta control vsebuje desloratadin.

Pred uporabo natančno preberite navodilo!
O tveganju in neželenih učinkih se posvetujte z zdravnikom ali s farmacevtom.

ActaChimicaSlovenica

ActaChimicaSlovenica

Kynurenic acid is metabolite of tryptophane that can be found in different foods, also in honey. The content of kynurenic acid was determined in more than 100 samples of different botanical sources. Results have shown that chestnut honey has much higher concentration of kynurenic acid than other honeys.



Year 2023, Vol. 70, No. 2

